Braincase anatomy in non-neosauropodan sauropodomorphs: evolutionary and functional aspects

Dissertation der Fakultät für Geowissenschaften der Ludwig-Maximilians-Universität München zur Erlangung des Doktorgrades in den Naturwissenschaften (Dr. rer. nat.)

Vorgelegt von

Mario Bronzati Filho

München, 15. März 2017

Erstgutachter: PD Dr. Oliver Rauhut

Zweitgutachter: Prof. Dr. Max Cardoso Langer

Tag der mündlichen Prüfung: 26.09.2017

I

Statutory declaration and statement

I hereby confirm that my thesis entitled "**Braincase anatomy in non-neosauropodan sauropodomorphs: evolutionary and functional aspects**", is the result of my own original work. Furthermore, I certify that this work contains no material which has been accepted for the award of any other degree or diploma in my name, in any university and, to the best of my knowledge and belief, contains no material previously published or written by another person, except where due reference has been made in the text. In addition, I certify that no part of this work will, in the future, be used in a submission in my name, for any other degree or diploma in any university or other tertiary institution without the prior approval of the Ludwig-Maximilians-University Munich.

Contents

Abstract of the thesis

The evolutionary history of sauropodomorphs starts in the Late Triassic, a period characterized by the extinction and radiations of distinct archosaur lineages. During the first c. 50 million years of sauropodomorph evolution, a great number of anatomical transformations are observed among non-sauropodan lineages of Sauropodomorpha, once thought as 'typical herbivore' and 'conservative'. All these transformations are reflected in the morphological disparity observed among sauropodomorph dinosaurs. The earliest members of the group, from the Late Triassic (Carnian) were small animals, faunivorous and omnivorous, and with a bauplan that differs significantly from the quintessential representatives of the group, the gigantic sauropods, the biggest land animals that ever lived on Earth. This morphological disparity, alongside a rich and globally distributed fossil record, represents a very interesting case to study morphological changes within a lineage. Notwithstanding, the anatomy of sauropodomorph was the topic of many studies, mainly aiming to understand the origins of the peculiar and distinct sauropod bauplan, especially the transition from a bipedal to a quadrupedal stance, and the evolution of a fully herbivore diet. The aim of this study is an analysis of patterns of transformation of the braincase in sauropodomorph dinosaurs and their implications for our understanding concerning the phylogenetic relationships and palaeobiology of these animals.

The analysis of two new fossils, the sauropodomorph dinosaur (*Buriolestes schultzi*) the lagerpetid (*Ixalerpeton polesinensis*), helps clarifying anatomical transformations of the braincase in the Dinosauromorpha lineage and the early evolution of dinosaur diets. The tooth morphology of *Buriolestes* indicates that it was a faunivorous animal. Thus, given its phylogenetic position as the sister group of all

the other sauropodomorphs, and the faunivorous diet of theropods and herrerasaurids, the new data indicate that faunivory is the ancestral condition of Sauropodomorpha.

The endocast of *Saturnalia tupiniquim* helps to understand one of the well-known traits of sauropodomorph dinosaurs, a short skull. *Saturnalia* has a well-developed flocculus (i.e. projecting into the space between the semi-circular canals of the inner ear), which is a feature observed in predatory dinosaurs, and absent in later sauropodomorphs, including sauropoda. Combining new information on the soft-tissues of the brain with data on skeletal anatomy and phylogeny of sauropodomorphs, it is proposed that skull reduction was firstly an adaptation to feed on small and elusive preys. As a small skull was later a 'key' trait for the evolution of a fully herbivorous diet (by diminishing the constraint on the neck), skull reduction in sauropodomorph can be now understood as an exaptation.

The osteological descriptions of the braincases of *Saturnalia tupiniquim* and *Efraasia minor* allow tracing the evolution of braincase anatomy in Sauropodomorpha in more details. Comparisons with lagerpetids, silesaurids, and other dinosaurs showed that features once thought to be absent or less widespread in dinosaurs, such as the semilunar depression (or subotic recess) and a basioccipital and subsellar recesses, are in fact found among members of the three main lineages of Dinosaria, and also among non-dinosaurian dinosauromorphs. Furthermore, the results of a phylogenetic analysis focusing on non-neosauropodan sauropodomorphs indicate that despite the existence of characters supporting a monophyletic 'Prosauropoda' (i.e. a calde encompassing the non-sauropodan sauropodomorphs), constrained phylogenetic analyses indicate that the paraphyletic condition of 'prosauropods' in relation to Sauropoda is still a much stronger hypothesis.

A great number of transformations in the braincase anatomy were also detected within sauropods in the phylogenetic analyses conducted for this thesis. Discrete character-taxon matrix analyses indicate a drastic transformation in the braincase of these animals in relation to their non-sauropodan relatives, with the results of a principal coordinate analysis showing that the morphospace occupation of sauropod braincases does not overlap with the morphospace of non-sauropodan sauropodomorpsh. Furthermore, analyses of rates of character evolution indicate that transformations shaping the braincase anatomy of sauropods occurred in a short period of time, during the Middle Jurassic, and can be linked to the further elongation of the neck also observed in Middle Jurassic taxa. Ultimately, these modifications in the cranio-cervical complex are likely related to a re-activation of the 'neck and head' cascade of gigantism, and potentially played a role in the differential survival of sauropodomorphs in the Early-Middle Jurassic.

Finally, differently from what is stated in a great number of previous studies on the evolution of Sauropodomorpha, the non-sauropodan sauropodomorphs (or "prosauropod") do not represent transitional forms between the hypothetical ancestor of Sauropodomorpha and Sauropoda. Nevertheless, sauropods and 'prosauropods' share part of their evolutionary history, and the data presented here emphasizes that tracing anatomical transformation in non-sauropodan lineages is crucial to understand the evolution of the gigantic sauropods.

CHAPTER 1

Introduction, objectives, and structure of the thesis

Author contributions:

Research design **Mario Bronzati**, Oliver W. M. Rauhut, Max C. Langer

Mario Bronzati wrote the chapter.

Chapter 1

INTRODUCTION

1.1. Introduction

Archosauria is the group of animals that includes extant birds and crocodylians (Gauthier & Padian, 1985; Benton & Clark, 1998), and a variety of other extinct lineages that lived during the Mesozoic Era (Nesbitt, 2011). Together with extinct archosaurs more closely related to them than to birds, living crocodylians compose Pseudosuchia; whereas birds and extinct archosaurs more closely related to them than to crocodylians form Avemetatarsalia (Benton & Clark, 1988). The fossil record of archosaurs dates back to the Early Triassic, a crucial period in the evolutionary history of vertebrates, as the aftermath of the Permo-Triassic mass extinction saw the origin and early radiation of many important new lineages (Benton *et al*., 2014). Recent analyses of the archosaur fossil record point to a dominance of forms belonging to the Pseudosuchia lineage during the Early-Middle Triassic (c. 240 – 230 Ma). Dinosaurs, with oldest fossils dating back to the Late Triassic (Carnian, c – 230 Ma), experienced a "slow" diversification during their first 30 million years of evolutionary history (Benton *et al., *2014), and by the last stages of the Triassic, pseusoduchian diversity was still higher than that of its closest archosaurian relatives (Brusatte *et al*., 2010a). It is only after the mass extinction event of the Late Triassic, which strongly affected pseudosuchians (Brusatte *et al., *2011), that non-avian dinosaurs started their more significant diversification, becoming the dominant

component of terrestrial faunas until the Cretaceous/Paleogene mass extinction event (Brusatte *et al*. 2010a, 2011; Nesbitt, 2011; Marsicano *et al*., 2015). During this period characterized by extinctions and radiations of distinct archosaur lineages (Nesbitt, 2011) starts the evolutionary history of sauropodomorphs, with the oldest fossils dating back to the Late Triassic, Carnian (Langer *et al*., 2010).

Dinosauromorpha

Avemetatarsalia has two major lineages, Pterosauromorpha, which included the flying reptiles, the pterosaurs, and Dinosauromorpha (Nesbitt, 2011). Dinosauromorpha (Fig 1.1) includes dinosaurs, today represented by birds, and other extinct lineages comprising Middle and Late Triassic taxa, such as lagerpetids and silesaurids (Nesbitt *et al*., 2010). Among dinosauromorphs, the position of Lagerpetidae as the sister-group of all other dinosauromorphs, which compose the less inclusive clade Dinosauriformes, is well established (Nesbitt *et al*., 2010; Cabreira *et al*., 2016; Martinez *et al*., 2016). However, a more controversial point is the position of Silesauridae, which are either recovered as the sister-group of Dinosauria (Kammerer *et al*., 2012; Bittencourt *et al*., 2014), or within Dinosauria, as the sister group of Ornithischia (Langer & Ferigolo, 2013; Cabreira *et al*., 2016). Moreover, the inclusivity of Silesauridae is also a matter of debate. Whereas some analysis indicate that *Lewisuchus admixtus* from the Middle Triassic of Argentina is a member of this clade (Nesbitt *et al*., 2010; Kammerer *et al*., 2012), other studies recover *Lewisuchus* as the sister taxon of silesaurids and dinosaurs (Bittencourt *et al*., 2014; Cabreira *et al*., 2016).
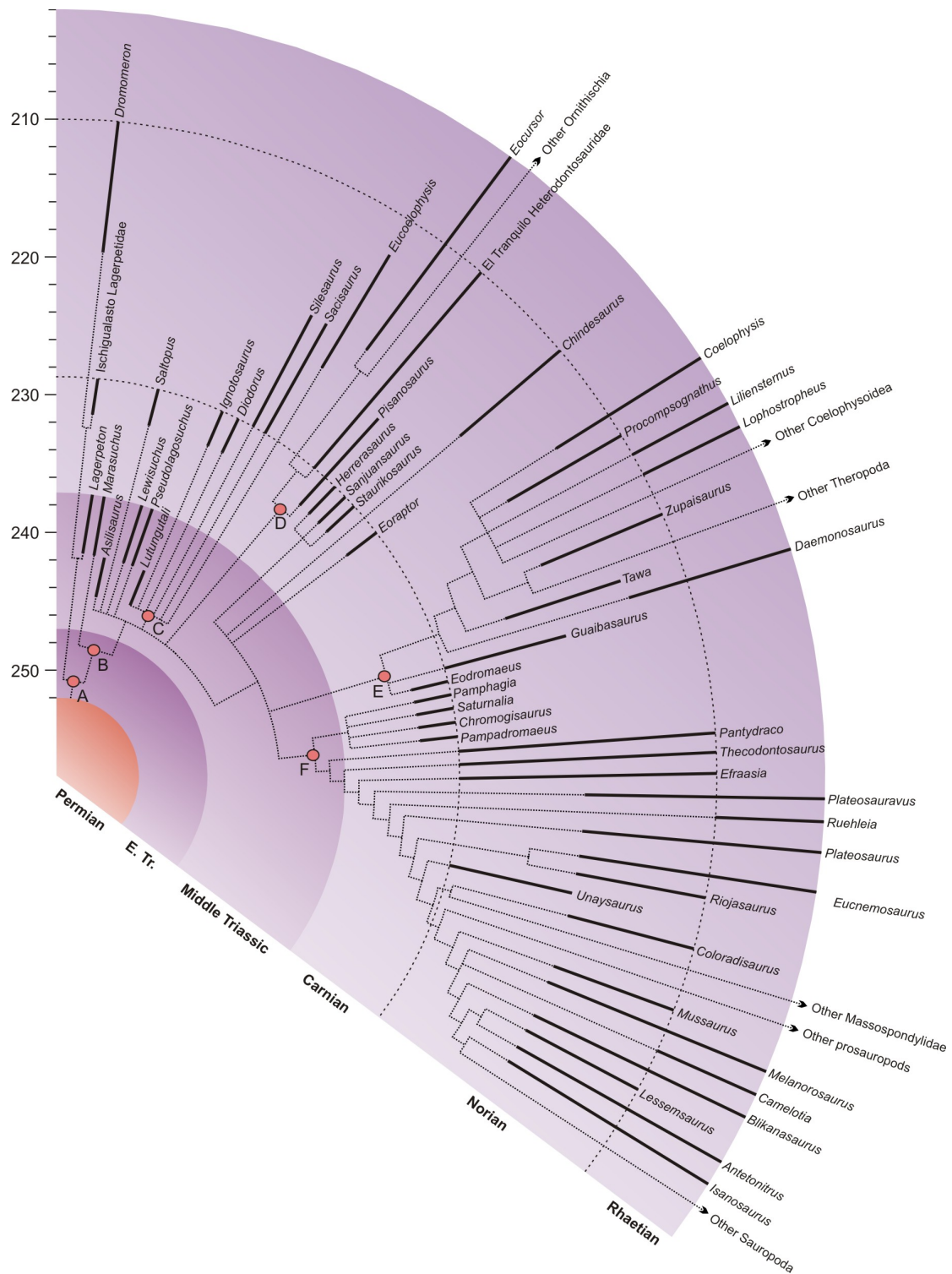
Figure 1.1: The phylogeny of Late Triassic dinosauromorphs (modified from Langer, 2014). Terminal taxa within the clades delimited by the nodes highlighted in the cladogram correspond to: A – dinosauromorphs; B – dinosauriforms; C – silesaurids; D – ornithischians; E – theropods; F – sauropodomorphs.

Phylogenetic relationships within Dinosauria are not less problematic (Fig 1.1). The group has three main established lineages, Ornithischia, Theropoda (including birds), and Sauropodomorpha (Langer *et al.,* 2010). Additionally, phylogenetic analysis have indicated that Sauropodomorpha and Theropoda are more closely related to each other than to Ornithischia (Langer & Benton, 2006). However, whereas the assignment of Jurassic and Cretaceous taxa to one of the three main lineages seems less problematic, the affinities of several Late Triassic taxa, especially Carnian animals such as *Herrerasaurus ischigualastensis, Eoraptor lunensis,* and *Eodromaeus murphy* remain disputed (Langer, 2014). *Herrerasaurus* and *Eodromaeus* are either found within Theropoda (Nesbitt *et al.,* 2009; Martinez *et al.,* 2011), or as non-eusaurischian saurischians, or in other words, more closely related to Theropoda and Sauropodomorpha than to Ornithischia (Cabreira *et al.,* 2016). Regarding *Eoraptor,* this taxon was originally described as a theropod (Sereno *et al.,* 1993), and has been recovered as such in subsequent phylogenetic analyses (Nesbitt *et al.,* 2009). However, other analyses recovered *Eoraptor* as a non-eusaurischian saurischian, or even as a member of Sauropodomorpha (Martinez *et al.,* 2011; Cabreira *et al.,* 2016).

Sauropodomorpha

 Sauropodomorpha (Fig. 1.2) was originally coined by von Huene (1932), to include "Prosauropoda", previously established by the same author in 1920, and Sauropoda, established by Marsh (1878). Later, definitions for Sauropodomorpha were proposed following the principles of phylogenetic nomenclature (de Queiroz & Gauthier, 1990, 1992, 1994). Some examples are the node-based definitions of Salgado et al. (1997), *"the clade including the most recent common ancestor of Prosauropoda and*

Sauropoda and all of its descendants", and Sereno (1998), *"the most recent common ancestor of* Plateosaurus *and* Saltasaurus *and all its descendants"*; and an alternative branch-based (= stem-based) definition presented Galton & Upchurch (2004), *"all taxa more closely related to* Saltasaurus *than to Theropoda"*. However, using "Prosauropoda" as a marker to define Sauropodomorpha as proposed by Salgado *et al.* (1997) is problematic, because this group, in its traditional sense (see below), is probably not monophyletic, and its content is unstable (Upchurch *et al.* 2007). Thus, the branch-based definition proposed by Galton & Upchurch (2004), even if not always explicitly mentioned by the authors of some studies, has been preferred (e.g. Yates *et al.*, 2010; Pol *et al.*, 2011; Apaldetti *et al.*, 2014; McPhee *et al.*, 2014, 2015). One of the reasons is that, contrary to the definition of Sereno (1989), the definition of Galton & Upchurch (2004) also encompasses a series of Carnian taxa that are more closely related to the "traditional sauropodomorphs" than to theropods. Among these are taxa such as *Saturnalia tupiniquim* (Langer et al., 1999), *Panphagia protos* (Martinez & Alcober, 2009), *Chromogisaurus novasi* (Ezcurra, 2010), and *Eoraptor lunensis* (Sereno *et al.,* 1993), described as a theropod, but found as a member of Sauropodomorpha in recent phylogenetic analysis, as mentioned above (e.g. Martinez *et al.,* 2012a; Cabreira *et al.,* 2016). Regardless of the still non-consensual scenario of early dinosaur evolution, and hence the assignment of Carnian taxa to one of the three main lineages of Dinosauria (Langer, 2014), the traditional "prosauropods" (see below) of the Late Triassic and Early Jurassic are consistently found as members of the Sauropodomorpha. Finally, the gigantic sauropods, found in deposits with ages ranging from the Late Triassic/Early Jurassic (obs. the uncertainty regarding the age of the oldest records of sauropods is a complex scenario related not only to the age of the fossils, but also to the assemblage of taxa encompassed by the different

phylogenetic definitions adopted for the group) till the end of the Cretaceous (McPhee *et al.,* 2015), are probably the most iconic members of the group (Wilson, 2005).
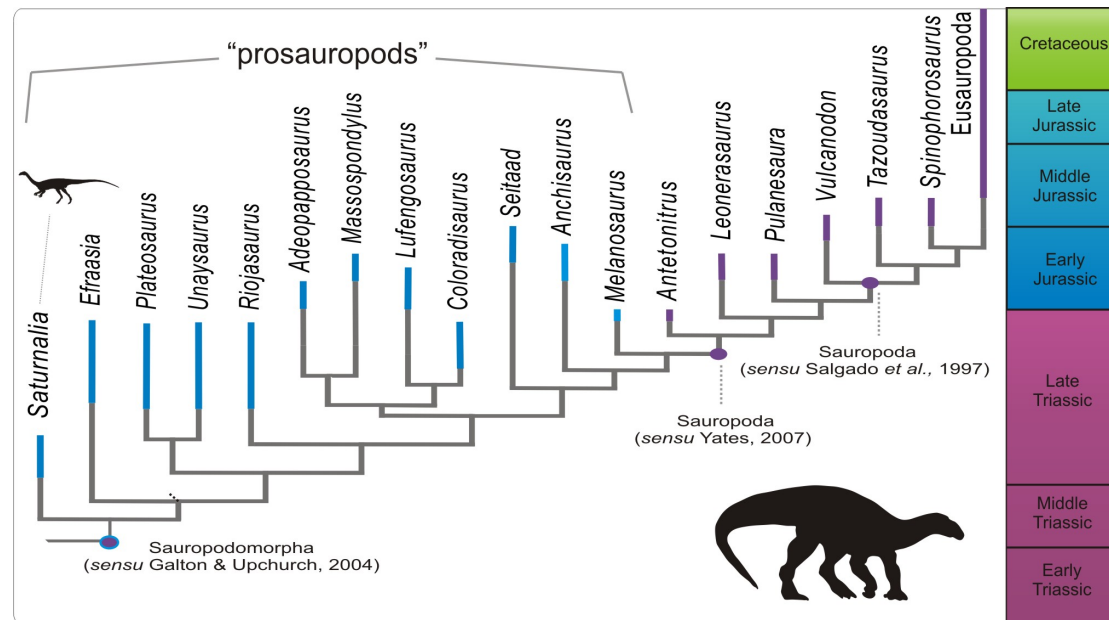
Figure 1.2: Simplified time-calibrated phylogeny of Sauropodomorpha.

"Prosauropoda": the non-sauropodan sauropodomorphs

Huene (1926) considered "Prosauropoda" as part of an assemblage of taxa referred to as Pachypodosaurier (the original term in German). According to Huene (1926), one major portion of Pachypodosaurier was a group of presumed carnivore taxa, the Carnosauria. Posterior studies showed that the taxonomy and systematics of carnosaurs were very problematic, and animals assigned to the group by Huene (1926; 1932) have been recognised as members of different archosaur lineages, including Pseudosuchia, Theropoda, and Sauropodomorpha (e.g. Benton, 1986; Galton, 1986). The other major portion of Huene's Pachydoposaurier was an assemblage of omnivore/herbivore animals. Within these, Huene (1926) considered the Triassic forms as belonging to "Prosauropoda", whereas the Jurassic and Cretaceous taxa were

part of Sauropoda. Later, Huene (1932) coined the term Sauropodomorpha to include both "Prosauropoda" and Sauropoda.

Only a few taxa of Huene's conception of "Prosauropoda" are still formally accepted as valid taxa today, such as *Plateosaurus, Thecodontosaurus, Massospondylus,* and, *Melanorosaurus* (see e.g. Benton *et al.,* 2000; Yates, 2003a; Yates, 2007). However, even during the pre-cladistic era, researchers started arguing that some of the members of "Prosauropoda" of Huene (1920) were probably more closely related to sauropods than to other "prosauropods" (Colbert, 1964; Charig et al. 1965). A paraphyletic "Prosauropoda" was also recovered in the pioneer cladistic analyses of Gauthier (1986) - this is not shown in the phylogenetic trees presented by the author but it is mentioned in his text (see also Sereno, 2007; Upchurch *et al.,* 2007). However, cladistic studies published not long after the work of Gauthier (1986) recovered the "prosauropods" as forming a natural group, i.e. monophyletic (Sereno, 1989; Galton, 1990). The two alternative hypotheses ("Prosauropoda" paraphyletic VS "Prosauropoda" monophyletic) were in debate for many years (Peyre de Fabrègues et al. 2015), and the matter is still not entirely resolved, although most recent analyses indicate that despite a number of less inclusive clades (e.g. Plateosauridae, Massospondylidae, Riojasauridae), the non-sauropodan sauropodomorphs (i.e. many of the classical prosauropods) correspond to a series of lineages that compose a paraphyletic assemblage in relation to Sauropoda (see below).

Because of the nature of phylogenetic definitions, the group corresponding to a definition will always be monophyletic (de Queiroz & Gauthier, 1990; 1992; 1994). Yet, applying different phylogenetic definitions for Sauropodomorpha in different tree topologies derived from cladistic analyses will result in different assemblages of

taxa. This occurs not only because the nature of the definitions (branch vs node based), but also because different tree topologies result in different arrangements of the taxa recovered within clades fitting the definitions (Langer, 2001). Thus, when the composition of "Prosauropoda" is analysed in an historical perspective, a more or less inclusive "Prosauropoda" is found among different phylogenetic analyses. A more inclusive "Prosauropoda", encompassing all or most of the non-sauropodan sauropodomorphs, as first recovered by Sereno (1989) and Galton (1990), was also recovered in later studies, such as Benton *et al*. (2000) and Galton & Upchurch (2004). However, other studies only found support for a less inclusive "Prosauropoda" (Yates & Kitching, 2003; Upchurch *et al*., 2007), which includes only an assemblage of taxa that came to be known as the "core prosauropods", consisting of taxa such as *Plateosaurus* and *Massospondylus* (Sereno, 2007). Today there is a growing consensus that the traditional 'Prosauropoda' of Huene, and even the "core prosauropods", represent a paraphyletic assemblage of taxa in relation to sauropods (e.g. Yates & Kitching 2003; Upchurch et al. 2007a; Yates 2007; Martínez 2009; Yates et al. 2010; Apaldetti et al. 2011; Pol et al. 2011). Thus, when applying existent definitions of "Prosauropoda" to different cladograms presented in the most recent studies (e.g. Apaldetti *et al*., 2014; McPhee *et al*., 2014, 2015; Otero *et al*., 2015), only a single "core prosauropod" taxon would form the clade, *Plateosaurus*. Furthermore, this clade would be equivalent to Plateosauridae (Yates, 2007). Thus, because the content of "Prosauropoda" would highly differ from its original concept, the name "Prosauropoda" as a clade has fallen into disuse (Yates, 2007). However, the term "prosauropods" is still sometimes employed to refer to the sauropodomorphs outside the Sauropoda clade (Otero & Salgado, 2015), a paraphyletic assemblage of taxa, which here in this thesis is also treated as the non-sauropodan sauropodomorphs.

1.2. Evolution of Sauropodomorpha

The morphological disparity among sauropodomorph dinosaurs represents a very interesting case of morphological change within a lineage. Early sauropodomorphs, such as *Saturnalia tupiniquim* (Langer et al. 1999) and *Panphagia protos* (Martinez & Alcober, 2009) were small and "gracile" animals, with a bauplan that differs significantly from later representatives of the group, the giant sauropods, the biggest land animals that ever lived on Earth (Rauhut *et al.,* 2011). By the end of the Triassic (c. 201 Ma), sauropodomorphs had already reached a broader distribution, with fossils found in most areas of the supercontinent Pangaea (Langer *et al.,* 2010). The latest Triassic (Norian – Rhaetian, c. 225 – 205 Ma) forms of "prosauropods*"* are typically the most abundant terrestrial vertebrates in places where they occur (Galton & Upchurch, 2004), representing the first large radiation of omnivorous/herbivorous dinosaurs for approximately 40 Ma, from the Late Triassic to the middle Early Jurassic (Sereno, 2007). With a rich and globally distributed fossil record, many studies (see below) have focused on the evolution of the Sauropodomorpha lineage, specially aiming to understand the origins of the peculiar and distinct sauropod bauplan (see e.g. Bates *et al.,* 2016).

Sauropods may be considered the best known members of the group, and their gigantic body size and strict herbivory represents an interesting case study to investigate extremes within the palaeobiology of terrestrial animals (Sander et al. 2011). Traditionally, "prosauropods" were generally regarded as conservative in respect to their general morphology (Sereno, 2007). However, the evolution of such peculiar and conspicuous morphology in sauropods, especially the adaptations to herbivory and quadrupedalism, happened through a series of morphological transformations that took place before the origin of Sauropoda, among non-

sauropodan sauropodomorphs (Wilson, 1999; Upchurch & Barrett, 2000; Yates & Kitching, 2003; Barrett & Upchurch, 2005, 2007; Parrish, 2005; Bonnan & Senter, 2007; Bonnan & Yates, 2007; Upchurch, et al. 2007; Remes, 2008; Fechner, 2009; Martinez, 2009; Yates et al. 2010; Pol et al. 2011; Rauhut et al. 2011).

A series of recent studies have investigated transformation patterns along the evolution of sauropodomorphs, mostly focusing in the transition from a bipedal to a quadrupedal stance, and also on the evolution of a fully herbivore diet (Barrett 2000; Yates & Kitching 2003, Barrett & Upchurch 2007; Bonnan & Yates 2007; Upchurch *et al.*, 2007b; Yates *et al.,* 2010; Rauhut *et al.*, 2011). These are ultimately linked to the evolution of gigantism in Sauropodomorpha, which was taken to the extreme by sauropods (Sander *et al.,* 2011). However, the evolution of the braincase and its associated soft tissues has not been studied in a comparative, evolutionary framework so far. Sauropod dinosaurs have one of the lowest encephalisation quotients amongst amniotes (Hopson 1979, 1980), and their braincase is highly derived and deviates from that of early saurischians in many respects (e.g. Janensch 1935-1936; Salgado & Calvo 1992; Paulina-Carabajal & Salgado 2007; Balanoff *et al*. 2010; Knoll *et al.*, 2012, Paulina-Carabajal *et al.*, 2014).

Evolution of herbivory

A recently described sauropodomorph from the Late Triassic (Carnian – c. 230 Ma) Santa Maria Formation of Brazil, *Buriolestes schultzi* (Cabreira *et al.,* 2016), revealed that the earliest sauropodomorphs possessed a tooth morphology that is more compatible with a strictly faunivorous diet. In light of this new finding, the most likely scenario is that faunivory represents the ancestral condition of Saurischia, or even Dinosauria, although the ancestral condition of the latter remains inconclusive

(Cabreira *et al.*, 2016). *Buriolestes* is additional evidence (see also Barrett & Upchurch, 2007; Barrett *et al.*, 2010) against the orthodox view of all Triassic sauropodomorphs as herbivore animals (e.g. Sereno, 2007).

The teeth of Carnian sauropodomorphs, such as *Buriolestes, Saturnalia* and *Eoraptor,* are recurved and bear small serrations perpendicular to the carina, as it is typical in carnivorous taxa (Barrett *et al.*, 2010; Nesbitt *et al.*, 2010). In a recent reassessment of *E. lunensis*, Sereno *et al.* (2012) stated that aspects of its tooth morphology, such as a first dentary tooth that is offset from the anterior end of the mandible and uncurved crowns, indicate that the diet of *E. lunensis* was partially or even fully herbivorous. As for the former feature, it has been demonstrated that such a morphology is not strictly correlated to a herbivorous diet in dinosaurs (Nesbitt *et al.*, 2010). As for the crown recurvature, it is indeed absent in some of the teeth of *E. lunensis*, but not in all. Thus, an at least partially faunivorous diet cannot be ruled out for that taxon, and the most parsimonious option is to treat *E. lunensis* as an omnivore. In this context, the acquisition of a fully herbivorous diet during the Carnian lacks support from the sauropodomorph fossil record (Barrett & Upchurch, 2007; Barrett *et al.*, 2011). Yet, among sauropodomorphs known from Norian (c. 228-208 Ma) and Rhaetian (c. 208-201Ma) deposits, such as *Efraasia* and *Plateosaurus,* the presence of lanceolate teeth with coarse denticles and overlap of adjacent crowns is observed (Barrett *et al.*, 2010; Nesbitt *et al.*, 2010). These features are compatible with an omnivorous or facultatively herbivorous diet (Barrett & Upchurch, 2007; Nesbitt *et al.*, 2010), indicating that strictly carnivorous sauropodomorphs are restricted to the Carnian, and that a transition to an obligatory herbivorous diet did not happen before the end of the Triassic (Barrett & Upchurch, 2007).

The time of the transition to a fully herbivorous diet in the evolutionary history of Sauropodomorpha is difficult to determine. If differentiation between a fully faunivorous and an omnivorous diet cannot rely only on tooth morphology, the same is true for that between an omnivorous and a fully herbivorous diet (Barrett & Upchurch, 2007). In addition, most non-sauropodan sauropodomorphs closely related to Sauropoda, and early sauropod taxa are known from incomplete materials, missing skulls (McPhee *et al.,* 2015), hampering inferences on their diet. In this context, a fully herbivorous diet is better associated with a fully quadrupedal stance (loss of grasping hands) and the increase in body size (enhanced absorption of nutrients during digestion), all appearing together during the Early Jurassic (Barrett & Upchurch, 2007; Sander *et al.,* 2011), with the anatomical traits related to this habit continuing to diversify along the next Mesozoic steps of sauropod evolution (see e.g. Christiansen, 2000; Upchurch & Barrett, 2000; Wilson, 2005; Sander *et al.,* 2011; Button *et al.,* 2014).

1.3. Braincase

The braincase is a complex structure formed by the ossification of several elements of the chondrocranium (Romer, 1976). Multiple cranial nerves and blood vessels pass through foramina and canals in the braincase, and it houses the inner walls of the middle ear; and its adjacent bones are often invaded by pneumatic diverticula from the middle ear air sac in archosaurs (Currie, 1997; Witmer, 1997). The position of these structures have a relatively constant distribution among all tetrapods (Romer, 1976), allowing inferences of the soft anatomy in fossil taxa based on the anatomy of extant animals (Witmer *et al.*, 2008). Hence, in many cases the information obtained from the shape, relative size, and position of each element of the braincase may

provide not only information with phylogenetic significance (Gower & Nesbitt, 2006; Rauhut, 2007; Nesbitt, 2011), but also clues about sensory abilities of extinct animals (Witmer *et al.,* 2003; Holliday & Witmer, 2004).

In recent years the use of non-destructive computed tomography (CT) scanning has allowed the visualization of the internal structures of the skull (Cunningham *et al.,* 2014). This new technology allows us not only to visualize inaccessible regions, but also to virtually reconstruct soft-tissue structures (e.g. inner ear, neurovascular canals, air sinuses), improving our understanding of paleoneurology and increasing the knowledge about brain evolution among dinosaurs or other extinct animals (e.g., Brochu, 2000, 2003; Larsson *et al.,* 2000; Larsson, 2001; Franzosa & Rowe, 2005; Sereno *et al.,* 2007; Sampson & Witmer, 2007; Witmer & Ridgely, 2008*a*, *b*, 2009; Witmer *et al.,* 2008; Lautenschlager *et al.,* 2012; Paulina-Carabajal *et al.,* 2014). This newly available information provides the empirical basis that allows inferring adaptations in the senses (e.g., vision, olfaction, hearing), or the level of neurological complexity among dinosaurs. At a broader scale, the interpretation of these attributes offers some clues about habits or lifestyle, ecological niches, and behaviour evolution of the extinct animals (Currie 1997; Evans *et al.,* 2009; Lautenschlager *et al.,* 2012).

The braincase in previous studies on sauropodomorphs

Braincase characters have been demonstrated to be important to establish the phylogenetic relationships of fossil vertebrates, such as archosaurs (Brusatte et al. 2010b; Gower, 2002; Gower & Nesbitt 2006), including Crocodylomorpha (e.g. Pol et al. 2013), or theropods (e.g. Carrano et al. 2012), and have also been incorporated in phylogenetic analyses of sauropodomorphs (Yates, 2003b, 2007). However, the

potential of this character complex for resolving non-neosauropodan sauropodomorph relationships has not been fully evaluated yet. Of the 353 characters used in the phylogenetic analysis of Yates (2007), only 12 (3.4 %) refer to the anatomy of the braincase, and a similar proportion is found in the matrix of Upchurch et al. (2007a), which uses 11 braincase characters, or 3.7 % of a total of 292 characters. Thus, this highly complex structure had less influence on the results of the phylogenetic analyses than, for instance, the morphology of a single limb-bone, the femur (19 characters in Yates [2007] and 15 characters in Upchurch et al. [2007]). One factor that might explain this scenario is that, apart from a few more detailed studies on the anatomy of the braincase (e.g. Galton, 1984, 1985; Galton & Kermack, 2010; Martinez *et al.*, 2012b; Apaldetti *et al.,* 2014), the morphology of this structure still plays a small role in morphological descriptions.

The last decade has witnessed a rapid development in the world of virtual palaeontology (Lautenschlager & Rücklin, 2014), and a series of studies analysed braincase anatomy of sauropodomorphs using the most modern techniques (e.g. Sereno *et al.,* 2007; Witmer *et al.,* 2008; Balanoff *et al.,* 2010; Knoll *et al.,* 2012; Paulina-Carabajal *et al.,* 2014). However, all of these studies were focused in sauropods. The last detailed study on the soft-tissue anatomy of a non-sauropodan sauropodomorph is the one of Galton (1985), who investigated the endocast of *Plateosaurus* still without the support of modern technologies.

1.4. Objectives of the dissertation

The aim of this study is an analysis of patterns of transformation of the braincase in sauropodomorph dinosaurs and their implications for our understanding concerning

the phylogenetic relationships and biology of these animals. The more specific goals of this thesis include the following:

- Document braincase osteology of non-sauropodan sauropodomorphs, especially *Saturnalia tupiniquim* from the Santa Maria Formation, Late Triassic of Brazil, and *Efraasia minor* from the Löwenstein Formation, Late Triassic of Germany.

- Construction of virtual endocasts for the sauropomorphs *Saturnalia tupiniquim* (Late Triassic – Carnian, c. 230 Ma), *Plateosaurus* (Late Triassic – Norian, c. 210 Ma), and a sauropod braincase tentatively referred to *Cetiosaurus oxoniensis* (Middle Jurassic, Bathonia, c. 165 Ma).

- Evaluate the utility and importance of braincase characters for phylogenetic analyses focusing on early dinosaurs and non-neosauropodan sauropodomorphs.

- Trace the morphological transformation of the braincase and its associated soft tissues from early sauropodomorphs (Late Triassic) to sauropods and evaluate the palaeobiological significance of these changes.

The study of these topics composes the next six chapters of this thesis. Each of these chapters was written to stand on its own as an independent publication. However, as all the individual chapters converge to the same main goal (patterns of braincase evolution in sauropodomorphs), some overlap in their content is unavoidable.

1.5. Overview of studies presented in Chapter 02 to Chapter 07

Chapter 02 addresses the long debated issue of the rise of dinosaurs in the early Mesozoic, particularly the transformation patterns along the initial stages in the evolution of Dinosauromoprha that shaped dinosaurs' ancestral anatomical traits and

dietary preferences (see e.g. Barrett & Rayfield, 2006; Nesbitt *et al.,* 2010; Barrett *et al.,* 2011). The study was prompted by the analysis of two new fossils, a sauropodomorph dinosaur (*Buriolestes schultzi*) and a dinosaur precursor (*Ixalerpeton polesinensis*), found together in the same outcrop of Late Triassic rocks (Carnian - Santa Maria Formation) in south Brazil. *Ixalerpeton polesinensis,* the first lagerpetid found with parts of the braincase, helps clarifying anatomical transformations of this structure in the Dinosauromorpha lineage. Additionally, *Buriolestes schultzi* shows a tooth morphology that better correlates to a strict faunivorous diet, providing strong evidence for an unexpected carnivore origin of the otherwise typically omnivorous/herbivorous sauropodomorph dinosaurs. The implications of these new findings are also discussed in more detail in chapters 03 and 04.

Chapter 03 addresses the intensely debated topics of the feeding behaviour of the earliest dinosaurs and the evolution of herbivory in Sauropodomorpha. It has previously been proposed that the reduction of the skull, a well-known trait of sauropodomorph dinosaurs, was the first step in the evolution of the peculiar body plan and herbivorous lifestyle of the later sauropods. However, the evolutionary significance of this remarkable anatomical modification of early sauropodomorphs has remained obscure. Using the technological support of Computed Tomography Scans, a virtual endocast was reconstructed for one of the oldest dinosaurs known, the sauropodomorph *Saturnalia tupiniquim* from the Late Triassic (c. 230 Ma) of Brazil. The results were unexpected: the brain anatomy *of Saturnalia tupiniquim* deviates from that of later sauropodomorphs. The animal has a well-developed flocculus, which is a feature observed in predatory animals, and so far unknown among sauropodomorph dinosaurs. This data was then analysed by combining skeletal anatomy and phylogenetic information. Based on that neurological information, it is

argued that an important adaptation for the herbivory in sauropodomorphs was related to predation, highlighting a process of exaptation in the evolution of herbivory in the group.

Regarding non-avian dinosaurs, braincase anatomy of non-sauropodan sauropodomorphs is still poorly explored in comparison to members of Sauropoda and Theropoda. The descriptions of the braincase anatomy of *Saturnalia tupiniquim* (Chapter 04) and *Efraasia minor* (Chapter 05) intend to provide new information regarding the knowledge of this structure in non-sauropodan sauropodomorphs.

Given its age and phylogenetic position, *Saturnalia tupiniquim* is a key taxon in order to trace the evolution of braincase anatomy in sauropodomorphs and dinosaurs as a whole. The postcranial anatomy of this taxon has been thoroughly investigated (Langer, 2003; Langer *et al.,* 2007), but its braincase has never been studied in details. Using computed tomography it was possible to access the complete braincase osteology of *Saturnalia* for the first time. Besides the osteological descriptions, a discussion regarding phylogenetic characters used to investigate the relationships of early dinosaurs and sauropodomorphs (in less detail for the latter, but see Chapter 05) is also provided in Chapter 04. This investigation showed that features once thought to be absent in dinosaurs are in fact widespread among different lineages.

Efraasia minor is a non-sauropodan sauropodomorph from the Late Triassic (Norian) Löwenstein Formation of Germany. A description of the braincase of *Efraasia* was first provided by Galton & Bakker (1985), but this structure is redescribed here in detail, adding new information based on CT-Scan data. Furthermore, an extensive discussion on phylogenetic characters related to braincase anatomy used in previous works focusing on non-neosauropodan sauropodomorphs is

also provided in Chapter 05. A series of problems in character construction was recognised in previous data matrices. These problematic characters were modified, and new characters were proposed. The results of the phylogenetic analysis using the new dataset indicate that a great number of features are exclusive of sauropods, pointing to a drastic morphological transformation in the early evolution of these taxa. This issue is more substantially analysed in Chapter 06.

The study in Chapter 06 is prompted by the re-analysis of a sauropod braincase from the Middle Jurassic (Bathonian – Oxfordshire Formation) of England, tentatively assigned to *Cetiosaurus*. This braincase was previously described by Galton & Knoll (2006), but the first virtual endocast for this specimen is now provided. Discrete character-taxon matrices analyses investigated morphospace occupation and rates of evolution of the braincase anatomy. The drastic transformation first detected in the analysis of chapter 05 is numerically demonstrated by the analysis of morphospace occupation, which shows that sauropod braincases occupy a different region of the morphospace in relation to non-sauropodan taxa. Additionally, the transformations in the braincase are understood as part of the anatomical transformations that allowed sauropods to reach sizes greater than non-sauropodan sauropodomorphs, which likely resulted in the differential survival of the lineages in the Early Jurassic.

Chapter 07 deals with the questionable use of the terms 'basal' and 'transitional', widely adopted in cladistic studies dealing with fossil taxa. In order to advocate this point of view, it brings an introductory example of sauropodomorph dinosaurs. This group was selected since the long-term interest in its evolutionary history places it as good example to illustrate the scenario of the current use of both terms. It is demonstrated that 'basal' and 'transitional' are often applied

inconsistently, and with inadequate justification. Moreover, it also has a problematic impact in the way scientific content is transmitted to a non-scientific audience by bringing an idea of an apparent direction to the evolutionary process. As a consequence, some journals in the Biological field (Kreel & Cranston, 2004 – Systematic Entomology; Zachos, 2016 – Mammalian Biology) have even suggested authors to avoid the use of 'basal', although it remains frequent in palaeontology, likely due to the lack of a discussion concerning fossil taxa. The core idea of this chapter is to show that cladograms are not evolutionary ladders. In this sense, despite probably representing the most iconic and well-known taxa within Sauropodomorpha, sauropods are not the final evolutionary product of this lineage. Accordingly, contrary to what is stated in a variety of previous studies on the evolution of Sauropodomorpha, the non-sauropodan sauropodomorph (or "prosauropod") taxa do not represent transitional forms between the hypothetical ancestor of Sauropodomorpha and Sauropoda. Nevertheless, tracing anatomical transformation in non-sauropodan lineages is crucial to understand the early evolution of the gigantic sauropods as demonstrated in other chapters of this thesis.

1.6. References

Apaldetti C, Martinez RN, Alcober OA, Pol D. 2011. A New Basal Sauropodomorph (Dinosauria: Saurischia) from Quebrada del Barro Formation (Marayes-El Carrizal Basin), Northwestern Argentina. *PLoS ONE* 6 (11), e26964.

Apaldetti C, Martinez RN, Pol D, Souter T. 2014. Redescription of the skull of *Coloradisaurus brevis* (Dinosauria, Sauropodomorpha) from the Late Triassic Los Colorados Formation of the Ischigualasto-Villa Union Basin, Northwestern Argentina. *Journal of Vertebrate Paleontology,* 34(5), 1113–1132.

Balanoff AM, Bever GS, Ikejiri T. 2010. The braincase of *Apatosaurus* (Dinosauria: Sauropoda) based on computed tomography of a new specimen with comments on

variation and evolution in Sauropod Neuroanatomy. *American Museum Novitates* 3677, 1–29.

Barrett PM. 2000. Prosauropods and iguanas: speculation on the diets of extinct reptiles, In: (ed. H.-D. Sues) *Evolution of Herbivory in Terrestrial Vertebrates: Perspectives from the Fossil Record*. Cambridge University Press, Cambridge , pp. 42–78 .

Barrett PM, Upchurch P. 2005. Sauropodomorph diversity through time, In: (eds. KC Rogers, JA Wilson) *The Sauropods; evolution and paleobiology*. University of California Press, Berkeley. pp. 126-156.

Barrett PM, Rayfield EJ. 2006. Ecological and evolutionary implications of dinosaur feeding behaviour. *Trends in Ecology and Evolution*, 21**,** 217–224.

Barrett PM, Upchurch P. 2007. The evolution of feeding mechanisms in early sauropodomorph dinosaurs. *Special Papers in Palaeontology*, 77, 91–112.

Barrett PM, Butler RJ, Nesbitt SJ. 2010. The roles of herbivory and omnivory in early dinosaur evolution. *Earth and environmental transactions of the Royal Society of Edinburgh*, 101, 383–396.

Bates KT, Mannion PD, Falkingham PL, Brusatte SL, Hutchinson JR, Otero A, Sellers WI, Sullivan C, Stevens KA, Allen V. 2016. Temporal and phylogenetic evolution of the sauropod dinosaur body plan. *Royal Society Open Science*, 3, 160636.

Benton MJ. 1986. The late Triassic reptile Teratosaurus - a rauisuchian, not a dinosaur. *Palaeontology*, 29, 293-301.

Benton MJ, Clark JM. 1988. Archosaur phylogeny and the relationships of the Crocodylia. In (ed: MJ Benton) *The phylogeny and classification of the tetrapods. Vol. 1. Amphibians and Reptiles*. Clarendon Press, Oxford. pp. 295-338.

Benton MJ, Juul L, Storrs GW, Galton PM. 2000. Anatomy and systematics of the prosauropod dinosaur Thecodontosaurus antiquus from the Late Triassic of Southwest England. *Journal of Vertebrate Paleontology*, 20, 77–108.

Benton MJ, Forth J, Langer MC. 2014. Models for the rise of the dinosaurs. *Current Biology*, 24(2), R87-R95.

Bittencourt JS, Arcucci AB, Marsicano CA, Langer MC. 2014. Osteology of the Middle Triassic archosaur Lewisuchus admixtus Romer (Chañares Formation, Argentina), its inclusivity, and relationships amongst early dinosauromorphs. *Journal of Systematic Palaeontology*, 13(3), 189–219.

Bonnan MF, Senter, P. 2007. Were the basal sauropodomorph dinosaurs *Plateosaurus* and *Massospondylus* habitual quadrupeds? *Special Papers* in *Palaeontology*, 77. 139-155.

Bonnan MF, Yates AM. 2007. A new description of the forelimb of the basal sauropodomorph *Melanorosaurus*: implications for the evolution of pronation, manus shape and quadrupedalism in sauropod. *Special Papers in Palaeontology*, 77, 157-168.

Brochu CA. 2000. A digitally-rendered endocast for *Tyrannosaurus rex*. *Journal of Vertebrate Paleontology*, 20, 1-6

Brochu CA. 2003. Osteology of *Tyrannosaurus rex*: Insights from a Nearly Complete skeleton and High-Resolution Computed Tomographic Analysis of the skull. Journal of Vertebrate Paleontology, 22(Suppl. 4, Memoir 7).

Brusatte SL, Nesbitt SJ, Irmis RB, Butler RJ, Benton MJ, Norell MA. 2010a. The origin and early radiation of dinosaurs. *Earth-Science Reviews,* 101, 68–100.

Brusatte SL, Benton MJ, Desojo JB, Langer MC. 2010b. The higher-level phylogeny of Archosauria (Tetrapoda: Diapsida). *Journal of Systematic Palaeontology,* 8(1), 3-47.

Brusatte SL, Benton MJ, Lloyd GT, Ruta M, Wang SC. 2011. Macroevolutionary patterns in the evolutionary radiation of archosaurs. *Earth and Enviromental transactions of the Royal Society of Edinburgh,* 101, 367-382.

Button DJ, Rayfield EJ, Barrett PM. 2014. Cranial biomechanics underpins high sauropod diversificaty in resource-poor environments. *Proceedings of the Royal Society B,* 281, 20142114.

Cabreira SF, Kellner AWA, Dias-da-Silva S, Silva LR, Bronzati M, Marsola JCA, Müller RT, Bittencourt JS, Batista BJ, Raugust T, Carrilho R, Brodt A, Langer MC. 2016. A unique Late Triassic dinosauromorph assemblage reveals dinosaur ancestral anatomy and diet. *Current Biology,* 26(22), 3090-3095.

Carrano MT, Benson RBJ, Sampson SD. 2012. The phylogeny of Tetanurae (Dinosauria:Theropoda). *Journal of Systematic Paleontology,* 10(2), 211-230.

Charig AJ, Attridge J, Crompton W. 1965. On the origin of the sauropods and the classification of the Saurischia. *Proceedings of the Linnean Society of London.* 176, 197-221.

Christiansen P. 2000. Feeding mechanisms of the sauropod dinosaurs *Brachiosaurus, Camarasaurus, Diplodocus* and *Dicraeosaurus*. *Historical Biology,* 14, 137-152.

Colbert EH. 1964. Relationship of saurischian dinosaurs. *American Museum Novitates.* 2181, 1-24.

Cunningham JA, Rahman IA, Lautenschlager S, Rayfield EJ, Donoghue PCJ. 2014. A virtual world of paleontology. *Trends in Ecology and Evolution,* 29(6), 347-357.

Currie PJ. 1997. Braincase anatomy. In: (eds. PJ Currie, K Padian) *Encyclopedia of Dinosaurs*. Academic Press, pp. 81-83.

Evans DC, Ridgely R, Witmer LM. 2009 Endocranial anatomy of lambeosaurine hadrosaurids (Dinosauria: Ornithischia): a sensorineural perspective on cranial crest function. *Anatomical Record,* 292, 1315–1337.

Ezcurra MD. 2010. A new early dinosaur (Saurischia: Sauropodomorpha) from the Late Triassic of Argentina: a reassessment of dinosaur origin and phylogeny. *Journal of Systematic Palaeontology,* 8(3), 371-425.

Ezcurra MD. 2016. The phylogenetic relationships of basal archosauromorphs, with an emphasis on the systematics of proterosuchian archosauriforms. *PeerJ,* 4, e1778.

Fechner R. 2009. Morphofunctional evolution of the pelvic girdle and hindlimb of Dinosauromorpha on the lineage to Sauropoda. Unpublished PhD thesis. Munich: Ludwig-Maximilians-University. 211 pp.

Franzosa J, Rowe T. 2005. Cranial endocast of the Cretaceous theropod dinosaur *Acrocanthosaurus atokensis*. *Journal of Vertebrate Paleontology,* 25(4), 859-864.

Galton PM. 1984. Cranial anatomy of the prosauropod dinosaur *Plateosaurus* from the Knollenmergel (Middle Keuper, Upper Triassic) of Germany. I. Two complete skulls from Trossingen/Württ, with comments on the diet. *Geologica et Palaeontologica,* 18, 139–171.

Galton PM. 1985. Cranial anatomy of the prosauropod dinosaur *Plateosaurus* from the Knollenmergel (Middle Keuper, Upper Triassic) of Germany. II. All the cranial material and details of soft-part anatomy. *Geologica et Palaeontologica,* 19, 119-159.

Galton PM. 1986. Prosauropod dinosaur *Plateosaurus* (=*Gresslyosaurus*) (Saurischia: Sauropodomorpha) from the Upper Triassic of Switzerland. *Geologica et Palaeontologica,* 20, 167–183.

Galton PM. 1990. Basal sauropodomorpha - Prosauropods. In: (eds. DB Weishampel, P Dodson, H Osmólska) *The Dinosauria*. University of California Press, Berkley. pp. 320–344.

Galton PM, Bakker RT. 1985. The cranial anatomy of the prosauropod dinosaur "*Efraasia diagnostica*", a juvenile individual of *Sellosaurus gracilis* from the Upper Triassic of Nordwürttemberg, West Germany. *Stuttgarter Beiträge zur Naturkunde B,* 117, 1–15

Galton PM, Knoll F. 2006. A saurischian dinosaur braincase from the Middle Jurassic (Bathonian) near Oxford, England: from the theropod *Megalosaurus* or the sauropod *Cetiosaurus*? *Geological Magazine,* 143, 905–921.

Galton PM, Upchurch P. 2004. Prosauropoda. In: (eds. DB Weishampel, P Dodson, H Osmólska) *The Dinosauria, second edition*. University of California Press, Berkley. pp. 232–258.

Galton PM, Kermack D. 2010. The anatomy of *Pantydraco caducus*, a very basal sauropodomorph dinosaur trom the Rhaetian (Upper Triassic) of South Wales, UK. *Revue de Paléobiologie,* 29(2), 341-404.

Gauthier J. 1986. Saurischian monophyly and the origin of birds. *Memoirs of the California Academy of Sciences.* 8, 1-55.

Gauthier J, Padian K. 1985. Phylogenetic, functional, and aerodynamic analyses of the origin of birds and their flight. In: (eds. JHOMK Hecht, G Viohl, P Wellnhofer), *The Beginning of Birds*, Freunde des Jura Museums, Eichstatt, pp. 185–197.

Gower DJ. 2002. Braincase evolution in suchian archosaurs (Reptilia: Diapsida): evidence from the rauisuchian *Batrachotomus kupferzellensis*. *Zoological Journal of the Linnean Society,* 136, 49–76.

Gower DJ, Nesbitt SJ. 2006. The braincase of *Arizonasaurus babbitti:* Further evidence for the non-monophyly of 'rauisuchian' Archosaurs. *Journal of Vertebrate Paleontology,* 26 (1), 79-87.

Holliday CM, Witmer LC. 2004. Anatomical domains within the heads of archosaurs and their relevance for functional interpretation. *Journal of Vertebrate Paleontology,* 24 (suppl 3), 71.

Hopson JA. 1979. Paleoneurology. In: (eds. C. Gans, RG Northcutt, P Ulinski). *Biology of the Reptilia.* Academic Press, New York, pp 39-146

Hopson JA. 1980. Relative brain size in dinosaurs: implications for dinosaurian endothermy. In: (eds: RDK Thomas, EC Olson) *A cold look at the warm blooded dinosaurs.* American Association for the Advancement of Science, Washington, DC, pp. 287-210

Huene F von.1926. Vollstandige Osteologie eines Plateosauriden ausdem Schwabischen Trias. *Geologie und Paläontologie Abhandlungen*, 15, 129–179

Huene F von. 1932. Die fossile Reptil-Ordnung Saurischia, ihre Entwicklung und Geschichte. *Monographien zur Geologie und Paläontologie,* 4, 1–361.

Janensch W. 1935-36. Die Schädel der Sauropoden *Brachiosaurus*, *Barosaurus* und *Dicraeosaurus* aus den Tendaguru-Schichten Deutsch-Ostafrikas. *Palaeontographica, Supplement* 7, 1(2),147-298.

Kammerer CF, Nesbitt SJ, Shubin NH. 2012. The First Silesaurid Dinosauriform from the Late Triassic of Morocco. *Acta Palaeontologica Polonica,* 57 (2), 277-284.

Knoll F, Witmer LM, Ortega F, Ridgely RC, Schwarz-Wings D. 2012. The braincase of the basal Sauropod dinosaur *Spinophorosaurus* and 3D reconstructions of the cranial endocast and inner ear. *Plos One* 7(1), e30060.

Krell FT, Cranston PS. 2004. Which side of the tree is more basal? *Systematic Entomology,* 29, 279-281.

Langer MC. 2001. Linnaeus and the PhyloCode: where are the differences? *Taxon,* 50(4), 1091-1096.

Langer MC. 2003. The pelvic and hindlimb anatomy of the stem-sauropodomorph *Saturnalia tupiniquim* (Late Triassic, Brazil). *Paleobios,* 23, 1-40.

Langer MC. 2014. The origins of Dinosauria: Much ado about nothing. *Palaeontology*, 57, 469-478

Langer MC, Benton MJ. 2006. Early dinosaurs: a phylogenetic study. *Journal of Systematic Palaeontology,* 4(4), 309-358.

Langer MC, Ferigolo J. 2013. The Late Triassic dinosauromorph *Sacisaurus agudoensis* (Caturrita Formation; Rio Grande do Sul, Brazil): anatomy and affinities. *Geological Society Special Publication,* 379, 353-392.

Langer MC, Abdala F, Richter M, Benton MJ. 1999. A sauropodomorph dinosaur from the Upper Triassic (Carnian) of southern Brazil. *Earth & Planetary Sciences* 329, 511–517.

Langer MC, França MAG, Gabriel S. 2007. The pectoral girdle and forelimb anatomy of the stem-sauropodomorph *Saturnalia tupiniquim* (Upper Triassic, Brazil). *Special Papers in Palaeontology.* 77, 113-137.

Langer MC, Ezcurra MD, Bittencourt JS, Novas FE. 2010. The origin and early evolution of dinosaurs. *Biological Reviews,* 85, 55-110.

Larsson HEC. 2001. Endocranial anatomy of *Carcharodontosaurus saharicus* (Theropoda, Allosauroidea) and its implications for theropod brain evolution. In: (eds. D Tanke, K Carpenter) *Mesozoic Vertebrate Life*. Indiana University Press, pp: 19-33.

Larsson HCE, Sereno PC, Wilson JA. 2000. Forebrain enlargement among nonavian theropod dinosaurs. *Journal of Vertebrate Paleontology,* 20(3), 615-618.

Lautenschlager S, Rayfield EJ, Altangerel P, Zanno LE, Witmer LM. 2012. The Endocranial Anatomy of Therizinosauria and Its Implications for Sensory and Cognitive Function. *PLoS ONE,* 7(12), e52289.

Lautenschlager S, Rücklin M. 2014. Beyond the print – Virtual paleontology in Science publishing, outreach, and education. *Journal of Paleontology,* 88(4), 727-734.

Marsh OC. 1878. Principal characters of American Jurassic dinosaurs. Part I. *American Journal of Science and Arts,* 16, 411–416.

Marsicano CA, Irmis RB, Mancuso AC, Mundin R, Chemale F. 2016. The precise temporal calibration of dinosaurs. *PNAS,* 113, 509-513.

Martinez RN. 2009. *Adeopapposaurus mognai*, gen. et sp. nov. (Dinosauria: Sauropodomorpha), with comments on adaptations of basal Sauropodomorpha. *Journal of Vertebrate Paleontology,* 29, 142–164.

Martinez RN, Alcober OA. 2009. A Basal Sauropodomorph (Dinosauria: Saurischia) from the Ischigualasto Formation (Triassic, Carnian) and the Early Evolution of Sauropodomorpha. *PLoS ONE,* 4(2), e4397.

Martinez RN, Sereno PC, Alcober OA, Colombi CE, Renne PR, Montanez IP, Currie BS. 2011. A basal dinosaur from the Dawn of the Dinosaur Era in Southwestern Pangaea. *Science,* 331, 206-210.

Martinez RN, Apaldetti C, Pol D. 2012a. Basal Sauropodomorphs from the Ischigualasto Formation. *Journal of Vertebrate Paleontology,* 32(suppl. 6), 51–69.

Martinez RN, Haro JA, Apaldetti C. 2012b. Braincase of *Panphagia protos* (Dinosauria, Sauropodomorpha). *Journal of Vertebrate Paleontology,* 32(suppl. 1): 70–82.

Martínez RN, Apaldetti C, Correa GA, Abelín D. 2016. A Norian lagerpetid dinosauromorph from the Quebrada del Barro Formation, northwestern Argentina. *Ameghiniana,* 53 (1), 1–13.

McPhee BW, Yates AM, Choiniere JN, Abdala F. 2014. The complete anatomy and phylogenetic relationships of *Antetonitrus longiceps* (Sauropodiformes, Dinosauria): implications for the origins of Sauropoda. *Zoological Journal of the Linnean Society,* 171, 151–205.

McPhee BW, Bonnan MF, Yates AM, Neveling J, Choiniere JN. 2015. A new basal sauropod from the pre-Toarcian Jurassic of South Africa: evidence of niche-partitioning at the sauropodomorph-sauropod boundary? *Scientific Reports,* 5, 13224.

Nesbitt SJ. 2011. The early evolution of archosaurs: relationships and the origin of the major clades. *Bulletin of the American Museum of Natural History,* 352, 1–292.

Nesbitt SJ, Smith ND, Irmis RB, Turner AH, Downs A, Norell MA. 2009. A complete skeleton of a Late Triassic saurischian and the early evolution of dinosaurs. *Science,* 326, 1530-1533.

Nesbitt SJ, Sidor CA, Irmis RB, Angielczyk KD, Smith RMH, Tsuji, LA. 2010. Ecologically distinct dinosaurian sister groups shows early diversification of Ornithodira. *Nature,* 464(4), 95-98.

Otero A, Salgado L. 2015. El registro de Sauropodomorpha (Dinosauria) de la Argentina. In: (eds. M. Fernández, Y Herrera) *Reptiles Extintos - Volumen en Homenaje a Zulma Gasparini. Publicación Electrónica de la Asociación Paleontológica Argentina,* 15(1): 69–89.

Otero A, Krupandan E, Pol D, Chinsamy A, Choiniere J. 2015. A new basal sauropodiform from South Africa and the phylogenetic relationships of basal sauropodomorphs. *Zoological Journal of the Linnean Society,* 174, 589–634.

Parrish JM. 2005. The origins of high browsing and the effects of phylogeny and scaling on neck length in sauropodomorphs. In: (eds. MT Carrano, TJ Gaudin, RW Blob, JR Wible). *Amniote paleobiology: perspectives on the evolution of mammals, birds, and reptiles.* University of Chicago Press, Chigaco, pp 201-223.

Paulina Carabajal A, Salgado L. 2007. Un basicráneo de titanosaurio (Dinosauria, Sauropoda) del Cretácico Superior del norte de Patagonia: descripción y aportes al conocimiento del oído interno de los dinosaurios. *Ameghiniana,* 44,109-120.

Paulina-Carabajal A, Carballido JL, Currie PJ. 2014. Braincase, neuroanatomy, and neck posture of *Amargasaurus cazaui* (Sauropoda, Dicraeosauridae) and its implications for understanding head posture in sauropods. *Journal of Vertebrate Palaeontology,* 34(4), 870–882.

Peyre de Fabrègues C, Allain R, Barriel V. 2015. Root causes of phylogenetic incongruence observed within basal sauropodomorph interrelationships. *Zoological Journal of the Linnean Society,* 175(3), 569-586.

Pol D, Garrido A, Cerda IA. 2011. A new sauropodomorh dinosaur from the Early Jurassic of Patagonia and the origin and evolution of the Sauropod-type sacrum. *Plos ONE,* 6(1), e14572

Pol D, Rauhut OWM, Lecuona A, Leardi JM, Xu X. Clark JM. 2013. A new fossil from the Jurassic of Patagonia reveals the early basicranial evolution and the origins of Crocodyliformes. *Biological Reviews,* 88, 862-872.

de Queiroz K, Gauthier J. 1990. Phylogeny as a central principle in taxonomy: phylogenetic definitions of taxon names. *Systematic Zoology,* 39, 307–322.

de Queiroz K, Gauthier J. 1992. Phylogenetic taxonomy. *Annual Review of Ecology and Systematics,* 23, 449–480.

de Queiroz K, Gauthier J. 1994. Toward a phylogenetic system of biological nomenclature. *Trends in Ecology and Evolution,* 9, 27–31.

Rauhut OWM. 2007. The myth of the conservative character: braincase characters in theropod phylogenies. *Hallesches Jahrbuch für Geowissenschaften, Beiheft,* 23, 51-54.

Rauhut OWM, Fechner R, Remes K, Moser K. 2011. How to get big in the Mesozoic: the evolution of the sauropodomorph body plan. In: (eds. N Klein, K Remes, CT Gee, PM Sander). *Biology of the sauropod dinosaurs: Understanding the life of giants*. Indiana University Press Bloomington, pp. 119-149.

Remes K. 2008. Evolution of the pectoral girdle and forelimb in Sauropodomorpha (Dinosauria, Saurischia): osteology, myology and function. Unpublished PhD thesis. Munich: Ludwig-Maximilians-University. 355 pp.

Romer AS. 1976. Osteology of the reptiles. The University of Chicago press, 772 pp.

Salgado L, Calvo JO. 1992. Cranial osteology of *Amargasaurus cazaui* Salgado and Bonaparte (Sauropoda, Dicraeosauridae) from the Neocomian of Patagonia. *Ameghiniana*, 29, 337-346.

Salgado L, Coria RA, Calvo JO. 1997. Evolution of titanosaurid sauropods. I. Phylogenetic analysis based on the postcranial evidence. *Ameghiniana*, 34, 3–32.

Sampson SD., Witmer LM. 2007 Craniofacial anatomy of *Majungasaurus crenatissimus* (Theropoda: Abelisauridae) from the Late Cretaceous of Madagascar. *Journal of Vertebrate Paleontology*, Memoir 8 (Suppl 2): 32-102.

Sander, P.M. et al., 2011. Biology of the sauropod dinosaurs: the evolution of gigantism. *Biological Reviews*, 86: 117-155.

Sereno PC. 1989. Prosauropod monophyly and basal sauropodomorph phylogeny. *Journal of Vertebrate Palaeontology*, 9(suppl. 3): 38A.

Sereno PC. 1998. A rationale for phylogenetic definitions, with application to the higher level taxonomy of Dinosauria. *Neues Jahrbuch für Geologie und Paläontologie Abhandlungen*, 210, 41-83.

Sereno PC. 2007. Basal Sauropodomorpha: Historical and recent phylogenetic hypotheses, with comments on *Ammosaurus major* (Marsh, 1889). *Special Papers in Palaeontology*, 77. 261–289.

Sereno PC, Forster CA, Rogers RR, Moneta AM. 1993. Primitive dinosaur skeleton from Argentina and the early evolution of the Dinosauria. *Nature*, 361,64-66.

Sereno PC, Wilson JA, Witmer LM, Whitlock JA, Maga A, Ide O, Rowe TA. 2007. Structural Extremes in a Cretaceous Dinosaur. *PLoS ONE*, 2(11), e1230.

Sereno PC, Martinez RN, Alcober OA. 2012. Osteology of *Eoraptor lunensis* (Dinosauria, Sauropodomorpha). *Journal of Vertebrate Paleontology*, 32(suppl. 6), 83–179.

Upchurch P, Barrett PM. 2000. The evolution of sauropod feeding mechanisms. In: (ed. HD Sues). *Evolution of herbivory in terrestrial vertebrates: perspectives from the fossil record*. Cambridge University Press, Cambridge, pp. 79-122.

Upchurch P, Barrett PM, Galton PM. 2007. A phylogenetic analysis of basal sauropodomorph relationships: implications for the origin of sauropod dinosaurs. *Special Papers in Palaeontology*, 77, 57–90.

Wilson JA. 1999. A nomenclature for vertebral laminae in sauropods and other saurischian dinosaurs. *Journal of Vertebrate Paleontology*, 19, 639-653.

Wilson JA. 2005. Overview of sauropod phylogeny and evolution. In: (eds. KC Rogers, JA Wilson) *The Sauropods: Evolution and Paleobiology*, University of California Press, Berkeley, pp. 15–49

Witmer LM. 1997. Craniofacial air sinus systems. In (eds. PJ Currie, K Padian) *Encyclopedia of dinosaurs*. Academic Press, San Diego, California, pp. 151–159.

Witmer LM. Ridgely RC. 2008. Structure of the brain cavity and inner ear of the centrosaurine ceratopsid *Pachyrhinosaurus* based on CT scanning and 3D visualization. In (ed. PJ Currie) *A New Horned Dinosaur from an Upper Cretaceous Bone Bed in Alberta*. National Research Council Research Press, Ottawa, pp. 117-144.

Witmer LM, Ridgely RC. 2008b. The paranasal air sinuses of predatory and armored dinosaurs (Archosauria: Theropoda and Ankylosauria) and their contribution to cephalic architecture. *Anatomical Record,* 291, 1362–1388.

Witmer LM, Ridgely RC. 2009. New insights into brain, braincase, and ear region of tyrannosaurs (Dinosauria, Theropoda), with implications for sensory organisation and behavior. *The Anatomical Record,* 292, 1266-1296.

Witmer LM, Chaterjee S, Franzosa J, Rowe T. 2003. Neuroanatomy of flying reptiles and implications for flight, posture and behaviour. *Nature,* 425, 950–953.

Witmer LM, Ridgely RC, Dufeau DL, Semones MC. 2008. Using CT to peer into the past: 3D visualization of the brain and ear regions of birds, crocodiles, and nonavian dinosaurs. In: (eds. H Endo, R Frey) *Anatomical imaging: towards a new morphology*. Springer-Verlag, Tokyo, pp. 67–87.

Yates AM. 2003a. The species taxonomy of the sauropodomorph dinosaurs from the Löwenstein Formation (Norian, Late Triassic) of Germany, *Palaeontology,* 46(2), 317-337.

Yates AM. 2003b. *Anchisaurus polyzelus* (Hitchcock): The smallest known sauropod dinosaurs and the evolution of gigantism among sauropodomorph dinosaurs. *Postilla,* 230, 1-58.

Yates AM. 2007. The first complete skull of the Triassic dinosaur M*elanorosaurus* Haughton (Sauropodomorpha: Anchisauria). *Special Papers in Palaeontology* 77, 9–55.

Yates AM, Kitching JW. 2003. The earliest known sauropod dinosaur and the first steps towards sauropod locomotion. *Proceedings of the Royal Society of London B* 270, 1753–1758.

Yates AM, Bonnan MF, Nevelling J, Chinsamy A, Blackbeard MG. 2010. A new transitional sauropodomorph dinosaur from the Early Jurassic of South Africa and the evolution of sauropod feeding and quadrupedalism. *Proceedings of the Royal Society of London B,* 277, 787–794.

Zachos FE. 2016. Tree thinking and species delimination: Guidelines for taxonomy and phylogenetic terminology. *Mammalian Biology,* 81, 185-188.

CHAPTER 2

A unique Late Triassic dinosauromorph assemblage reveals dinosaur ancestral anatomy and diet

Chapter published as: Cabreira SF, Kellner AWA, Dias-da-Silva S, Silva LR, Bronzati M, Marsola JCA, Müller RT, Bittencourt JS, Batista BJ, Raugust T, Carrilho R, Brodt A, Langer MC. 2016. A unique Late Triassic dinosauromorph assemblage reveals dinosaur ancestral anatomy and diet. *Current Biology,* 26(22), 3090-3095.

Author contributions:

Conceptualization, Supervision, and Project Administration, M.C.L., A.W.A.K. and S.F.C.; Methodology, Validation and Formal Analysis, M.C.L., J.S.B., **M.B**., J.C.A.M. and R.T.M.; Investigation, M.C.L., S.F.C., J.S.B., **M.B.**, J.C.A.M. and R.T.M.; Resources and Funding Acquisition M.C.L. and S.F.C.; Data Curation, S.F.C., L.R.S. and B.J.B.; Writing – Original Draft, M.C.L., A.W.A.K., **M.B.**, J.C.A.M. and R.T.M.; Writing – Review and Editing, S.D.S., T.R., R.C. and A.B; Visualization, M.C.L., S.F.C., **M.B.** and J.C.A.M.

*All figures of Chapter 2 are modified after Cabreira *et al*. (2016)

CHAPTER 2

A unique Late Triassic dinosauromorph assemblage reveals dinosaur ancestral anatomy and diet

Sergio F. Cabreira,[1] Alexander W. A. Kellner, [2] Sérgio Dias-da-Silva,[3] Lúcio R. da Silva,[1,3] **Mario Bronzati,[4]** Júlio C. de A. Marsola,[5,6] Rodrigo T. Müller,[3] Jonathas S. Bittencourt,[7] Brunna J. Batista,[1] Tiago Raugust,[8] Rodrigo Carrilho,[9] André Brodt,[9] and Max C. Langer[5,*]

[1] Museu de Ciências Naturais; Universidade Luterana do Brasil; Canoas-RS 92425-900; Brazil.; [2] Departamento de Geologia e Paleontologia; Museu Nacional-UFRJ; Rio de Janeiro-RJ 20940-040; Brazil.; [3] Centro de Apoio à Pesquisa Paleontológica, Universidade Federal de Santa Maria, Santa Maria-RS, 97105-900, Brazil.; [4] Ludwig–Maximilians–Universität & Bayerische Staatssammlung für Paläontologie und Geologie; Munich 80333; Germany.; [5] Laboratório de Paleontologia, FFCLRP; Universidade de São Paulo; Ribeirão Preto-SP 14040-901; Brazil.; [6] School of Geography, Earth and Environmental Sciences; University of Birmingham; Birmingham B15 2TT; United Kingdom.; [7] Departamento de Geologia; Universidade Federal de Minas Gerais; Belo Horizonte-MG, 31270-901; Brazil.; [8] Instituto de Geociências; Universidade Federal do Rio Grande do Sul; Porto Alegre-RS 91540-000; Brazil.; [9] Centro Universitário La Salle; Canoas-RS 92010-000; Brazil.

2.1. ABSTRACT

Dinosauromorpha includes dinosaurs and other much less diverse dinosaur precursors of Triassic age, such as lagerpetids (Langer *et al.*, 2013). Joint occurrences of these taxa with dinosaurs are rare, but more common during the latest part of that period (Norian-Rhaetian, 228-201 Myr ago) (Irmis *et al.*, 2007; Niedzwiedzki *et al.*, 2014). In contrast, the new lagerpetid and saurischian dinosaur described here were unearthed from one of the oldest rock units with dinosaur fossils worldwide, the Carnian (237-228 Myr ago) Santa Maria Formation of south Brazil (Da Rosa, 2014), a record only matched in age by much more fragmentary remains from Argentina (Martinez *et al.*, 2013). This is the first time nearly complete dinosaur and non-dinosaur dinosauromorph remains are found together in the same excavation, clearly showing that these animals were contemporaries since the first stages of dinosaur evolution. The new lagerpetid preserves the first skull, scapular and forelimb elements, plus associated vertebrae, known for the group, revealing how dinosaurs acquired several of their typical anatomical traits. Besides, a novel phylogenetic analysis shows the new dinosaur as the most basal Sauropodomorpha. Its plesiomorphic teeth, strictly adapted to faunivory, provides crucial data to infer the feeding behaviour of the first dinosaurs.

2.2. RESULTS

Here we report one of the oldest (and the best preserved) association of dinosaur and dinosaur precursor, respectively represented by new species of Lagerpetidae and Sauropodomorpha. These provide unequivocal evidence that those animals shared the same landscapes during Late Triassic times, also suggesting that faunivory was the ancestral diet of dinosaurs. There is evidence of four individuals in the association,

two lagerpetids and two dinosaurs. The lagerpetids are represented by a semi-articulated skeleton and a pair of fragmentary femora. As for the dinosaurs, a large articulated individual was preserved, together with smaller and non-duplicated bone elements that indicate the presence of another individual (either a juvenile or a smaller taxon). The two articulated specimens correspond to the type-specimens of the new taxa proposed below.

Systematic Paleontology

Locality, stratigraphy, and age

The specimens were collected side by side at the Buriol ravine (29°39'30.78''S; 53°26'08.97''W), São João do Polêsine-RS, Brazil; Alemoa Member, Santa Maria Formation; Candelária Sequence, Paraná Basin (Horn *et al.*, 2014); *Hyperodapedon* Assemblage Zone, Carnian, Late Triassic (Langer *et al.*, 2007).

Archosauria Cope, 1869 (Gauthier, 1986)

Dinosauromorpha Benton, 1985 (Sereno, 1991)

Lagerpetidae Arcucci, 1986 (Nesbitt *et al.,* 2009)

Ixalerpeton polesinensis gen. et sp. nov.

Holotype. ULBRA-PVT059. Partially articulated skeleton including skull roof, braincase, 23 presacral, two sacral, and nine tail vertebrae, right scapula, left humerus, paired pelvic girdle, femur, tibia, and fibula (Figures 2.1A-2.1H).

Etymology. The genus name combines the Greek words ιξαλος (=leaping) and ἑρπετόν (=reptile). The specific epithet refers to São João do Polêsine, town where the specimens were found.

Diagnosis. *Ixalerpeton polesinensis* differs from other Lagerpetidae by a unique suite of traits (autapomorphies marked with an asterisk): iliac antitrochanter, dorsoventrally deep distal end of the ischial shaft, pubis lacking ambiens process*, crest shaped fourth trochanter, medial condyle of distal end of the femur with low angled craniomedial* and sharp angled caudomedial corners, and proximal end of the tibia with deep caudal groove.

Dinosauriformes Novas, 1992 (Novas, 1992)

Dinosauria Owen, 1842 (Padian & May, 1993)

Saurischia Seeley, 1887 (Gauthier, 1986)

Sauropodomorpha Huene, 1932 (Upchurch, 1997)

Buriolestes schultzi gen. et sp. nov.

Holotype. ULBRA-PVT280. Articulated skeleton including partial skull, few pre-sacral, three sacral, and 42 tail vertebrae, left scapula and forelimb lacking most of the manus, paired ilia and ischia, partial left pubis and nearly complete left hind limb (Figures 2.1I-2.1P).

Etymology. The genus name combines the Greek word ληστής (= robber) and the family name (Buriol) of the type-locality owners. The specific epithet honours the paleontologist Cesar Schultz.

Diagnosis. *Buriolestes schultzi* differs from other sauropodomorphs by an autapomorphic caudal projection of the medial condyle of the tibia (Figure 2.1O), medial to the intercondylar notch, a full differential diagnosis is provided in the Supplemental Experimental Procedures.
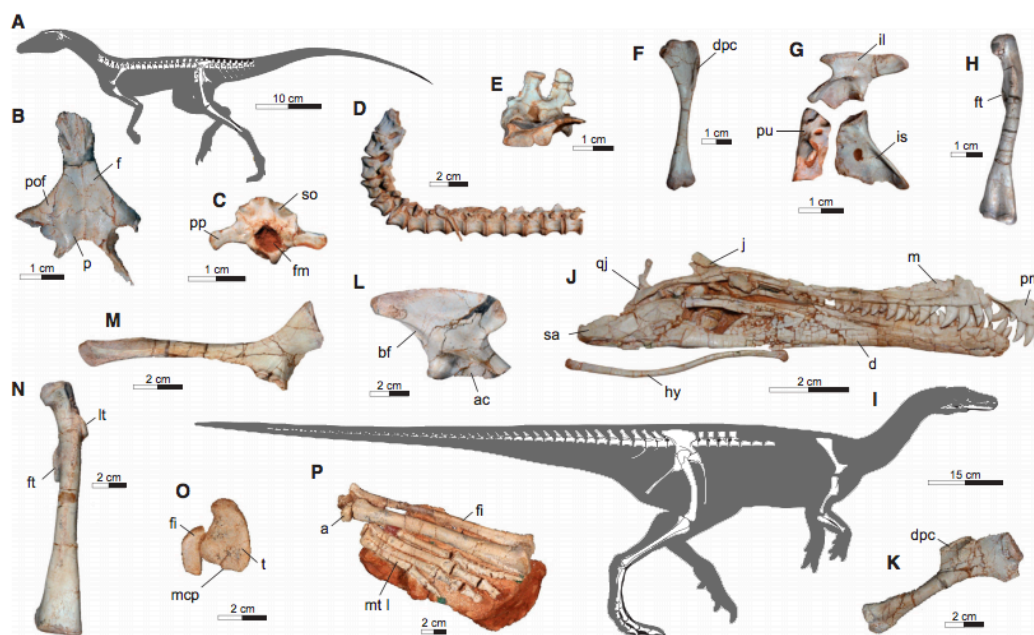
Figure 2.1. Skeletal features of *Ixalerpeton polesinensis* and *Buriolestes schultzi*. Abbreviations: a, astragalus; ac, acetabulum; bf, brevis fossa; d, dentary; dpc, deltopectoral crest; f, frontal, fi, fibula; fm, foramen magnum; ft, fourth trochanter; hy, hyoid apparatus; il, ilium; is, ischium; j, jugal; lt, lesser trochanter; m, maxilla; mcp, medial condyle projection; mt I, metatarsal I; p, parietal; pu, pubis; pm, premaxilla; pof, postfrontal; pp, paroccipital process; qj, quadratojugal; sa, surangular; so, supraoccipital; t, tibia. (A-H) *I. polesinensis* (ULBRA-PVT059). (A) skeletal reconstruction. (B) skull roof. (C) braincase. (D) presacral vertebrae. (E) sacral vertebrae. (F) humerus. (G) pelvis. (H) femur. (I-P) *B. schultzi* (ULBRA-PVT280). (I) skeletal reconstruction. (J) skull. (K) humerus. (L) ilium. (M) ischium. (N) femur. (O) tibia/ fibula proximal articulation. (P) epipodium and pes. Some figured bones are still partially imbedded in the rock matrix, which has been digitally removed (Modified from Cabreira *et al.*, 2016).

Descriptions

The parietal and frontal bones of *Ixalerpeton polesinensis* form a skull roof broader than that of most early dinosaurs. A large postfrontal fits laterally to the frontal, as more common to non-archosaur archosauromorphs (Nesbitt, 2011). Unlike dinosaurs (Langer & Benton, 2006), *I. polesinensis* retains a frontal not excavated by the supratemporal fossa and a post-temporal opening not reduced to a foramen sized aperture. Medial to that, a notch in the supraoccipital indicates the path of the middle

cerebral vain, which also laterally pierces the braincase, dorsal to the trigeminal foramen. The lateral braincase wall hosts the anterior tympanic recess (Nesbitt, 2011; Witmer, 1997) and a shallow depression on the caudoventral surface of the parabasisphenoid (also seen in *Lewisuchus admixtus*, *Saturnalia tupiniquim*, and *Eodromaeus murphy*) that resembles the semilunar depression of non-archosaur archosauriforms (Ezcurra, 2016). Comparisons to other dinosauromorphs (Sereno & Arcucci, 1994; Dzik, 2003; Bittencourt *et al.,* 2014) indicate that *I. polesinensis* preserves presacral vertebrae 6-20, the first two of which are longer and may correspond to the last neck vertebrae. The trunk series starts with transitional morphologies, including a trapezoidal second vertebra as in *Marasuchus lilloensis* (Sereno & Arcucci, 1994). Unlike silesaurids (Dzik, 2003) and most dinosaurs (Langer & Benton, 2006), the lateral surface of the neural arches lack laminae radiating from the apophyses, and the caudalmost vertebra lacks the cranially inclined neural spines described for *Lagerpeton chanarensis* (Sereno & Arcucci, 1994). The two-vertebrae sacrum fits the archosaur plesiomorphic pattern (Nesbitt, 2011). The ilium has a fully closed acetabulum, the caudal margin of which bears an antitrochanter. This is continuous to the ischial antitrochanter, which forms the entire acetabular margin of the bone, as in *L. chanarensis* (Sereno & Arcucci, 1994). *Ixalerpeton polesinensis* also shares an extensive ventromedial flange of the ischium with the latter taxon, forming the laminar symphysis and a deep articulation with the pubis. Its femur has various lagerpetid (Nesbitt *et al.,* 2009; Martinez *et al.,* 2013) traits such as a large caudomedial tuber of the proximal portion, a lateral emargination ventral to the head, and a large tibiofibular crest separated from the lateral condyle by a deep groove. The fourth trochanter forms a large crest, differing from that of *Dromomeron* spp (Nesbitt *et al.,* 2009).

Buriolestes schultzi lacks usual sauropodomorph traits such as a reduced skull and an enlarged external naris (Sereno *et al.*, 2013). As in all early dinosaurs (Nesbitt, 2011), the frontal is excavated by the supratemporal fossa. A sharp ridge forms the ventral border of the antorbital fenestra, as typical of neotheropods (Yates, 2005), but a subnarial gap/diastema is lacking in the premaxilla-maxilla junction. The dentary tip resembles those of other Carnian sauropodomorphs, with 2-3 large foramina and the ventrally sloping surface housing the first two teeth. Most teeth are caudally curved, with serrations (six per millimetre) forming straight angles to the crown margin, but these are not seen in the mesial carina of the elongate rostral teeth, a feature also reported for some neotheropods (Yates, 2005). As typical of sauropodomorphs (Yates, 2007), the humerus is longer than 60% the length of the femur and the deltopectoral crest extends for more than 40% of its length. The last of the three sacral vertebrae lacks dorsoventrally expanded ribs and, as in *Saturnalia tupiniquim* and *Plateosaurus engelhardti* (Pol *et al.*, 2011), was surely incorporated from the tail series. The iliac preacetabular ala is short and dorsoventrally expanded, whereas the long postacetabular ala is ventrally excavated by a brevis fossa. The ventral margin of the acetabular wall is plesiomorphically straight (Nesbitt, 2011), as in *Panphagia protos* and *S. tupiniquim*. The pubic shaft is straight, laminar, and slightly expanded at the distal end, lacking typical traits found in major dinosaur groups (Langer & Benton, 2006); e.g. sauropodomorph "apron", theropod "boot", ornithischian retroversion. The femoral head is expanded and kinked, as typical of dinosaurs (Langer & Benton, 2006), but not completely inturned (states 304-2 and 305-1 in [Nesbit, 2011]). The iliofemoral musculature attaches to a subtle anterior trochanter and a marked trochanteric shelf. The tibia is slightly longer than the femur, but not as much as in early ornithischians and theropods, which also have an expanded outer

malleolus (Langer & Benton, 2006), absent in *B. schultzi*. As in most non-theropod saurischians (Langer & Benton, 2006), the calcaneum is proximodistally flattened and has a reduced tuber. The third metatarsal is the longest, as typical of dinosaurs (Nesbitt, 2011), and the fifth element is proximally expanded. The distalmost of the 42 preserved tail vertebrae lack elongated prezygapophyses, differing from those of *Tawa hallae*, herrerasaurids, and neotheropods (Langer & Benton, 2006; Nesbitt, 2011).

2.3. DISCUSSION

A new phylogenetic analysis (see Supplemental Experimental Procedures) places *Ixalerpeton polesinensis* and *Buriolestes schultzi* respectively within Lagerpetidae and Sauropodomorpha (Figure 2.2, Appendix for Chapter 1). The joint record of sauropodomorphs and lagerpetids in the Santa Maria Formation matches a similar find in the coeval Ischigualasto Formation of Argentina (Martinez *et al.*, 2013). Based on much more complete remains, the new discovery confirms that the co-occurrence between non-dinosaurian Dinosauromopha and dinosaurs was not restricted to later stages of the Triassic and to the northern parts of Pangaea, where silesaurids and lagerpetids have been found together with theropod dinosaurs (Irmis *et al.*, 2007, Niedzwiedzki *et al.*, 2014), reinforcing rapid replacement as a very unlikely scenario for the initial radiation of dinosaurs (Irmis *et al.*, 2007; Brusatte *et al.*, 2010; Benton *et al.*, 2014].

The discovery of *Ixalerpeton polesinensis* helps defining traits of anatomical parts previously unknown for lagerpetids that are either unique to Dinosauromorpha or diagnose less inclusive groups.
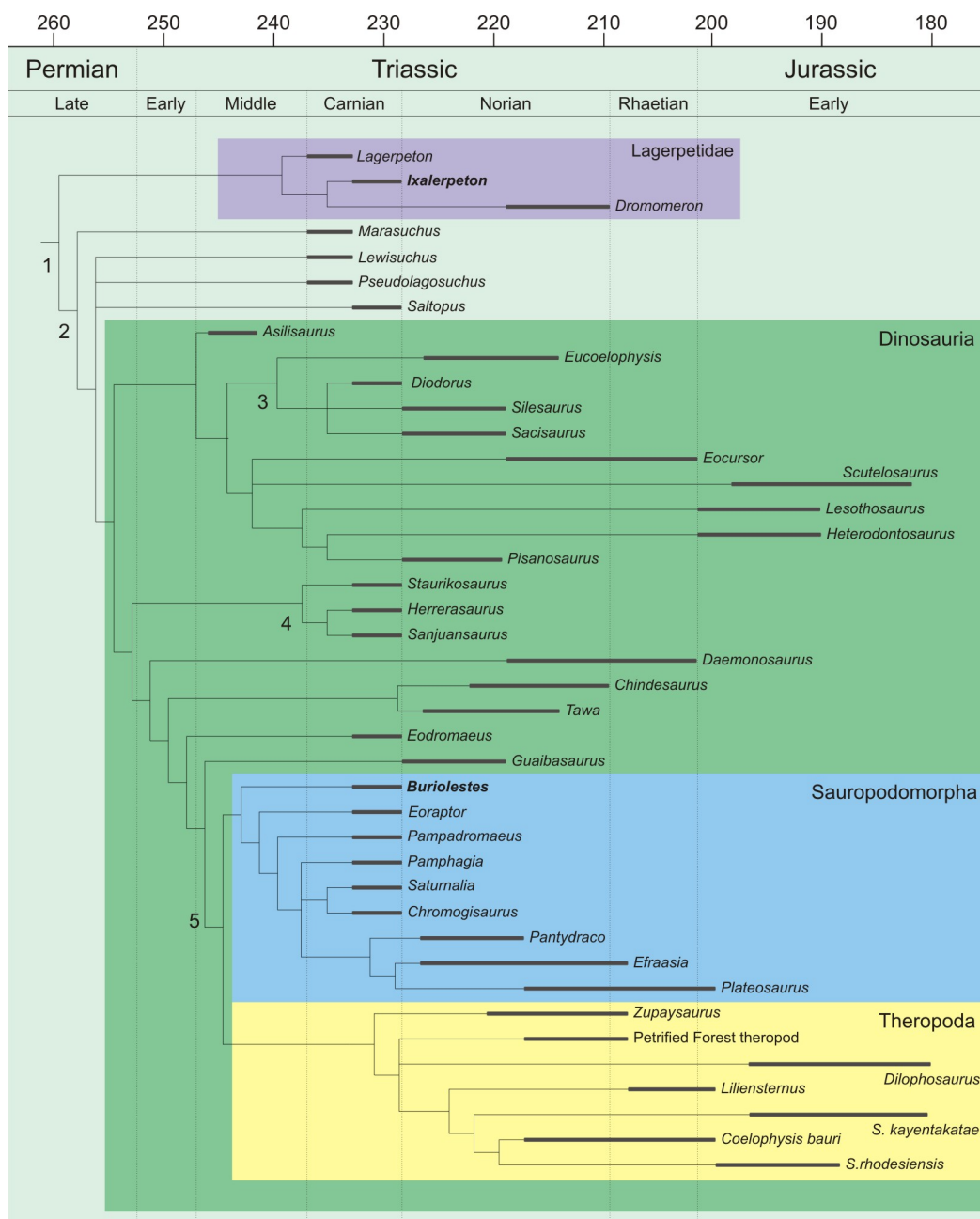
Figure 2.2. Time calibrated phylogeny of early dinosauromorphs. Simplified version of the strict consensus tree. Lagerpetidae, Dinosauria, Saurischia, Theropoda, and Sauropodomorpha are marked as colour blocks. Numbered nodes represent Dinosauromorpha (1), Dinosauriformes (2), Ornithischia (3), Silesauridae (4), Herrerasauridae (5), Eusaurischia (6). Silhouettes represent the newly described *Ixalerpeton polesinensis* and *Buriolestes schultzi*. Stratigraphic ranges mark uncertainties about the age of the fossil occurrences, not the actual duration of the lineage (Modified from Cabreira *et al.*, 2016).

For example, *I. polesinensis* bears a anterior tympanic recess in the braincase, as typical of Dinosauriformes (Nesbitt, 2011) and more recently also found out of the dinosaur-line of archosaurs (Sobral *et al.*, 2016), but retains traits unknown to that

group, such as a large post-temporal fenestra, a postfrontal bone, and a frontal not excavated by the supratemporal fossa (Nesbitt, 2011). Also, its glenoid faces slightly laterally, a plesiomorphic condition modified in Dinosauriformes to a fully caudally facing articulation (Langer & Benton, 2006). On the contrary, its deltopectoral crest extending for more than 30% of the humerus demonstrates that his condition is plesiomorphic for Dinosauromorpha.

Buriolestes schultzi adds to the recently found plethora of Carnian dinosaurs (Martinez & Alcober, 2009; Ezcurra, 2010; Cabreira *et al.*, 2011; Sereno *et al.*, 2013), but its unique position as the sister-taxon to all other sauropodomorphs helps clarifying the sequence of character acquisition in the early evolution of the group. Sauropodomorphs share a ventrally bent dorsal margin of the dentary tip (usually with an inset first tooth) and a low mandibular articulation. Their humeri bear a long deltopectoral crest, particularly in the sister-clade to *B. schultzi*. The sister-clade to *Eoraptor lunensis* is characterized by a broader distal end of the humerus and the prevalence of teeth with leaf-shaped crowns and large denticles (four per millimetre). More caudal teeth with significantly shorter crowns are only seen in members of the clade formed by *Saturnalia tupiniquim*, *Chromogisaurus novasi*, *Panphagia protos*, and norian sauropodomorphs. Among these, *P. protos* has a skull that surpasses two-thirds of the femoral length, suggesting that it may represent an earlier slit compared to *S. tupiniquim*.

Dental traits of *Buriolestes schultzi* are compatible with a faunivorous diet (Figure 2.3 and Appendix for Chapter 2), the animal probably praying on small vertebrates and non-hardly-skeletonized invertebrates. Its discovery confirms that early members of the otherwise typically herbivorous Sauropodomorpha were likely predators. In consequence, regardless of the affinities of herrerasaurids and other

putative theropods (Brusatte *et al.*, 2010), our results consistently show faunivory as the ancestral diet of saurischian dinosaurs. Indeed, in the evolutionary hypothesis advocated here, the ancestral of all dinosaurs would also be faunivorous, with herbivory/omnivory appearing independently in Ornithischia (including silesaurids), the bulk of Sauropodomorpha, and later in various theropod groups (Zanno & Makovicky, 2011). Yet, alternative scenarios have to be considered, and the ancestral dinosaur diet is ambiguous if, for example, Silesauridae is accepted both as the sister-group to dinosaurs and not to include *Lewisuchus admixtus* (Figure 2.3). In any case, new discoveries like *Ixalerpeton* and *Buriolestes* will continue to provide the kind of data necessary to ever more reliably test the patterns of early dinosaur evolution.
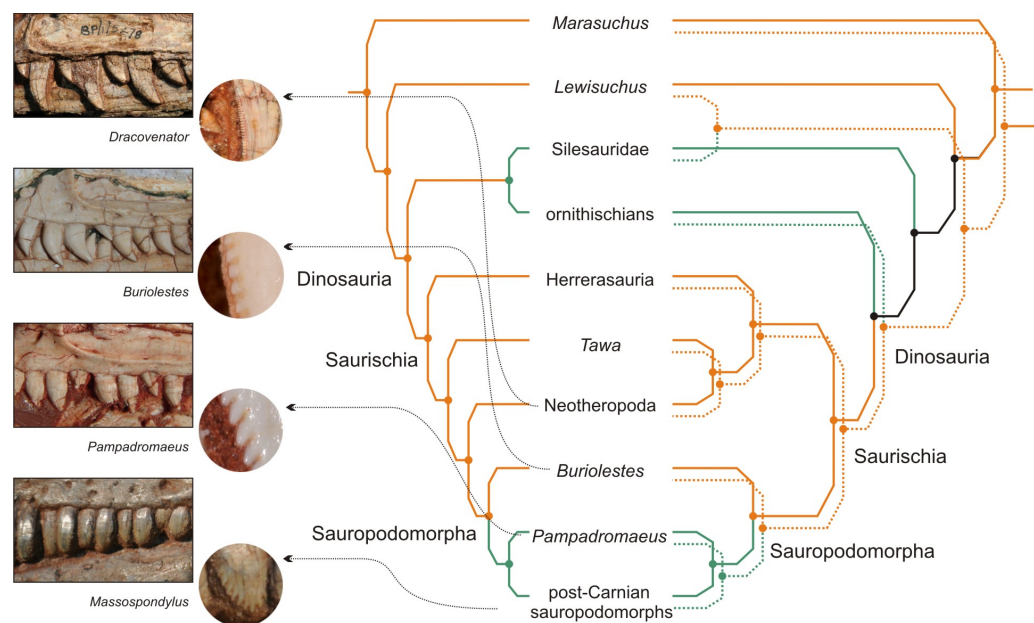
Figure 2.3. Dietary preferences represented on early dinosauromorph phylogenies. Hypothesis advocated here is shown in the left cladogram, with alternative arrangements shown on the right. Colour of the branches represent reconstructed ancestral feeding habits of the lineages; green = herbivory/omnivory; black = ambiguous; orange = faunivory. Photographs illustrate (top to bottom) increasing levels of tooth adaptation towards herbivory/omnivory among eusaurischians. *Dracovenator* (BP/1/5278) and *Plateosaurus* (GPIT-18318a), left photograph scale bar = 10 mm, right photograph total high = 3 mm; *Buriolestes* (ULBRA-PVT280) *Pampadromaeus* (ULBRA-PVT016), left photograph scale bar = 5 mm, left photograph total high = 1 mm (Modified from Cabreira *et al.*, 2016).

2.4. ACKNOWLEDGMENTS

2.5. REFERENCES

Benton MJ, Forth J, Langer MC. 2014. Models for the Rise of the Dinosaurs. *Current Biology*, 24, R87-R95.

Bittencourt JS, Arcucci AB, Marsicano CA, Langer MC. 2014. Osteology of the Middle Triassic archosaur *Lewisuchus admixtus* Romer (Chañares Formation, Argentina), its inclusivity, and relationships among early dinosauromorphs. *Journal of Systematic Palaeontology*, 13, 189–219.

Brusatte SL., Nesbitt SJ, Irmis RB, Butler RJ, Benton MJ, Norell MA. 2010. The origin and early radiation of dinosaurs. *Earth-Science Reviews*, 101, 68–100.

Cabreira SF, Schultz CL, Bittencourt JS, Soares MB, Fortier DC, Silva LR, Langer, MC. 2011. New stem-sauropodomorph (Dinosauria, Saurischia) from the Triassic of Brazil. *Naturwissenschaften*, 98, 1035–1040.

Dzik J. 2003. A beaked herbivorous archosaur with dinosaur affinities from the early Late Triassic of Poland. *Journal of Vertebrate Paleontology*, 23, 556–574.

Ezcurra MD. 2010. A new early dinosaur (Saurischia: Sauropodomorpha) from the Late Triassic of Argentina: a reassessment of dinosaur origin and phylogeny. *Journal of Systematic Palaeontology*, 8, 371-425.

Ezcurra MD. 2016. The phylogenetic relationships of basal archosauromorphs, with an emphasis on the systematics of proterosuchian archosauriforms. *PeerJ*, 4, e1778.

Gauthier J. 1986. Saurischian monophyly and the origin of birds. *Memoirs of the California Academy of Sciences*, 8, 1–55.

Horn BLD, Melo TP, Schultz CL, Philipp RP, Kloss HP, Goldberg K. 2014. A new third-order sequence stratigraphic framework applied to the Triassic of the Paraná Basin, Rio Grande do Sul, Brazil, based on structural, stratigraphic and paleontological data. *Journal of South-American Earth Sciences*, 55, 123–132.

Irmis RB, Nesbitt SJ, Padian K, Smith ND, Turner AH, Woody D, Downs A. 2007. A Late Triassic dinosauromorph assemblage from New Mexico and the rise of dinosaurs. *Science*, 317, 358–361.

Langer MC, Benton MJ. 2006. Early dinosaurs: A phylogenetic study. *Journal of Systematic Palaeontology*, 4, 309–358.

Langer MC, Ribeiro AM, Schultz CL, Ferigolo J. 2007. The continental tetrapod-

bearing Triassic of South Brazil. *New Mexico Museum of Natural History Sciences Bulletin*, 41, 201–218.

Langer MC, Nesbitt SJ, Bittencourt JS, Irmis RB. 2013. Non-dinosaurian Dinosauromorpha. *Geological Society Special Publications,* 379, 157–186.

Martinez RN, Alcober OA. 2009. A basal sauropodomorph (Dinosauria: Saurischia) from the Ischigualasto Formation (Triassic, Carnian) and the early evolution of Sauropodomorpha. *PLoS One*, 4, e4397.

Martínez RN, Apaldetti C, Alcober OA, Colombi CE, Sereno PC, Fernandez E, Santi Malnis P, Correa GA, Abelin D. 2013. Vertebrate succession in the Ischigualasto Formation. *Journal of Vertebrate Paleontology,* 32, suppl. 6, 10–30.

Nesbitt SJ. 2011. The early evolution of archosaurs: relationships and the origin of major clades. *Bulletin of the American Museum of Natural History,* 352, 1–292.

Nesbitt SJ, Irmis RB, Parker WG, Smith ND, Turner AH, Rowe T. 2009. Hindlimb osteology and distribution of basal dinosauromorphs from the Late Triassic of North America. *Journal of Vertebrate Paleontology,* 29, 498–516.

Niedzwiedzki G, Brusatte SL, Sulej T, Butler RJ. 2014. Basal dinosauriform and theropod dinosaurs from the mid–Late Norian (Late Triassic) of Poland: implications for triassic dinosaur evolution and distribution. *Palaeontology*, 57, 1121–1142.

Novas FE. 1992. Phylogenetic relationships of the basal dinosaurs, the Herrerasauridae. *Palaeontology*, 35, 51–62.

Padian K, May CL. 1993. The earliest dinosaurs. *New Mexico Museum of Natural History Sciences Bulletin,* 3, 379–381.

Pol D, Garrido A, Cerda IA. 2011. A New Sauropodomorph Dinosaur from the Early Jurassic of Patagonia and the Origin and Evolution of the Sauropod-type Sacrum. *PLoS ONE,* 6, e14572.

da Rosa AA. 2014. Geological context of the dinosauriform-bearing outcrops from the Triassic of Southern Brazil. *Journal of South American Earth Sciences,* 61, 108–119.

Sereno PC. 1991. Basal archosaurs: phylogenetic relationships and functional implications. *Journal of Vertebrate Paleontology, Memoir* 2, 1–53

Sereno PC, Arcucci AB. 1994. Dinosaurian precursors from the Middle Triassic of Argentina: *Lagerpeton chanarensis. Journal of Vertebrate Paleontology,* 13, 385–3991.

Sereno PC, Martínez RN, Alcober OA. 2013. Osteology of *Eoraptor lunensis* (Dinosauria, Sauropodomorpha). *Journal of Vertebrate Paleontology,* 32 (sup. 1), 83–179.

Sobral G, Sookias RB, Bhullar B-AS, Smith R, Butler RJ, Müller J. (2016). New information on the braincase and inner ear of *Euparkeria capensis* Broom: implications for diapsid and archosaur evolution. *Royal Society Open Science,* 3: 160072.

Upchurch, P. 1997. Sauropodomorpha. In (eds. PJ Currie, K Padian), Encyclopedia of Dinosaurs San Diego, Academic Press, pp. 658–660.

Witmer LM. 1997. Craniofacial air sinus systems. In (eds. PJ Currie, K Padian), Encyclopedia of Dinosaurs San Diego, Academic Press, pp. 151–159.

Yates AM. 2005. A new theropod dinosaur from the Early Jurassic of South Africa and its implication for the early evolution of theropods. *Palaeontologia Africana,* 41, 105–122.

Yates AM. 2007. The first complete skull of the Triassic dinosaur *Melanorosaurus* Haughton (Sauropodomorpha:Anchisauria). *Special Papers in Palaeontology,* 77, 9–55.

Zanno LE, Makovicky PJ. 2011. Herbivorous ecomorphology and specialization patterns in theropod dinosaur evolution. *PNAS* USA, 108, 232–237.

CHAPTER 3

Early dinosaur brain indicates faunivorous exaptation in the early evolution of sauropodomorph herbivory

Chapter submitted to *Scientific Reports* as: Early dinosaur brain indicates faunivorous exaptation in the early evolution of sauropodomorph herbivory. Manuscript number: SREP-17-05851

Authors: Mario Bronzati[1,2,*], Oliver W. M. Rauhut[1,2], Jonathas S. Bittencourt[3], Max. C. Langer[4]

Author contributions:

M.B. and M.C.L. conceptualized the study; **M.B.** segmented the CT-Scan data; **M.B., O.W.M.R., and M.C.L.** analysed the results; **M.B**., O.W.M.R., M.C.L., and J.S.B. wrote the manuscript.

<div align="right">**Chapter 3**</div>

Early dinosaur brain indicates faunivorous exaptation in the early evolution of sauropodomorph herbivory

Mario Bronzati[1,2,*], Oliver W. M. Rauhut[1,2], Jonathas S. Bittencourt[3], Max. C. Langer[4]

[1] Bayerische Staatssammlung für Paläontologie und Geologie, Richard-Wagner-Straße 10, 80333 Munich, Germany.

[2] Department of Earth and Environmental Sciences and GeoBioCenter, Ludwig-Maximilians-Universität, Richard-Wagner-Straße 10, 80333 Munich, Germany.

[3] Departamento de Geologia, Universidade Federal de Minas Gerais, Av. Presidente Antônio Carlos 6627, 31270-901, Belo Horizonte MG, Brazil

[4] Laboratório de Paleontologia, FFCLRP, Universidade de São Paulo, Av. Bandeirantes 3900, 14040-901, Ribeirão Preto SP Brazil.

3.1. ABSTRACT

Sauropod dinosaurs are iconic Mesozoic herbivores that have a very characteristic bauplan, including a small skull, long neck, and a massive body. Interestingly, this morphology deviates from that observed in other large herbivores, such as most living mammals, which tend to have a rather large, robust skull with teeth suitable for mastication. The reduced sauropod skull is a heritage from their Late Triassic precursors, but the evolutionary drive behind its origin remained enigmatic. Here, we investigate the feeding behaviour of early sauropodomorphs, combining information

on hard and soft cranial anatomy, including new neurological data for one of the oldest dinosaurs known, *Saturnalia tupiniquim* from the Late Triassic (c. 230 Ma) of Brazil. The neurological features, especially the presence of a well-developed flocculus of the cerebellum, are consistent with an adaptation for refined capture of small prey items. In this context, we argue that the reduction of the skull in sauropodomorphs represents a primary predatory adaptation to hunt small, elusive animals by rapid neck/head movements. Later in the Mesozoic, the skull reduction triggered the evolution of gigantism in sauropods by minimizing the biomechanical constraint to further elongation of the neck, a crucial step for the evolution of herbivory in the group.

3.2. Introduction

Recent fossil discoveries have provided new perspectives for the study of the dietary evolution of early dinosaurs, but the ancestral condition for the group is still unclear, with faunivory and omnivory being equally likely (Barrett & Rayfield, 2006; Nesbitt *et al.*, 2010; Cabreira *et al.*, 2016). Less controversial is the independent acquisition of full herbivorous diets in the three main dinosaur lineages, Ornithischia, Theropoda, and Sauropodomorpha (Nesbitt *et al.*, 2010; Barrett *et al.*, 2010; Novas *et al.*, 2015). Within the latter clade, sauropods are iconic giant terrestrial herbivores, achieving great evolutionary success during the Mesozoic (Upchurch *et al.*, 2004; Wilson, 2005). These animals include the largest terrestrial vertebrates yet recorded, and have a characteristic body plan, with massive bodies, reaching up to 90,000 kg (Mazzetta *et al.*, 2014; Benson *et al.*, 2014), combined with elongated necks and tails, and extremely small heads relative to their body size. The presence of small heads is

uncommon in other large herbivores, which typically exhibit large and robust skulls, with tooth batteries suitable for mastication (Sander *et al*., 2011).

The small skull of sauropods has been inherited from early sauropodomorphs precursors (Langer *et al*., 2010), from which they significantly differ in ecology (Barrett *et al*., 2010; Rauhut *et al*., 2011; Sander *et al*., 2011). The earliest sauropodomorphs were small (1-2 m in body length), with a body mass not exceeding 50 kg (Benson *et al*., 2014), and faunivory was their ancestral diet (Cabreira *et al*., 2016). Osteological changes related to the transition from faunivory to full herbivory are well documented in the Late Triassic and Early Jurassic sauropodomorph fossil record (Rauhut *et al*., 2011; Barrett & Upchurch, 2007). However, characterizing the feeding behaviour of early forms is not always straightforward, especially because tooth morphology alone does not allow a clear separation between herbivore and partially faunivore (omnivore) habits (Barrett *et al*., 2010; Nesbitt *et al*., 2010).

Here, diet evolution in early sauropodomorphs is investigated using new paleoneurological data for *Saturnalia tupiniquim* (Langer *et al*., 1999), from the Late Triassic (Carnian – c. 230 Ma) Santa Maria Formation of Brazil. Together with the Ischigualasto Formation of Argentina, those strata contain the oldest unequivocal dinosaurs (Langer *et al*., 2010). Cranial remains are not scarce (e.g. Sereno & Novas, 1993; Sereno *et al*., 1993; Cabreira *et al*., 2011; Martinez *et al*., 2011; Martinez *et al*., 2013), but information on the soft tissues associated with the braincase (e.g. brain, inner ear, cranial nerves) remained poorly studied. Indeed, given its age and phylogenetic position (Langer *et al*., 2010), *S*. *tupiniquim* is a key-taxon to understand the early evolution of sauropodomorph feeding behaviours.

3.3. Results

Endocasts

Based on the CT-Scan data, it was possible to reconstruct the endocast of *Saturnalia tupiniquim*, including the inner ear, cranial nerves, and parts of the brain, including the cerebellum. The spatial distribution, number, and general morphology of cranial nerves V, VI, VII, and XII (Figure 3.1) mostly correspond to that of other dinosaurs (see e.g. Sampson & Witmer, 2007; Witmer *et al.*, 2008; Evans *et al.*, 2009; Knoll *et al.*, 2012; Paulina-Carabajal, 2012; Paulina-Carabajal *et al.*, 2014) and non-dinosaurian dinosauriforms (Bittencourt *et al.*, 2014). Located on the lateral wall of the braincase, anterior to the flocculus of the cerebellum and the semi-circular canals of the inner ear, cranial nerve V (trigeminal nerve) is the thickest of the cranial nerves, ventral to which lays cranial nerve VI (abducens nerve). In contrast to other cranial nerves, the exit of the abducens nerve is located ventrally in the braincase, in the anterior portion of the pasabasisphenoid. The exit of cranial nerve VII (facial nerve) is completely enclosed by the prootic. As typical in dinosaurs, it is located ventral to the anterior semi-circular canal of the inner ear and is thinner than that of cranial nerves V and VI. Cranial nerve XII (hypoglossal nerve) of *S. tupiniquim* had two branches that independently exited the posterolateral portion of the braincase through the otoccipital. This is seen in most dinosaurs, but some sauropods have a single exit for that nerve (Balanoff *et al.*, 2010).

The CT data allowed a detailed reconstruction of the inner ear anatomy of *Saturnalia tupiniquim*. The anterior semi-circular canal is approximately 1.5 times higher than wide and the longest of the three canals, similar to the condition in some theropods (Witmer *et al.*, 2008; Lautenschlager *et al.*, 2012), and early sauropods (Knoll *et al.*, 2012). In contrast, titanosaurian sauropods have an anterior semi-

circular canal that is slightly higher than wide (Knoll *et al.*, 2012; Paulina-Carabajal, 2012). In dorsal view, the anterior and posterior semi-circular canals diverge from one another, forming an angle of approximately 80 degrees. The portion of the inner ear ventral to the semi-circular canals is shorter than the anterior semi-circular canals, but this region is not very well preserved, and the ventralmost limit of the cochlea is unclear. However, the flocculus of the cerebellum is clearly recognized in the anterior portion of the virtual endocast. It is large and well-developed, projecting into the space between the semi-circular canals.
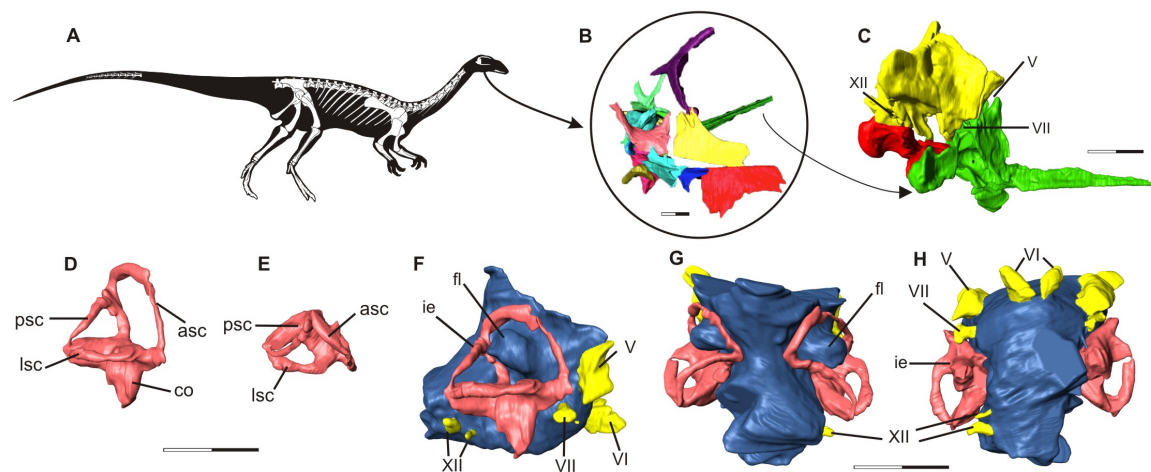
Figure 3.1: The early sauropodomorph *Saturnalia tupiniquim*. Skeletal reconstruction (A). Virtual preparation of cranial bones as preserved inside the matrix (B), with braincase highlighted in lateral (C) view. Reconstruction of the soft tissues associated to the braincase: right inner ear in lateral (D) and dorsal (E) views, and endocast in lateral (F), dorsal (G), and, ventral (H) views. Abbreviations: asc – anterior semicircular canal; co – cochleae; fl – flocculus; ie – inner ear; lsc – lateral semicircular canal; psc – posterior semicircular canal; V – trigeminal nerve; VI – abducens nerve; VII – facial nerve; XII hypoglossal nerve. Scale bars = 1cm.

3.4. Discussion

When inferring the lifestyle of a fossil taxon, multiple aspects should be taken into consideration. These can be categorised as historical (i.e. which take into account the phylogenetic history of an organism) and ahistorical (i.e. form-function correlation of

anatomical traits) evidences (*sensu* Barrett & Rayfield, 2006). The feeding behaviour of dinosaurs can, thus, be ahistorically analysed by combining anatomical information from hard (e.g. tooth morphology, postcranial elements) and soft (e.g. brain) tissues (Barrett & Rayfield, 2006). In this sense, the original interpretation of *Saturnalia tupiniquim* as a herbivorous animal (Langer *et al.*, 1999) mostly took into account historical evidences (i.e. its affinities to Sauropodomorpha, hitherto interpreted as typical herbivore clade), rather than specific aspects of its anatomy. Indeed, the tooth morphology of *Saturnalia tupiniquim* shows features also found in dinosaurs able to use food sources other than plants (Barrett *et al.*, 2010; Nesbitt *et al.*, 2010; Cabreira *et al.*, 2016). Its teeth are recurved and bear small serrations perpendicular to the carina, as typical of carnivorous taxa (Barrett *et al.*, 2010; Nesbitt *et al.*, 2010), also seen in the coeval *Buriolestes schultzi* (Cabreira *et al.*, 2016). Hence, based on tooth morphology alone, carnivorous or omnivorous diet reconstructions are equally likely for these early sauropodomorphs (Barrett *et al.*, 2010; Nesbitt *et al.*, 2010). Yet, the new soft tissue data presented here provide additional evidence for their faunivore feeding behaviour. *Saturnalia tupiniquim* has an enlarged flocculus of the cerebellum, a structure that plays an important role in the control of head and neck movements (Butler & Hodos, 1996; Winship & Wylie, 2003). Indeed, a well-developed flocculus leads to an enhanced gaze capacity (Witmer *et al.*, 2003), which enables animals to better focus on prey while coordinating the neck and skull during fast movements.

The enlarged flocculus occupied most of the inner ear labyrinth of *Saturnalia tupiniquim* (Figure 3.1). Based on the size of the floccular recess in the medial surface of the braincase, this also seems to be the condition in other faunivore archosaurs, such as the non-archosaurian archosauriform *Euparkeria capensis* (Sobral *et al.*, 2016) and the non-dinosaurian dinosauriforms *Marasuchus lilloensis* (pers. obs) and

Lewisuchus admixtus (Bittencourt *et al.,* 2014). In non-avian theropods, the flocculus projects into the space of the semi-circular canals of the inner ear, but with a great variation in size among different taxa (Rogers, 1998; Witmer *et al.,* 2008; Lautenschlager *et al.,* 2012). In contrast, the flocculus of the herbivorous sauropods (Witmer *et al.,* 2008; Balanoff *et al.,* 2010 Knoll *et al.,* 2012; Paulina-Carabajal, 2012) and ornithischians (Evans *et al.,* 2009; Paulina-Carabajal *et al.,* 2016; Cruzado-Caballero *et al.,* 2016) does not project into the labyrinth of the inner ear.

The reduction of the flocculus in sauropods has been associated with the adoption of a quadrupedal stance (Chaterjee & Zheng, 2002; Paulina-Carabajal, 2012). Nevertheless, early sauropodomorph endocasts show that the transition to quadrupedalism was not the major force shaping flocculus anatomy in the evolution of the group (Figure 3.2). For example, *Plateosaurus engelhardti* was a bipedal animal (Bonnan & Senter, 2007; Mallison, 2010) and already has a reduced flocculus. On the other hand, an interesting correlation is observed when the development of the flocculus of sauropodomorphs is analysed alongside osteological aspects in a phylogenetic context.

When characters are mapped on a phylogeny of sauropodomorphs, it is clear that the loss of neurological traits potentially related to an efficient predation (i.e. the reduction of the flocculus) occurred together with modifications associated with a more obligate herbivorous diet. Contrary to the dentition of the oldest Carnian sauropodomorphs, other Late Triassic members of the group, such as *Efraasia minor* and *Plateosaurus engelhardti* possess lanceolate teeth with coarse denticles, features that are usually considered to indicate a diet mainly based on plants (Barrett & Upchurch, 2007). Yet, these taxa could eventually complement their diet with scavenging (Barrett, 2000), a less "active" means of gathering animal food. Still, the

first steps towards body size increase in Sauropodomorpha happened in the minimal clade including *Plateosaurus* and sauropods (Rauhut *et al.*, 2011; Sander *et al.*, 2011; Benson *et al.*, 2014). The increase in body size has been demonstrated as having been crucial for the evolution of a fully herbivorous diet in Sauropodomorpha (Sander *et al.*, 2011). Thus, we suggest that the reduction of the flocculus in sauropodomorphs correlates to a change in feeding behaviour (i.e. from active predators to herbivores or scavenger omnivores) rather than to the adoption of an obligatory quadrupedal stance, which happened later in the evolutionary history of the group (Bonnan & Yates, 2007).

The neurological support for predatory behaviour in *Saturnalia tupiniquim* provides new insights for the scenario regarding the acquisition of one of the most remarkable sauropodomorph traits, the reduced skull (Figure 3.2). In the phylogenetic hypotheses so far proposed (Nesbitt *et al.*, 2010; Cabreira *et al.*, 2016; Langer *et al.*, 2010; Martinez *et al.*, 2011; Martinez *et al.*, 2013; Bittencourt *et al.*, 2014; Ezcurra, 2010), the reduction of the skull length (to less than 2/3 of the femoral length) was recovered as a synapomorphy of the less inclusive clade containing *S. tupiniquim* and sauropods. However, the driving force behind this anatomical modification remained enigmatic, with the only explanation offered being that a small skull on a long neck might have allowed an omnivorous animal to secure small prey items by rapid head and neck movements (Rauhut *et al.*, 2011). The well-developed flocculus and reduced skull of the oldest sauropodomorph, as well as the importance of the former structure to coordinate rapid neck and head movements is consistent with this idea. Given its small body size and reduced head, *S. tupiniquim* was probably unable to prey on other medium-sized tetrapods of the Santa Maria Formation fauna. However, a small, light skull on a relatively elongated neck (see Appendix for Chapter 3) would be ideal to

allow rapid head movements in pursuit of small, elusive prey items, such as insects and small vertebrates. In this context, a large flocculus would have helped to coordinate such head and neck movements and the visual fixation of prey (Winship & Wylie, 2003; Witmer *et al.*, 2003), making such a behaviour more effective.

The proposed feeding behaviour of *Saturnalia tupiniquim* is not unexpected in the context of early dinosaur evolution, as the ancestral condition of the group was most probably faunivory (Cabreira *et al.*, 2016). Nevertheless, seen in the context of sauropodomorph evolution, the skull reduction of *S. tupiniquim,* initially representing a predatory specialisation, can be understood as an example of an important but frequently underestimated aspect of the evolutionary process, exaptation (Gould & Vrba, 1982). It has been demonstrated that a series of evolutionary innovations were necessary for establishing the highly efficient strictly herbivorous lifestyle of sauropods (Sander, 2013). Among these, the small skull significantly reduced biomechanical constraints for neck elongation (Witzel & Preuschoft, 2005). In turn, an elongated neck allowed access to food sources that were unavailable for other herbivores and created a larger feeding envelope, reducing energy consumption during food intake (Sander *et al.*, 2011). Thus, the fact that skull reduction is first seen in a predatory sauropodomorph implies a scenario where a trait related to one habit (faunivory) was crucial for the evolution of a complete different lifestyle (herbivory) in a subsequently different selection regime.
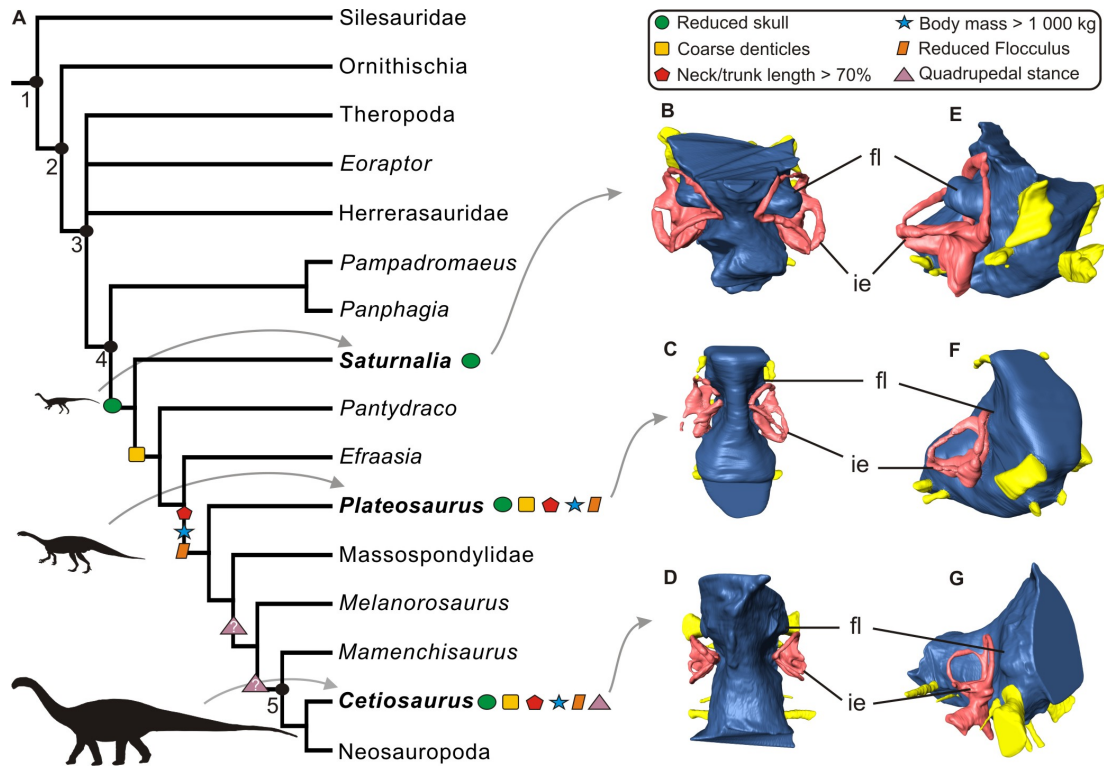
Figure 3.2: Simplified Dinosauria phylogeny highlighting character acquisition in Sauropodomorpha (A). Endocasts of *Saturnalia tupiniquim* (MCP-3845-PV), *Plateosaurus* (MB.R.5586-1), and a sauropod specimen tentatively reffered to *Cetiosaurus* (OUMNH J13596) in dorsal (B, C, D) and anterolateral (E, F, G) views showing the morphology of the flocculus in sauropodomorph dinosaurs. Abbreviations: fl – flocculus, ie – inner ear, 1 – Dinosauriformes, 2 – Dinosauria, 3 – Saurischia, 4 – Sauropodomorpha, 5 – Sauropoda.

In conclusion, it is worth stressing out that making inferences on the lifestyle of fossil taxa using a single criterion can be misleading. Form/function correlations should be very carefully made (Walsh *et al.*, 2013), and other parameters (historical and ahistorical) should be taken into account. Here we demonstrated the correlation between the reduction of the flocculus with other anatomical modifications related to the adoption of a herbivorous diet. This indicates that the transition to herbivory also involved neurological modifications in Sauropodomorpha (Figure 3.2). In this

context, the small flocculus of most sauropodomorphs is thus understood as a vestigial trait, retained in a reduced version from the bipedal, predatory early sauropodomorphs. Finally, head reduction certainly played an important role in sauropodomorph evolution, reducing the biomechanical constraints to neck elongation, triggering the evolutionary cascade that led to the unusual sauropod body plan and, ultimately, their gigantism (Sander, 2013). The small skull of faunivorous early sauropodomorphs can, therefore, be seen as a case of exaptation, which constrained the evolution of the highly efficient plant-eating strategy of sauropods.

3.5. Material & Methods

Specimen and CT-Scan

Saturnalia tupiniquim is known from three specimens: MCP 3844-PV (holotype), 3845-PV, and MCP 3946-PV (14). The fossils come from the Late Triassic (Carnian – c. 230 Ma) Santa Maria Formation, in southern Brazil, from a locality commonly known as Cerro da Alemoa or Waldsanga (53°45' W; 29°40' S). The braincase is only preserved in MCP 3845-PV, which also has great part of the postcranium preserved (Langer, 2003; Langer *et al.,* 2007). Computed tomography data was used to produce a virtual model of the soft tissues associated with the braincase of *S. tupiniquim*. The specimen was scanned at the Zoologische Staatsammlung München (Bavaria State Collection of Zoology, Munich, Germany) in a Nanotom Scan (GE Sensing & Inspection Technologies GmbH, Wunstorf Germany) using the following parameters: Voltage: 100 Kv; Current: 130 μA; 3,1 μm voxel size. 1,440 x-ray slices were generated, which were downsampled by half and segmented in the software Amira (version 5.3.3, Visage Imaging, Berlin, Germany).

Size of the flocculus

In order to quantify the size of the flocculus of the cerebellum we opted for using a qualitative approach regarding the projection of this structure into the space between the semi-circular canals of the middle-ear. Thus, if the flocculus projects into the space between the semi-circular canals, it is here considered as well developed. On the other hand, if the flocculus does not project into this space, it is considered as poorly developed. One alternative approach to measure the development of this structure would be more quantitative, based on the ratio between the volume of the flocculus and the total volume of the brain. However, the endocast of *Saturnalia tupiniquim* is not complete, lacking its anterior portion, and thus the exact ratio of flocculus to brain size could not be estimated. Another factor that hampers the use of such an approach in this study is the lack of more data regarding brain and flocculus volumes of other early dinosaurs and non-dinosaurian dinosauromorphs. Nevertheless, the qualitative approach taken here is objective and based on an easily distinguishable feature of the endocast.

Phylogeny of Sauropodomorpha

In order to trace morphological transformations and major changes in the feeding behaviour along sauropodomorph evolution, we constructed an informal supertree based on the results of the most recent phylogenetic analyses for the group (e.g. Ezcurra, 2010; Langer *et al.,* 2010; Nesbitt *et al.,* 2010; Yates, *et al.,* 2010; Martinez *et al.,* 2011, 2013; Pol *et al.,* 2011; McPhee *et al.,* 2015; Novas *et al.,* 2015; Otero *et al.,* 2015; Cabreira *et al.,* 2016). The discovery of new taxa, such as *Panphagia protos* (Martinez & Alcober, 2009), *Chromogisaurus novasi* (Ezcurra, 2010), *Pampadromaeus barbarenai* (Cabreira *et al.,* 2011), and *Buriolestes schultzi*

(Cabreira *et al.*, 2016), along with the reassessment of the phylogenetic position of *Eoraptor lunensis* as a sauropodomorph (Martinez *et al.*, 2013), provided new data and interpretations, but the relationships of the earliest sauropodomorphs from the Carnian Santa Maria and Ischigualasto formations are still uncertain (see e.g. Laner, 2014). Nevertheless, the nesting of *Saturnalia tupiniquim* within sauropodomorphs has been consistently confirmed by independent studies (Ezcurra, 2010; Langer *et al.*, 2010; Nesbitt *et al.*, 2010; Yates, *et al.*, 2010; Martinez *et al.*, 2011, 2013; Pol *et al.*, 2011; McPhee *et al.*, 2015; Novas *et al.*, 2015; Otero *et al.*, 2015; Cabreira *et al.*, 2016). Regarding other non-sauropod sauropodomorphs, there is a growing consensus that no clade congregates all (nor most) taxa classically treated as 'Prosauropoda' to the exclusion of Sauropoda. Instead, these taxa have recently been found to represent a paraphyletic array in relation to Sauropoda (Ezcurra, 2010; Langer *et al.*, 2010; Yates, *et al.*, 2010; Pol *et al.*, 2011; McPhee *et al.*, 2015; Otero *et al.*, 2015).

3.6. Acknowledgements

3.7. References

Balanoff AM, Bever GS, IkejiriT. 2010. The braincase of *Apatosaurus* (Dinosauria: Sauropoda) based on computed tomography of a new specimen with comments on variation and evolution in Sauropod Neuroanatomy. *American Museum Novitates*. 3677, 1–29.

Barrett, P. M. 2000. Prosauropod dinosaurs and iguanas: speculations on the diets of extinct reptiles. In (ed. HD Sues) *Evolution of Herbivory in Terrestrial Vertebrates: Perspectives from the Fossil Record,* Cambridge University Press, Cambridge, pp. 42-78.

Barrett PM, Rayfield EJ. 2006. Ecological and evolutionary implications of dinosaur feeding behaviour. *Trends in Ecology and Evolution,* 21**,** 217–224.

Barrett PM, Upchurch P. 2007. The evolution of feeding mechanisms in early sauropodomorph dinosaurs. *Special Papers in Palaeontology,* 77, 91–112.

Barrett PM, Butler RJ, Nesbitt SJ. 2010. The roles of herbivory and omnivory in early dinosaur evolution. *Earth and Enviromental transactions of the Royal Society of Edinburgh,* 101, 383–396.

Benson RBJ. *et al*. 2014. Rates of Dinosaur Body Mass Evolution Indicate 170 Million Years of Sustained Ecological Innovation on the Avian Stem Lineage. *PLoS Biolgy,* 12(5), e1001853.

Bittencourt JS, Arcucci AB, Marsicano CA, Langer MC. 2014 Osteology of the Middle Triassic archosaur *Lewisuchus admixtus* Romer (Chañares Formation, Argentina), its inclusivity, and relationships amongst early dinosauromorphs. *Journal of Systematic Palaeontology,* 13(3), 189–219.

Bonnan MF, Senter P. 2007. Were the basal sauropodomorph dinosaurs *Plateosaurus* and *Massospondylus* habitual quadrupeds? *Special Papers in Palaeontology,* 77, 139–135.

Bonnan MF, Yates AM. 2007. A new description of the forelimb of the basal sauropodomorph *Melanorosaurus*: implications for the evolution of pronation, manus shape and quadrupedalism in sauropod dinosaurs. *Special Papers in Palaeontology,* 77, 157–168.

Butler AB, Hodos W. 1996. *Comparative Vertebrate Neuroanatomy: Evolution and Adaptation* 514 (Wiley-Liss, New York, 1996).

Cabreira SF. *et al*. 2011. New stem-sauropodomorph (Dinosauria, Saurischia) from the Triassic of Brazil. *Naturwissenchaften*. 98**,** 1035-1040.

Cabreira SF. *et al*. 2016. A unique Late Triassic dinosauromorph assemblage reveals dinosaur ancestral anatomy and diet. *Current Biology*.

Chatterjee S, Zheng Z. 2002. Cranial anatomy of *Shunosaurus*, a basal sauropod dinosaur from the Middle Jurassic of China. *Zoological Journal of the Linnean Society,* 136, 145–169.

Cruzado-Caballero P, Fortuny J, Llacer S, Canudo J. 2015. Paleoneuroanatomy of the European lambeosaurine dinosaur Arenysaurus ardevoli. *PeerJ,* 3, e802.

Evans DC, Ridgely R, Witmer LM. 2009. Endocranial anatomy of lambeosaurine hadrosaurids (Dinosauria: Ornithischia): a sensorineural perspective on cranial crest function. *Anatomical Record*, 292, 1315–1337.

Ezcurra MD. 2010. A new early dinosaur (Saurischia: Sauropodomorpha) from the Late Triassic of Argentina: a reassessment of dinosaur origin and phylogeny. *Journal of Systematic Palaeontology*, 8(3), 371-425.

Gould SJ, Vrba ES. 1982. Exaptation – a missing term in the science of form. *Paleobiology*, 8, 4–15.

Knoll F., *et al*. 2012 The braincase of the basal Sauropod dinosaur *Spinophorosaurus* and 3D reconstructions of the cranial endocast and inner ear. *PlosOne*, **7(1)**, e30060.

Langer MC. 2003. The sacral and pelvic anatomy of the stem-sauropodomorph *Saturnalia tupiniquim* (Late Triassic, Brazil). *Paleobios*, 23(2), 1–40.

Langer MC. 2014. The origins of Dinosauria: much ado about nothing. *Palaeontology*, 57(3), 469–478.

Langer MC, França MAG, Gabriel S. 2007. The pectoral girdle and forelimb anatomy of the stem sauropodomorph *Saturnalia tupiniquim* (Late Triassic, Brazil). *Special Papers in Palaeontology*, 77, 113–137.

Langer MC, Abdala F, Richter M, Benton MJ. 1999. A sauropodomorph dinosaur from the Upper Triassic (Carnian) of southern Brazil. *Earth and Planetary Science Letters*, 329, 511–517.

Langer MC, Ezcurra MD, Bittencourt JS, Novas FE. 2010. The origin and early evolution of dinosaurs. *Biological Reviews*, 85**,** 55–110.

Lautenschlager S, Rayfield EJ, Altangerel P, Zanno LE, Witmer LM. 2012. The Endocranial Anatomy of Therizinosauria and Its Implications for Sensory and Cognitive Function. *PLoS ONE*, 7(12), e52289.

Mallison H. The digital *Plateosaurus* I: Body mass, mass distribution and posture assessed using CAD and CAE on a digitally mounted complete skeleton. *Palaeontologia Electronica*, 13(2), 8A.

Martinez RN, Alcober OAA. 2009. Basal Sauropodomorph (Dinosauria: Saurischia) from the Ischigualasto Formation (Triassic, Carnian) and the Early Evolution of Sauropodomorpha. *PLoS ONE*, 4(2), e4397.

Martinez RN. e*t al*. 2011. A basal dinosaur from the dawn of the dinosaur Era in Southwestern Pangaea. *Science*, 331, 206-210.

Martinez RN, Apaldetti C, Abelin D. 2013. Basal Sauropodomorphs from the Ischigualasto Formation. *Journal of Vertebrate Palaeontology,* 32(suppl. 6), 51-69.

Mazzetta GM, Christianssen P, Farina RA. 2004. Giants and bizarres: body size of some Southern American Cretaceous dinosaurs. *Historical Biology,* **16**, 1.13.

McPhee BW *et al*. 2015. A new basal sauropod from the pre-Toarcian Jurassic of South Africa: evidence of niche-partitioning at the sauropodomorph-sauropod boundary? *Scientific Reports*, 5, 13224.

Nesbitt SJ. *et al*. 2010. Ecologically distinct dinosaurian sister group shows early diversification of Ornithodira. *Nature,* 464(4), 95–98.

Novas FE. *et al*. 2015. An enigmatic plant-eating theropod from the Late Jurassic period of Chile. *Nature,* 522, 331–334.

Otero A. *et al*. 2015. A new basal sauropodiform from South Africa and the phylogenetic relationships of basal sauropodomorphs. *Zoological Journal of the Linnean Society,* 174, 589-634.

Paulina-Carabajal A. 2012. Neuroanatomy of Titanosaurid Dinosaurs from the Upper Cretaceous of Patagonia, with comments on endocranial variability within Sauropoda. *Anatomical Record,* 295, 2141–2156.

Paulina-Carabajal A, Lee YN, Jacobs LL. 2016. Endocranial Morphology of the Primitive Nodosaurid Dinosaur *Pawpawsaurus campbelli* from the Early Cretaceous of North America. *PLoS ONE,* 11(3), e0150845.

Pol D, Garrido A, Cerda IA. 2011. A new sauropodomorh dinosaur from the Early Jurassic of Patagonia and the origin and evolution of the Sauropod-type sacrum. *Plos ONE,* 6(1), e14572.

Rauhut OWM, Fechner R, Remes K, Reis K. 2011. How to get big in the Mesozoic. In (eds. N Klein, K Remes, CT Gee, PM. Sander) *Biology of the sauropod dinosaurs: understanding the life of giant*. Indiana University Press, Bloomington and Indianapolis pp. 119-149.

Rogers SW. 1998. Exploring dinosaurs neuropaleobiology: Viewpoint, computed tomography, and analysis of an *Allosaurus fragilis* endocast. *Neuron,* 21, 673-679.

Sampson SD, Witmer LM. 2007. Craniofacial anatomy of *Majungasaurus crenatissimus* (Theropoda: Abelisauridae) from the Late Cretaceous of Madagascar. *Journal of Vertebrate Palaeontology,* 2, 32–102.

Sander PM. 2013. An Evolutionary Cascade Model for Sauropod Dinosaur Gigantism - Overview, Update and Tests. *PLoS ONE,* 8(10), e78573.

Sander PM. *et al*. 2011. Biology of the sauropod dinosaurs: the evolution of gigantism. *Biological Reviews,* 86, 117–155.

Sereno PC, Novas FE. 1993. The skull and neck of the basal theropod *Herrerasaurus ischigualastensis*. *Journal of Vertebrate Paleontology,* 13, 451-476.

Sereno PC, Forster CA, Rogers RR, Moneta AM. 1993. Primitive dinosaur skeleton from Argentina and the early evolution of Dinosauria. *Nature,* 361, 64-66.

Sobral G. *et al*. 2016. New information on the braincase and inner ear of *Euparkeria capensis* Broom: implications or diapsid and archosaur evolution. *Royal Society Open Science,* 3, 160072.

Upchurch P, Barrett PM, Galton PM. 2007. A phylogenetic analysis of basal sauropodomorph relationships: implications for the origin of sauropod dinosaurs. *Special Papers* in *Palaeontology,* 77, 57–90.

Walsh SA, *et al*. 2013. Avian cerebellar floccular fossa size is not a proxy for flying ability in birds. *Plos One,* 8(6), e67176.

Wilson JA. 2005. Sauropoda. In (eds. KA Curry Rogers, JA Wilson) *The sauropods: Evolution and Paleobiology,* University of California Press, Berkeley.

Winship IR, Wylie DRW. 2003. Zonal organization of the vestibulocerebellum in pigeons (*Columba livia*): I. Climbing fiber input to the flocculus. *Journal of Computational Neurology*, 456, 127–139.

Witmer LM, Chaterjee S, Franzosa J, Rowe T. 2003. Neuroanatomy of flying reptiles and implications for flight, posture and behaviour. *Nature*, 425, 950–953.

Witmer LM, Ridgely RC, Dufeau DL, Semones MC. 2008. Using CT to Peer into the Past: 3D Visualization of the Brain and Ear Regions of Birds, Crocodiles, and Nonavian Dinosaurs. In (eds E Hideki, F Roland) *Anatomical imaging: towards a new morphology*, Springer-Verlag, Tokyo, pp. 67-87.

Witzel U, Preuschoft H. 2005. Finite-element model construction for the virtual synthesis of the skulls in vertebrates: case study of Diplodocus. *Anatomical Record* 283, 391–401.

Yates AM, Bonnan MF, Nevelling J, Chinsamy A, Blackbeard MG. 2010. A new transitional sauropodomorph dinosaur from the Early Jurassic of South Africa and the evolution of sauropod feeding and quadrupedalism. *Proceedings of the Royal Society of London, B*, 277(1682), 787-794.

CHAPTER 4

Braincase anatomy of the early sauropodomorph *Saturnalia tupiniquim* (Late Triassic, Brazil)

Authors: Mario Bronzati[1,2,*], Max C. Langer, Oliver W. M. Rauhut[1,2]

Author contributions:

All authors conceptualized the study; **M.B.** segmented the CT-Scan data; **All authors** wrote the manuscript.

Chapter 4

Braincase anatomy of the early sauropodomorph *Saturnalia tupiniquim* (Late Triassic, Brazil)

Mario Bronzati[1,2,*], Max C. Langer[3], Oliver W. M. Rauhut[1,2]

[1] Bayerische Staatssammlung für Paläontologie und Geologie, Richard-Wagner-Straße 10, 80333 Munich, Germany.

[2] Faculty of Geosciences, Ludwig-Maximilians-Universität, Munich, Germany, Richard-Wagner-Straße 10, 80333 Munich, Germany.

[3] Faculdade de Filosofia Ciências e Letras de Ribeirão Preto, Universidade de Sao Paulo, Av. Bandeirantes 3900, 14040-901 Ribeirão Preto, São Paulo, Brazil.

4.1. Abstract

The braincase anatomy of the sauropodomorph dinosaur *Saturnalia tupiniquim* from the Late Triassic (Carnian) Santa Maria Formation of Brazil is described for the first time, using information based on CT-Scan data. The comparative description here provided fills a gap in the knowledge of braincase anatomy of early dinosaurs, still poorly known in comparison to the anatomy of later representatives of the group. In addition, we provide a discussion on the braincase features recently employed to investigate the phylogenetic relationships of early dinosaurs and dinosauromorphs. Our investigation indicates that the use of different nomenclatures in previous studies dealing with different archosauromorph sub-groups likely hampered the recognition of equivalent traits in taxa across different lineages. This is the case for the otic (or

semilunar depression) and the basioccipital recesses, which are more widespread among dinosaurs and its closest archosauriform relatives than previously suggested. Finally, the reassessment of previously proposed phylogenetic characters provides a stronger basis for future studies on dinosauromorph phylogeny.

4.2. Introduction

The braincase anatomy of dinosaurs has been deeply investigated. However, with a few exceptions (e.g. Galton, 1984, 1985; Galton & Bakker, 1985; Apaldetti *et al*., 2014; Nesbitt, 2011; Martinez *et al*. 2012a), most of these works were focused on Jurassic and Cretaceous taxa (e.g. Sampson & Witmer, 2007; Knoll *et al*., 2012; Lautenschlager *et al*., 2012; Sobral *et al*., 2012; Paulina-Carabajal *et al*., 2014). On the other hand, studies providing detailed anatomical descriptions of the earliest representatives of the clade (e.g. Martinez *et al*., 2012a), or of non-dinosaurian dinosauromorphs (Bittencourt *et al*., 2014), are scarce. Furthermore, these studies have mainly analysed braincase evolution in the context of a specific dinosaur lineage, especially Sauropodomorpha (e.g. Galton, 1984; Galton & Baker, 1985; Yates, 2007; Apaldetti *et al*., 2014). In this context, it is probably not misleading to state that the braincase anatomy of early dinosaurs is still poorly known in comparison to other parts of their skeleton (see e.g. Langer, 2003; Langer *et al*., 2007; Butler, 2010; Sereno *et al*, 2012). Various factors contribute to this relatively poor knowledge scenario. The braincase is not preserved in many Triassic taxa (e.g. *Chromogisaurus novasi*, *Staurikosaurus pricei*, *Guaibasaurus candelariensis*, *Chindesaurus briansmalli*, *Pisanosaurus mertii*); other have incomplete or fragmentary braincases (e.g. *Eocursor parvus*, *Eodromaeus murphi*, *Pampadromaeus barberenai*) or the braincase is preserved but not entirely visible (e.g. *Herrerasaurus*

ischigualastensis, *Eoraptor lunensis*). Additionally, more detailed descriptions of the braincase anatomy is still a lacking for many taxa with a complete or almost complete braincase, as is the case for *Tawa hallae* and *Saturnalia tupiniquim* (see Table 1).

Here, we describe the braincase anatomy of *Saturnalia tupiniquim*, from the Late Triassic (Carnian – c. 230 Ma) of Brazil. *Saturnalia tupiniquim* was firstly described by Langer *et al*. (1999) and it is consistently found as a sauropodomorph in phylogenetic analyses (e.g. Nesbitt *et al*., 2009, 2012; Ezcurra, 2010; Martinez *et al*., 2011, 2012 Cabreira *et al*., 2016). The post-cranial, particularly appendicular anatomy of *S*. *tupiniquim* is well known (Langer, 2003; Langer *et al*., 2007), but its braincase has never been described in detail. Given its age and phylogenetic position, *S*. *tupiniquim* corresponds to a key taxon in studies about the origin and the early evolution of Dinosauria and Sauropodomorpha. As the braincase anatomy of non-sauropodan sauropodomorphs has been discussed elsewhere (Chapter 5), this study will mostly focus on braincase evolution in the context of early dinosaurs and non-dinosaurian dinosauromorphs.

Institutional Abbreviations

BPI - Bernard Price Institute for Palaeontological Research, University of the Witwaaterstrand, Johannesburg, South Africa; **CAPPA/UFSM** – Centro de Apoio à Pesquisa Paleontológica, Universidade Federal de Santa Maria, Santa Maria, Brazil; **GR** - Ghost Ranch Ruth Hall Museum of Palaeontology, Abiquiu, USA; **MB** - Museum für Naturkunde, Berlin, Germany; **MCP PV** - Museu de Ciências e Tecnologia, Pontificia Universidade Católica do Rio Grande do Sul, Porto Alegre, Brazil; **NHMUK** - British Museum of Natural History; **OUMNH** - Oxford University Museum of Natural History, Oxford, UK; **PVL** - Paleontologia de Vertebrados Lillo,

Tucuman, Argentina; **PVSJ** - Museo de Ciencias Naturales, San Juan, Argentina; **PULR** - Universidad Nacional de La Rioja, La Rioja, Argentina; **QG** - Queen Victoria Museum, Salisbury, Zimbabwe; **SAM** - Iziko South African Museum, Capetown, South Africa; **SMNS** - Staatliches Museum für Naturkunde, Stuttgart, Germany; **ULBRA-PV** - Museu de Ciências Naturais, Universidade Luterana do Brasil, Canoas, Brazil; **ZPAL** – Institute of Paleobiology of the Polish Academy of Sciences, Warsaw, Poland.

4.3. Material & Methods

The braincase of *Saturnalia tupiniquim*

Saturnalia tupiniquim is known on the basis of three fairly complete specimens: MCP–3844–PV (holotype); MCP–3845–PV and 3846–PV (paratypes); see Langer (2003) for more details. Langer et al. (1999) provided a very preliminary description of *S. tupiniquim*, and more detailed acconts on specific parts of the skeleton were provided latter. Langer (2003) described the anatomy of pelvic girdle and hind limb, and Langer et al. (2007) focused on the shoulder girdle and forelimb anatomy. The braincase is only preserved in MCP-3845-PV. An account about the soft tissues of the braincase has been presented in Chapter 3, but its osteology has not been addressed in detail.

Table 4.1 (next two pages): List of dinosauromorphs commonly used as Operational Taxonomic Units in phylogenetic analysis focusing on early dinosaurs. Their phylogenetic affinities, and respective bones of the braincase known for each of the taxon.

TAXA	PHYLOGENETIC STATUS	FRONTAL	PARIETAL	BASIOCCIPITAL	PARABASISPHENOID	PROOTIC	OTOCCIPITAL	SUPRAOCCIPITAL	LATEROSPHENOID	DESCRIPTION
MIDDLE TRIASSIC										
Lagerpeton chanarensis	Lagerpetidae (e.g. Langer, 2014)	Unknown	Unknown	Unknown	Unknown	Unknown	Unknown	Unknown	Unknown	--
Marasuchus lilloensis	Dinosauriform, sister group of all other dinosauriforms and dinosaurs (Nesbitt, 2011; Bittencourt *et al.*, 2014)	Unknown	Unknown	Preserved	Preserved	Preserved	Preserved	Preserved	Unknown	Briefly Described (Sereno & Arcucci, 1994)
Asilisaurus kongwe	Uncertain: Silesauridae (e.g. Nesbitt *et al.*, 2010/ Dinosauriform sister group of silesaurids plus dinosaurs(e.g. Bittencourt *et al.*, 2014)	Unknown	Unknown	Unknown	Unknown	Unknown	Unknown	Unknown	Unknown	--
Lewisuchus admixtus	Uncertain: Silesauridae (e.g. Nesbitt *et al.*, 2010) / Dinosauriform, sister group of silesaurids plus dinosaurs (e.g. Bittencourt *et al.*, 2014)	Unknown	Poorly Preserved	Preserved	Preserved	Preserved	Preserved	Preserved	Preserved	Described (Bittencourt *et al.,* 2014)
Pseudolagosuchus major	Uncertain: Silesauridae (e.g. Nesbitt *et al.*, 2010) / Dinosauriform, sister group of silesaurids plus dinosaurs (e.g. Bittencourt *et al.*, 2014)	Unknown	Unknown	Unknown	Unknown	Unknown	Unknown	Unknown	Unknown	--
Lutungutali sitwensis	Silesauridae (Peecock *et al.,* 2014)	Unknown	Unknown	Unknown	Unknown	Unknown	Unknown	Unknown	Unknown	--
Ixalerpeton polesinensis	Lagerpetidae (Cabreira *et al.*, 2016)	Preserved	Preserved	Preserved	Preserved	Preserved	Preserved	Preserved	Unknown	Briefly Described (Cabreira *et al.,* 2016)
LATE TRIASSIC - CARNIAN										
Dromomeron gigas		Unknown	Unknown	Unknown	Unknown	Unknown	Unknown	Unknown	Unknown	--
Saltopous elginensis	Uncertain: Dinosauriform (Benton *et al.*, 2011)	Unknown	Unknown	Unknown	Unknown	Unknown	Unknown	Unknown	Unknown	--
Ignotosaurus fragilis	Silesauridae (Martinez et al., 2013, 2016)	Unknown	Unknown	Unknown	Unknown	Unknown	Unknown	Unknown	Unknown	--
Diodorus scytobrachion	Silesauridae (Kammerer et al., 2012)	Unknown	Unknown	Unknown	Unknown	Unknown	Unknown	Unknown	Unknown	--
Pisanosaurus mertii	Ornithischia (Langer et al., 2010)	Unknown	Unknown	Unknown	Unknown	Unknown	Unknown	Unknown	Unknown	--
Herrerasaurus ischigualastensis	Uncertain: Theropoda (e.g. Nesbitt *et al.*, 2010)/"stem"- Saurischia (e.g. Langer *et al.*, 2010)	Preserved	Preserved	Preserved	Preserved	Unknown	Preserved	Preserved	Unknown	Briefly Described (Sereno & Novas, 1993)
Sanjuansaurus gordilloi	Herrerasauridae (e.g. Alcober & Martinez, 2010; Bittencourt *et al,*. 2014)	Unknown	Unknown	Unknown	Unknown	Unknown	Unknown	Unknown	Unknown	--
Staurikosaurus pricei	Herrerasauridae: within Theropoda (Sues *et al.,* 2011)/"stem"-Saurischia (Bittencourt *et al*., 2014)	Unknown	Unknown	Unknown	Unknown	Unknown	Unknown	Unknown	Unknown	--
Eoraptor lunensis	Uncertain: Theropoda (e.g. Nesbitt *et al*., 2011)/Sauropodomorpha (e.g. Martinez *et al*., 2013)/Saurischia outside Theropoda or Sauropodomorpha (Bittencourt *et al*., 2014)	Preserved	Preserved	Unknown	Preserved	Unknown	Unknown	Poorly Preserved / Misidentified	Unknown	Briefly Described (Sereno *et al*., 2012)
Eodromaeus murphi	Theropoda (e.g. Martinez *et al*., 2011; Bittencourt *et al*., 2014)	Unknown	Unknown	Preserved	Preserved	Preserved	Poorly Preserved	Unknown	Unknown	Briefly Described (Martinez *et al.,* 2011)
Panphagia protos	Sauropodomorpha (e.g. Martinez & Alcober, 2009)	Preserved	Preserved	Unknown	Unknown	Preserved	Unknown	Preserved	Unknown	Described (Martinez *et al.,* 2012)
Saturnalia tupiniquim	Sauropodomorpha (e.g. Langer *et al*., 2010; Bittencourt *et al*., 2014)	Preserved	Preserved	Preserved	Preserved	Preserved	Preserved	Preserved	Preserved	Described here
Chromogisaurus novasi	Sauropodomorpha (e.g. Ezcurra, 2010; Bittencourt *et al*., 2014)	Unknown	Unknown	Unknown	Unknown	Unknown	Unknown	Unknown	Unknown	--
Pampadromaeus barbarenai	Sauropodomorpha (e.g. Cabreira *et al*., 2011)	Unknown	Unknown	Unknown	Unknown	Unknown	Unknown	Unknown	Unknown	--
Buriolestes schultzi	Sauropodomorpha (Cabreira *et al*., 2016)	Preserved	Unknown	Unknown	Unknown	Unknown	Unknown	Unknown	Unknown	Briefly Described (Cabreira *et al.,* 2016)

LATE TRIASSIC - NORIAN

Taxon	Classification									Description
Dromomeron romeri and *D. gregorii*	Lagerpetidae (Martinez *et al.,* 2016)	Unknown	Unknown	Unknown	Unknown	Unknown	Unknown	Unknown	Unknown	--
Silesaurus opolensis	Silesauridae (e.g. Nesbitt *et al.*, 2010; Bittencourt *et al.,* 2014)	Preserved	Preserved	Preserved	Preserved	Preserved	Preserved	Preserved	Unknown	Briefly Described (Dzik, 2003)
Sacisaurus agudoensis	Silesauridae (e.g. Langer & Ferigolo, 2013; Bittencourt *et al.,* 2014)	Unknown	Unknown	Unknown	Unknown	Unknown	Unknown	Unknown	Unknown	--
Eucoelophysis baldwini	Theropoda (e.g. Nesbitt *et al.*, 2010)									
Eocursor parvus	Ornithischia (Butler *et al.*, 2007; Cabreira *et al.,* 2016)	Unknown	Unknown	Unknown	Preserved	Unknown	Unknown	Preserved	Unknown	Described (Butler, 2010)
El Tranquilo Heterodontosaurid		Unknown	Unknown	Unknown	Unknown	Unknown	Unknown	Unknown	Unknown	--
Chindesaurus bryansmalli	Herrerasauridae (Sues *et al.*, 2011)	Unknown	Unknown	Unknown	Unknown	Unknown	Unknown	Unknown	Unknown	--
Coelophysis	Theropoda (e.g. Nesbitt *et al.*, 2010; Bittencourt *et al*., 2014)	Preserved	Preserved	Preserved	Preserved	Preserved	Preserved	Preserved	Preserved	--
Procompsognathus triassicus	Theropoda (Langer, 2014)									
Zupaisaurus rougieri	Theropoda (Ezcurra, 2007)	Preserved	Preserved	Preserved	Unknown	Unknown	Preserved	Preserved	Unknown	Described (Ezcurra,2007)
Tawa hallae	Theropoda (Nesbitt *et al*., 2009) / "stem"-Saurischia (Cabreira *et al.,* 2016)	Preserved	Preserved	Preserved	Preserved	Preserved	Preserved	Preserved	Preserved	Briefly Described (Nesbitt *et al.,* 2009)
Daemonosaurus chauliodus	Theropoda (Sues et al. 2011)									
Guaibasaurus candelariensis	Uncertain: Theropoda (e.g. Langer *et al.,* 2011)/Sauropodomorpha (Ezcurra, 2010)/"stem"-Saurischia (Cabreira *et al.,* 2016)	Unknown	Unknown	Unknown	Unknown	Unknown	Unknown	Unknown	Unknown	--
Pantydraco caducus	Sauropodomorpha (Yates, 2007)	Preserved	Preserved	Preserved	Preserved	Preserved	Preserved	Preserved	Preserved	Described (Galton & Kermack, 2010)
Thecodontosaurus antiquus	Sauropodomorpha (Yates, 2007)	Preserved	Preserved	Preserved	Preserved	Preserved	Preserved	Preserved	Unknown	Briefly Described (Benton *et al.,* 2000)
Efraasia minor	Sauropodomorpha (Yates, 2007)	Preserved	Preserved	Preserved	Preserved	Preserved	Preserved	Preserved	Preserved	Described (Bronzati & Rauhut, xxxx)
Plateosaurus	Sauropodomorpha (Yates, 2007)	Preserved	Preserved	Preserved	Preserved	Preserved	Preserved	Preserved	Preserved	Described (Galton, 1985)

LATE TRIASSIC - RHAETIAN

Taxon	Classification									Description
Liliensternus liliensterni	Theropoda (Sues *et al.,* 2011)									
Lophostropheus airelensis	Theropoda (Ezcurra & Cuny, 2007)	Unknown	Unknown	Unknown	Unknown	Unknown	Unknown	Unknown	Unknown	--

EARLY JURASSIC

Taxon	Classification									Description
Lesothosaurus diagnosticus	Ornithischia (Nesbitt *et al.,* 2009; Langer *et al.,* 2010)	Preserved	Preserved	Preserved	Preserved	Preserved	Preserved	Preserved	Preserved	Described (Porro *et al.,* 2015)
Heterodontosaurus	Ornithischia (Norman *et al.,* 2011; Cabreira *et al.,* 2016)	Preserved	Preserved	Preserved	Preserved	Preserved	Preserved	Preserved	Preserved	Described (Norman *et al.,* 2011)

CT-Scan

The block containing the specimen (Fig. 4.1) is heavily fractured, so that its mechanical preparation could be potentially risky. Hence, computed tomography was employed in order to access the braincase anatomy of *Saturnalia tupiniquim*. The specimen was scanned at the Zoologische Staatsammlung München (Bavaria State Collection of Zoology, Munich, Germany) in a Nanotom Scan (GE Sensing & Inspection Technologies GmbH, Wunstorf Germany) using the following parameters: Voltage: 100 Kv; Current: 130 µA; 3,1 µm voxel size). 1440 x-ray slices were generated; these were down sampled by half and then segmented in the software Amira (version 5.3.3, Visage Imaging, Berlin, Germany).
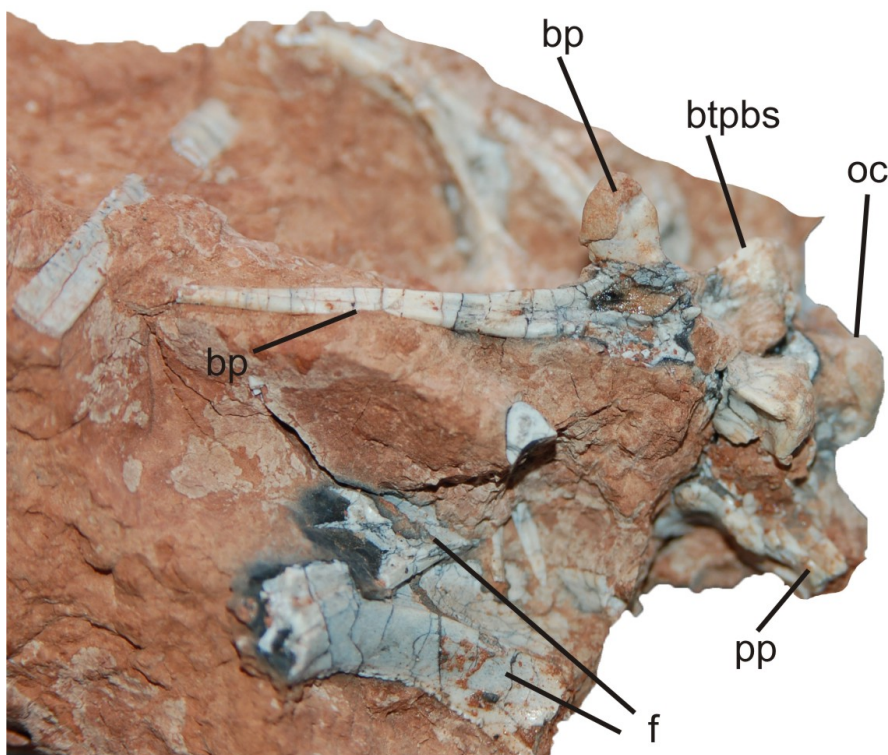
Figure 4.1: General view of the block containing the braincase of the specimen MCP 3845 PV of *Saturnalia tupiniquim*. Abbreviations: **bp** – basipterygoid process; **btpbs** – basisphenoid component of the basal tubera; **cpp** – cultriform process of the parabasisphenoid; **f** – frontal; **oc** – occipital condyle; **pp** – paroccipital process.

4.4. RESULTS

In the following description we employed traditional anatomical and directional terms such as 'anterior' and 'posterior' rather than using the veterinary terms 'cranial' and 'caudal', respectively. Taxa used for comparisons are detailed in Table 4.2.

Table 4.2: List of comparative taxa used in the present study. Specific collection numbers represent specimens analysed first-hand by the authors, whereas other comparative data were obtained from the literature listed within the table

Taxon	Source of information
Adeopapposaurus mognai	PVSJ 568; PVSJ 610
Buriolestes schultzi	UFSM XXXX
Coelophysis "Syntarsus" rhodesiensis	QG 195; QG 197
Coloradisaurus brevis	PVL 3967
Eocursor parvus	SAM-PK-K8025
Eoraptor lunensis	PVSJ 512; Sereno *et al.*, 2013
Euparkeria capensis	SAM-PK-7696; SAM-PK-5867
Herrerasaurus ischigulastensis	PVSJ 407
Hypsilophodon foxii	OUMNH R2477
Ixalerpeton polesinensis	ULBRA-PVT059
Lesothosaurus diagnosticus	NHMUK PV R8501
Lewisuchus admixtus	PULR 01
Marasuchus lilloensis	PVL 3872
Massospondylus carinatus	SAM-PK-K1314
Panphagia protos	PVSJ 8743
Pantydraco caducus	NHMUK - P.24; P.141/1
Plateosaurus engelhardti	MB.R.5586-1; SMNS 13200; Prieto-Marquez & Norell, 2011
Prolacerta broomi	BPI 5066
Silesaurus opolensis	ZPAL Ab III/361; ZPAL Ab III/362
Sphenosuchus acutus	SAM-PK-K3014
Tawa hallae	GR 241
Thecodontosaurus antiquus	Benton *et al.*, 2000
Unaysaurus tolentinoi	UFSM11069

General aspects of the braincase

CT-Scan data shows that all the braincase bones are preserved inside the matrix. This includes right and left frontals and parietals (the skull roof), parabasisphenoid, basioccipital, supraoccipital, both otoccipitals (= exoccipital + opisthotic *sensu* Sampson & Witmer, 2007), and laterosphenoids. However, bone sutures are not all

visible, probably due to an advanced stage of fusion between the elements and also for some aspects of the tomographic procedure. For instance, a suture line between the exoccipitals and the basioccipital is clearly visible on the occipital condyle of the specimen to the naked eye. Furthermore, the pattern of this suture, at the dorsolateral portion of the occipital condyle, corresponds to the morphology observed in other dinosauriforms analysed for this study. Nevertheless, this suture was not recognised in the CT-Scan of *Saturnalia tupiniquim*.

The laterosphenoids, frontals, and parietals are preserved as isolated elements, whereas the supraoccipital, otoccipitals, parabasisphenoid, basioccipital, and prootic are preserved in articulation (Fig. 4.2). Yet, a previous breakage separated parts of the basioccipital and otoccipital, including the occipital condyle, from the other elements. These were glued to the remaining of the braincase before the CT-Scan procedure. Based on the segmentation results, it is also possible to observe a line of fracture at the level of the lateral cranial openings (Fig. 4.2). That fracture was, most likely, not restricted to the natural limits of the bones forming the dorsal (prootic, otoccipitals, supraoccipital) and ventral (basioccipital and parabasisphenoid) portions of the braincase. Instead, it might correspond to a fracture at the dorsoventral portion of the braincase where it is most fragile (i.e. at the level of the lateral openings of the fenestra ovalis, trigeminal and facial foramina, and 'metotit' foramen), thus more susceptible to fractures. Indeed, the portion of the otoccipital containing the apertures related to cranial nerve XII (hypoglossal) is preserved articulated to the ventral piece of the braincase, which includes the basioccipital and parabasisphenoid. On the other hand, the major portion of the otoccipital is separate from that piece, preserved instead in articulation with elements of the dorsal portion of the braincase, such as the prootic and the otoccipitals. This preservation pattern is also seen in two braincases of

the sauropodomorph *Plateosaurus engelhardti* (MB.R. 5855.1 and AMNH 6810). It is important to stress this situation because the difficulty to recognize all bone limits in the CT-Scan data hampers a more detailed description of some elements, and also the exact identification of the part each bone takes in well-recognized structures of the braincase. Moreover, this has also implications in what concerns the maturity of the individual.

Langer et al. (2007) argued that the more gracile aspect of the bones of MCP-3845-PV in relation to those of the holotype could indicate that the specimen dealt with here was most likely a juvenile or sub-adult that had already reached the adult size. Regarding the anatomy of the braincase, sauropodomorph specimens considered as juvenile individuals (based on evidences of their cranial and postcranial anatomy), such as *Efraasia minor* (Galton & Bakker, 1985 1983), *Pantydraco caducus* (Galton & Kermack, 2010), and *Unaysaurus totentinoi* (J. Bittencourt, pers. comm.), do not exhibit a firm junction at the parabasisphenoid-basioccipital contact, with these elements preserved disarticulated from one another (Chapter 5). Outside Sauropodomorpha, the lack of closed braincase sutures in the holotype of *Tawa hallae* has been considered as an indication of its juvenile condition (Nesbitt *et al.*, 2009). In this context, the well-developed articulation between the basioccipital and parabasisphenoid of MCP-3845-PV, with both elements firmly attached to one another, suggests that the specimen most likely does not represent a juvenile of *Saturnalia tupiniquim*.
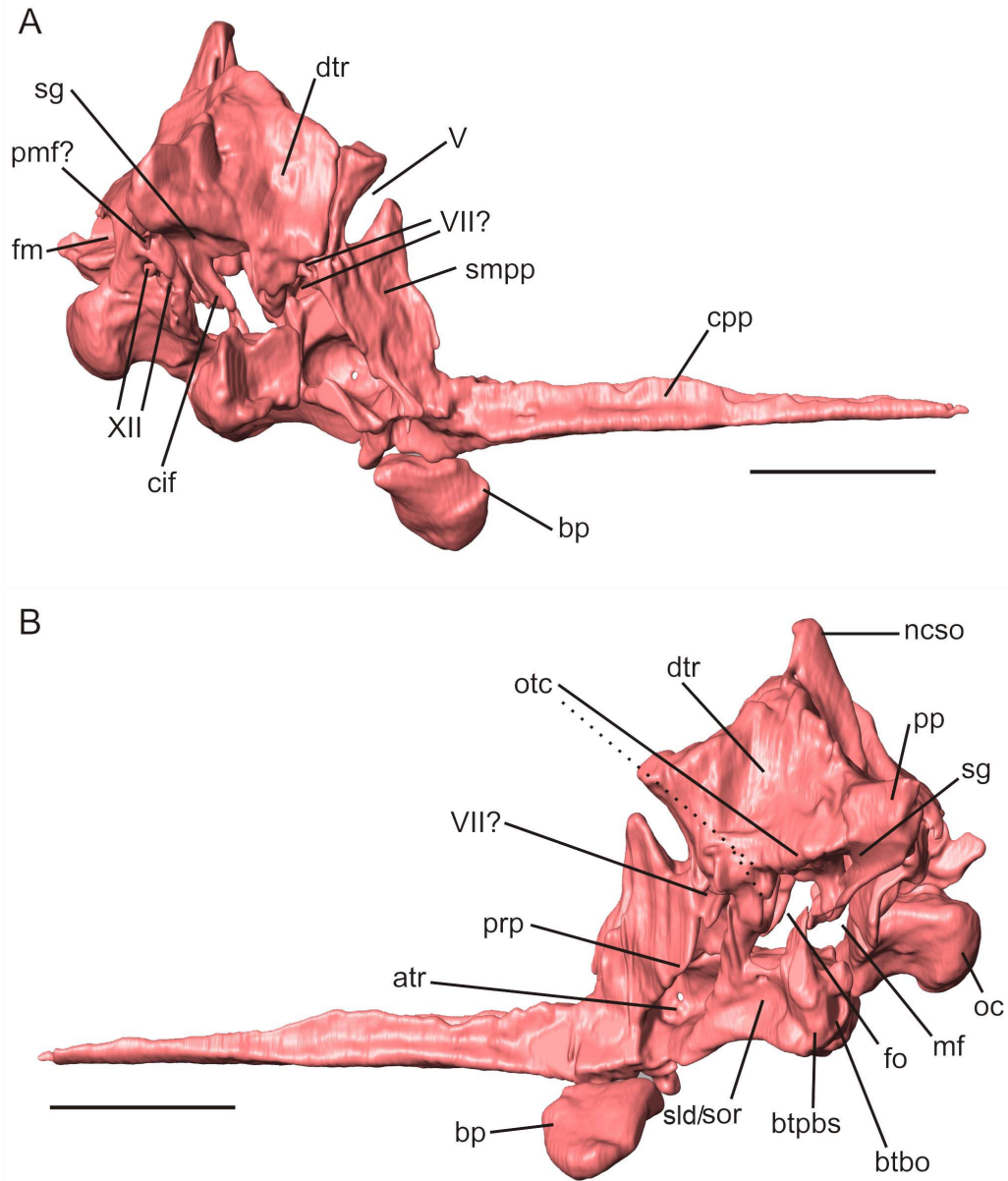
Figure 4.2: Braincase of the specimen MCP 3845 PV of *Saturnalia tupiniquim* in right (A) and left (B) lateral views. Abbreviations: **atr** – anterior tympanic recess; **bp** – basipterygoid process; **btbo** – basioccipital component of the basal tubera; **btpbs** – basisphenoid component of the basal tubera; **cif** – crista interfenestralis; **cpp** – cultriform process of the parabasisphenoid; **dtr** – dorsal tympanic recess; **fm** – foramen magnum; **fo** – fenestra ovalis; **mf** – metotic foramen; **ncso** – nuchal crest of the supraoccipital; **oc** – occipital condyle; **otc** – otosphenoidal crest; **pmf** – additional foramen posterior to the metotic foramen; **pp** – paroccipital process; **prp** – preotic pendant; **sg** – stapedial groove; **smpp** – surface for attachment of the *protractor pterygoideus* muscle; **sld/sor** – semilunar depression / subotic recess; **V** – notch for the trigeminal nerve; **VII** – foramen for the facial nerve; **XII** – foramen for the hypoglossal nerve. Scale bars = 1 cm.

The anteroposterior length of the braincase, from the occipital condyle to the tip of the cultriform process is c. 54 mm, approximately half of the total skull length, estimated in 98 mm (Appendix for Chapter 3). This ratio (anteroposterior length of the braincase/skull) is not possible to be precisely established for most early dinosaurs, because the anterior tip of the cultriform process is hidden by matrix or other bones (e.g. *Eoraptor lunensis*, *Herrerasaurus ischigualastensis*), or simply because the skull including the braincase is not entirely preserved (e.g. *Panphagia protos*, *Pantydraco caducus*). Nevertheless, the ratio in *Saturnalia tupiniquim* roughly approaches that of the sauropodomorph *Massospondylus carinatus* (0.5 in BP I 5241; c. 0.6 in SAM-PK-K1314) and the ornithischian *Lesothosaurus diagnosticus* (c. 0.5, Porro *et al*., 2016); the latter, however, lacks the anterior tip of the pre-maxilla.

Skull Roof

Frontal

CT-scan data shows both frontals of MCP-3845-PV preserved inside the matrix (Fig. 4.3). Each frontal is arched dorsally in the anteroposterior axis, with the most dorsal point approximately at the mid-point of that axis. This results in a concave ventral surface in lateral/medial views. Even probably lacking a small part of its anterior tip (see discussion below), the frontal is c. 1.7 times longer than wide (maximal length – c. 29 mm /maximal width – c. 17 mm). A similar condition is observed in all taxa analysed for this study. Martinez et al. (2012a, p.80) stated that some sauropodomorphs, such as *Plateosaurus engelhardti*, *Adeopapposaurus mognai*, and *Massospondylus carinatus* possess a wider than long frontal, differing from the condition of some Carnian dinosaurs. However, the frontal of *P. engelhardti*, *A.*

mognai, and *M. carinatus* is also longer than wider. The width is only greater than the length if measurements are taken from both frontals together.
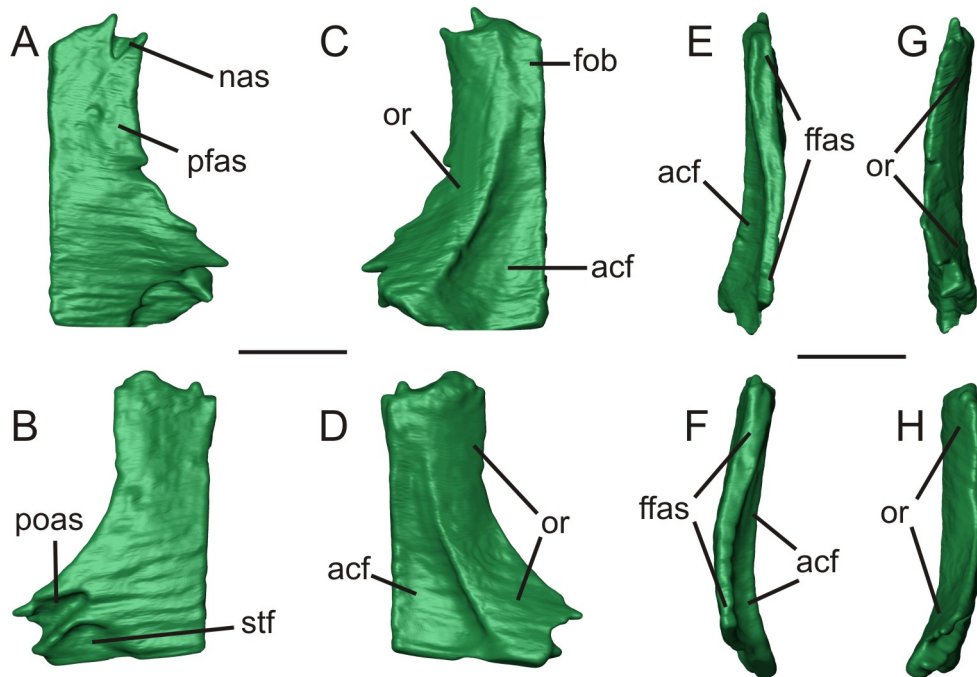
Figure 4.3: Right and left frontals of the specimen MCP 3845 PV of *Saturnalia tupiniquim* in dorsal (A, B), ventral (C, D), medial (E, F), and lateral (G, H) views, respectively. Abbreviations: **acf** – anterior cranial fossa; **ffas** – frontal/frontal articulation surface; **fob** – fossa for the olfactory bulb; **nas** – articulation surface with the nasal; **or** – orbital roof; **pfas** – articulation surface with the prefrontal; **poas** – articulation surface with the postorbital; **stfo** – supratemporal fossa. Scale bars = 1 cm

The frontal pair of *Saturnalia tupiniquim* has a sub-rectangular anterior half and is T-shaped in dorsal/ventral views (Fig. 4.3), as in *Herrerasaurus ischigualastensis* and *Plateosaurus engelhardti*. This is because these taxa lack a lateral expansion in the anterior half of the bone, as seen in forms such as *Panphagia protos* and *Tawa hallae*. In these taxa, such lateral expansion gives an hour-glass shape to the bones. Furthermore, from its mid-length, each frontal of *S. tupiniquim*

gets progressively wider posteriorly, as in *P. engelhardti*, *H. ischigualastensis*, and *Lesothosaurus diagnosticus*. This gives a broader aspect to this portion of the skull roof of those animals, in relation to other forms such as *Panphagia protos*, *Silesaurus opolensis*, and *Buriolestes schultzi*, in which the lateral expansion of the frontal occurs more posteriorly (in the antero-posterior axis).

A slot in the anterolateral corner of the dorsal surface of the frontal probably corresponds to the articulation for the nasal (Fig. 4.3). Slightly posterior to this notch, a shallow, half-moon shaped depression most likely corresponds to the pre-frontal articulation (Fig. 4.3). This depression extends for slightly more than one third of the anteroposterior length of the frontal, and medially it reaches half of the width of the bone in this region. Also at the dorsal surface of the bone, the articulation area for the postorbital is located at the posterolateral corner, anterolateral to the portion of the frontal that contributes to the anterior margin of the supratemporal fossa. The slot for the postorbital extends anteromedially, reaching the mid-length of the anterior margin of the supratemporal fossa, from which it is separated by a crest. The supratemporal fossa occupies the lateral-half of the posterior margin of the frontal. A portion of the supratemporal fossa excavating the frontal is seen in all dinosauriforms, but not in the lagerpetid *Ixalerpeton polesinenis* (Cabreira *et al*. 2016).

In *Saturnalia tupiniquim*, the posterior margin of the frontal is lateromedially straight to slightly convex (Fig. 4.3), differing from the more concave aspect seen in *Plateosaurus engelhardti*. In both taxa, the frontal does not participate in the border of the supratemporal fenestra, from which it is excluded by an anterolateral projection of the parietal (see below) that contacts the postorbital along the anteromedial corner of the fenestra. As for the participation of the frontal in the supratemporal fenestra of other early dinosaurs, fractures and the preservation of the fossil do not allow the

recognition of a posterior projection of the bone reaching the supratemporal fenestra in *Herrerasaurus ischigualastensis*, as proposed by Sereno & Novas (1993, fig. 1c) and Martinez et al. (2012a, fig. 2). In addition, the irregular shape of the posterior margin of the frontals of *Panphagia protos* is most likely due to breakage, and it is also not possible to be sure about the presence of that posterior projection.

In *Saturnalia tupiniquim*, a crest extends along the entire anteroposterior axis of the ventral surface of the frontal (Fig. 4.3), setting two distinct surfaces appart, the orbital roof laterally and the endocranial surface medially. This configuration as a single ridge is also seen in the sauropodomorphs *Efraasia minor* and *Plateosaurus engelhardti*, and the lagerpetid *Ixalerpeton polesinensis*. A different condition is observed in *Panphagia protos*, in which two parallel ridges extend along the entire separation of the two regions. *Silesaurus opolensis* and *"Syntarsus" rhodosiensis* also have a double crest in the posterior two thirds of the frontal, but these merge into a single one anteriorly, at the limit between orbital roof and endocranial surface of these taxa.

The lateral margin of the frontal is formed by the crest corresponding to the roof of the orbit (Fig. 4.3). This is more dorsally raised at its midpoint, following the general condition of the whole bone. Thus, the orbital roof is dorsally arched in lateral view. Yet, it is ventrally concave in transverse section, raising dorsally towards the lateral margin at an angle of c. 45 degrees to the endocranial roof. This inclination resembles the condition of *Panphagia protos*. In *Silesaurus opolensis*, the orbital roof is more 'verticalized', an angle of c. 60 degrees is formed between the two regions of the ventral surface of the frontal. In *"Syntarsus" rhodosiensis* and *Plateosaurus engelhardti*, the angle between those regions is less than 30 degrees, and the orbital roof is more horizontal.

In *Saturnalia tupiniquim*, the lateral margin of the orbital roof parallels the crest that sets its medial limit. Hence, the width of the orbital roof remains constant along its entire anteroposterior length. Also, the orbital roof extends along the entire lateral margin of the frontal as preserved. This differs from the condition observed in *Silesaurus opolensis*, *"Syntarsus" rhodosiensis*, *Panphagia protos*, and *Plateosaurus engelhardti*, in which the orbital roof is restricted to the posterior two thirds of the ventral surface of the frontal. On the contrary, the orbital roof of *Lesothosaurus diagnosticus* is restricted to the anterior two-thirds of ventral surface of the frontal.

Two fossae are present on the endocranial surface of the frontals in *Saturnalia tupiniquim* (Fig. 4.3). The more posterior probably represents the anterior cranial fossa (*fossa cranii anterioris* in Martinez *et al.*, 2012a), where the frontal roofed part of the anterior portion of the brain (telencephalon). That fossa extends for c. 75% of the anteroposterior length of the frontal, reaching the posterior margin of the bone. It occupies most of the endocranial surface of the frontal, except for its lateroposterior corner, where the ventral surface of the bone is flat. This fossa is also found in other early dinosaurs such as *"Syntarsus" rhodosiensis* and *Panphagia protos*, but divided into anterior and posterior parts by a low crest. In *Lesothosaurus diagnosticus* the ridge is absent, and the cranial fossa is continuous. Anterior to the fossa cranii rostralis, in the anterior fourth of the frontal of *S. tupiniquim*, another depression corresponds to the fossa for the olfactory bulb. This is elliptical in shape and approximately five times smaller than the anterior cranial fossa.

Parietal

The description of the parietal is based only on the left element, which is completely preserved (Fig. 4.4). The right parietal is broken and partially preserved in separate

pieces, adding no extra anatomical information. The total length of the parietal is c. 22 mm, and its maximum width, from the posterolateral corner of the parietal wing to the medial suture to its counterpart, is 13 mm (Fig. 4.4). The bone is composed of two parts, the anterior body (sometimes treated as the main body of the parietal – e.g. Martinez *et al.*, 2012a) and the parietal wing. The former corresponds the portion extending from the anterior margin of the bone to the point where its long transverse axis is twisted from a horizontal to a vertical plane. The parietal is isolated, but its anterior body probably contacted the frontal anteriorly, the supraoccipital posteroventrally, the laterosphenoid lateroventrally, and eventually the postorbital laterally. The parietal wing would have contacted the supraoccipital medially, the paraocciptal process of the otoccipital ventrally, and the squamosal distally. In *Saturnalia tupiniquim*, the anteroposterior lengths of those two regions are nearly the same, as in *Ixalerpeton polesinensis, Herrerasaurus ischigualastensis*, and *Eoraptor lunensis*. In contrast, the anteroposterior length of the anterior body corresponds to c. 0.8 of that of the parietal wing in *Plateosaurus engelhardti*, and to c. 1.5 in *Panphagia protos*.

The anterior margin of the parietal contacts the posterior margin of the frontal via an interdigitating suture in taxa such as *Ixalerpeton polesinensis, Herrerasaurus ischigualastensis*, and *Plateosaurus engelhardti*. In *Saturnalia tupiniquim* (Fig. 4.4), the anterior margin of the parietal is mostly straight (the same is true for the posterior margin of the frontal), but bears two slots that may represent articulation points with the posterior margin of the frontal. The opposite was suggested for *Panphagia protos* (Martinez et al. 2012a), but we could not observe any evidence of an interdigitating suture in this taxon after first hand analysis of the specimens. Yet, the absence of an interdigitating suture could be a preservation bias seen in both *S. tupiniquim* and *Pa.*

protos. In these taxa, the parietal and frontal are not preserved in articulation, and the small and delicate projections of an interdigitating suture could have been lost during preservation or preparation. Other possibility for *S. tupiniquim* is that the CT-Scan data could not reconstruct the delicate morphology of an interdigitating suture, as suggested for *Lesothosaurus diagnosticus* (Porro et al. 2015).
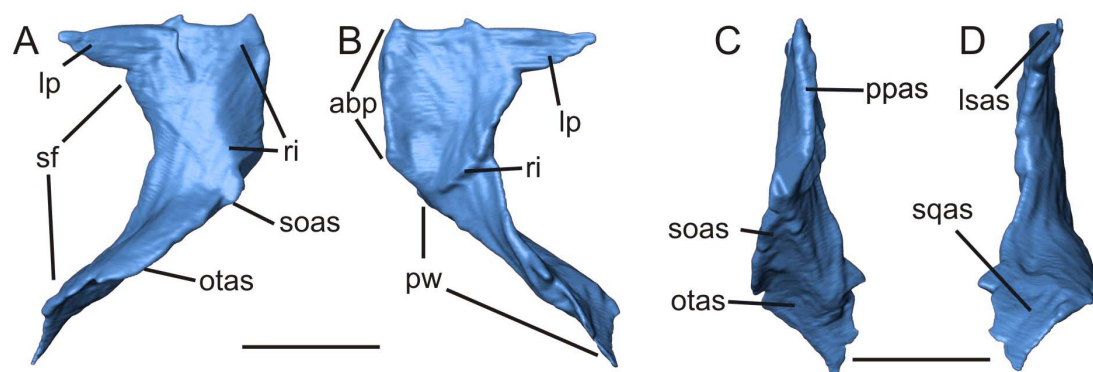
Figure 4.3: Left parietal of the specimen MCP 3845 PV of *Saturnalia tupiniquim* in dorsal (A), ventral (B), medial (C), and lateral (D) views. Abbreviations: **abp** – anterior body of the parietal; **lp** – lateral projection; **otas** – articulation surface with the otoccipital; **ri** – ridge; **ppas** – parietal/parietal articulation surface; **lsas** – articulation surface with the laterosphenoids; **pw** – parietal wing; **sf** – margin of the supratemporal fenestra; **soas** – articulation surface with the supraoccipital; **sqas** – articulation surface with the squamosal. Scale bars = 1 cm.

The anterior body of the parietal has a lateral projection at its anterolateral corner (Fig. 4.4). It is 5 mm long anteroposteriorly, which corresponds to about one fourth of the anteroposterior length of the bone. The anterior margin of the projection is mostly straight, corresponding to one third of the total anterior width of the parietal. The projection is subtriangular in dorsal/ventral views and its anteroposterior long axis is oblique to the horizontal, with the posterior margin more ventrally positioned than the anterior. Its dorsal surface corresponds to part of the supratemporal fossa, and would be continuous to the part of the fossa entering the frontal, as described above.

When segmented parietal and frontal are virtually articulated, the lateral projection of the former reaches the postorbital slot in the posterolateral margin of the latter. Thus, we infer that the frontal was excluded from the margin of the supratemporal fenestra by the parietal/postorbital contact, as in *Adeopapposaurus mognai* (see e.g. Martinez, 2009). A triangular lateral projection is also present in the parietals of other dinosaurs such as *Herrerasaurus ischigualastensis, Plateosaurus engelhardti, Panphagia protos, Efraasia minor*), but it is absent in the lagerpetid *Ixalerpeton polesinensis*. Instead, this taxon possesses a post-frontal bone (absent in dinosaurs) that contacts the anterolateral surface of the anterior body of the parietal.

The dorsal surface of the anterior body of the parietal (Fig. 4.4), excluding the anterolateral projection, is transversally convex and roughly sub-rectangular in shape, with a concave lateral margin and a retracted posteromedial corner (but this can be a breakage artefact). A low ridge extends anteroposteriorly from the anterolateral corner of the body, curving medially towards its posterior margin, but does not reach the parietal/parietal suture. This gives a half-moon shape aspect to the portion of the parietal medial to the ridge, which form the skull roof. A topologically equivalent ridge is lacking in *Lesothosaurus diagnosticus*, but seen in *Plateosaurus engelhardti*, *Panphagia protos*, and *Herrerasaurus ischigualastensis*. It is sharper (with the dorsal surface projecting slightly laterally) in the former taxon than in *Saturnalia tupiniquim* and *Pa. protos*, and broader in *H. ischigualastensis* than in the above mentioned sauropodomorphs. This ridge marks the medial limit of the supratemporal fossa in the parietal. In *S. tupiniquim*, the ridge projects more dorsally than the medial margin of the anterior body of the parietal. Thus, with the parietals articulated, the dorsal surface of the pair, between the ridges, is concave, as also seen in *H. ischigualastensis* and *Pl. engelhardti*. This surface is flat to slight concave in *L. diagnosticus,* whereas in

Heterodontosaurus tucki and *Adeopapposaurus mognai*, the supratemporal fossa extends until the medial limit of the parietal in the posterior half of its anterior body, and a single crest extends along the interparietal contact.

In ventral view, the surface of the anterior body of the parietal is transversely and anteroposteriorly concave, mainly following the corresponding convexity of the dorsal surface of the bone (Fig. 4.4). A posteromedially to anterolateraly oriented ridge separates the anterior body of the parietal from the parietal wing. It extends anteriorly forming the edge of the parietal, but does not continues medially, as in *Panphagia protos*, the crest of which is C-shaped (see Martinez *et al.,* 2012a, fig. 4c). Instead, in *Saturnalia tupiniquim* the ridge extends anterolaterally, reaching the posterior limit of the subtriangular anterolateral projection. In addition, the CT-Scan data did not allow recognising the sulcus present anterior to the ridge as seen in *P. protos* (Martinez et al. 2012a).

The parietal wing corresponds to a tall, posterolaterally extending lamina (Fig. 4.4). Its anteroposterior length is c. 10 mm. The ventral and dorsal margins parallel one another for c. 90% of the long axis of the process, but the latter descents ventrally at the tip, approching the ventral margin, which remains at the same dorsoventral level (horizontal). The lateral surface of the parietal wing forms the medial and posteromedial margin of the supratemporal fossa. Its ventral half is transversally concave, following the shape of the ventral portion of the anterior body of the parietal that forms the supratemporal fossa. The distal portion of this concave surface represents the articulation area with the parietal ramus of the squamosal, where both bones formed together the posterior margin of the supratemporal fenestra. A low ridge marks the dorsal limit of that concave region, dorsal to which the lateral surface of the

parietal wing is transversally convex, shaping the dorsal limit of the supratemporal fossa in the region.

Based on the shape of the lateral surface of the parietal, it is very likely that the supratemporal fenestra was longer than wide in *Saturnalia tupiniquim*, as in other taxa such as *Plateosaurus engelhardti, Lesothosaurus diagnosticus,* and *Herrerasaurus ischigualastensis*. A wider than long supratemporal fenestra is typical of sauropods, which have anteroposteriorly short parietals (Wilson, 2005).

Braincase

The laterosphenoids are isolated from the rest of the braincase elements, whereas the supraoccipital, otoccipitals, prootics, parabasisphenoid, and basioccipital have been preserved in articulation (Fig. 4.2). However, bone limits are not entirely clear in the CT- Scan data, hampering a more detailed description of the general morphology of the elements preserved inside the matrix. Nevertheless, most structures associated to the braincase (e.g. cranial nerve apertures, recesses) were identified and described in detail below.

Basioccipital

The basioccipital is the more exposed bone in the surface of the block containing the braincase, and some of it limits are also more easily recognisable in the CT-Scan data (Figs. 4.2, 4.5, 4.6). It forms the posteroventral portion of the braincase, contacting the parabasisphenoid anteriorly and the otoccipital dorsally. The bone is preserved in two separate pieces, a posterior piece including the occipital condyle and an anterior piece attached to the parabasisphenoid (Fig. 4.5). The former was glued to the anterior portion of the braincase before the CT-Scan imaging. The basioccipital is almost

completely preserved in MCP-3845-PV, except for a small part of its ventral surface, between the posterolateral projections of the parabasisphenoid, where the bone is damaged, and a part of the surface that would have contacted the otoccipital on the left side, anterior to the otoccipital condyle (Figs. 4.1, 4.2). In general, the bone is composed of an anterior portion, corresponding to an anterior projection extending between the posterolateral projections of the parabasisphenoid, and a posterior portion including the occipital condyle.

The basioccipital-parabasisphenoid contact is U/V shaped, with an anterior projection of the former extending between two posterolateral expansions of the latter (Fig. 4.5). The anterior projection of the basioccipital has an anteroposterior length of c. 5 mm, which corresponds to slightly less than half the total anteroposterior length of the bone, which is c. 11mm (Fig. 4.2). The lateromedial width of the projection at its posterior third is also c. 5 mm, and this subtly reduces anteriorly, ending in a rounded margin and giving a U-shape to this portion of the bone (Fig. 4.5). The CT-scan data show that the ventral surface of that projection is transversely concave, confluent with, and deeper than the basisphenoid recess. However, this region is damaged and mostly covered by matrix, hampering a more precise reconstruction.

The posterior portion of the basioccipital is narrower (Fig. 4.5) at the occipital condyle (width = 6 mm), than at the level of the basioccipital part of the basal tubera (width = 9.5 mm). The ventral surface of this portion of the bone is anteroposteriorly concave, and as smooth as in *Lewisuchus admixtus*, *Silesaurus opolensis*, and *Adeopapposaurus mognai*. These taxa lack the parallel ridges extending from the occipital condyle to the basal tubera as described for *Efraasia minor* (Chapter 5), and also seen in *Plateosaurus engelhardti* and *Tawa hallae*.
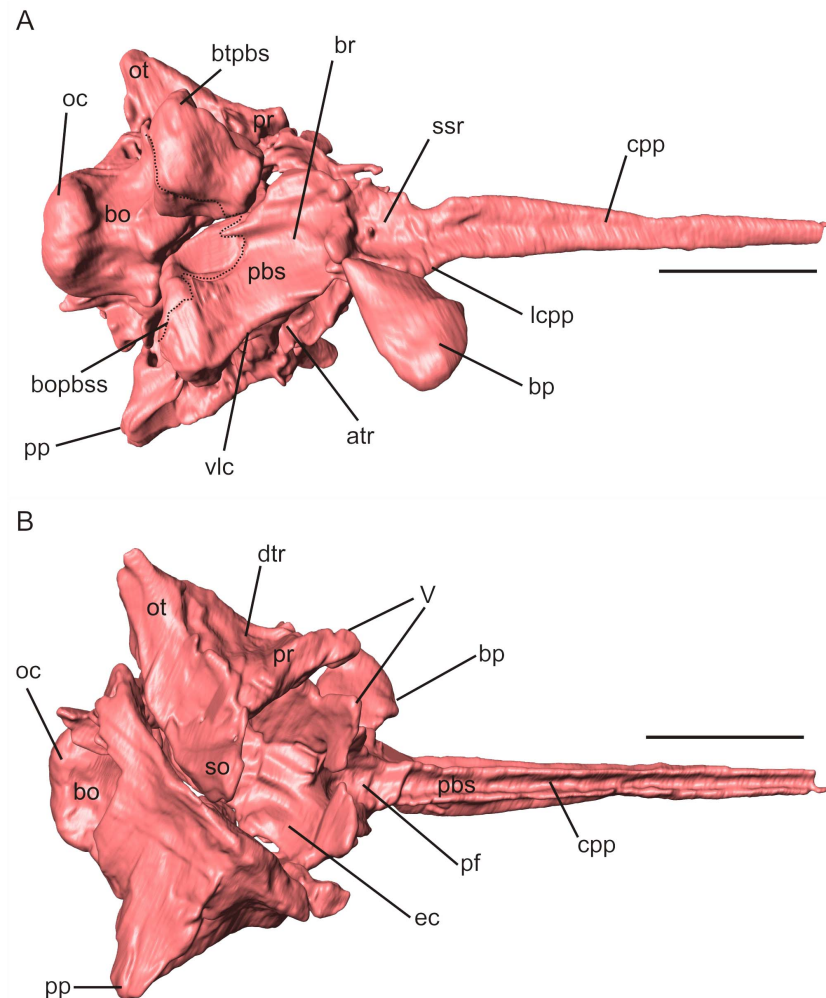
Figure 4.5: Braincase of the specimen MCP 3845 PV of *Saturnalia tupiniquim* in ventral (A) and dorsal (B) views. Abbreviations: **atr** – anterior tympanic recess **bo** – basioccipital; **bp** – basipterygoid process; **bopbss** – basioccipital/parabasisphenoid suture (dashed line) **br** – basisphenoid recess; **btbo** – basioccipital component of the basal tubera; **btpbs** – basisphenoid component of the basal tubera; **cpp** – cultriform process of the parabasisphenoid; **dtr** – dorsal tympanic recess; **ec** – endocranial cavity; **lcpp** – lamina of the cultriform process of the parabasisphenoid; **oc** – occipital condyle; **ot** – otoccipital; **pbs** – parabasisphenoid; **pf** – pituitary fossa; **pp** - paroccipital process; **pr** – prootic; **so** – supraoccipital; **ssr** – subsellar recess; **vlc** – ventrolateral crest; **V** – notch for the trigeminal nerve. Scale bars = 1 cm.

In cross-section, the posterior portion of the basioccipital of MCP-3845-PV has ventrolaterally facing surfaces forming an angle of approximately 120 degrees to

one another. This V-shaped morphology, together with the lack of the paired ridges mentioned above, makes the distinction between ventral and lateral surfaces unclear. Nevertheless, a fossa is seen in each anterolateral corner of this basioccipital portion (Fig. 4.5), which is topologically correspondent to the neotheropod sub-condylar recess (Witmer et al. 1997). With a certain degree of subjectivity, it is possible to state that the fossa of *Saturnalia tupiniquim* is not as well-developed as that of *Tawa hallae* or *Buriolestes schultzi*, mostly resembling those of *Efraasia minor* and *Plateosaurus engelhardti*.
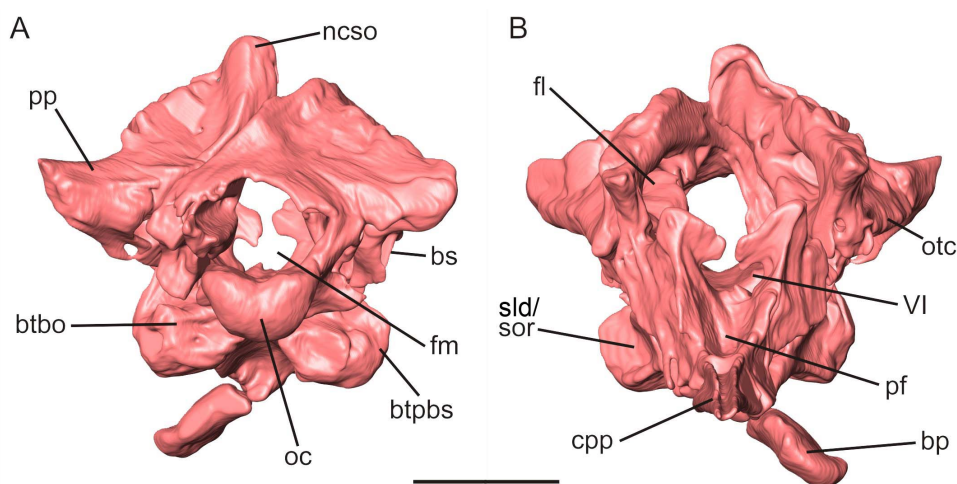
Figure 4.6: Braincase of the specimen MCP 3845 PV of *Saturnalia tupiniquim* in posterior (A) and anterior (B) views. Abbreviations: **bp** – basipterygoid process; **bs** – bony strut; **btbo** – basioccipital component of the basal tubera; **btpbs** – basisphenoid component of the basal tubera; **cpp** – cultriform process of the parabasisphenoid; **fl** – floccular lobe of the cerebellum; **fm** – foramen magnum; **ncso** – supraoccipital nuchal crest; **oc** – occipital condyle; **otc** – otosphenoidal crest; **pf** – pituitary fossa; **pp** – paroccipital process; **sld/sor** – semilunar depression / subotic recess; **VI** – notch for the abducens nerve. Scale bars = 1cm.

The dorsal surface of the occipital condyle is lateromedially concave at its mid-point, whereas the ventral margin is rounded, giving a kidney-shape for this structure in occipital view (Fig. 4.6). As for all dinosauromorphs (Sampson &

Witmer, 2007; Bittencourt *et al.,* 2014; Chapter 5), the occipital condyle is mostly composed by the basioccipital, with a small contribution of the otoccipital to its dorsolateral corners. The condyle has a lateromedial width of c. 8 mm, half of which corresponds to the basioccipital, and the other half to the otoccipital, 2 mm on each side. Its height is c. 4 mm at the centre, where the condyle has no contribution of the otoccipital. This remains relatively constant along the lateromedial extension of the structure, as its dorsal and ventral surfaces are concave/convex, respectively.

The posterodorsal corner of the basioccipital forms the medioventral portion of the foramen magnum (Figs. 4.5, 4.6). In dinosaurs, the foramen is typically surrounded by the basioccipital medioventrally, the supraoccipital mediodorsally, and the otoccipital laterodorsally, with their contribution varying in different taxa (Sampson & Witmer, 2007; Chapter, 5). Yet, only the basioccipital contribution can be precisely defined in MCP-3845-PV. The maximum width of the foramen is c. 95 mm, reached at mid-length of its dorsoventral axis. From this point, the foramen width diminishes progressively, both ventrally and dorsally. As its maximum height is c. 55 mm, the foramen magnum of MCP-3845-PV is wider than tall, as in *Lewisuchus admixtus*. In *Silesaurus opolensis, Herrerasaurus ischigualastensis,* and *Plateosaurus engel hardi,* the foramen is approximately as wide as tall.

The morphology of the dorsal surface of the basioccipital is accessible based on the CT-Scan data (Fig. 4.5). It forms most of the endocranial cavity floor in the posterior half of the braincase, except for a small contribution of the otoccipitals to its lateral portion, at the level of the occipital condyle. The dorsal surface of the bone is transversely concave (mainly as an extension of the concave above mentioned dorsal surface of the occipital condyle), forming a U-shaped neural canal in this region. The floor of the neural canal is slightly narrower posteriorly, at the anterior limit of the

occipital condyle, than anteriorly, where the anterodorsal portion of the basioccipital forms the ventral border of the metotic foramen.

Parabasisphenoid

In dinosauriforms (Bittencourt *et al*. 2014), including dinosaurs (Sampson & Witmer, 2007), the parasphenoid and basisphenoid are usually fused to one nother, forming the parabasisphenoid (*sensu* Sampson & Witmer, 2007). In MCP-3845-PV, it contacts the prootics anterodorsally, the otoccipitals posterodorsally, and the basioccipital posteriorly (Figs. 4.2, 4.5). It forms the anterior portion of the braincase floor, and also a great part of its lateral walls, and has a series of associated structures, such as the cultriform and basipterygoid processes, the basisphenoid component of the basal tubera, the preotic pendant (see prootic description below), and the subsellar, basisphenoid, otic, and anterior tympanic recesses.

The cultriform process is here considered the portion of the parabasisphenoid extending from the subsellar recess, between the basipterygoid processes, posteriorly, to the anterior tip of the bone (Fig. 4.5). In MCP-3845-PV, the process is c. 30 mm long, corresponding to c. 55% of the total anteroposterior length of the braincase. The process is 4 mm broad at its posterior end, and gradually narrows anteriorly, with a distal width of 1.5 mm. The height of the process also decreases anteriorly; it is c. 5.3 mm proximally, and no more than 2 mm distally. In cross-section, the cultriform process is U-shaped at its anterior third, with a rounded ventral margin. Posteriorly, the cross section assumes an inverted-T shape, with the presence of short (c. 1mm) bulbous lateral projections that are the cross-sectional expression of ridges extending along the ventral surface of the bone. These ridges extend for about half of the length of the cultriform process, becoming lower anteriorly. Anterior to that, the ventral

surface of the process becomes flat, rather than concave as more posteriorly between the ridges. The ridges parallel one another for their entire length in the process. Posteriorly, they merge with the base of the basipterygoid processes (Fig. 4.5), forming the lamina of the cultriform process of the parasphenoid (Chapter 5), i.e. the triangular lateral lamina of the parabasisphenoid rostrum of Apaldetti *et al*. (2014). Medial to these laminae, a recess at the anterior portion of the main body of the parabasisphenoid is here identified as the subsellar recess (Fig. 4.5). The region corresponding to the recess is preserved only in the left side of the braincase; covered by matrix, but visible with the CT-scan data. On the right side, this region is greatly damaged. The recess is c. 5 mm lateromedially wide and c. 4.5 mm dorsoventrally deep. Although its anterior margin is not entirely preserved, the recess would likely have a sub-circular outline in ventral view if both sides were preserved.

The ventral surface of the parabasisphenoid, excluding the cultriform process, would assume an X-shape with both basipterygoid processes preserved (Fig. 4.5). The basipterygoid processes corresponding to the anterolateral projections, and the two posterolateral projections bearing the basisphenoidal component of the basal tubera (Fig. 4.5). As such, the parabasisphenoid body has a total anteroposterior length of 12 mm. Immediately posterior to the subsellar recess, the parabasisphenoid is 7 mm wide lateromedially, expanding laterally towards the basisphenoidal portions of the basal tubera as it process posteriorly, where it is 19 mm wide. It is worth mentioning that this width includes the "gap" in the parabasisphenoid that receives the anterior projection of the basioccipital. The ventral edge of the posterior margin of the bone is dorsally located in relation to the ventral extension of its main body, so that a curved posteroventral margin is formed in lateral view.

Each posterior projection of the parabasiphenoid is 6 mm long. Its width remains relatively constant, but expands at the posterior tip, where the basisphenoidal component of the basal tubera is located (Fig. 4.5). This corresponds to a bulbous structure, with an uneven surface covered in small/shallow pits for muscle attachment. The pits are mostly concentrated in the posterior and ventral surfaces of the tuber, but they are also cover at the ventral portion of the lateral surface of the parabasisphenoid in this area.

The depression on the ventral surface of the parabasisphenoid main body (Fig. 4.5), located posterior to the subsellar recess and anterior to the lateral projections of the basisphenoidal component of the basal tubera, is here identified as the basisphenoid recess (*sensu* Witmer, 1997 – see discussion below). A thin and low bone wall sets the anterior limit of the depression, marking its separation from the subsellar recess. Laterally, the basisphenoid recess is bounded by the ventrolateral crest [*sensu* Kurzanov, 1976 (= lateral lamina of the basiphenoid of Apaldetti *et al.*, 2014)]. In *Saturnalia tupiniquim*, this crest is laminar, setting the boundary between the ventral and lateral surfaces of the parabasisphenoid. It extends along the entire anteroposterior length of the main body of the bone, starting at the anterior margin of the anterior tympanic recess and becoming posteriorly confluent with the basisphenoidal component of the basal tubera.

The left basipterygoid process was originally preserved separated from the braincase, but it was glued to the parabasisphenoid before the CT-Scan procedure (Figs. 4.2, 4.5). The breakage surface was slightly damaged, but it was possible to determine the original position of the process, and it is thus safe to establish its orientation. The right basipterygoid process is also preserved, but the preservation of the right side does not allow defining its original position. The basipterygoid process

projects anterioventrally, with its anterior margin forming an angle of c. 60 degrees with the ventral surface of the cultriform process in lateral view. An anteriorly oriented basipterygoid process is also observed in *Silesaurus opolensis*, whereas it is posteriorly oriented in *Plateosaurus engelhardti*, and strictly ventrally in *Tawa hallae* (Nesbitt *et al.,* 2009). Nevertheless, defining the orientation of the process is not trivial, as it is sometimes difficult to establish the orientation of the whole braincase, resulting in different interpretation by different authors. The process also has a lateral projection, forming an angle of 45 degrees to the sagittal plane. Thus, left and right processes would form an angle of 90 degrees to one another. The basipterygoid process is 7.5 mm long, and has a maximum width of 6 mm. It has a lanceolate shape in lateral view, wider proximally and gradually narrowing distally. Its outer surface is irregular, with alternate concave and convex regions. Yet, it is generally slightly compressed mediolaterally, and thicker at its posterior margin than anteriorly. Despite some subjectivity, this condition resembles that of *Lewisuchus admixtus,* which may be considered as an intermediate between the more laminar process of *Eodromaeus murphi, T. hallae,* and *Si. opolensis*, and the more rounded one of sauropodomorphs such as *Pl. engelhardti* and *Thecodontosaurus antiquus* (Benton *et al.*, 2000).

The main body of the parabasisphenoid bears a large excavation on its lateral surface (Fig. 4.2), considered here as the anterior tympanic recess (but see discussion below). In dinosaurs, that recess usually extends from the anteroventral to the posterodorsal portions of the basisphenoid, invading the ventral margin of the lateral surface of the prootic (e.g. Rauhut, 2004; Sampson & Witmer, 2007; Chapter 5*)*. In MCP-3845-PV, the boundary between the basisphenoid and prootic is not clear, but the dorsal edge of the recess is located directly ventral to the lateral opening for the facial nerve, indicating that the recess of *Saturnalia tupiniquim* also invades the

prootic. However, differently from what is observed in *Thecodontosaurus antiquus* and *Efraasia minor*, in which the recess forms a single and continuous excavation, two different regions are clearly devised in the anterior tympanic recess of *Saturnalia tupiniquim* (but see discussion below), resembling the condition seen in *Lewisuchus admixtus* (M.B. pers. obs). The recess has a maximum (anteroventral-posterodorsal) length of 9 mm, and a maximal transverse width of c. 3 mm. Its anteroventral portion is elyptical in shape, and corresponds to approximately two thirds of its total length. It is confluent with the ventrolateral crest described above. At the deepest point of the excavation, around the mid-point of the anteroventral region, a small circular aperture (c. 1 mm diameter) is seen and likely corresponds to the lateral aperture of the vidian canal (= foramen for the internal carotid artery). The internal carotid artery and the palatine branch of facial nerve (VII) enter the internal cavity of the braincase through this aperture (Sampson & Witmer, 2007). The posterodorsal portion of the recess is shallower, and has only half the size of the anteroventral portion.

Posterior to the anterior tympanic recess, the posteroventral corner of the parabasisphenoid has a large depression on its lateral surface (Fig. 4.2), which is here identified as the semilunar depression (see discussion below). The surface between the subotic- and anterior tympanic recesses is better preserved in the left side of the braincase. The ventral limit of the semilunar depression is clearly marked by a c. 1 mm thick anteroposteriorly extending lamina, which also marks the lateral edge of the ventral surface of the parabasisphenoid. The recess is also well defined posteriorly by a gently rounded ridge (c. 2.5 mm thick) that also marks the transition between the lateral and posterior surfaces of the parabasisphenoid. Dorsally, the depression is confluent with the fenestra ovalis, with the parabasisphenoid forming the ventral margin of this aperture. Anteriorly there is also no clearly marked limit, but the

depression get shallower until the level of the posterior margin of the anterior tympanic recess.

In the dorsal surface of the parabasisphenoid, the pituitary fossa (Sampson & Witmer, 2007) is located posterior to the cultriform process (Figs. 4.5, 6.6). In anterior view, the fossa has a V-shape format, with a rounded ventral margin. It is posteriorly bordered by a vertical, c. 1 mm thick bone wall, setting it apart from the posteriormost dorsal surface of the parabasisphenoid. Usually, the medioventral portion of the fossa is perforated by the internal carotid artery. However, in MCP-3845-PV we found no sign of a foramen in this area of the parabasisphenoid, leading to two possible scenarios. One is that the condition of *Saturnalia tupiniquim* is similar to that of non-archosauria archosauriforms, the internal carotid of which does not enter the pituitary fossa anteriorly, but via a path on the ventral surface of the parabasisphenoid (Nesbitt, 2011). However, when the internal carotid enters the braincase through the pituitary fossa, it exits the fossa laterally via a foramen within the anterior tympanic recess here identified in *S. tupiniquim*. Thus, we consider the absence of the foramen as most likely an artefact, caused by the preservation and/or the CT-Scan segmentation, rather than a condition deviating from that of all other dinosauriforms.

At the dorsal portion of the wall posteriorly bordering the pituitary fossa (Fig. 4.6), a perforation corresponds to the passage of cranial nerve VI (abducens). Typically, the left and right foramina have independent apertures. Indeed, in the left side it is possible to see that the dorsal part of the wall curves ventrally, almost reaching a dorsal projection from the ventral margin, what would have enclosed the nerve. It is, however, not clear if there is an additional opening between those for the abducens

nerves, presumably for the basilar artery (Balanoff *et al.*, 2010). Such an additional foramen is present in *Plateosaurus engelhardti*, but absent in *Silesaurus opolensis*.

Supraoccipital, otoccipitals, and prootics: bones limits

The supraoccipital, otoccipitals, prootics, and the laterosphenoids, form together the dorsal portion of the braincase. In MCP-3845-PV, the laterosphenoids are isolated, but the supraoccipital, otoccipitals, and prootics, are preserved articulated inside the matrix containing the braincase (Figs. 4.2, 4.5, 4.6). The sutures between these bones are not entirely clear in the CT-Scan data, hampering a more detailed description of each of them. Thus, the below descriptions will mainly attempt to identify the structures associated to those bones, such as cranial foramina and recesses.

Prootic

Left and right prootics of MCP-3845-PV are entirely preserved inside the rock matrix (Figs. 4.2, 4.5), only the posterior portion of the lateral surface of the right bone being exposed. Contacts with other bones include the parabasisphenoid ventrally, otoccipital posteriorly, laterosphenoids anteriorly, and supraoccipital mediodorsally. A series of structures are at least partially associated to the prootic in all dinosariforms analysed for this study, namely: the floccular recess of the cerebellum, the prootic pendant, the metotic foramen (see discussion below), the fenestra ovalis, the dorsal tympanic recess, and the foramina for cranial nerves VII (facial) and V (trigeminal).

Immediately anterodorsal to the anterior tympanic recess (Fig. 4.2), the lateral surface of the braincase corresponds to the region for the attachment of *M. protractor pterygoideus* (Sampson & Witmer, 2007). This attachment surface is typically formed by the prootic dorsally, with a contribution from the parabasisphenoid ventrally

(Sampson & Witmer, 2007; Chapter 5), but we could not recognise any detail of the suture in that area. Such a surface extends from the proximal part of the cultriform process (anteroventrally) to the ventral margin of the notch for the trigeminal nerve (posterodorsally). It has a sub-rectangular shape with a maximum length of 13 mm, and maximum and minimal width of 7 mm and 4 mm respectively at its dorsalmost and ventralmost portions. As observed in *Efraasia minor*, *Saturnalia tupiniquim* does not have a well-developed preotic pendant. Accordingly, the ventral margin of that surface mainly follows the curvature of the dorsal portion of the anterior tympanic recess (Fig. 4.2). In some theropods, the preotic pendant forms a laminar structure covering part of the anterior tympanic recess (Sampson & Witmer, 2007). A relatively well-developed lamina covering part of the anterior tympanic recess in lateral view is also observed in *Eodromaeus murphi*. In *Tawa hallae*, the preotic pendant also forms a lamina, but this projects less posteroventrally than in *E. murphi*. On the other hand, the preotic pendant of *Silesaurus opolensis* is more robust and rounded, resembling the condition of sauropodomorphs such as *Plateosaurus engelhardti* and *Massospondylus carinatus* (Chapter 5).

The ventral margin of the trigeminal nerve notch in *Saturnalia tupiniquim* is located dorsal to the surface for the attachment of *M. protractor pterygoideus* (Fig. 4.2). The notch is elongated and U-shaped, with the anterior margin located slightly more medial than the posterior margin (Fig. 4.5). The dorsal margin of the notch is c. 7.2 mm long. It is relatively straight for most of its length, but curves slightly ventrally at its anterior third. The ventral margin of the notch is shorter, c. 5.1 mm, and also curves slightly dorsally at its anterior end. The notch has a 3.2 mm width that is relatively constant along its length. The anterior margin of the bone would have

contacted the laterosphenoid, enclosing the foramen for the trigeminal nerve (see below).

A feature that has been discussed in previous studies on dinosaur braincases (e.g. Nesbitt, 2011; Chapter 5) concerns the arrangement of the trigeminal nerve and middle cerebral vein exits in the lateral wall of the braincase. Three distinct morphologies have been recognised. Some neotheropods exhibit separate foramina for the nerve and the vein (Rauhut, 2004), whereas forms such as the sauropodomorph *Coloradisaurus brevis* have a single foramen for both (Apaldetti *et al*., 2014). A third case correspond to the presence of a partially subdivided notch in the prootic, with the vain occupying a more posteromedial position (Nesbitt, 2011; Chapter 5), as observed in sauropodomorphs such as *Efraasia minor* and *Plateosaurus engelhardti*. No separate notch or path for the middle cerebral vein, as that observed in *Efraasia minor* (Chapter 5), was found in the medial surface of the prootic of *Saturnalia tupiniquim*. Yet, the prootic notch of MCP-3845-PV is relatively elongated, suggesting that the trigeminal nerve and the vein would exit the braincase through a single foramen. In addition, as mentioned above, the ventral and dorsal tips of the notch aperture are curved in *S. tupiniquim*, suggesting a partial separation between the nerve and vein paths (Figs. 4.2, 4.4).

Posteroventral to the trigeminal nerve, MCP-3845-PV bears a small circular foramen on both sides of the braincase (Fig. 4.2), here interpreted as for the facial nerve (VII). One important aspect to be considered is its position in relation to the anterior tympanic recess. In *Panphagia protos* (Martinez *et al*., 2012a, fig. 8C) and *Tawa hallae* (pers. obs.), the facial nerve foramen is outside and dorsal to the anterior tympanic recess. On the other hand, in *Lewisuchus admixtus* lacks a clear separation between the foramen and the anterior tympanic recess, with the former either within

or confluent with the dorsal limit of the latter (Bittencourt *et al.*, 2014, fig. 4B). In *Saturnalia tupiniquim*, the results of the segmentation in left and right sides differ, the former matching the condition of *P. protos* and *T. hallae,* and the latter that of *L. admixtus*. Below, we describe the different morphology of both sides, which could be the original condition of the braincase or the result of biases on preservation and/or segmentation of the CT data.

In the left side of the braincase, the aperture is c. 0.8 mm and separated from the anterior tympanic recess by a 1 mm bone surface that forms the dorsal roof of the recess (Fig. 4.2). In this context, a depression in the lateral surface of the prootic would most likely correspond to the path of the palatine ramus of the facial nerve, which turns anteroventrally after leaving the braincase (Galton, 1985; Sampson &Witmer, 2007). Likewise, a depressed surface between the two anterior rami of the otosphenoidal crest would represent the path of the hyomandibular ramus of the facial nerve in the lateral surface of the prootic (Fig. 4.2), which turns posterolaterally after leaving the braincase (Galton, 1985; Sampson &Witmer, 2007). In the right side of the braincase, the surface between the notch for the trigeminal nerve and the rounded aperture is twice the length of that of the left side (c. 2 mm). As mentioned above, the ventral margin of the foramen is confluent with the dorsal portion of the tympanic recess. Finally, regardless the existence of those two alternative scenarios, in none of the sides of the braincase of MCP-3845-PV it is possible to see a lamina partially covering (laterally) the foramen for the facial nerve, as seen in *Lewisuchus admixtus* (pers. obs) and *Panphagia protos* (Martinez *et al.*, 2012, fig. 8a and 8c). Such a lamina also seems to be absent in *Tawa hallae*.

The crista prootica is here termed the otosphenoidal crest (Sampson & Witmer 2007), as this structure can be formed by three different bones: prootic, otoccipital,

and parabasisphenoid. As mentioned above, it is not possible to clearly visualize the limits between the prootic and otoccipital, but it seems that the otosphenoidal crest of MCP-3845-PV has an otoccipital component, extending until the proximal portion of the parocipital process (Fig. 4.2). Typically, the prootic overlaps the otoccipital at their contact, but this is not clear in the results of the segmentation. In this portion of the braincase, the otosphenoidal crest forms a low and rounded (c. 3 mm thick) ridge. From its posterior tip, at the proximal part of the paroccipital process, the crest extends anteriorly as a single ridge for c. 8.5 mm, and bifurcates at the level of the fenestra ovalis. The ventral branch of the crest forms the anterior margin of that fenestra, contacts the parabasisphenoid ventrally, setting the boundary between the fenestra ovalis and the anterior tympanic recess. The dorsal branch forms the dorsal margin of the facial nerve foramen. It is important to stress that we treat both rami of the otosphenoidal crest as part of this structure because no discontinuity between them and the posteriormost portion of the crest is seen (Sobral *et al.* 2016; Chapter 5).

Dorsal to the otosphenoidal crest, the prootic contacts the supraoccipital dorsally, the otoccipital posteriorly, and the laterosphenoid anteriorly (Figs. 4.2, 4.4). A large depression (= dorsal tympanic recess *sensu* Witmer, 1997) occupies this area, forming c. 60% of the lateral surface of the braincase, from the paroccipital process posteriorly to the trigeminal notch anteriorly. Left and right sides of the braincase exhibit small differences, probably related to the preservation of the bones inside the matrix. The ventral limit of the recess is rounded, giving a half-moon aspect to the whole structure in lateral view (Figs. 4.2, 4.5, 4.6). Its anterior limit is, however, more sharply defined on the left side, where a triangular flat surface of bone separates the recess from posterior margin of the trigeminal nerve notch. The anterior margin of the recess is vertical, extending from the otosphenoidal crest ventrally, to the prootic

margin that would probably contact the parietal/laterosphenoid dorsally. On the right side, the recess is anteriorly shallower and no so sharply defined. It becomes even shallower dorsally, but it is not clear if it would have also excavated the parietal (e.g. Witmer, 1997). Finally, the recess is continuous on the left side of the braincase, but the right bears two deeper regions separated by a low and thick crest. This crest extends from the dorsal margin of the stapedial groove to the portion of the prootic/otoccipital that would contact the anterodorsal surface of the supraoccipital.

The medial surface of the prootic is dorsoventrally concave (Fig. 4.6). Together with the concave dorsal surface of the parabasisphenoid and basioccipital, this gives a rounded aspect to the endocranial cavity. A large and deep circular depression dominates the medial surface of the prootic and corresponds to the flocullar recess of the cerebellum (Fig. 4.6). This morphology is similar to that of other dinosauriforms such as *Lewisuchus admixtus*, *Silesaurus opolensis*, *Tawa hallae*, and *Panphagia protos*, and the non-archosaurian archosauriform *Euparkeria capensis* (Sobral *et al*. 2016). Later sauropodomorphs have a shallower depression on the medial surface of the prootic, indicating the absence of a well-developed flocculus of the cerebellum (Chapter 3). Unfortunately, details of the auricular recess, typically located at the posterior margin of the prootic, where it contacts the otoccipital (Gower, 2002; Nesbitt, 2011), are not possible to be observed in the CT-Scan data.

Otoccipital

The term otoccipital is here employed for the single element formed by the fusion of the exoccipital and opistothic (Sampson & Witmer, 2007). Both otoccipitals are preserved in MCP-3845-PV, (Figs. 4.2, 4.5, 4.6), but the paroccipital processes are broken, lacking their most distal portions. The lateral surfaces of both otoccipitals are

partially exposed, and additional details of their morphology are provided by the CT-Scan data. In dinosaurs, the otoccipital usually contacts the supraoccipital medially, the parabasisphenoid anteroventrally, the basioccipital posterodorsally, and the prootic anterodorsally (Galton, 1984; Sampson & Witmer, 2007). Yet, except for the contact with the basioccipital in the occipital condyle (not covered by sediment), those with the other bones cannot be precisely identified MCP-3845-PV. The otoccipital can be roughly divided into a dorsal portion that contacts the supraoccipital medially and the prootic anteriorly, and three projections that originate from this dorsal portion. One of these is the paroccipital process, which originates in the posterolateral corner of the bone. Ventral to the paroccipital process, a more robust projection forms parts of the foramen magnum and occipital condyle, enclosing the foramina for the hypoglossal nerve. Anteriorly, a second ventral projection consists of the crista interfenestralis, between the metotic foramen and the fenestra ovalis. The posterodorsal region of the braincase, formed by the otoccipital and supraoccipital, will be discussed in a separate section, because the related bone limits are not at all clear (Figs. 4.2, 4.5, 4.6).

As mentioned above, the occipital condyle is a two-bone structure, formed mostly by the basioccipital, but having an otoccipital contribution to its dorsolateral portion. The contact between both bones is not seen in the CT-Scan data, but visible in the actual specimen. From the above described posteroventral projection of the otoccipital, an smaller, additional posterior projection abuts the basioccipital portion of the condyle laterally. This projection is pyramidal and c. 5 mm long. Medially, it contributes to the floor of the endocranial cavity, forming its posterolateral edge. The ventral surface is flat at the contact with the basioccipital, whereas the dorsal surface

is concave and anterodorsally confluent with the portion of the otoccipital forming the lateral margins of the foramen magnum.

The total participation of the otoccipital in the borders of the foramen magnum cannot be precisely determined, because its suture to the supraoccipital is not visible both in the fossil and in the CT-Scan data. However, in all other taxa analysed for this study in which those bone limits are seen (e.g. *Lewisuchus admixtus*, *Plateosaurus engelhardti*), the otoccipital forms the lateral margin and at least part of the dorsal margin of the foramen. In MCP-3845-PV, the medial surface of the otoccipital that bonds the foramen magnum extends ventromedially to dorsolaterally for c. 0.6 mm, and curves medially dorsal to this, assuming a dorsoventral orientation (Fig. 4.6). In MCP-3845-PV, this change in orientation is more marked, forming an angle of c. 100 degree and resembling the morphology of *L. admixtus* and in *Silesaurus opolensis* (see Bittencourt *et al.*, 2014, fig. 3). On the other hand, the lateral margins of the foramen magnum of *Herrerasaurus ischigualastensis* and *P. engelhardti* have a more rounded aspect.

Anterior to the pyramidal projection forming the condyle, the ventral portion of the otoccipital is pierced by two foramina (Fig. 4.2). These are identified as passages for the two branches of cranial nerve XII (hypoglossal), reconstructed only on the right side. Both foramina have a circular shape, the posterior being slightly larger (2 mm diameter) than the anterior (1.5 mm diameter). The former is also more dorsally located than the latter, with its ventral margin located at the same dorsoventral level as the dorsal margin of the anterior foramen. Dorsal to the hypoglossal foramina, an additional fossa posterior to the metotic foramen is seen. However, the presence of an additional foramen in this area, which could indicate a

division of the metotic foramen (see Gower & Weber, 1998; Chapter 5), remains uncertain.

Anterior to the foramina for the hypoglossal nerve, two larger apertures are seen on the lateral wall of the braincase (Fig. 4.2). The posterior of which is identified as the metotic foramen (see also Gower & Weber, 1998; Sobral *et al.,* 2012; Chapter 5), whereas the anterior corresponds to the fenestra ovalis (or fenestra vestibule, Sampson & Witmer, 2007). They are divided by a lateromedially expanded (c. 3 mm) sheet of bone, the crista interfenestralis (Sampson & Witmer, 2007). On the left side, where it is better preserved, the preserved dorsal portion of the crista is c. 5 mm height, but we estimate a total height of 7 mm. As in other dinosaurs, the crista interfenestralis has its dorsal tip at the ventral surface of the proximal portion of the paroccipital process, where both structures are confluent. From the paroccipital process, the crista extends anteroventrally. It is curved, with concave anterior and convex posterior margins.

In MCP-3845-PV, the fenestra ovalis is of about the same size as the metotic foramen (Fig. 4.2), resembling the condition of *Plateosaurus engelhardi* and *Efraasia minor*. If the cultriform process of the parasphenoid is horizontally positioned, the fenestra ovalis is not strictly vertical, but has its ventral margin located anteriorly to the dorsal margin. The crista interfenestralis borders the fenestra posteriorly, and as mentioned above, its anterior margin gives a convex aspect to the posterior margin of the fenestra. The anterior limit of the fenestra ovalis is defined by the anteroventral ramus of the otosphenoidal crest. The dorsal margin of the fenestra has a depression that extends posteriorly until the proximal portion of the paroccipital process, which is here identified as the stapedial groove (Fig. 4.2).

The paroccipital process projects from the posterolateral corner of the dorsal portion of the otoccipital (Figs. 4.2, 4.5, 4.6). In taxa such as *Silesaurus opolensis, Tawa hallae,* and *Plateosaurus engelhardti,* the depression corresponding to the stapedial groove extends posterolaterally for only a short length of the paroccipital process. In *Saturnalia tupiniquim,* the stapedial groove extends along the entire anteroventral margin of the paroccipital process as preserved. Yet, as only the proximal portion of this structure is preserved in MCP-3845-PV, it is not possible to estimate the total length of the groove.

Otoccipital/Supraoccipital – Posteromedial region of the dorsal portion of braincase

As previously mentioned, although the corresponding surface is exposed in the block, the supraoccipital-otoccipital boundary is not apparent in MCP-3845-PV, neither reachable via the CT-Scan data. Therefore, we here describe the dorsal region of the braincase, from the foramen magnum to the anterior margin of the supraoccipital, without attempting to precisely identify bone limits.

The dorsal margin of the foramen magnum of archosaurs is typically formed by the supraoccipital medially and the otoccipitals laterally (Nesbitt, 2011), but the contributions of each bone can not be defined in MCP-3845-PV. The dorsal surface of the braincase, anterior do the dorsal margin of the foramen magnum, is transversely concave, mainly following the curvature of the foramen magnum and endocranial cavity (Fig. 4.6). Based on comparisons with *Silesaurus opolensis, Lewisuchus admixtus,* and *Plateosaurus engelhardti,* in which both bones are preserved in articulation, the region with a more marked dorsoventral inclination in MCP-3845-PV might correspond to the supraoccipital. With the cultriform process horizontally

aligned, the dorsal margin of the supraoccipital forms an angle of c. 70 degrees in relation to the horizontal plane at its anterior portion (Fig. 4.2). A thick supraoccipital crest extends anteroposteriorly for half the length of the supraoccipital dorsal surface, starting at its anterior edge, along the midline of the bone. Lateral to this crest, the dorsal surface of the braincase is slightly concave transversely, as defined by its dorsally raised lateral margins.

Laterosphenoid

Both laterosphenoids are preserved isolated inside the block containing the other braincase elements of MCP-3845-PV. The right element lacks some of its processes, but the left laterosphenoid is entirely preserved (Fig. 4.7). As the preserved portions of both bones show no differences, this description is solely based on the left element. The laterosphenoid would have formed the anterodorsal portion of the braincase. It can be roughly divided in a central main body, which would eventually contact the orbitospenoid anteriorly, and four projections contacting other adjacent bones. The posterior process would have contacted the prootic, the anterolateral process the postorbital, the anteromedial process the frontal, and the ventral process the prootic or/and the parabasisphenoid.

The lateral surface of the laterosphenoid main body of *Saturnalia tupiniquim* is concave, and its corresponding medial surface is convex (Fig. 4.7). This is similar to the condition observed in other sauropodomorphs such as *Plateosaurus engelhardti* and *Efraasia minor*. The convex medial surface of the laterosphenoid of *S. tupiniquim* forms the anterodosal portion of the endocranial cavity, and might have contacted the orbitosphenoid anteriorly. However, the CT-Scan data provided no evidence of a preserved orbitosphenoid in the block.
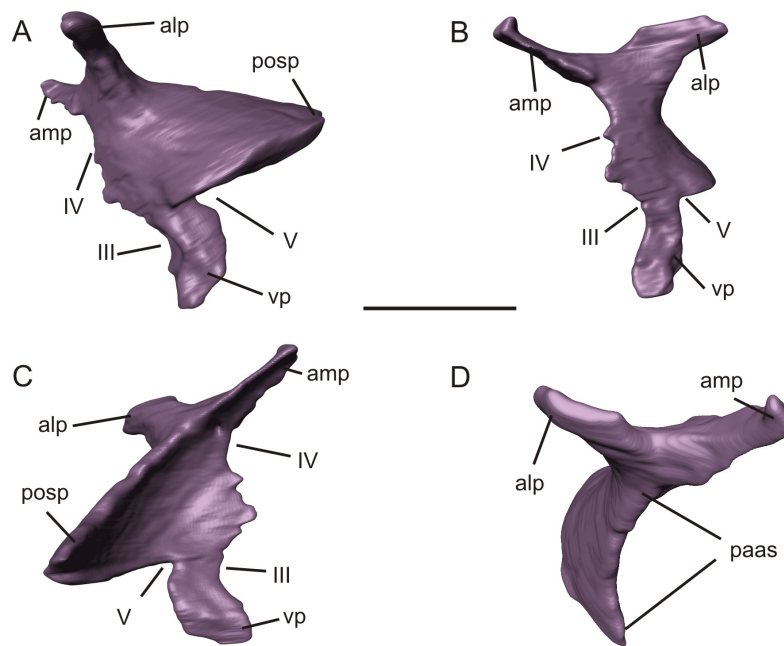
Figure 4.7: Left laterosphenoid of the specimen MCP 3845 PV of *Saturnalia tupiniquim* in lateral (A), anterolateral (B), medial (C), and dorsal (D) views. Abbreviations: **alp** – anterolateral process; **amp** – anteromedial process; **paas** – articulation surface with the parietal; **posp** – posterior process; **vp** – ventral process; **III** – path of the oculomotor nerve; **IV** – path of the trochlear nerve; **V** – path of the trigeminal nerve. Scale bars = 1 cm

The ventral process represents slightly less than one third the total height of the laterosphenoid (Fig. 4.7). Its posterior margin forms, together with the ventral margin of the posterior process of the bone, the dorsal portion of the trigeminal nerve foramen. The transition between these two processes forms a sharp angle. As the prootic-parabasisphenoid suture is not clear in the trigeminal nerve area, it is also not clear which bone would have contacted the posterior margin of the ventral process of the laterosphenoid to define the trigeminal nerve foramen.

The anterior margin of the ventral process is slightly convex in lateral-medial views. It merges with the main body of the bone dorsally, forming an indentation that corresponds to the passage of cranial nerve III (oculomotor). Dorsal to that, the anterior margin of the main laterosphenoid body is also concave, forming the posterior margin of the passage of cranial nerve IV (trochlear), below the

anteromedial process. The anterior projection of the laterosphenoid margin, which sets the passages for cranial nerves III and IV apart, probably contacted the orbitosphenoid anteriorly.

Dorsal to the passage for the trochlear nerve, the anterior margin of the laterosphenoid gives rise to a lateromedially compressed anteromedial process that projects medially from the main body of the bone (Fig. 4.7) and probably contacted the ventral surface of the frontal. The anteromedial process of *Saturnalia tupiniquim* is as long as the ventral process. Other sauropodomorphs such as *Plateosaurus engelhardti* and *Massospondylus carinatus* have a relatively shorter process, less than half the length of the ventral process (Gow, 1990; Prieto-Marquez & Norell, 2011) – although it may be incompletely preserved in *P. engelhardti* (AMNH 6810). Given the length of those processes , it is possible that their tips contacted one another in *S. tupiniquim*, ventral to the frontal, similar to the condition observed in some theropods such as *Allosaurus* (*pers. obs.*).

The anteromedial and anterolateral laterosphenoid processes of *Saturnalia tupiniquim* diverge from one another forming an angle of approximately 150 degrees in dorsal view (Fig. 4.7). The anterolateral process, which contacted the postorbital, is rounded and slightly shorter than the anteromedial process. From the anterolateral process (anteriorly) to the posterior process (posteriorly), the dorsal margin of the laterosphenoid would have contacted the ventral surface of the anterior body of the parietal (including its lateral projection). Together, laterosphenoid and parietal formed the anterolateral portion of the supratemporal fenestra/fossa of *S. tupiniquim*.

4.5. DISCUSSION

Here we discuss braincase anatomy features that have been used in phylogenetic constructions focusing on early dinosaurs and non-neosauropodan sauropodomorphs (e.g. Nesbitt, 2011; Nesbitt *et al.,* 2012; Bittencourt *et al.,* 2014; Cabreira *et al.,* 2016; Chapter 5). Because of the high level of disagreement among the recent phylogenetic hypotheses proposed (Langer, 2014), we chose to discuss dinosauriforms braincase evolution by examining particular anatomical traits under distinct phylogenetic arrangements. Proposing a new phylogenetic hypothesis for dinosauromorphs is beyond the scope of this work.

Recesses

Witmer (1997) presented a detailed review on the pneumatic recesses of the dinosaur skull. We provide here a brief overview on the presence of these structures in early dinosaurs and non-dinosaurian dinosauromophs, also discussing some nomenclatural issues.

Subsellar recess: The subsellar recess is located on the ventral surface of the proximal portion of the cultriform process of the parabasisphenoid (Witmer, 1997). Such a depression is seen in all dinosauromorphs examined for this study, in which that area is preserved or visible (Fig. 4.8). Hence, it is safe to infer the presence of the subsellar recess as the ancestral condition for dinosaurs. Regarding the ancestral condition for dinosauromorphs, we remain largely ignorant on the presence of a subsellar recess, but a depression is clearly present in archosauromorphs such as *Prolacerta broomi* and *Youngina capensis* (M.B. pers. obs.).

Regarding the three main dinosaur lineages, the presence of a subsellar recess has been extensively reported for theropod dinosaurs, including birds (Rauhut, 2004; Witmer & Ridgely, 2009; Bever *et al.*, 2013). Recently, Bronzati & Rauhut (Chapter 5) mentioned that the term had not been previously used in sauropodomorph literature, but that the structure is common to all sauropodomorphs. In Ornithischia, a cultriform process recess is present in *Hypsilophodon foxi* and *Dysalotosaurus lettowvorbecki* (see Sobral *et al.*, 2012; fig. 1B). We are not aware of the absence of such structure in any member of Dinosauria; obs. it seems absent in one specimen of *Lesothosaurus diagnosticus* (NHMUK PV RU B17), but is clearly present in another (BMNH R 8501). Hence, a phylogenetic character only dealing with the presence or absence of the subsellar recess is non-informative in order to establish relationships within Dinosauromorpha.
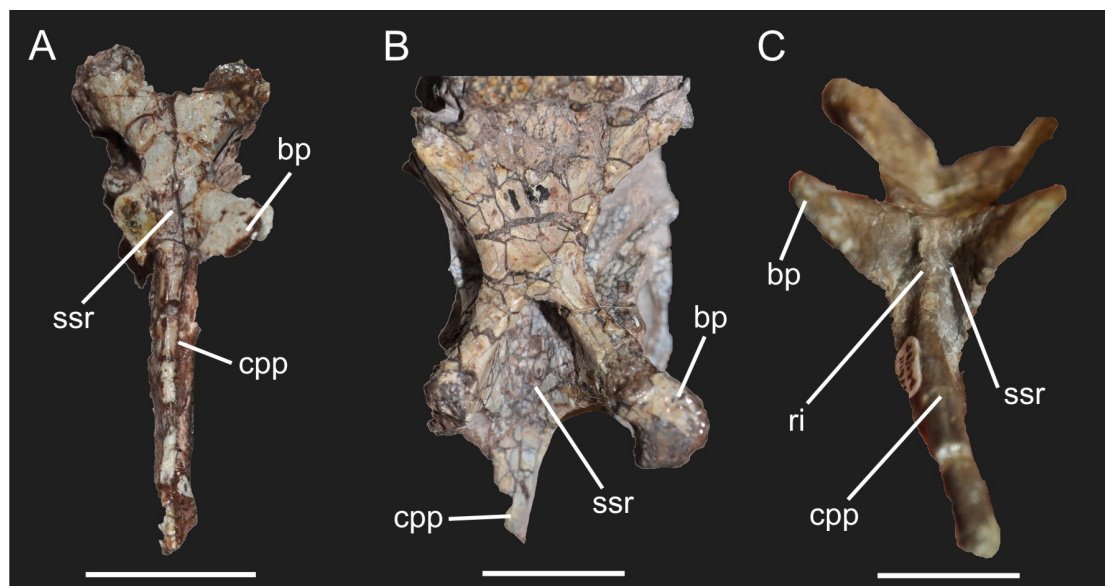
Figure 4.8: Parabasisphenoid of the specimens SAM-PK-K8025 of *Eocursor parvus* (A), SMNS 12667 of *Efraasia minor* (B), ZPAL ABIII361/88 of *Silesaurus opolensis* (C), in anteroventral view. Abbreviations: **bp** – basipterygoid process; **cpp** – cultriform process of the parabasisphenoid; **ri** – ridge; **ssr** – subsellar recess. Scale bars = 1 cm

Two characters related to the subsellar recess have been proposed in Bronzati & Rauhut (Chapter 5) in the context of sauropodomorphs evolution. One of these is related to the ridges that extend in the ventral surface of the cultriform process. In *Saturnalia tupiniquim*, these ridges originate from the lamina connecting the cultriform and basipterygoid processes and extend parallel to one another until they fade away anteriorly. Thus, the subsellar recess is not as clearly defined anteriorly as in *Efraasia minor* and *Massospondylus carinatus*. In *Plateosaurus engelhardti* and *Lewisuchus admixtus,* the ridges converge anteriorly in the ventral surface of the parabasisphenoid giving a triangular aspect to the anterior margin of the recess. On the other hand, in *Silesaurus opolensis*, the ridges extend parallel to one another, as in *S. tupiniquim,* but instead of merging with the ventral surface of the cultriform process, they extend along the dorsal portion of the lateral surface of the cultriform process.

A second character discussed by Bronzati & Rauhut (Chapter 5) deals with the depth/width ratio of the subsellar recess. For instance, taxa such as *Eocursor lunensis* exhibit a "shallow" recess, with the total width greater than the dorsoventral depth. On the other hand, *Efraasia minor* has a "deep" recess, which is as deep as wide (Fig. 4.8). Another trait with possible phylogenetic implications, not discussed in Bronzati & Rauhut (Chapter 5) is the presence/absence of a ridge medially dividing the subsellar recess (Fig. 4.8). This is present in *Silesaurus opolensis* and *Lewisuchus admixtus*, but not in *E. minor* and *Tawa hallae* (Fig. 4.8).

Basisphenoid recess vs "median pharyngeal recess": Posterior to the subsellar recess, another depression in the ventral surface of the parabasisphenoid corresponds to the basisphenoid recess of Witmer (1997). Latter, a series of studies (e.g. Gower, 2002;

Martz & Small, 2006; Sobral *et al.*, 2016) used the term "median pharyngeal recess" to refer to similarly positioned depression. Those authors often quote Witmer (1997) as a reference, but the term "median pharyngeal recess" does not appear in his work. Instead, Witmer (1997) mentions that the basisphenoid recess originates from a median pharyngeal system (see also Witmer & Ridgely, 2009), and a literature survey did not find any work refering to a "median pharyngeal recess" before Witmer (1997). In this context, the use of the term "median pharyngeal recess" might correspond to an equivocal interpretation of Witmer (1997), or to other interpretations of the authors no further clarified in their works. Other works have commented on the equivalence of the terms basisphenoid recess and "median pharyngeal recess" (e.g. Nesbitt, 2011; Ezcurra, 2016; Sobral *et al.*, 2016), but we rather suggest that works citing Witmer (1997) should only employ the term basisphenoid recess, or justify the choice for "median pharyngeal recess".

A basisphenoid recess has been extensively reported for theropods (e.g. Rauhut, 2004; Sampson & Witmer, 2007) and recently demonstrated to be also present in sauropodomorph dinosaurs (Chapter 5), and non-archosaurian archosauriforms (Sobral *et al*. 2016). Such a widespread distribution was already mentioned by Witmer (1997), and more recently by Dufeau (2011, PhD thesis). In fact, a depression in the ventral surface of the basisphenoid, even if very subtle (e.g. *Lesothosaurus diagnosticus*, *Eocursor lunensis*), was identified for all taxa analysed for this study, in which the ventral surface of the bone is visible (Fig. 4.9). Instead, Nesbitt (2011) stated that the recess is absent in the archosauromorphs *Prolacerta bromi* and *Euparkeria capensis,* and in the dinosaurs *L. diagnosticus, Plateosaurus engelhardti*, and *Herrerasaurus ischigualastensis*. However, as already mentioned by Sobral *et al*. (2016) for *E. capensis*, we cannot recognise any difference between the

ventral parabasisphenoid depressions of these taxa and those of, for example, *Silesaurus opolensis,* scored by Nesbitt (2011) as having the recess. It is also worth stressing that this disagreement is not related to the different terminologies (i.e. "median pharyngeal recess" vs basisphenoid recess), but most likely the result variation in the recess development in different taxa. For instance, the recess in non-archosaurian archosauriforms such as *P. bromi* and *E. capensis* (Sobral *et al.*, 2016) and some sauropodomoporhs such as *Efraasia minor* (Bronzati & Rauhut, Chapter 5) is clearly not as developed as that of some theropods (see Rauhut, 2004) such as *Coelophysis* ("*Syntarsus*") *rhodosiensis*. In this context, a "less-developed" recess might be coded as absent for some taxa, according to the interpretation of the authors. Thus, the size/depth of the basisphenoid recess may be a better way to express such variation in a phylogenetic context.

Finally, Sobral *et al*. (2016) argued that Nesbitt (2011) scored the "median pharyngeal recess" as absent in *Euparkeria capensis* due to different interpretations on what consists in the basisphenoid recess. According to the authors, Nesbitt (2001) understood the recess as a "pronounced depression at the anterior extreme of the ventral fossa at the midline", differing from the most widely used definition of the term. However, the pronounced depression mentioned by Sobral *et al*. (2016), i.e. that of character 107 in Nesbitt (2011), is not the basisphenoid recess ("median pharyngeal recess"), but another depression in the basioccipital. Nesbitt (2011) deals with the basisphenoid recess (or "median pharyngeal recess") in his character 100, which is clearly in accordance with the most used definition of the term (Witmer, 1997).
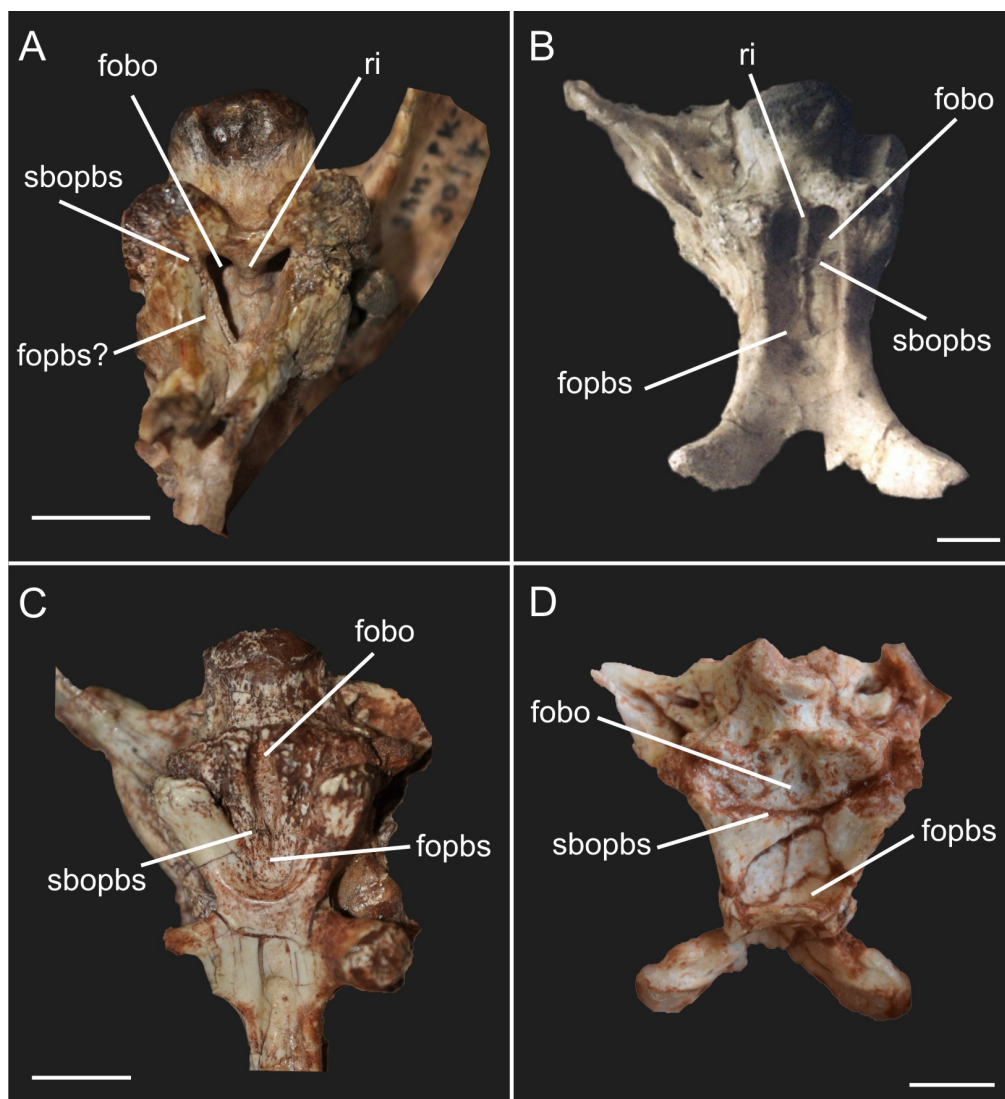
Figure 4.9: Parabasisphenoid and basiocciptal of the specimens SAM 3014 of *Sphenosuchus acutus* (A), QG 195 of *Coelophysis "Syntarsus" rhodesiensis* (B), SAM PK K 1314 of *Massospondylus carinatus* (C), and CAPPA/UFSM 0035 of *Buriolestes schultzi* (D) in ventral view. Abbreviations: **fobo** – fossa in the basioccipital; **fopbs** – fossa in the parabasisphenoid; **ri** – ridge; **sbopbs** – basioccipital/parabasisphenoid suture. Scale bars = 1 cm

Recess in the basioccipital: According to Witmer (1997), the "basisphenoid sinus" can be highly expanded in some taxa, reaching the basioccipital posteriorly. This matches the morphology observed in some dinosaurs (Fig. 4.9). In this case, it is possible that the depressions in the ventral surface of the parabasisphenoid and

basioccipital are related to the same system, the median pharyngeal system (see Witmer, 1997). Nevertheless, differences in the development of this system (i.e. a depression in the basioccipital, a depression in the basisphenoid, or both) can still be phylogenetic informative (Nesbitt, 2011). For instance, in his character 107, Nesbitt (2011) discusses the presence of a deep recess in the basioccipital, which is illustrated by the blind pit present in *Protosuchus fergusi* and the more deep and wide recess of *Sphenosuchus acutus* (see Nesbitt, 2011, fig. 24a and 24e). Nesbitt (2011) set that depression apart from the parabasisphenoid recess, because the latter is exclusive to the basisphenoid. However, when scoring the presence/absence of the basioccipital recess one has to take into consideration the posterior extension of the basisphenoid recess into the basioccipital, which is not usually sharply defined posteriorly, but fades away towards the anteromedial projection of that bone. This morphology was observed in all the dinosauriform braincases we analysed for this study.

Nesbitt (2011) scored the presence of the basioccipital recess (character 107) only for members of Pseudosuchia, but this structure is widespread among dinosaurs. In fact, a depression in the ventral surface of the basioccipital that is continuous with the parabasisphenoid recess anteriorly was observed in all the taxa analysed for this study as mentioned above. Thus, regarding the presence of a basioccipital recess, we suggest that future studies should incorporate different aspects of its morphology, which seems more informative than the simple presence/absence of a recess. For instance, a blind pit within the depression in the anteroventral surface of the basioccipital (Fig. 4.9) was observed in all dinosauriforms, with the exception of *Efraasia*. The situation is not clear in *Herrerasaurus ischigualastensis* because the contact between basioccipital and parabasisphenoid is not possible to be traced, but it seems that this taxon exhibit an anteroposteriorly elongated pit. Furthermore, a single

blind pit is present in the ornithischians *Lesothosaurus diagnosticus* and *Hypsilophodon foxi*, and also in the saurischians *Buriolestes schultzi* (undivided single blind pit); *Massospondylus carinatus* (SAM PK K1314; single pit but anteroposteriorly elongated), *Plateosaurus engelhardti* (AMNH 6810; single pit but anteroposteriorly elongated), and *Eoraptor lunensis* (undivided, single blind pit; but see comment regarding the shape of the basioccipital above). A blind pit seems also to be present in *Lewisuchus admixtus*, and in one specimen of *Silesaurus opolensis* (ZPAL AB III 361/88), whereas it seems to be absent in another specimen of the latter (ZPAL AB III 364/4). Differently, a pair of pits divided by a ridge is observed in the ornithischian *Dysalotosaurus lettowvorbecki*, and theropods such as *Coelophysis* (*"Syntarsus"*) *rhodosiensis* (pit divided by a septum), *Piatnitzkysaurus floresi* (Rauhut, 2004) and *Fukuivenator paradoxus* (Azuma *et al*. 2016, fig. 4).

Regarding the taxa analysed for this study, the presence of a single bind pit in the anteroventral surface of the basioccipital is the condition of all sauropodomorphs and non-dinosaurian dinosauriforms, including *Silesaurus*. Differently, all theropods have a pair of pits divided by a ridge (the only exception would be if *Eoraptor* is a member of Theropoda, as this taxon exhibit a single blind pit). In ornithischians, the two conditions are found.

Anterior tympanic recess and semilunar depression: The anterior tympanic recess (Fig. 4.10), which originates from diverticula of the middle ear sac, is located at the lateral surface of the parabasisphenoid, ventral to the foramen for facial nerve (VII) and the otosphenoidal crest (Witmer, 1997). Still according to Witmer (1997), the anterior tympanic recess can become sub-divided, with the presence of a prootic recess anteriorly and a subotic recess posteriorly (see Witmer, 1997, fig. 3). A divided

anterior tympanic recess has been reported for theropods (e.g. Norell *et al*. 2000, 2009; Makovicky *et al.,* 2003), whereas only an anterior tympanic recess (i.e. undivided) has been recognised as present in all other dinosauriforms (Nesbitt, 2011), and recently also identified in the dinosauromorph *Ixalerpeton polesinensis* (Cabreira *et al.,* 2016). Furthermore, Sobral *et al*. (2016) stated that the depression on the lateral surface of the parabasisphenoid of the non-archosaurian archosauriform *Euparkeria capensis* is topologically equivalent, hence homologous, to the anterior tympanic recess of dinosaurs. However, nomenclatural issues have possibly hampered the recognition of a divided anterior tympanic recess in some previous studies, as taxa such as *I. polesinensis* (see Cabreira *et al*. 2016) and *E. capensis* (see Sobral *et al*. 2016) have been considered to have a semilunar depression (*sensu* Gower & Weber, 1988), rather than a subotic recess (*sensu* Witmer, 1997).
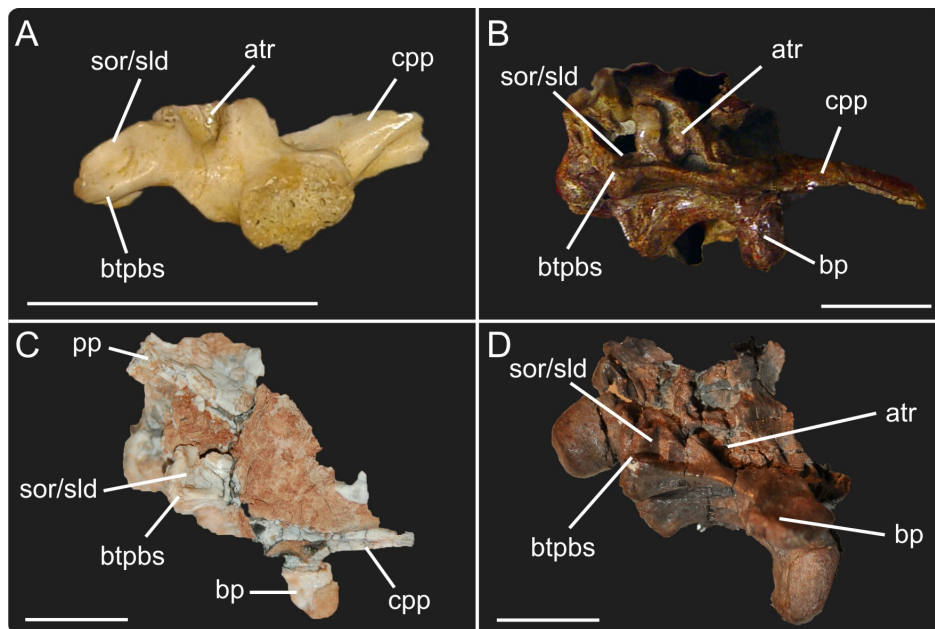
Figure 4.10: Parabasisphenoid of the specimens ZPAL RV/413 of *Osmolskina czatkowicensis* (A), PULR 01 of *Lewisuchus admixtus* (B), MCP 3845 PV of *Saturnalia tupiniquim* (C), and PVSJ 562 of *Eodromaeus murphy* (D) in lateral view. Abbreviations: **atr** – anterior tympanic recess; **bp** – basipterygoid process; **btpbs** – basisphenoid component of the basal tubera; **cpp** – cultriform process of the parabasisphenoid; **pp** – paroccipital process; **sor/sld** – subotic recess / semilunar depression. Scale bars = 1 cm

A detailed discussion on the non-archosaurian archosauromorphs semilunar depression is given by Gower & Weber (1988), where the authors homologized a depression on the lateral surface of the parabasisphenoid of *Euparkeria capensis* with a similar structure previously identified by Evans (1986, figs. 1 and 4) for the non-archosauriform archosauromorph *Prolacerta broomi*. According to Gower & Weber (1998), among non-archosauria archosauriforms, this depression is consistently present on the posteroventral corner of the parabasisphenoid, anterior (and/or dorsal; M.B. pers. obs) to the basisphenoidal component of the basal tubera. Additionally, as they stated that the semilunar depression was absent in crown-group archosaurs, we can assume that Gower & Weber (1998) considered their semilunar depression not homologous to the subotic recess of Witmer (1997). However, both Gower & Weber (1998, fig. 3) and Witmer (1997, fig. 3) were clearly dealing with a depression on the posteroventral region of the lateral surface of the parabasisphenoid dorsal to the basisphenoidal component of the basal tubera. Thus, given their topological equivalence, we prefer to treat the semilunar depression and the subotic recess as *a priori* homologues among all archosauromorphs. Yet, we prefer to adopt the term anterior tympanic to refer to the anterior one of the recesses in the case of a division *sensu* Witmer (1997). This is because a great portion of the anterior recess is located in the basisphenoid, and thus the term prootic recess might be misleading for some readers. Furthermore, this is the term adopted in previous works on early dinosauromorphs (Nesbitt, 2011; Cabreira *et al.*, 2016), and its usage here intends to avoid confusion. Regarding the posterior recess, here we treat it as the semilunar depression because this is also the nomenclature adopted in previous studies on early dinosaurs and non-archosaurian archosauriforms (Nesbitt, 2011; Sookias *et al.*, 2014;

Cabreira *et al.,* 2016; Sobral *et al.,* 2016), and it is therefore potentially less confuse for the following discussion.

The presence/absence of an anterior tympanic recess (Nesbitt *et al.,* 2009; Nesbitt, 2011; Bittencourt *et al.* 2014) and of a semilunar depression (Nesbitt *et al.* 2009; Nesbitt, 2011; Cabreira *et al.,* 2016) have been used as characters in previous phylogenetic studies of early dinosaurs. However, the absence/presence of an anterior tympanic recess (in the general sense discussed above) is non-informative for dinosauromorphs, because the structure is present in all taxa, as already indicated in Nesbitt (2011).

Regarding the semilunar depression, it was scored as present in *"Syntarsus" kayentakatae* in Nesbitt *et al.* (2009), but later Nesbitt (2011) mentioned that this structure was absent in crown-group archosaurs. We did not analyse the braincase of *"Syntarsus" kayentakatae,* but a depression in the posteroventral corner of the lateral surface of the basisphenoid is present in *Coelophysis* ("*Syntarsus*") *rhodesiensis.* Recently, a similar depression has been reported for the lagerpetid *Ixalerpeton polesinensis* (Cabreira *et al.,* 2016), and our observations indicate that such a depression is also present in non-dinosaurian dinosauriforms such as *Marasuchus lilloensis* and *Lewisuchus admixtus*, as well as in the saurischians *Eodromaeus murphi* and *Saturnalia tupiniquim* (Figs. 4.2, 4.10). It is, however, absent in *Silesaurus opolensis, Herrerasaurus ischigualastensis, Tawa hallae, Efraasia minor, Plateosaurus engelhardti, Eocursor parvus*, and *Lesothosaurus diagnosticus.*

We remain largely ignorant regarding the presence of semilunar depression in non-archosaurian archosauriforms, but the presence of this structure in *Euparkeria* and in the non-dinosaurian dinosauromorphs *Ixalerpeton polesinensis* and *Marasuchus liloensis* might indicate that the presence of a semilunar depression is the

ancestral condition of Dinosauromorpha. For Dinosauria, the presence of a semilunar depression in *Saturnalia tupiniquim, Eodromaeus murphi,* and tetanuran theropods [although treated as the subotic recess in the latter, see e.g. Norell *et al.,* (2000); Makovicky *et al.,* (2003)], and its absence in taxa such as *Herrerasaurus ischigualastensis, Tawa hallae,* and *Buriolestes schultzi* so far indicates a scenario of multiple acquisitions and/or losses of this structure. Finally, it is worth stressing that, unlike for the other recesses mentioned above, we could not recognise a shallower depression in the region of the semilunar depression in taxa that do not have the structure.

Relative position of the elements of the ventral portion of the braincase: One aspect that has been analysed (e.g. Yates, 2007) in the context of sauropodomorph evolution is the relative position of some structures at the ventral margin of the braincase, i.e. the cultriform process of the parabasisphenoid, the basal tuberae, and the ventral limit of the occipital condyle. The relations between these elements have also been used as a phylogenetic character in the study of Bittencourt *et al.* (2014), more focused on early dinosauriforms. Regarding Sauropodomorpha, previous studies (Yates, 2007) have found that the plesiomorphic condition is the alignment of all these elements in nearly the same dorsoventral plane. Indeed, this is the condition assumed for taxa such as *Thecodontosaurus antiquus* (Benton *et al.,* 2000) and *Pantydraco caducus*.

A problematic aspect of this character is that the sauropodomorph basal tubera is not a single and/or continuous structure, but a set of knobs and protuberances spanning the basioccipital and the parabasisphenoid that have different positions in the dorsoventral axis (see Chapter 5). In *Thecodontosaurus antiquus*, for example, the basisphenoidal component of the basal tubera is in the same dorsoventral level of the

ventral surface of the parasphenoid rostrum and the ventral limit of the occipital condyle, but part of its basioccipital component is dorsal to these elements. Thus, the "basal tuberae complex" as a whole does not represent a good marker to analyse variations in the alignment of those elements. Nevertheless, comparisons between the ventral surfaces of the occipital condyle and the cultriform process are feasible. In this sense, *Saturnalia tupiniquim* has a stepped braincase, with the ventral surface of the cultriform process ventrally located in relation to the ventral limit of the occipital condyle (Fig. 4.2). This is the same morphology observed in other sauropodomorphs such as *Plateosaurus engelhardti* and *Massospondylus carinatus*. On the other hand, *T. antiquus* has a braincase with the ventral limit of the occipital condyle at the same level of the ventral margin of the cultriform process, which is also the condition observed in *Lewisuchus admixtus*.

Unfortunately, the relative position of these elements in other taxa outside Sauropodomorpha is difficult to establish, as they are either hidden by other bones, or not preserved in articulation. This hampers the elaboration of a more detailed scenario of morphological variation, but we believe that using solely the relative position of the cultriform process of the parabasisphenoid and the occipital condyle is a better approach than adding information on the basal tubera complex.

4.6. CONCLUSIONS

Computed tomography allowed a detailed investigation of the braincase anatomy of the Late Triassic sauropodomorph *Saturnalia tupiniquim*, as previously undone for such an old dinosaur. The description provided here adds to previous publications focusing on the braincase anatomy of Late Triassic sauropodomorphs, contributing to enhance our understanding of this structure in early dinosaurs and its closest

dinosauromorph relatives. Regarding the recesses of the braincase, as mentioned by Witmer (1997), birds are the maximal exponents of skull pneumatisation in archosaurs, but non-avian theropods also exhibit a well-developed pneumatic cranial system. Indeed, in comparison to other dinosaurs, the braincase recesses of theropods are more easily recognised, but various of these recesses, even if "less-developed", are also widespread among other dinosaurs and non-dinosaurian dinosauromorphs.

Finally, the phylogeny of early dinosauriforms is still in the state of flux (Ezcurra, 2010; Langer *et al.*, 2010; Nesbitt *et al.*, 2010; Martinez *et al.*, 2011, 2012b; Langer & Ferigolo, 2013; Bittencourt *et al.*, 2014; Cabreira *et al.*, 2016). Despite few exceptions, such as *Saturnalia tupiniquim,* the affinity of most Triassic taxa to one of the three main dinosaur lineages (Ornithischia, Sauropodomorpha, Theropoda) or to non-dinosaurian dinosauriform clades is still ambiguous (see e.g. Langer, 2014). In this context, future studies might incorporate the information discussed here in the form of phylogenetic characters, which may help stabilising a clearer pattern about the braincase evolution of dinosauromorphs.

4.7. REFERENCES

Apaldetti C, Martinez RN, Pol D, Souter T. 2014. Redescription of the skull of *Coloradisaurus brevis* (Dinosauria, Sauropodomorpha) from the Late Triassic Los Colorados Formation of the Ischigualasto-Villa Union Basin, Northwestern Argentina. *Journal of Vertebrate Paleontology,* 34(5), 1113–1132.

Azuma Y, Xu X, Shibata M, Kawabe S, Miyata K, Imai T. 2016. A bizarre theropod from the Early Cretaceous of Japan highlights mosaic evolution among coelurosaurians. *Scientific Reports,* 6, 20478.

Balanoff AM, Bever GS, Ikejiri T. 2010. The braincase of *Apatosaurus* (Dinosauria: Sauropoda) based on computed tomography of a new specimen with comments on variation and evolution in Sauropod Neuroanatomy. *American Museum Novitates,* 3677, 1–29.

Benton MJ, Juul L, Storrs GW, Galton PM. 2000. Anatomy and systematics of the prosauropod dinosaur Thecodontosaurus antiquus from the Late Triassic of Southwest England. *Journal of Vertebrate Paleontology,* 20, 77–108.

Benton MB, Walker AD. 2011. *Saltopus*, a dinosauriform from the Upper Triassic of Scotland. *Earth and Environmental Science Transactions of the Royal Society of Edinburgh*, 101(3-4), 285-299.

Bever GS, Brusatte SL, Carr TD, Xu X, Balanoff AM, Norell MA. 2013. The braincase anatomy of the Late Cretaceous dinosaur Alioramus (Theropoda: Tyrannosauroidea). *Bulletin of the American Museum of Natural History,* 376, 1–72.

Bittencourt JS, Arcucci AB, Marsicano CA, Langer MC. 2014. Osteology of the Middle Triassic archosaur Lewisuchus admixtus Romer (Chañares Formation, Argentina), its inclusivity, and relationships amongst early dinosauromorphs. Journal of Systematic Palaeontology, 13(3), 189–219.

Butler RJ. 2010. The anatomy of the basal ornithischian dinosaur *Eocursor parvus* from the Lower Elliot Formation (Late Triassic) of South Africa. *Zoological Journal of the Linnean Society,* 160, 648-684.

Butler RJ, Smith RMH, Norman DB. 2007. A primitive ornithischian dinosaur from the Late Triassic of South Africa, and the early evolution and diversification of Ornithischia. *Proceedings of the Royal Society B*, 274 (1621), 2041–2046.

Cabreira SF, Kellner AWA, Dias-da-Silva S, Silva LR, Bronzati M, Marsola JCA, Müller RT, Bittencourt JS, Batista BJ, Raugust T, Carrilho R, Brodt A, Langer MC. 2016. A unique Late Triassic dinosauromorph assemblage reveals dinosaur ancestral anatomy and diet. *Current Biology*, 26(22), 3090-3095.

Dufeau DL. 2011. The evolution of the cranial pneumaticity in Archosauria: Patterns of paratympanic sinus development. PhD thesis. College of Arts and Sciences of Ohio University.

Evans SE. 1986. The braincase of *Prolacerta broomi* (Reptilia, Triassic). *Neues Jahrbuch für Geologie und Paläontologie, Abhandlungen,* 173(2), 181-200.

Ezcurra MD. 2007. The cranial anatomy of the coelophysoid theropod *Zupaysaurus rougieri* from the Upper Triassic of Argentina. *Historical Biology,* 19, 185-202.

Ezcurra MD. 2010. A new early dinosaur (Saurischia: Sauropodomorpha) from the Late Triassic of Argentina: a reassessment of dinosaur origin and phylogeny. *Journal of Systematic Palaeontology,* 8(3), 371-425.

Ezcurra MD. 2016. The phylogenetic relationships of basal archosauromorphs, with an emphasis on the systematics of proterosuchian archosauriforms. *PeerJ,* 4, e1778.

Ezcurra MD, Cuny G. 2007. The coelophysoid *Lophostropheus airelensis*, gen. nov.: a review of the systematics of "*Liliensternus*" *airelensis* from the Triassic-Jurassic boundary outcrops of Normandy (France). *Journal of Vertebrate Paleontology*, 27 (1), 73–86.

Galton PM. 1984. Cranial anatomy of the prosauropod dinosaur *Plateosaurus* from the Knollenmergel (Middle Keuper, Upper Triassic) of Germany. I. Two

complete skulls from Trossingen/Württ, with comments on the diet. *Geologica et Palaeontologica*, 18, 139–171.

Galton PM. 1985. Cranial anatomy of the prosauropod dinosaur *Plateosaurus* from the Knollenmergel (Middle Keuper, Upper Triassic) of Germany. II. All the cranial material and details of soft-part anatomy. *Geologica et Palaeontologica*, 19, 119-159.

Galton PM, Bakker RT. 1985. The cranial anatomy of the prosauropod dinosaur "*Efraasia diagnostica*", a juvenile individual of *Sellosaurus gracilis* from the Upper Triassic of Nordwürttemberg, West Germany. *Stuttgarter Beiträge zur Naturkunde B*, 117, 1–15

Galton PM, Kermack D. 2010. The anatomy of *Pantydraco caducus*, a very basal sauropodomorph dinosaur trom the Rhaetian (Upper Triassic) of South Wales, UK. *Revue de Paléobiologie*, 29(2), 341-404.

Gow CE. 1990. Morphology and growth of the *Massospondylus* braincase (Dinosauria, Prosauropoda). *Paleontologia Africana*, 27, 59–75.

Gower DJ. 2002. Braincase evolution in suchian archosaurs (Reptilia: Diapsida): evidence from the rauisuchian *Batrachotomus kupferzellensis*. *Zoological Journal of the Linnean Society*, 136, 49–76.

Gower DJ, Weber E. 1998. The braincase of *Euparkeria*, and the evolutionary relationships of avialans and crocodilians. *Biological Reviews*, 73: 367–411.

Kammerer CF, Nesbitt SJ, Shubin NH. 2012. The First Silesaurid Dinosauriform from the Late Triassic of Morocco. *Acta Palaeontologica Polonica*. 57(2), 277-284.

Knoll F, Witmer LM, Ortega F, Ridgely RC, Schwarz-Wings D. 2012. The braincase of the basal Sauropod dinosaur *Spinophorosaurus* and 3D reconstructions of the cranial endocast and inner ear. *Plos One*, 7(1), e30060.

Kurzanov SM. 1976. Brain-case structure in the carnosaur *Itemirus* N. gen. and some aspects of the cranial anatomy of dinosaurs. *Paleontological Journal*, 1976, 361–369.

Langer MC. 2003. The pelvic and hindlimb anatomy of the stem-sauropodomorph *Saturnalia tupiniquim* (Late Triassic, Brazil). *Paleobios*, 23, 1-40.

Langer MC. 2014. The origins of Dinosauria: Much ado about nothing. *Palaeontology*, 57, 469-478

Langer MC, Ferigolo J. 2013. The Late Triassic dinosauromorph *Sacisaurus agudoensis* (Caturrita Formation; Rio Grande do Sul, Brazil): anatomy and affinities. *Geological Society Special Publication*, 379, 353-392.

Langer MC, Abdala F, Richter M, Benton MJ. 1999. A sauropodomorph dinosaur from the Upper Triassic (Carnian) of southern Brazil. *Earth & Planetary Sciences*, 329, 511–517.

Langer MC, França MAG, Gabriel S. 2007. The pectoral girdle and forelimb anatomy of the stem-sauropodomorph *Saturnalia tupiniquim* (Upper Triassic, Brazil). *Special Papers in Palaeontology*, 77, 113-137.

Langer MC, Ezcurra MD, Bittencourt JS, Novas FE. 2010. The origin and early evolution of dinosaurs. *Biological Reviews*, 85, 55-110.

Lautenschlager S, Rayfield EJ, Altangerel P, Zanno LE, Witmer LM. 2012 The Endocranial Anatomy of Therizinosauria and Its Implications for Sensory and Cognitive Function. *PLoS ONE,* 7(12), e52289.

Makovicky PJ, Norell MA, Clark JM, Rowe T. 2003. Osteology and relationships of *Byronosaurus jaffei* (Theropoda: Troodontidae). *American Museum Novitates,* 3402, 1-32.

Martinez RN. 2009. *Adeopapposaurus mognai,* gen. et sp. nov. (Dinosauria: Sauropodomorpha), with comments on adaptations of basal Sauropodomorpha. *Journal of Vertebrate Paleontology,* 29, 142–164.

Martinez RN, Alcober OA. 2009. A Basal Sauropodomorph (Dinosauria: Saurischia) from the Ischigualasto Formation (Triassic, Carnian) and the Early Evolution of Sauropodomorpha. *PLoS ONE,* 4(2), e4397.

Martinez RN, Sereno PC, Alcober OA, Colombi CE, Renne PR, Montanez IP, Currie BS. 2011. A basal dinosaur from the Dawn of the Dinosaur Era in Southwestern Pangaea. *Science,* 331, 206-210.

Martinez RN, Haro JA, Apaldetti C. 2012a. Braincase of *Panphagia protos* (Dinosauria, Sauropodomorpha). *Journal of Vertebrate Paleontology,* 32(suppl. 1), 70–82.

Martinez RN, Apaldetti C, Pol D. 2012b. Basal Sauropodomorphs from the Ischigualasto Formation. *Journal of Vertebrate Paleontology,* 32(suppl. 6), 51–69.

Martínez RN, Apaldetti C, Correa GA, Abelín D. 2016. A Norian lagerpetid dinosauromorph from the Quebrada del Barro Formation, northwestern Argentina. *Ameghiniana,* 53 (1), 1–13.

Martz JW, Small BJ. 2006. *Tecovasuchus chatterjeei,* a new aetosaur (Archosauria: Stagonolepididae) from the Tecovas Formation (Carnian, Upper Triassic) of Texas. *Journal of Vertebrate Paleontology,* 26, 308–320.

Nesbitt SJ. 2011. The early evolution of archosaurs: relationships and the origin of the major clades. *Bulletin of the American Museum of Natural History,* 352, 1–292.

Nesbitt SJ, Smith ND, Irmis RB, Turner AH, Downs A, Norell MA. 2009. A complete skeleton of a Late Triassic saurischian and the early evolution of dinosaurs. *Science,* 326, 1530-1533.

Nesbitt SJ, Sidor CA, Irmis RB, Angielczyk KD, Smith RMH, Tsuji, LA. 2010. Ecologically distinct dinosaurian sister groups shows early diversification of Ornithodira. *Nature,* 464(4), 95-98.

Norell MA, Makovicky PJ, Clark JM. 2000. A new troodontid theropod from Ukhaa Tolgod, Mongolia. *Journal of Vertebrate Paleontology,* 20(1), 7-11.

Norell MA, Makovicky PJ, Bever GS, Balanoff AM, Clark JM, Barsbold R, Rowe T. 2009. A review of the Mongolian Cretaceous dinosaur *Saurornithoides* (Troodontidae:Theropoda). *American Museum Novitates.* 3654, 1-63.

Norman DB, Crompton AW, Butler RJ, Porro LB, Charig AJ. 2011. The Lower Jurassic ornithischian dinosaur *Heterodontosaurus tucki* Crompton & Charig,

1962: cranial anatomy, functional morphology, taxonomy, and relationships. *Zoological Journal of the Linnean Society*, 163, 182-276.

Paulina-Carabajal A, Carballido JL, Currie PJ. 2014. Braincase, neuroanatomy, and neck posture of *Amargasaurus cazaui* (Sauropoda, Dicraeosauridae) and its implications for understanding head posture in sauropods. *Journal of Vertebrate Palaeontology,* 34(4), 870–882.

Peecook BR, Sidor CA, Nesbitt SJ, Smith RMH, Steyer JS, Angielczyk KD. 2013. A new silesaurid from the upper Ntawere Formation of Zambia (Middle Triassic) demonstrates the rapid diversification of Silesauridae (Avemetatarsalia, Dinosauriformes). *Journal of Vertebrate Paleontology*, 33(5), 1127.

Porro LB, Witmer LM, Barrett PM. 2015. Digital preparation and osteology of the skull of *Lesothosaurus diagnosticus* (Ornithischia: Dinosauria). *PeerJ,* 3, e1494.

Prieto-Márquez A, Norell MA. 2011. Redescription of a nearly complete skull of *Plateosaurus* (Dinosauria: Sauropodomorpha) from the Late Triassic of Trossingen (Germany). *American Museum Novitates*, 3727, 1–58.

Rauhut OWM. 2004. Braincase structure of the Middle Jurassic theropod dinosaur *Piatnitzkysaurus*. *Canadian Journal of Earth Sciences*, 41, 1109–1122.

Sampson SD, Witmer LM. 2007. Craniofacial anatomy of *Majungasaurus crenatissimus* (Theropoda: Abelisauridae) from the Late Cretaceous of Madagascar. *Journal of Vertebrate Paleontology*, 27, 32–102.

Sereno PC, Novas FE. 1993. The skull and neck of the basal theropod *Herrerasaurus ischigualastensis*. *Journal of Vertebrate Paleontology,* 13, 451–476.

Sereno PC, Arcucci AB. 1994. Dinosaurian precursors from the Middle Triassic of Argentina: *Marasuchus lilloensis* gen. nov. *Journal of Vertebrate Paleontology,* 14, 53-73

Sereno PC, Martinez RN, Alcober OA. 2012. Osteology of *Eoraptor lunensis* (Dinosauria, Sauropodomorpha). *Journal of Vertebrate Paleontology*, 32(suppl. 6), 83–179.

Sobral G, Hipsley CA, Müller J. 2012. Braincase redescription of Dysalotosaurus lettowvorbecki (Dinosauria, Ornithopoda) based on computed tomography. *Journal of Vertebrate Paleontology*, 32, 1090–1102.

Sobral G, Sookias RB, Bhullar B-AS, Smith R, Butler RJ, Müller J. 2016. New information on the braincase and inner ear of *Euparkeria capensis* Broom: implications or diapsid and archosaur evolution. *Royal Society Open Science,* 3, 160072.

Sookias RB, Sennikov AG, Gower DJ, Butler RJ. 2014. The monophyly of Euparkeriidae (Reptilia: Archosauriformes) and the origins of Archosauria: a revision of *Dorosuchus neoetus* from the Mid-Triassic of Russia. *Palaeontology,* 57(6), 1177–1202.

Sues H-D, Nesbitt SJ, Berman DS, Henrici AC. 2011. A late-surviving basal theropod dinosaur from the latest Triassic of North America. *Proceedings of the Royal Society B*, 278(1723), 3459–3464.

Wilson JA. 2005. Overview of sauropod phylogeny and evolution. In (Eds. KA Curry Rogers, JA Wilson) *The Sauropods: Evolution and Paleobiology*, University of California Press, Berkeley, pp. 15–49.

Witmer LM. 1997. Craniofacial air sinus systems. In (Eds. PJ Currie, K Padian) *Encyclopedia of dinosaurs*. Academic Press, San Diego, pp. 151–159.

Witmer LM, Ridgely RC. 2009. New Insights Into the brain, braincase, and ear region of Tyrannosaurs (Dinosauria, Theropoda), with implications for sensory organization and behaviour. *The Anatomical Record*, 292, 1266–1296.

Yates AM. 2007. The first complete skull of the Triassic dinosaur M*elanorosaurus* Haughton (Sauropodomorpha: Anchisauria). *Special Papers in Palaeontology*, 77. 9–55.

CHAPTER 5

Braincase redescription of *Efraasia minor* (Huene, 1908) (Dinosauria, Sauropodomorpha) from the Late Triassic of Germany, with comments on the evolution of the sauropodomorph braincase.

Chapter re-submitted to the *Zoological Journal of the Linnean Society* after the first round of peer review as: Braincase redescription of *Efraasia minor* (Huene, 1908) (Dinosauria, Sauropodomorpha) from the Late Triassic of Germany, with comments on the evolution of the sauropodomorph braincase. Manuscript number: ZOJ 12-2016-2832.

Authors: Mario Bronzati[1,2,*], Oliver W. M. Rauhut[1,2]

Author contributions:

M.B. and O.W.M.R. conceptualized the study; **M.B.** segmented the CT-Scan data; **M.B.** performed the phylogenetic analysis; **M.B.,** and O.W.M.R. analysed the results; **M.B**., and O.W.M.R. wrote the manuscript.

Chapter 5

Braincase redescription of *Efraasia minor* (Huene, 1908) (Dinosauria, Sauropodomorpha) from the Late Triassic of Germany, with comments on the evolution of the sauropodomorph braincase

Mario Bronzati[1,2], and Oliver W. M. Rauhut[1,2]

[1] Department of Earth and Enviromental Sciences, Ludwig–Maximilians–Universität, Richard-Wagner-Strasse, 10, 80333, Munich, Germany.

[2] Bayerische Staatssammlung für Paläontologie und Geologie; Richard-Wagner-Strasse, 10, 80333, Munich, Germany.

5.1. Abstract

The braincase anatomy of the sauropodomorph dinosaur *Efraasia minor* (Late Triassic, Norian, Löwenstein Formation of Germany) is redescribed in detail, adding new information based on CT-Scan data. We discuss the evolution of sauropodomorph braincases from a phylogenetic perspective, focusing on non-neosauropodan representatives. For this, we revised braincase characters used in data matrices focused on these assemblage of taxa. This led to the recognition of problems with some of the phylogenetic characters, which did not accurately reflect the morphological variation observed among taxa within the group. We also discuss the presence of a divided metotic foramen in members of the group. This has implications

for the recognition of soft tissues associated with braincase foramina in non-sauropodan sauropodomorphs, and we propose that the the path for the jugular vein was either through the posterior foramen resulting from this division or through the foramen magnum. Finally, our study demonstrates a series of differences regarding braincase anatomy between "prosauropods" and sauropod taxa. However, it remains unclear if these differences might be due to a drastic morphological change at the basis of the Sauropoda or if they simply reflect the lack of braincase materials of non-neosauropodan sauropods, which might exhibit transitional morphologies.

5.2. INTRODUCTION

Sauropoda includes the largest land animals in earth history (Upchurch *et al*. 2004; Wilson, 2005), which exhibit a peculiar morphology that largely deviates from the body plan of the earliest representatives of Sauropodomorpha (see e.g. Rauhut *et al*. 2011). The earliest sauropodomorphs are well known from the Late Triassic of South America, and were small, gracile, and probably bipedal and omnivore/carnivore animals (e.g. Langer *et al*., 1999; Martinez & Alcober, 2009; Ezcurra, 2010; Martinez *et al*., 2012a; Cabreira *et al*., 2016). Anatomical transformations related to quadrupedalism, a herbivorous diet, and increase in body size is observed in non-sauropodan sauropodomorph lineages (Upchurch *et al*., 2007; Rauhut *et al*., 2011; McPhee *et al*., 2015). This shows that the peculiar and conspicuous morphology of sauropods is a product of morphological transformations including those that happened earlier in the evolutionary history of sauropodomorphs (e.g., Upchurch & Barrett, 2000; Barrett & Upchurch, 2007; Parrish, 2005; Bonnan & Senter, 2007; Upchurch *et al*., 2007; Martinez, 2009; Yates *et al*., 2010; Pol *et al*., 2011; McPhee *et*

al., 2014; 2015), among lineages once thought to be conservative (Sereno, 2007a). These lineages are classically referred to as "prosauropods" (see e.g. Galton & Upchurch 2004), but this grouping (in its traditional sense) is now generally regarded as a paraphyletic array of taxa that are consecutively closer to Sauropoda (e.g. Upchurch *et al.*, 2007; Yates 2007b; Pol *et al.*, 2011; McPhee *et al.*, 2015; Otero *et al.*, 2015). In this scenario of major evolutionary changes happening among the "prosauropodan" lineages, the conspicuous braincase morphology of sauropods, which may be related to the lowest encephalisation quotients amongst amniotes (Hopson 1979, 1980), probably stems from anatomical modifications within non-sauropodan sauropodomorphs. However, this particular structure has received rather limited attention in evolutionary studies of non-sauropodan sauropodomorphs.

Braincase anatomy in general has received greater attention in the last years. The development of computed tomography and virtual reconstruction techniques (e.g., Witmer & Ridgely, 2009; Balanoff *et al.*, 2010; Knoll *et al.*, 2012) together with the recognition of this structure as an important character complex in phylogenetic analyses (Brusatte *et al.*, 2010; Carrano *et al.*, 2012; Gower, 2002; Gower & Nesbitt, 2006; Nesbitt, 2011; Pol *et al.*, 2013) contributed to placing the braincase in the forefront of archosaur studies. In dinosaur literature, the anatomy of these complex structures has been mainly investigated in detail in theropods (e.g., Sampson & Witmer, 2007; Lautenschlager *et al.*, 2012; Bever *et al.*, 2013), ornithischian dinosaurs (e.g., Evans *et al.*, 2007, 2009; Sobral *et al.*, 2012), and sauropods (e.g., Balanoff *et al.*, 2010; Knoll *et al.*, 2012; Rowe *et al.*, 2010). For non-sauropodan sauropodomorph dinosaurs, however, the significance of this structure has not yet been explored in its totality. Apart from a few more detailed studies on the anatomy of the braincase (e.g. Galton; 1985; Galton & Kermack, 2010; Martinez *et al.*, 2012b;

Apaldetti *et al.,* 2014), the morphology of this structure still plays a small role in morphological descriptions.

We herein re-describe the braincase of *Efraasia minor* Huene, 1908, a Late Triassic (Norian) sauropodomorph from Germany. The material used as basis for this study, the skull of the specimen SMNS 12667, was previously described in a paper by Galton & Bakker (1985). However, a more detailed description of the braincase morphology, including data obtained from CT-Scans is provided here. The comparative nature of this study led to the recognition of problematic issues in the literature on sauropodomorph braincase. These include the misidentification of structures and problems in the definition of characters used in phylogenetic studies of the group, which are also discussed here.

5.3. MATERIAL & METHODS

Institutional Abbreviations

Abbreviations: **AMNH** – American Museum of Natural History; **BMNH** – British Museum of Natural History; **BPI** – Bernard Price Institute for Palaeontological Research, University of the Witwaaterstrand; **MB** – Museum für Naturkunde Berlin; **MCP-PV** – Museu de Ciência e Tecnologia da PUC-RS; **PVL** – Paleontologia de Vertebrados Lillo, Universidad Nacional de Tucuman; **PVSJ** – Museo do Ciencias Naturles, Universidad Nacional de San Juan; **SAM** – Iziko South African Museum; **UFSM** – Universidade Federal de Santa Maria, Santa Maria, Brazil; YPM – Yale Peabody Museum; **ZPAL** – Institute of Paleobiology of the Polish Academy of Science

Taxonomic History of SMNS 12667

The braincase described here belongs to specimen SMNS 12667 of *Efraasia minor,* and is housed in the Staatliches Museum für Naturkunde (Stuttgart, Germany). SMNS 12667 consists of a fairly complete skeleton preserved in 4 blocks (Galton, 1973; Galton & Bakker, 1985), the smallest of which contains the skull elements (Fig. 5.1). Besides the incomplete skull, preserved bones in the other three blocks include cervical, dorsal, sacral and caudal vertebrae, ribs, gastralia, left and right scapulae, right coracoid, left humerus, metacarpals, left ilium, left and right pubis, left and right femora, right tibia, right fibula, right astragalus, right calcaneum, and the proximal end of the right pes (see Galton, 1973). The block in which braincase elements of SMNS 12667 are preserved contains not only these remains but also other cranial bones, such as the quadrate, pterygoid, squamosal, articular, and surangular, and also the atlas.

The bones were excavated by the German palaeontologist Eberhard Fraas, who named this specimen in his 1913 paper as a new species of the genus *Thecodontosaurus* Riley & Stuchbury, 1836, *T. diagnosticus* Fraas, 1913. At that time, Fraas referred two specimens to *T. diagnosticus,* SMNS 12667 and another skeleton discovered in the same excavation, SMNS 12668. However, Fraas (1913) did not provide a description or diagnosis, so that *Thecodontosaurus diagnosticus* Fraas, 1913, has to be regarded as a *nomen nudum*. Later, Huene (1932) validated the species name and described the material under the name *Palaeosaurus*(?) *diagnosticus*. It was not until Galton (1973) that the genus *Efraasia* Galton, 1973 was firstly proposed, with specimens SMNS 12667 and SMNS 12668 assigned to the species *E. diagnosticus*. Initial works on SMNS 12667 mainly dealt with the postcranial elements preserved (Fraas, 1913; Huene, 1932; Galton, 1973). Huene (1932) described the braincase in a very preliminary way. Following further

preparation of the block containing the cranial elements, Galton & Bakker (1985) presented the first detailed description of the skull remains, including the braincase. In their paper, the authors also proposed a new taxonomic change, suggesting that the specimen SMNS 12667 should be considered a junior synonym of *Sellosaurus gracilis* von Huene, 1908 (see also Galton, 1985).
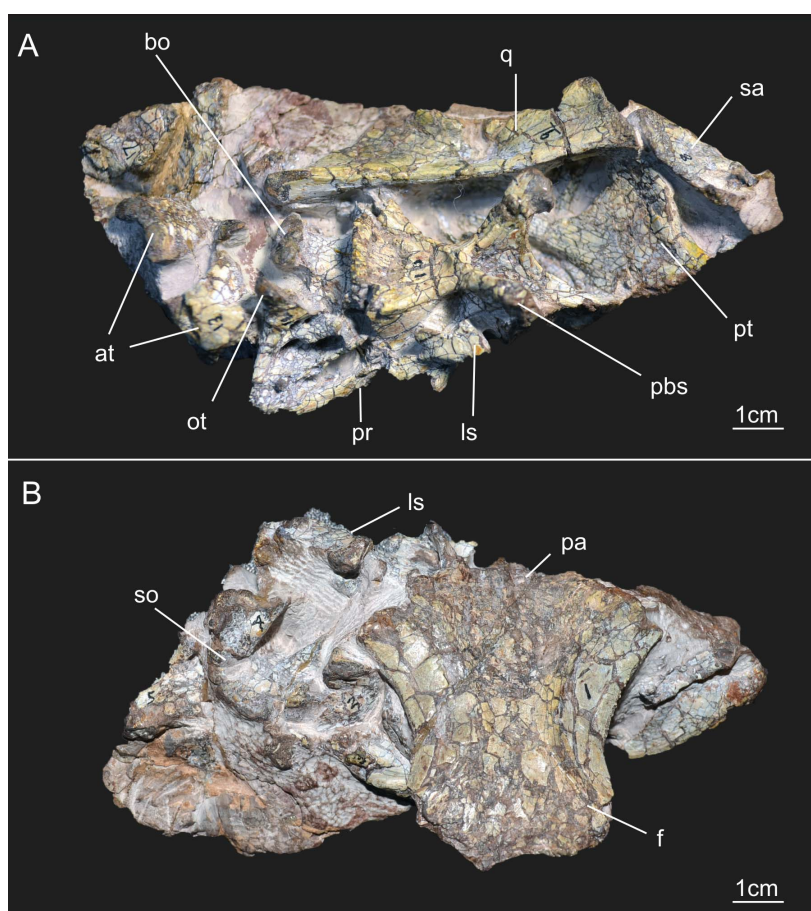
Figure 5.1: General view of the block containing the braincase of the specimen SMNS – 12667 of *Efraasia minor*. Abbreviations: **at** – atlas; **bo** – basioccipital; **f** – frontals; **ls** – laterosphenoid; **ot** – otoccipital; **p** – parietal; **pbs** – parabasisphenoid; **pr** – prootic; **pt** – pterygoid; **q** – quadrate; **sa**: surangular; **so** – supraoccipital.

In a more recent study, Yates (2003) conducted a taxonomic analysis of the sauropodomorph materials of the Löwenstein Formation, Late Triassic, Germany.

Yates came to the conclusion that sauropodomorph fossils coming from this formation belong to two different genera, *Plateosaurus* von Meyer, 1837, including *P. gracilis* Huene, 1908 and *P. engelhardti* von Meyer, 1837, and *Efraasia*. Together with other materials, SMNS 12667 was assigned to the latter genus, but under the species name *Efraasia minor,* which was first proposed by Huene (1908) as a new species of *Teratosaurus* Huene, 1908 (see Galton, 1973). This taxonomic assignment to *Efraasia minor* proposed by Yates (2003) has been adopted widely in the literature (e.g. Yates *et al.,* 2010; Pol *et al.,* 2011; Apaldetti *et al.,* 2011; McPhee *et al.,* 2014), and is also the one followed in this study.

Systematic Terminology

Here we follow the definitions proposed by Galton & Upchurch (2004) and Yates (2007a) for Sauropodomorpha and Sauropoda, respectively.

CT-Scan Procedure

The block containing the braincase of the specimen SMNS 12667 was scanned in a Nanotom Scan (GE Sensing & Inspection Technologies GmbH, Wunstorf Germany), located at the Zoologische Staatsammlung München (Bavaria State Collection of Zoology, Munich, Germany). In a 55 minutes scanning procedure (Voltage: 80Kv; Current: 240 μA; 0,1 mm, diamond filter), 1651 x-ray slices were generated, which yielded a volume dataset with the following dimensions: 2063x1553x2398 with 3,1 μm voxel size. Because of the poor contrast between matrix and bones, an automatic volume rendering did not bring any result. The slices obtained in the scanning procedure were therefore downsampled by half and then segmented in the software Amira (version 5.3.3, Visage Imaging, Berlin, Germany) by hand.

5.4. RESULTS

In the following description we employed traditional anatomical and directional terms such as 'anterior' and 'posterior' rather than using the veterinary terms 'cranial' and 'caudal', respectively. Taxa used for comparisons are detailed in Table 1.

Table 1: List of comparative taxa used in the present study. Specific collection numbers represent specimens analysed first-hand by the authors, whereas other comparative data were obtained from the literature listed within the table

Taxon	Source of Information
Adeopapposaurus mognai	PVSJ 568; PVSJ 610; Martinez, 2009
Coloradisaurus brevis	PVL 3967; Apaldetti *et al.,* 2014
Dicraeosaurus hansemanni	MB.R.2379.1-3
Eoraptor lunensis	PVSJ 512; Sereno *et al.,* 2012
Giraffatitan brancai	MB.R.2180.22.1-4
Herrerasaurus ischigualastensis	PVSJ 407; Sereno & Novas, 1993
Massospondylus carinatus	SAM-PK-K1314
Massospondylus kaalae	SAM-PK-K1325; Barrett, 2009
Melanorosaurus readi	Yates, 2007
Melanorosaurus sp.	Jay Nair pers. comm.
Panphagia protos	PVSJ 874; Martinez *et al.,* 2012
Pantydraco caducus	BMNH - P.24; P.141/1; Galton & Kermack, 2010
Plateosaurus	MB.R.5586-1; SMNS 13200; Prieto-Marquez & Norell, 201
Riojasaurus incertus	PULR 56
Sarahsaurus aurifontanalis	Rowe *et al.,* 2010
Saturnalia tupiniquim	MCP 3845-PV
Silesaurus opolensis	ZPAL AB III/361; ZPAL Ab III/362
Thecodontosaurus antiquus	Benton *et al.,* 2000
Tornieria africana	MB.R.2386
Unaysaurus tolentinoi	UFSM 11069
Sauropoda indet.	MB.R. 2387.1-3,4; Remes, 2006

General aspects of the braincase

Braincase bones that are preserved include the parabasisphenoid (= parasphenoid + basisphenoid – *sensu* Gower & Weber, 1998), basioccipital, otoccipital (= exoccipital + opisthotic – *sensu* Sampson & Witmer, 2007), prootics, left laterosphenoid, supraoccipital, frontals, and a fragment of the anterior portion of the parietals (Fig.

5.1). Based on the CT-Scan data, it is very likely that most of the separation between bones of SMNS 12667 did not happen due to breakage, but through disarticulation, testifying to the skeletally immature status of the specimen at the time of its death (see below). The frontals, the left laterosphenoid, and the supraoccipital are displaced from their original position. The assemblage of bones including the basioccipital, parabasisphenoid, prootics, and otoccipitals, which represent the ventral and lateral portion of the braincase, are preserved almost in the position these bones would occupy in the animal in life, although only the left prootic and otocipital are still articulated with each other (Fig. 5.2). Most of the left side of the braincase is visible, except for the contact of the parabasisphenoid and prootic (hidden by the displaced laterosphenoid), and also the anteriormost region of the parabasisphenoid (Fig. 5.1). With the data from the CT-Scan it was possible to reconstruct the morphology of the entire lateral surface of these bones and also to access details of some of the cranial openings. Moreover, the CT-Scan showed that the right prootic and otoccipital are partially preserved inside the matrix (Fig. 5.2). Finally, CT-Scan data also shows that most of the medial surface of the bones of the lateral wall and also the floor of the braincase are preserved in a way that makes an accurate reconstruction of the internal elements (e.g. soft tissues such as the inner ear) impossible (see also Appendix for this chapter).
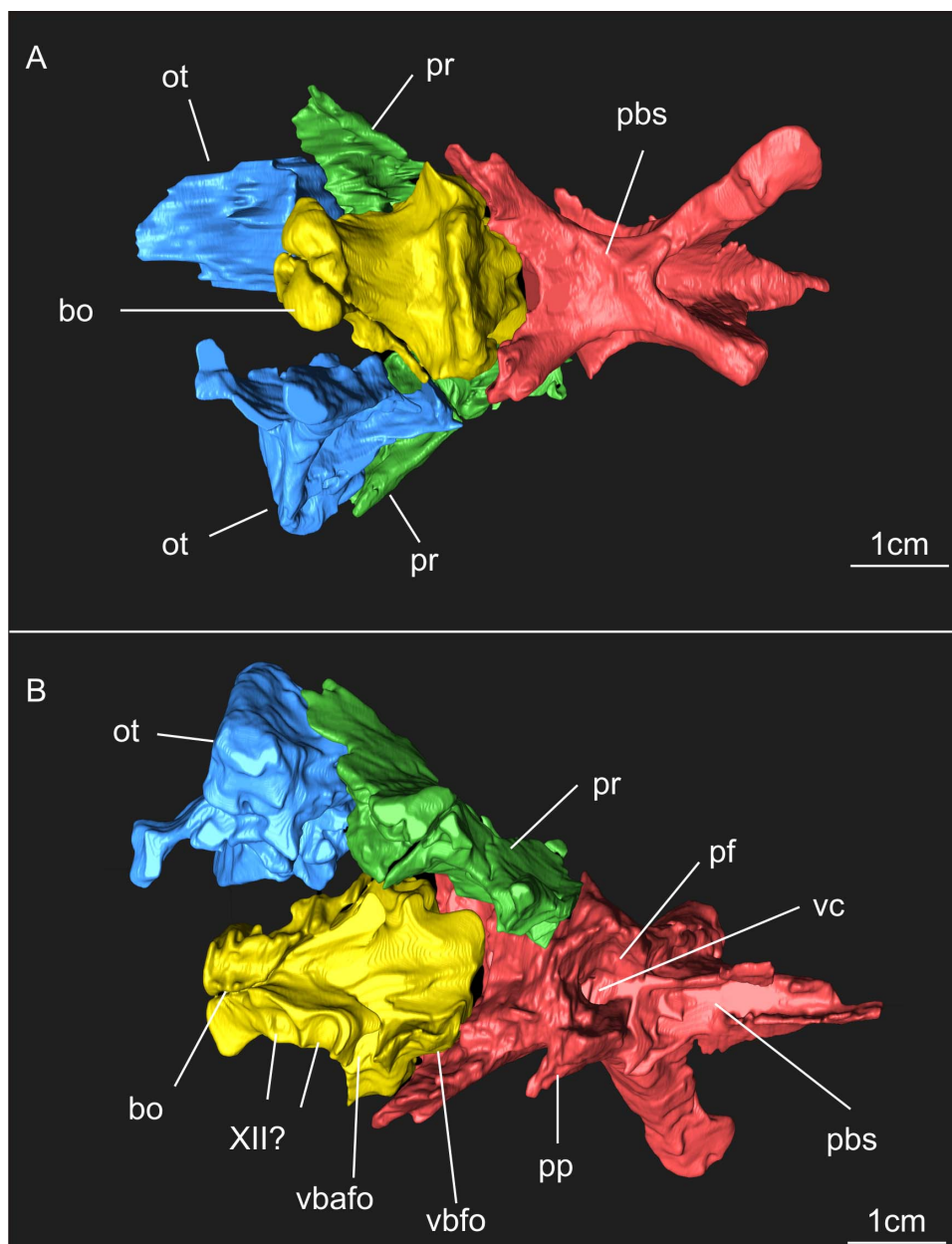
Figure 5.2: Results of the segmentation of CT-Scan data showing some of the braincase bones of the specimen SMNS - 12667 preserved in the block – the laterosphenoid was omitted because it was strongly displaced from its original position (but see Fig. 5.11). A: ventral view of the braincase. B: Dorsal view of the braincase (right prootic and otoccipital were excluded in order to show details of the dorsal surface of basioccipital and parabasisphenoid). Abbreviations: **bo** – basioccipital; **ot** – otoccipital; **pbs** – parabasisphenoid; **pf** – pituitary fossa; **pp** – preotic pendant; **pr** – prootic; **vbafo** – ventral border of the anterior foramen of the otoccipital between the exoccipital pillar and the fenestra ovalis; **vbfo** – ventra border of the fenestra ovalis; **vc** – vidian canal; **XII** – foramen for cranial nerve XII.

In the original description by Galton & Bakker (1985), the authors point out that the elements of the ventral surface of the braincase (cultriform process of the parasphenoid, proximal part of the basipterygoid processes, basal tubera and occipital condyle) were positioned at the same dorsoventral level, a condition classically regarded as the plesiomorphic condition for Sauropodomorpha (Yates, 2007b). A different interpretation from that of Galton & Bakker (1985) was given by Yates (2003), who stated that the occipital condyle is located slightly dorsally in relation to the ventral elements of the braincase.

Determining the exact condition in *Efraasia minor* is not trivial, because of fractures, displacement, and complete disarticulation of some elements. In the basioccipital, a line of fracture is present slightly posterior to the basioccipital component of the basal tubera, indicating a ventral dislocation of the posterior portion of the basioccipital, including the condyle. Furthermore, the parabasisphenoid and basioccipital were almost completely disarticulated from each other, in a way that makes it impossible to determine if the basioccipital was displaced ventrally or if it is in its original position. Thus, to securely establish the position of the occipital condyle in relation to the ventral margin of the braincase would require more complete material with less displacement of its elements. However, if the condyle was displaced dorsally, this displacement was rather small, and certainly considerably less than that seen in sauropodomorphs such as *Plateosaurus*, *Massospondylus carinatus* Owen, 1854, or *Coloradisaurus brevis* Bonaparte, 1978.

Frontal

The frontals (Fig. 5.3) were originally identified as parietals by Huene (1932). Galton & Bakker (1985) correctly re-identified these bones as the frontals, and also mention in their paper that a small portion of the parietals is attached to the posterior margin of the frontals. Both frontals are preserved in SMNS 12667 (Fig. 5.3) and exposed in ventral view. There is no traceable suture between the left and right elements, nor was it possible to visualize bone limits in the CT-scan. However, as sutures are rather untraceable in the entire braincase, and the frontals are affected by numerous fractures, the lack of suture might be related to the preservation rather than representing real fusion of the left and right elements. In *Plateosaurus* (Prieto-Marquez & Norell, 2011) and *Massospondylus kaalae* Barrett, 2009, it is possible to observe a suture in the midline between both bones in the ventral surface. Likewise, early sauropodomorphs such as *Panphagia protos* Martinez & Alcober, 2009 and *Eoraptor lunensis* Sereno *et al.*, 1993 do not have fused frontals. Thus, it seems unlikely that these bones would have been fused in *Efraasia*. The frontals are longer than wide. The total length of the frontal is about 45 mm, and its maximum width, in the posterior third of the bone, is 25 mm. This is an intermediate condition in relation to *Panphagia* (Martinez *et al.*, 2012b), in which the anteroposterior length is twice the width of the frontal, and *Plateosaurus* (AMNH 6810), in which this relation is approximately 1,5. Due to preservation, the right frontal shows the distinction between two regions of the ventral surface of the bone, the orbital and endocranial roofs (Fig. 5.3), better than the left element. The orbital roof corresponds to the region of the frontal that forms the dorsal border of the orbit, whereas the endocranial cavity houses the olfactory tract (Sampson & Witmer, 2007). Both regions are delimited by a single crest (the *crista cranii* – see e.g. Martinez *et al.*, 2012), a condition similar to

Saturnalia tupiniquim Langer *et al.* 1999, *Plateosaurus* (AMNH 6810), *Massospondylus kaalae*, and most other sauropodomorphs. *Panphagia* exhibits 2 parallel crests between the distinct regions of the ventral surface of the frontal (Martinez *et al.*, 2012b). The crest in SMNS 12667 is developed as a broad, transversely rounded ridge that is not offset from either the surface of the orbital nor the endocranial facet, but marks a change in orientation of the ventral surfaces. The crest runs parallel to the lateral margin of the frontals, which is concave in ventral view, for most of its length. The anterior portion of the orbital roof is not completely preserved but it is possible to see that the crest converges laterally towards the lateral margin of the frontal in the anterior portion of the frontals. Thus, the width of the orbital roof remains more or less the same along the anteroposterior axis of the ventral surface, but decreases towards its anterior end, at about the level where the fossa for the olfactory bulb is located on the endocranial roof of the bone (see below). The orbital roof of SMNS 12667 is slightly concave transversely and raises dorsally towards the lateral margin. The lateral margin of the frontal is slightly vaulted, being more raised dorsally at its midpoint than in its anterior and posterior ends, resulting in an anteroposteriorly concave aspect for the ventral surface of the orbital roof in lateral view. In anterior view, at the level where the frontal reaches its maximum dorsal projection, the angle between the ventral and dorsal surfaces of the bone is approximately 30 degrees, a condition similar to that in *Panphagia* (Martinez *et al.*, 2012b), *M. kaalae*, and *Pantydraco caducus* Galton *et al*, 2007.
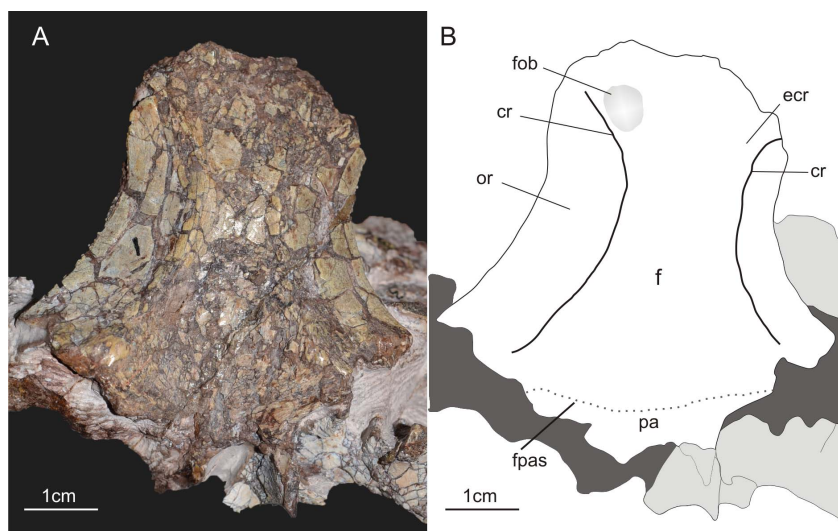
Figure 5.3: A: Ventral view of the frontals of the specimen SMNS – 12667 of *Efraasia minor*. B – Schematic drawing of A. Abbreviations: **cr** – crest; **ecr** – endocranial roof; **f** – frontals; **fob** – fossa for the olfactory bulb; **fpas** – fronto-parietal suture; **or** – orbital roof; **pa** parietal.

At about mid-length of the frontal, the area between the orbital facets is slightly narrower than each of the latter (Fig. 5.3). However, this area widens gradually both posteriorly towards the roof of the endocranial cavity and anteriorly towards the olfactory bulbs and the antorbital skull roof. The fossa for the olfactory bulb is located at the anterior third of the endocranial roof, being positioned closer to the crest delimitating the orbital roof than to the medial limit of the bone. It is developed as a very shallow, sub-circular fossa, deeper at its center than at its corners, and with lengths varying from approximately 7mm anteroposteriorly to 5 mm transversely. In the posteriormost region of the bone, the surface of the endocranial roof is slightly wider than the orbital margin. In this respect, the morphology of SMNS 12667 is mostly similar to *Panphagia* (Martinez *et al*., 2012b). In *Plateosaurus* (AMNH 6810), the surface corresponding to the orbital roof is also wider than the one corresponding to the roof of the endocranial cavity at the mid-length of the frontal. However in this taxon, the difference is much more marked, with

the bone surface of the orbital roof being 3 to 4 times wider than that of the endocranial roof. The condition in *Pantydraco* differs from that in *Efraasia, Panphagia,* and *Plateosaurus* (AMNH 6810) in that even at the mid-length of the bones, the medial surface of the frontal is wider than the orbital roof.

The posterior margin of the frontal extends slightly beyond the posterior limit of the orbital roof (Fig. 5.3). The posterior region of the articulated frontals of SMNS 12667 is deeply concave transversely. The concavity is deepest posteriorly but decreases gradually anteriorly towards the median portion of the bones. Anteriorly, the ventral surface is flat except for the region of the fossa for the olfactory bulb. The articular facets for the prefrontals and postorbitals are not preserved.

Parietal

Only the anteriormost portion of the parietals is preserved in SMNS 12667, visible in ventral view (Fig. 5.3). The total anteroposterior length of the preserved portion of the main body of the left parietal is 7 mm, and it is no more than 3 mm in the right parietal. The parietals articulate with the frontals anteriorly. The suture can be more easily recognized on the left side, but its exact course is not entirely clear. From the left lateral limit of the preserved parietal the suture runs posteromedially, giving a concave aspect to the anterior margin of the parietal in the medial portion of the bone, similar to the morphology observed in *Adeopapposaurus mognai* Martinez, 2009. In contrast, *Plateosaurus* has a parietal with a straight anteromedial margin, and *Panphagia* with a concave anterior margin.

The anterolateral ramus of the parietal of SMNS 12667 probably contacted the laterosphenoid ventrally, together forming the anteromedial border of the external and internal supratemporal fenestra. The anterolateral ramus of the parietal is preserved

only in the left parietal. It has a triangular shape, with a linear anterior margin with a total length of 9 mm, and a concave posterior margin, which formed the anterior and medial margin of the supratemporal fenestra. The anterolateral ramus extends laterally until the level of the medial limit of the orbital roof of the frontal. As the preserved posterolateral margin of the frontal curves anterolaterally and does not extend posteriorly, this indicates an absence of the frontals from the anterior margin of the supratemporal fenestra, with the anterolateral ramus of the parietal contacting the postorbital in this region. However, given the preservation of the specimen and the variation of the composition of the anterior border of the supratemporal fenestra (i.e. if frontals participate or not) observed in sauropodomorphs (Martinez *et al.*, 2012b), this remains speculative.

In its medial portion, the ventral surface of the parietals is concave, following the concavity in the posterior portion of the frontal described above. The concavity in the ventral surface diminishes progressively laterally until the level of the medial limit of the anterolateral ramus. From this point the surface becomes concave up to the lateral limit of the preserved part of the anterolateral ramus of the parietal.

Basioccipital

The basioccipital forms the posteroventral portion the braincase (Figs. 5.2, 5.4). In SMNS 12667, only the ventral and lateral portion of the bone is visible. The CT-Scan showed that the dorsal part of the basioccipital, which is hidden in the matrix, is partially damaged (Fig. 5.2), but some inferences about its morphology are still possible. Bones contacting the basioccipital include the parabasisphenoid anteriorly and the otoccipital dorsolaterally. Except for a possible fragment of the otoccipital

still being attached to the basioccipital, the latter bone is completely isolated from other elements, as revealed by CT-Scan data.
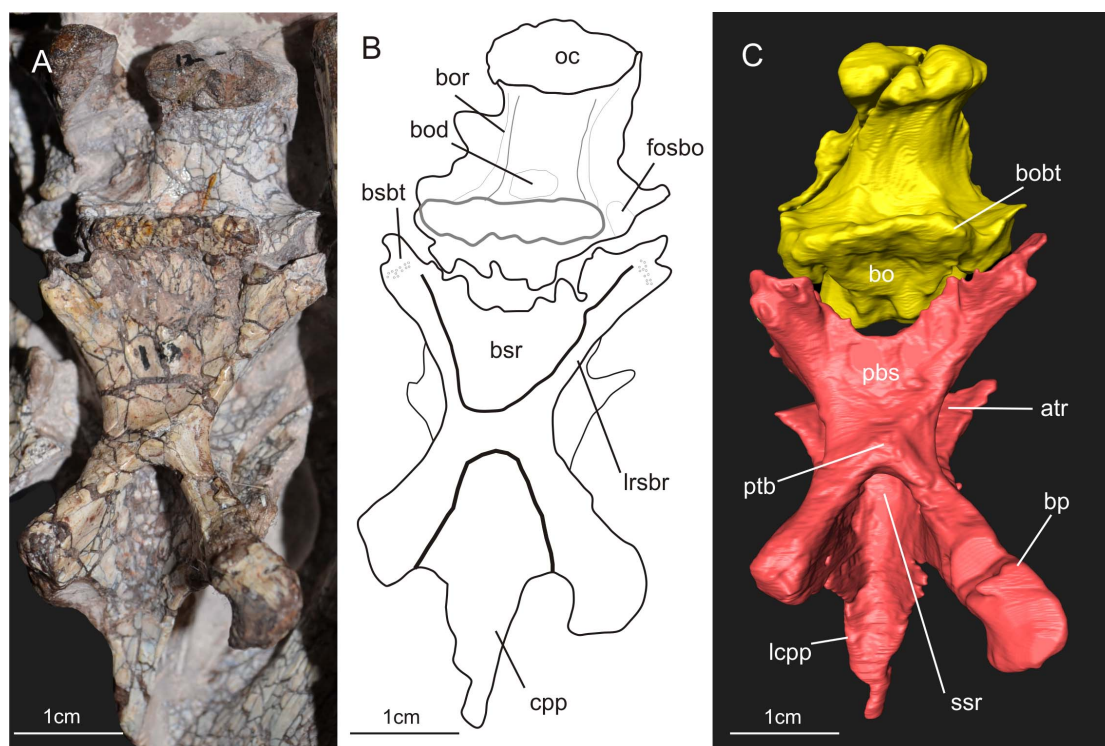
Figure 5.4: A – Ventral view of the basioccipital and parabasisphenoid of the specimen SMNS – 12667 of *Efraasia minor*. B – Schematic drawing of A. C Virtual reconstruction of A. Abbreviations: **atr** – anterior tympanic recess; **bo** – basioccipita; **bobt** – basioccipital component of the basal tubera; **bod** – basioccipital depression; **bor** – basioccipital ridge; **bp** – basipterygoid process; **bsr** – basisphenoid recess; **bsbt** – basisphenoidal component of the basal tubera; **cpp** – cultriform process of the parabasisphenoid; **fosbo** – fossa of the basioccipital; **lcpp** – lamina of the cultriform process of the parabasisphenoid; **lrsbr** – lateral ridge of the subsellar reess; **pbs** – parabasisphenoid; **ssr** – subsellar recess.

In SMNS 12667, the dorsal portion of the basioccipital forms the major part of the floor of the braincase (Fig. 5.2), with a small contribution of the otoccipital to the lateroposterior portion at the level of the occipital condyle. This condition is similar to other sauropodomorphs, such as *Plateosaurus* (see Galton, 1985), *Leyesaurus tolentinoi* Apaldetti *et al.*, 2011, *Adeopapposaurus, Coloradisaurus brevis* Bonaparte, 1978, and *Melanorosaurus* Haughton, 1924 (see Galton, 1985). Thus, in SMNS

12667 and other sauropodomorphs the posterior-most surface of the basioccipital forming the floor of the braincase is narrower than the anterior part at the level of the basioccipital component of the basal tubera (Fig. 5.2).

The posterior portion of the dorsal surface of the basioccipital is transversely concave, resulting in a U-Shape of the floor of the posterior part of the braincase and the beginning of the neural canal in posterodorsal view, as in *Plateosaurus*. The anterodorsal portion of the basioccipital forms the ventral border of the anterior foramen of the otoccipital between the exoccipital pillar and the fenestra ovalis (Fig. 5.2 - see discussion below for the terms anterior and posterior foramen of the otoccipital). Prieto-Marquez & Norell (2011) stated that the border of the metotic foramen of *Plateosaurus* (see discussion below) is formed by the parabasisphenoid, but we disagree with their interpretation based on the pictures provided in the manuscript (Prieto-Marquez & Norell, 2011: fig. 27A), and on the analysis of another specimen of *Plateosaurus* (MB.R-5586-1), which also shows that this border is formed by the basioccipital. *Leyesaurus* also exhibits the same morphology as *Plateosaurus* and *Efraasia*.

For the description of the ventral portion of the basioccipital of SMNS 12667 (Fig. 5.4), two regions are delimited, an anterior one, which represents the region of the basioccipital anterior to the basioccipital component of the basal tubera, and a posterior one, posterior to this structure. Because this division is based on the basioccipital component of the basal tubera, this structure will be dealt with first.

The basal tubera of sauropodomorphs are usually formed by two ossifications, with contributions from the parabasisphenoid and basioccipital (see Yates, 2004). In the previous description of SMNS 12667, Galton & Bakker (1995) considered the basioccipital/parabasisphenoid suture to traverse the basal tubera. In this case, the

latter structure would represent the anterior limit of the basioccipital. We agree with Galton & Bakker (1985) in respect to the structures that they indicated as being part of the basal tubera complex of SMNS 12667 (see Galton & Bakker, 1985: fig. 2C). Thus, this complex consists of a sharp and straight median transverse ridge and a bulbous lateral expansion on either side, which is lower than the ridge and marked by a deep incision extending from lateral into its central part. The latter was considered to be an unossified, cartilaginous part by Galton & Bakker (1985: 3). However, the transverse ridge is only formed by the basioccipital (i.e. it is part of the basioccipital component of the basal tubera), and the median contact between basioccipital and parabasisphenoid lies anterior to this ridge. In SMNS 12667, the basioccipital has thus a broadly triangular anteromedial projection that extends anteriorly between two posterolateral projections of the parabasisphenoid. This morphology is the same as observed in other non-sauropodan sauropodomorphs, such as *Adeopapposaurus*, *Massospondylus*, *Pantydraco*, *Unaysaurus tolentinoi* Leal *et al.*, 2004, *Coloradisaurus*, *Anchisaurus polyzelus* Hitchcock, 1865, and *Plateosaurus*. Sauropods such as *Giraffatitan brancai* Janensch, 1914 and *Dicraeosaurus hansemanni* Janensch, 1914, have a more linear and horizontal contact between both bones. The anterior surface of the transverse ridge shows rugose striations, as already mentioned by Galton & Bakker (1985).

Because the basal tubera morphology of the basioccipital of SMNS 12667 may be confused with a structure in theropods named the basituberal web by Bakker *et al.* (1988; = intertuberal lamina, Witmer & Ridgely, 2010), it is worth commenting on the difference between both. As the term used by Witmer & Ridgely (2010) indicates, the lamina in theropods connects the left and right parts of the basisphenoidal component of the basal tubera. In SMSN 12667, the ridge is part of

the basioccipital components of the basal tubera, and is not located between basisphenoidal components of the tubera, but situated slightly posterior to these. Furthermore, as in other sauropodomorphs (e.g. *Plateosaurus, Massospondylus*), the posterior surface of the basioccipital basal tubera in SMNS 12667 is very rugose, related to the muscle attachment in this area (Romer, 1967; Snively & Russell, 2007), and not a smooth lamina as in the theropods exhibiting a similar structure (Bakker *et al.*, 1998). So far, a lamina similar to that seen in some theropods is unknown in sauropodomorphs.

As in other sauropodomorphs (e.g. *Coloradisaurus, Plateosaurus, Massospondylus*), SMNS 12667 exhibits a distinctive neck in the posterior region of the basioccipital, separating the occipital condyle from the main body of the bone (Figs. 5.2, 5.4). The condyle of SMNS 12667 is formed by two components, the basioccipital ventrally and mediodorsally, and the otoccipital laterodorsally. The same condition is present in other sauropodomorphs, such as *Massospondylus carinatus, Massospondylus kaalae, Plateosaurus,* and *Melanosaurus*, but it differs from that in *Coloradisaurus,* in which the otoccipital contribution to the condyle is minimal, with most of the structure being formed solely by the basioccipital. In SMNS 12667, the dorsolateral limit of the basioccipital in the occipital condyle is well marked by the disarticulation of the basioccipital and the otoccipital in this region on the left side of the braincase. However, a small fragment of the otoccipital might still be attached to the basioccipital on the right side. The condyle is not entirely preserved dorsally, and marks of preparation and an unclear limit between bones and sediment in the CT–Scan data does not allow a secure interpretation of its morphology in posterior view. As preserved, the condyle has a width of 15 mm, 10 mm of which correspond to the

basioccipital component of the condyle, and 5mm to the otoccipital component (2.5 mm on each side).

In SMNS 12667, the portion of the basioccipital delimited by the occipital condyle posteriorly and by the basioccipital component of the basal tubera anteriorly is trapezoidal in shape in ventral view, with the anterior and posterior margins forming parallels sides (Fig. 5.4). This trapezoidal outline is due to the fact that the lateral wall of the basioccipital just behind the tubera is not strictly vertical but slopes laterodorsally, and is thus visible in ventral view. In *Plateosaurus* (MB.R.5586-1; Prieto-Marquez & Norell, 2011), the lateral side of the basioccipital is more vertically oriented in the anterolateral region, resulting in a more rectangular shape for this portion of the bone in ventral view.

The ventral side of the basioccipital of SMNS 12667 exhibits a shallow longitudinal groove delimited by two parallel longitudinal ridges (Fig. 5.4B). The groove extends from the neck of the occipital condyle to the posterior limit of the medial ridge forming the basioccipital component of the basal tubera, where it becomes deeper and wider. The lateral ridges mark the transition from the ventral to the lateral surface of the basioccipital. In other sauropodomorphs (e.g. *Massospondylus carinatus*, *Melanorosaurus*, *Plateosaurus*, *Giraffatitan*), these ridges also extend from the occipital condyle to the basioccipital component of the basal tubera. The ridges, and consequently the fossa between them, are evident to different degrees among sauropodomorpha. In *Plateosaurus* (MB.R.5586-1) and the sauropod *Giraffatitan*, the ridges and the groove are easily recognized in ventral view. On the other hand, these structures are much less pronounced in another specimen of *Plateosaurus* (AMNH 6810), and are absent (or imperceptible) in some taxa, such as *Saturnalia* and *Adeopapposaurus*. Regarding the groove in SMNS 12667, it exhibits a

deeper, semi-circular fossa in its most anterior part, just posterior to the transverse ridge of the basioccipital component of the basal tubera (Fig. 5.4B). This fossa is also present in other sauropodomorphs, such as *Aardonyx celestae* Yates *et al*, 2010; *Giraffatitan*, and *Plateosaurus*. In *Plateosaurus* (MB.R.5586-1) and *Aardonyx*, the fossa is deeper than in SMNS 12667.

Laterally and slightly anterior to the semi-circular fossa, the basioccipital surface exhibits another depression, which marks the division of medial and lateral portions of the basiocciptal component of the basal tubera (Fig. 5.4B). The depression is only preserved on the right side and corresponds to a similar structure observed by Prieto-Marquez & Norell (2001: fig. 30B, 'fos bo') in *Plateosaurus* (AMNH 6810). However, it seems that in SMNS 12667, the fossa does not have a well defined ventral limit, as it is the case in *Plateosaurus* (Prieto-Marquez & Norell, 2011). In the latter, the fossa also marks the division between the two portions of the basioccipital component of the tubera.

CT-Scan data indicates a complete separation of the basioccipital and parabasisphenoid in SMNS 12667 (Fig. 5.5).
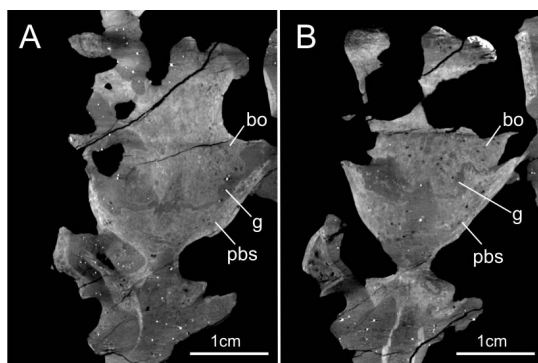
Figure 5.5: X-ray slices obtained from the CT-Scan procedure showing the complete separation of basioccipital and parabasisphenoid in two distinct regions of the braincase of the specimen SMNS - 12667 of *Efraasia minor*. The region depicted in A is more dorsally located in relation to the region depicted in B. Abbreviations: **bo** – basioccipital; **g** – gap; **pbs** – parabasisphenoid.

A complete disarticulation between the basioccipital and the parabasisphenoid is usually observed in braincase materials of individuals of sauropodomorphs regarded as juveniles (e.g. Fedak & Galton, 2007; Galton & Kermack, 2010), indicating that SMNS 12667 is a juvenile specimen of *Efraasia minor* (see also Galton & Bakker, 1985; Yates, 2003). Similar disarticulation between the basioccipital and parabasisphenoid is present in the braincases of *Unaysaurus* and *Anchisaurus* (Fedak & Galton, 2007). Regarding *Anchisaurus*, recent papers have considered this specimen as representing a juvenile (see Fedak & Galton, 2007 and Yates, 2010). In *Unaysaurus*, there is only an incipient contact between the bones by a connection between the basioccipital and basisphenoidal component of the tubera. Although not treated as a juvenile in its original description (Leal *et al*., 2004), ongoing study of the specimen of *Unaysaurus* has found characteristics supporting this assessment (J. Bittencourt – *pers. comm*.). In the holotype of *Pantydraco*, probably a very immature specimen (Galton & Kermack, 2010), the parabasisphenoid and basioccipital are completely disarticulated from each other. This indicates a very weak junction between these two bones in earlier ontogenetic stages of Sauropodomorpha, before complete maturity of the animals.

Parabasisphenoid

The parabasisphenoid forms the anterior part of the floor of the braincase (Figs. 5.2, 5.4). In SMNS 12667, the parabasisphenoid would have contacted the basioccipital posteriorly, the otoccipital posterodorsally, the prootic dorsally, and potentially the laterosphenoid anterodorsally. The parabasisphenoid possesses a series of associated structures, which include the cultriform process, basipterygoid processes, subsellar

and basisphenoid, recesses, and a part of the basal tubera (in addition to the basioccipital component, as detailed above).

In SMNS 12667 the parasphenoid is completely fused to the basisphenoid (Fig. 5.4), as in all other dinosaurs (Currie, 1997) and archosauriforms (Walker, 1990; Bittencourt *et al.*, 2014). Because of this it is necessary to emphasize that, despite recognizing a portion of the parabasisphenoid as the cultriform process and treating it as a distinct region in the description herein, it is impossible to precisely delimitate the posterior limit of the process and the suture between parasphenoid and basisphenoid. Furthermore, it is very likely that only the most proximal part of the cultriform process is preserved in SMNS 12667, because, by comparison with other non-sauropodan sauropodomorphs that have a more completely preserved cultriform process (e.g. *Saturnalia*, *Plateosaurus*, *Pantydraco*), the anteroposterior length of this structure might be greater than the length of the rest of the braincase. Only the ventral surface of the parabasisphenoid and parts of the lateral sides are exposed in SMNS 12667, but more details of its morphology can be established with the help of the CT-scan data.

The parabasisphenoid is slightly longer (25 mm) than wide (22 mm) between the basal tubera and the base of the cultriform process (Figs. 5.2, 5.4). In ventral view, it is notably X-shaped, being strongly constricted in its central part and expanding rapidly laterally posteriorly towards the basisphenoidal portions of the basal tubera and anteriorly towards the basipterygoid processes. The lateral expansion of both of these structures is approximately equal, but the minimal width of the bone of c. 8.5 mm is less than half of the width across the basal tubera (c. 22 mm).

In lateral view, the ventral margin of the parabasisphenoid between the proximal limit of the basipterygoid process and the basisphenoidal component of the

tubera is curved, with its posterior and anterior ends located ventrally in respect to the surface between them. Dorsally, a deep excavation in the lateral surface of the bone corresponds to the anterior tympanic recess of theropods in respect to its relative position (Witmer, 1997). The surface posteroventral to this recess is flat, and the lateral side of the bone would have contacted the prootic dorsally and the otoccipital posteriorly.

Posterior to the cultriform process, the dorsal surface of the parabasisphenoid has the pituitary fossa preserved anteriorly, which is separated from the posterior-most surface by a vertical wall of bone perforated by the vidian canal medioventrally. This canal is represented by a single opening in *Efraasia*, similar to the condition observed in *Thecodontosaurus*, which indicates that the right and left carotids converge within the bone and enter the pituitary fossa through a single foramen. On the other hand, *Adeopapposaurus* (PVSJ 568), *Massospondylus* (BP I 5231), and *Plateosaurus* (MB.R. 5586-1) exhibit two small foramina in this region, indicating a posterior convergence of the left and right carotid within the pituitary fossa. However, it is necessary to point out that this region of the braincase is poorly preserved in both *Efraasia* and *Thecodontosaurus*. Thus, the absence of a sub-divided vidian canal might be an artefact, especially because the septum dividing the canal in *Adeopapposaurus* and *Plateosaurus* consists of a thin and delicate structure.

The basisphenoidal component of the basal tubera is a bulbous structure located at the tip of the posterolateral projections of the parabasisphenoid (Fig. 5.4). From the anterior limit of the parabasisphenoid/basioccipital contact, the length of the projections is c. 8 mm. The surface of the tubera shows a series of small and shallow circular pits that represent the scars of the muscle attachment in this region. The pits

are present in the posterior end of the ventral surface of the projection, and also in the posteroventral corner of the lateral side of parabasisphenoid.

Here we adopt the term basisphenoid recess (*sensu* Witmer, 1997) to refer to the depression on the ventral surface of the parabasisphenoid (Fig. 5.4), located anterior to the posterolateral projections of the tubera and posteriorly to the subsellar recess (see below). In SMNS 12667, the depression is very shallow and anteriorly defined by a protuberance on the ventral surface of the parabasisphenoid located between the proximal bases of the basipterygoid processes. A protuberance is also observed in other taxa, such as *Plateosaurus* (Prieto-Marquez & Norell, 2011), *Unaysaurus,* and *Adeopapposaurus* (PVSJ 568), whereas other taxa, such as *Massospondylus, Coloradisaurus,* and *Pantydraco* do not possess a protuberance in this region of the parabasisphenoid. The lateral limit of the basisphenoid recess of SMNS 12667 is more distinguishable on the right side of the braincase. On this side, a low-rounded ridge extends along the lateral margin of the ventral surface of the parabasisphenoid. Posteriorly this ridge becomes confluent with the basisphenoidal component of the basal tubera.

The presence of a basisphenoid recess is a widespread characteristic among non-sauropodan sauropodomorphs, probably being present in all the members of the group (pers. obs.). As mentioned above, the usage of terms shallow and deep is subjective, but obvious differences are also notable in relation to the depth of the basisphenoid recess among different taxa. The basisphenoid recess of SMNS 12667 is shallow, resembling more the morphology observed in taxa such as *Adeopapposaurus* and *Pantydraco,* than the one of *Coloradisaurus,* which exhibits a deeper basisphenoid recess. However, a basisphenoid recess as deep as that observed in most theropod taxa (e.g. Rauhut, 2003, 2004) is not observed in non-sauropodan

sauropodomorphs. In SMNS 12667, as in other non-sauropodan sauropodomorphs we analysed, the recess does not have a clearly defined posterior limit in the parabasisphenoid, but fades towards the ventral surface of the basioccipital projected between the posterolateral margins of the parabasisphenoid. This differs from theropods (Witmer, 1997; Rauhut, 2004; Sampson & Witmer, 2007) and sauropods such as *Tornieria africana* Fraas, 1908, the recess is also clearly defined posteriorly, configuring a rounded/circular outline to this structure in ventral view. In SMNS 12667, the shape of the recess in the parabasisphenoid is triangular/trapezoidal, similar to the condition in other non-sauropodan sauropodomorphs analysed for this study. The ridges delimiting the basisphenoid recess laterally correspond to the transitional surface between the ventral and lateral side of the parabasisphenoid (Fig. 5.6). This transitional surface, from the ventral side of the bone to the level of the anterior tympanic recess laterally, was named the lateral lamina of the basisphenoid (= *crista ventrolateralis* in Theropoda; Sampson & Witmer, 2007, following Kurzanov, 1976) by Apaldetti *et al*. (2014) in their redescription of the skull of *Coloradisaurus*. In SMNS 12667, this transitional surface is not developed as a lamina, but rather as a rounded lateral edge.

The lateral surface of the parabasisphenoid of SMNS 12667 is better exposed on the right side of the braincase, with the left side being partially covered by matrix and hidden by the dislocated right laterosphenoid (Fig. 5.6A). Nevertheless, with CT-Scan data it is possible to access the whole morphology of the lateral portion of the bone, and the region of the parabasisphenoid that would have made contact with the prootic in the left side of the braincase (Fig. 5.6B). Although the precise limits of the bones are still uncertain, it is possible that the separation of parabasisphenoid and both prootic and ottoccipital on the left side of the braincase happened in the original

region of articulation between these bones, based on the morphological similarity of what is preserved of the parabasisphenoid on both sides (Fig. 5.2 and Appendix for this chapter).

The excavation on the lateral side of the parabasisphenoid (Fig. 5.6) is topologically correlated to the structure usually named the anterior tympanic recess in theropods (Witmer, 1997; Rauhut, 2004), which is also present in representatives of the Avemetatarsalia lineage outside Dinosauria (Nesbitt, 2011; Bittencourt *et al.*, 2014; pers. obs.), in the non-archosaurian archosauriform *Euparkeria capensis* Broom, 1913 (Sobral *et al.* 2016), and in all the non-sauropodan sauropodomorphs analysed for this study. In SMNS 12667, the anterior tympanic recess is mainly located in the parabasisphenoid, but its posterodorsal limit is within the anteroventral limit of the lateral surface of the prootics (see below). The anteroventral limit of the recess in the parabasisphenoid is situated close to the base of the basipterygoid process. From this point, the recess extends posterodorsally, occupying approximately one third of the lateral surface of the bone. From the anteroventral to the posterodorsal limit, the length of the recess is approximately 15 mm. The lateral surface of the parabasisphenoid roofing the dorsal limit of the anterior tympanic recess is the region of the preotic pendant. This structure is formed by the parabasisphenoid and the prootics (see description below).
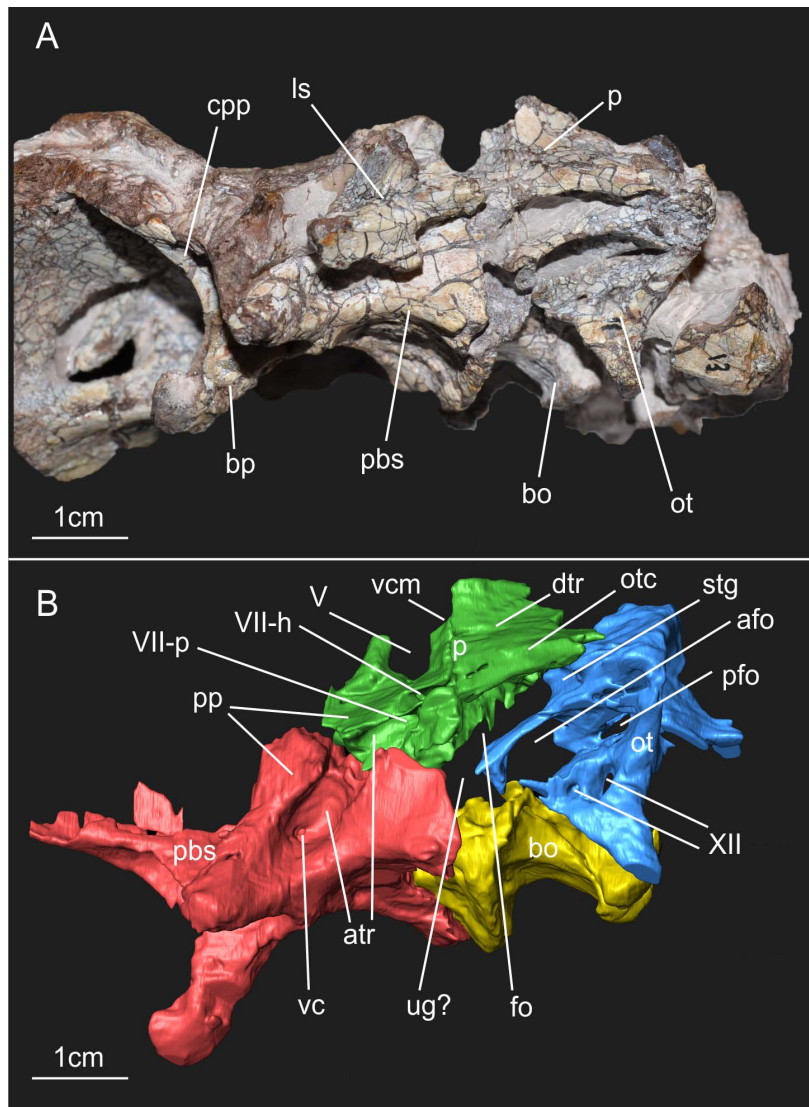
Figure 5.6: A: Ventrolateral view of the braincase of the specimen SMNS – 12667 of *Efraasia minor*. B: Virtual reconstruction of A (excluding the laterosphenoid) detailing the cranial openings. Abbreviations: **afo** – anterior foramen of the otoccipital between the exoccipital pillar and the fenestra ovalis; **atr** – anterior tympanic recess; **bo** – basioccipital; **bp** – basipterygoid process; **cpp** – cultriform process of the parabasisphenoid; **dtr** – dorsal tympanic recess; **fo** – fenestra ovalis; **ls** – laterosphenoid; **mpp** – attachment region of the *m. protractor pterygoideus*; **ot** – otoccipital; **otc** – otosphenoidal crest; **p** – prootic; **pbs** – parabasisphenoid; **pfo** – posterior foramen of the otoccipital between the exoccipital pillar and the fenestra ovalis; **pp** – preotic pendant; **stg** – stapedial groove; **ug** – unossified gap; **vc** – vidian canal; **vcm**: path of the mid-cerebral vein; **V** – notch of the 5th cranial nerve (trigeminal); **VII-h** – foramen for hyomandinbular ramus of the 7th cranial nerve (facial); **VII-p** – foramen for palatine ramus of the 7th cranial nerve (facial); **XII** – foramina for the 12th cranial nerve (hypoglossal).

The aperture of the vidian canal lies in the anteroventral portion of the anterior tympanic recess of SMNS 12667 (Fig. 5.6). The vidian canal (or foramen for

the internal carotid artery) represents the opening through which the internal carotid artery and the palatine branch of the facial nerve (VII) enter the internal cavity of the braincase (Galton, 1985; Sampson & Witmer, 2007). In their description of the skull of *Coloradisaurus*, Apaldetti *et al*. (2014) treated the vidian canal and the foramen for the internal carotid artery as two distinct structures. This would make *Coloradisaurus* distinct from SMNS 12667 and other sauropodomorphs; however, it rather reflects a confusion in the usage of different terms related to the same structure. As explained in Müller *et al*. (2011), the path of the internal carotid artery varies among amniotes. However, in those groups where a vidian canal is present, by definition, it represents the aperture through which the internal carotid artery enters the braincase. The dorsal opening in *Coloradisaurus* might be related to the palatine branch of the facial nerve (see below).

The aperture of the vidian canal in the lateral surface of the parabasisphenoid connects to an aperture located at the ventromedial portion of the posterior limit of the pituitary fossa (Fig. 5.2). The pituitary fossa (or *sella turcica*), which houses the pituitary gland (Galton, 1985), is a structure present in the anterior portion of the dorsal surface of the parabasisphenoid, posterodorsal to the cultriform process. The posterior limit of the pituitary fossa is a wall of bone (c. 2 mm thick and 7 mm tall), which would have contacted the prootics dorsally at the region of dorsum sellae, which is not preserved in SMNS 12667. The lateral borders of the pituitary fossa correspond to the medial surface of the portion of the parabasisphenoid that laterally forms the preotic pendant. From its ventral limit, the lateral margins of the fossa diverge posterolaterally. Thus, the pituitary fossa is triangular in outline in anterior view, but with a rounded ventral apex (Fig. 5.2), similar to the morphology observed in *Plateosaurus*. Posterior to the wall of bone defining the fossa, the shape of the

dorsal region of the parabasisphenoid follows the general morphology of the corresponding ventral surface described above.

Because of its basically identical morphology and position to the condition seen in many theropods, we interpret the deep ventral concavity at the base of the cultriform process (Fig. 5.4) as the subsellar recess (sensu Witmer, 1997). The term subsellar recess is widely used in the literature on theropod braincases (e.g. Rauhut, 2004; Sampson & Witmer, 2007; Paulina Carabajal, 2011; Bever *et al.*, 2013), but has not yet been applied to sauropodomorphs. In fact, not only is the use of the term subsellar recess uncommon in studies on sauropodomorphs, but even the respective structure is rarely described. One of the few exceptions is the paper by Gow (1990), in which the author used the term "blind pocket" to refer to the subsellar recess of *Massospondylus carinatus;* however, no detailed description or comparisons with other taxa were provided. Nevertheless, notable differences regarding the depth of the subsellar recess among sauropodomorphs are obvious (although the usage of deep and shallow may be subjective). The recess of SMNS 12667 is very deep, similar to the condition in *Coloradisaurus* and *Plateosaurus* (MB.R.2285-1). Other taxa, such as *Pantydraco*, *Massospondylus carinatus* (only SAM PK K1314)*,* and *Giraffatitan* exhibit a shallower recess (see discussion below). Although not mentioned in the description by Galton & Bakker (1985), subsequent phylogenetic studies (e.g. Yates, 2007b; Yates *et al.*, 2010; Apaldetti *et al.*, 2011; Pol *et al.*, 2014; Mcphee *et al.*, 2014; 2015) treated the braincase of *Efraasia* as possessing a deep transverse septum between the basipterygoid processes (character 83 of Yates, 2007b). These authors probably interpreted the posterior border of the deep subsellar recess (*sensu* Witmer, 1997) as such a septum, but the bony connection between the processes is actually low when compared to other taxa (see discussion below).

The right basipterygoid process of SMNS 12667 is entirely preserved, lacking only a small fragment of the anteromedial surface distally, whereas only the proximal part of the left process is preserved (Figs. 5.2, 5.4, 6). The relatively robust proximal portion of the basipterygoid process is formed by a complex array of bony struts that results in a roughly T- to H-shaped cross-section of this part. Thus, the ventral part of the base of the process is formed by a stout vertical strut between the anterior tympanic recess and the subsellar recess; this strut has a slightly transversely expanded ventral surface in its proximal part. More dorsally, the base of the basipterygoid process is formed by a thin anterodorsomedially directed lamina that extends from the basipterygoid process towards the cultriform process and thus forms the dorsolateral wall of the subsellar recess, and a more robust, almost horizontal lamina that arises from the dorsal roof of the anterior tympanic recess. The distal part of the basipterygoid process is lateromedially compressed, as preserved on the right side. In its distalmost portion, where the process would have contacted the pterygoid, the tip of the basipterygoid process curves laterally. The process projects ventrolaterally, as in *Unaysaurus, Giraffatitan, Massospondylus,* and *Thecodontosaurus*. Establishing the anteroposterior orientation of the basipterygoid processes can be problematic because it is sometimes difficult to determine the exact orientation of the parabasisphenoid in the braincase. Using *Plateosaurus* as an example, Prieto-Marquez & Norell (2011) stated in their description of AMNH 6810 that the basipterygoid process projects anteriorly in this specimen. However, according to our interpretation of the illustrations (Prieto-Marquez & Norell, 2011: fig. 27) the processes are clearly posteroventrally oriented in AMNH 6810, as in other specimens of *Plateosaurus* (e.g. MB.R. 5581.6; MB.R. 1937; SMNS 13200). In SMNS 12667, the basipterygoid processes are notably anteriorly oriented. A vertical

or even posterior orientation of these processes would imply an inclination of the ventral surface of the parabasisphenoid of more than 45 degrees in relation to the anteroposterior axis, and consequently a strong verticalization of the internal cavity of the braincase. This is very unlikely, and not supported by the relative position of the basioccipital (and thus the occipital condyle) towards the parabasisphenoid. At about the level of the proximal limit of the cultriform process (Figs. 5.2, 5.4), the distance between the medial margins of the basipterygoid processes is c. 10 mm, but the bases of the processes converge posteromedially to a minimal distance of 2 mm at the posterior end of the subsellar recess. This approximation of the proximal portions of the basipterygoid processes in SMNS 12667 resembles the morphology observed in *Thecodontosaurus,* rather than that of *Adeopapposaurus, Coloradisaurus, Massospondylus,* and *Plateosaurus,* which have a greater separation of the basipterygoid processes proximally.

The cultriform process of the parabasisphenoid is only partially preserved (Figs. 5.2, 5.4). The exact proximal limit of the process is difficult to establish because the process arises gradually from the laminae of the basipterygoid processes mentioned above and the subsellar recess. The preserved portion is no longer than 15 mm anteroposteriorly and 9 mm high. In dorsal view, the lateral margins of the proximal portion of the cultriform process contact each other dorsally anterior to the pituitary fossa in sauropodomorphs such as *Plateosaurus* and *Saturnalia*, forming a short, closed canal. In SMNS 12667 the lateral margins do not converge dorsally (Fig. 5.2B), but it is not possible to affirm if this represents the original morphology or results from the poor preservation of the fossil in this region. In anterior view, the cultriform process is U-shaped, with its lateral margins diverging laterodorsally from each other.

The ventral surface of the proximal part of the cultriform process of SMNS 12667 is concave transversely (Fig. 5.4), as in other sauropodomorphs, such as *Coloradisaurus*, *Plateosaurus*, *Massospondylus*, and the sauropod *Giraffatitan*. The lateral margins of the concave surface are delimited by sharp-rimmed laminae, which extend from the basis of the basipterygoid processes to the lateral edges of the cultriform process. In contrast, *Plateosaurus, Massospondylus, Giraffatitan,* and *Coloradisaurus* do not exhibit such a sharp lamina (triangular lateral lamina of the parasphenoid rostrum in Apaldetti *et al*. 2014), but rather have a more rounded crest, which extends from the basipterygoid process to the cultriform process. In lateral view, the anteroventral border of the laminae is notably concave. In SMNS 12667 and some other taxa, such as *Massospondylus* and *Coloradisaurus,* these laminae/crests are inclined ventrolaterally, so that their bases are parallel to each other along their entire length, whereas the laminae diverge posteroventrally in anterior view. They fade into the ventral surface of the cultriform process slightly anterior to the level of the anterior end of the basipterygoid processes, from where the ventral surface becomes slightly convex transversely (Fig. 5.4). A different condition is present in *Plateosaurus, Unaysaurus, Sarahsaurus aurifontanalis* Rowe *et al*., 2011, and in the sauropod *Giraffatitan*. In these taxa, the two ridges converge medially in the portion of the cultriform process where the surface becomes flat/convex, resulting in a triangular shape of the concavity on the ventral surface of the proximal portion of the process, providing a well-defined anterior limit for the subsellar recess (see below) in these taxa.

Prootic

Both prootics of SMNS 12667 are preserved (Fig. 5.2) but the description provided here is mainly based on the left element (Figs. 5.6, 5.7), as the right prootic is preserved inside the matrix and its surface is greatly damaged. The left prootic has its lateral surface exposed, except for the anteroventral surface that contacted the parabasisphenoid ventrally (Figs. 5.6A, 5.7). This area is covered by the right laterosphenoid in the block, but can be visualized with CT-Scan data (Fig. 5.6B). The CT-scan also shows that the medial surface of this bone, including the inner ear cavity, is greatly damaged. The only recognizable feature in the medial surface is a large depression in the region that corresponds to the position of the flocculus of the cerebellum. However, any detail of this structure, or of the semicircular canals of the inner ear within the prootic, is impossible based on the CT-scan data.
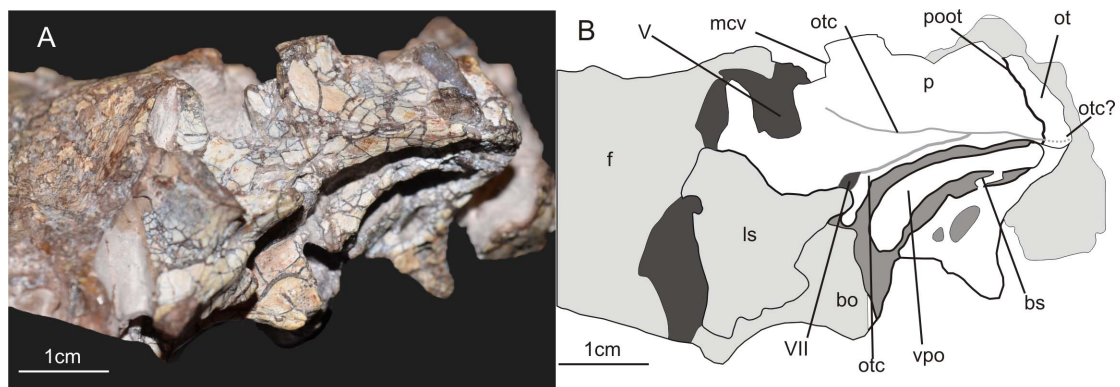
Figure 5.7: Lateral view of the left prootic of the specimen SMNS – 12667 of *Efraasia minor*. Abbreviations: **bs** – bony strut; **f** – frontal; **ls** – laterosphenoid; **ot** – otoccipital; **otc** – otosphenoidal crest; **p** – prootic; **pbs** – parabasisphenoid; **poot** – posterior limit of of the prootic overlapping the otoccipital; **vcm** – notch of the mid-cerebral vein; **vpo** – ventral process of the otoccipital; **V** – notch of the trigeminal nerve; **VII** – foramen for the cranial nerve VII.

The prootic forms most of the laterodorsal wall of the braincase. In SMNS 12667 the prootic is still articulated with the paroccipital process of the otoccipital posteriorly (Fig. 5.7). The posterodorsal part of the prootic probably contacted the

parietal dorsally, and potentially also the supraoccipital, as in some other sauropodomorphs, such as *Thecodontosaurus* (Benton *et al*., 2000), *Adeopapposaurus* (Martinez, 2009), and *Plateosaurus* (Galton, 1984). Other contacts of the prootic include the parabasisphenoid anteroventrally and the laterosphenoid anterodorsally. Several foramina either pierce the prootic or are bordered by this element in conjunction with other bones. These include the foramina for cranial nerves V and VII, the opening for the mid-cerebral vein, and the fenestra ovalis (Figs. 5.6, 5.7).

The surface of the prootic overlapping the otoccipital represents the posterior third of a subrectangular bone surface that extends from the base of the paroccipital process posterior to the level of the notch for the mid-cerebral vein anteriorly (Fig. 5.7). The rectangle is flexed in its anterior third, so that the anterior part is directed slightly anterodorsaly, whereas the posterior part is oriented considerably posterodorsally; this flexure results in a notched anterior half of the dorsal margin. The maximal length of this sub-rectangular surface is 19 mm and its height is 11 mm posterior and 9 mm anteriorly, it being delimited by the otosphenoidal crest (= crista prootica; see Sampson & Witmer, 2007) ventrally. The anterodorsal margin of this surface would have contacted the laterosphenoid, enclosing the aperture of the mid cerebral vein (see below). Posteriorly, the dorsal part of the prootic overlaps the otoccipital, thus forming the anterior part of the base of the paroccipital process, as in other archosaurs. The surface of this dorsal portion of the prootic is anteroposteriorly concave towards the anterior rim, but flat in its posterior half. In theropods, this is the position where the dorsal tympanic recess is located (Witmer, 1997; Rauhut, 2004). Our observations indicate that a very shallow concavity is present among many non-sauropodan sauropodomorphs (e.g. *Plateosaurus, Adeopapposaurus,*

Massospondylus), including *Efraasia,* but it is not developed as a pneumatic recess as in some theropod taxa (Witmer, 1997).

As noted above, the dorsal portion of the prootic is separated from the ventral part by a bony crest. We here adopt the term otosphenoidal crest instead of crista prootica, because, as discussed by Sampson & Witmer (2007), the crest extends beyond the limits of the prootics in some taxa. In SMNS 12667, the posterior end of the crest is unclear due to preservation, but it seems that the crest extended posteriorly onto the proximal part of the paroccipital process (Fig. 5.7). At the ventral margin of the subrectangular surface described above, the crest is developed as a low rounded ridge, and it defines the dorsal margin of the fenestra ovalis and the laterodorsal margin of the stapedial groove on the basis of the paroccipital process. The crest bifurcates anteriorly at the anteroposterior level where the dorsal surface of the prootic curves anterodorsally (Figs. 5.6 and 5.7). The dorsal component of this bifurcation extends anteriorly towards the notch for the mid-cerebral vein, where it meets the anterior border of the bone at about the mid-height of this notch. In the anterior portion, the crest becomes more prominent and overhangs the more ventral part of the lateral side towards the foramen. It thus might have formed the dorsal border of a posterior course of the mid-cerebral vein on the outside of the braincase. This anterodorsal component of the otosphenoidal crest is not present in all taxa, and in those taxa where it is present, it is often not regarded as part of the structure (see e.g. Martinez *et al.,* 2012b). Usually, the crest extends only ventrally or anteroventrally, bordering the foramen for the facial nerve (Sampson & Witmer, 2007). However, as we see no discontinuity between the ridge extending anteriorly and the posterior component of the otosphenoidal crest, we consider this anterodorsal component as part of the otosphenoidal crest in SMNS 12667. This anterodorsal

component is also observed in *Panphagia* (see Martinez *et al*., 2012b: fig. 8C), *Massospondylus* (BP 1 5231), and *Plateosaurus* (MB.R. 5581.6), but not in *Adeopapposaurus*.

The portion of the otosphenoidal crest that extends anteoventrally borders the foramen for the facial nerve (Fig. 5.7 - see below). As it is the case in other non-sauropodan sauropodomorphs, such as *Plateosaurus, Melanorosaurus, Adeopapposaurus,* and *Massospondylus,* the portion of the crest bordering the facial foramen is low and do not expand laterally in SMNS 12667. In contrast, many neosauropods, such as *Dicraeosaurus, Tornieria,* and *Giraffatitan* exhibit a well-developed, high and laterally expanded otosphenoidal crest. In these taxa, the crest is developed as a sheet of bone projecting lateroposteriorly, hiding the fenestra ovalis in lateral view. Anteroventral to the foramen for the nerve VII, the otosphenoidal crest becomes confluent with the posterior rim of the preotic pendant.

The preotic pendant (sensu Madsen & Welles, 2000; = *ala basisphenoidalis*, see Sampson & Witmer, 2007) is a structure usually formed by a bone expansion in the anteroventral portion of the prootics and the dorsal margin of the parabasisphenoid (Figs. 5.2, 5.6, 5.7), dorsal to the vidian canal (Sampson & Witmer, 2007). This structure is present in dinosauriforms (e.g. *Silesaurus opolensis* Dzik, 2003), and also in all dinosaur clades (pers. obs.). However, as for the subsellar and basisphenoid recesses, it is usually more developed in the braincase of some theropod taxa, where it is expanded as a posteroventrally directed lamina (e.g. Chure & Madsen, 1996, 1998; Rauhut, 2004; Sampson & Witmer, 2007). Sauropodomorph taxa, such as *Plateosaurus, Melanosaurus, Thecodontosaurus,* and *Massospondylus* exhibit relatively well-developed preotic pendants, but they do not overlap a significant portion of the anterior tympanic recess in lateral view, as in some

theropods. In SMNS 12667, there is no such well-developed structure, with the preotic pendant projecting no more than two millimeters ventrally in the area of the anterior tympanic recess. The length of the preotic pendant surface of SMNS 12667 in the prootic, measured from the ventral border of the foramen for the facial nerve up to the anteroventral limit of the bone, is c. 5mm. The preotic pendant marks the anterodorsal limit of the anterior tympanic recess. The posterodorsal limit of the preotic pendant is more difficult to establish, as the dorsal surface becomes confluent with the surface of the prootic anteroventral to the notch of the trigeminal nerve, which does not participate in the preotic pendant. The portion of the pendant formed by the parabasisphenoid is similar in size to the one formed by the prootic, and it overhangs the dorsal margin of the anterior tympanic recess in this bone. The preotic pendant represents the attachment surface for the *m. protractor pterygoideus* (Figs. 5.6, 5.7), as in other sauropodomorphs (Prieto-Marquez & Norell, 2011; Martinez *et al.*, 2012b) and theropods (Sampson & Witmer, 2007).

In SMNS 12667, the notch for the trigeminal nerve (V) is located dorsally and slightly posteriorly to the attachment surface for the *m. protractor pterygoideus* (Fig. 5.6), as in all other sauropodomorphs (e.g. *Plateosaurus, Panphagia, Coloradisaurus, Melanorosaurus*). As is typical for members of the group, the foramen for cranial nerve V in SMNS 12667 is bordered by the prootic ventrally and posteriorly, and would be enclosed by the laterosphenoid anterodorsally (Prieto-Marquez & Norell, 2011; Martinez *et al.*, 2012b; Apaldetti *et al.*, 2014; Yates, 2007b). In *Thecodontosaurus,* the foramen for cranial nerve V is completely enclosed by the prootic (Benton *et al.*, 2000), which is also observed in the ornithischian *Dysalotosaurus lettowvorbecki* Virchow, 1919 (Sobral *et al.*, 2012), but this represents an unusual configuration for non-sauropod sauropodomorphs, which was

not observed in any other taxa we examined for this study (pers. obs.). In SMNS 12667, the anteroventral margin of the trigeminal notch formed by the prootic is broken and slightly dislocated. As preserved, this margin has a length of 5 mm, which is also the width of the foramen. However, because of the breakage, part of the anteroventral margin is ventrally dislocated, and its total length could be some millimeters greater than the width of the notch. The ventral border of the notch is concave. The posterodorsal margin of the notch in the prootic is shorter than the anteroventral margin (3mm). The small triangular projection of the prootic forming the posterodorsal notch of the trigeminal nerve also forms the anteroventral margin of the notch for the mid-cerebral vein. In contrast to the concave ventral margin of the notch for the trigeminal nerve, the notch for the mid-cerebral vein has a more straight ventral margin. As with the trigeminal foramen, the laterosphenoid probably enclosed the notch for the mid-cerebral vein anterodorsally. A complete separation of the foramen for the trigeminal nerve and mid-cerebral vein is also observed in other taxa, such as *Plateosaurus* and *Adeopapposaurus*, but not in *Coloradisaurus*. In this taxon, there is a single notch for the trigeminal nerve and the mid-cerebral vein, with the latter probably passing through the dorsal portion of the opening (Apaldetti *et al.*, 2014).

Posteroventral to the trigeminal notch, other openings in the prootic correspond to the foramen for the facial nerve (VII). Galton & Bakker (1985) did not mention the passage for this nerve, probably because the region was obscured by matrix, but with the CT-Scan data it was possible to identify the internal and external apertures in the prootic related to this nerve (Fig. 5.6). As is typical for dinosaurs, an opening is found posteroventral to the trigeminal foramen, associated with the otosphenoidal crest. Regarding the relationship between the otosphenoidal crest and

the foramen for cranial nerve VII in non-sauropodan sauropodomorphs, several statements can be found in the literature. Gow (1990) stated that the crest borders the opening of the foramen for the facial nerve in *Massospondylus* (BP 1 5231) anteriorly, but noted a second ridge ventral to it, which he called the *crista subfacialis*. On the other hand, Galton (1985) mentioned that it borders the posterior margin in *Plateosaurus*, and Martinez *et al*. (2012b) considered the foramen to be enclosed by the crista in *Panphagia*. However, it seems that the difference stated by the authors is not the result of different morphologies among taxa, but different interpretations of what was regarded as the ventral ramus of the otosphenoidal crest bordering the facial nerve foramen. In SMNS 12667, there is no indication that the crest runs only along the anterior or posterior margin of the foramen. The borders of the foramen are continuous with the otosphenoidal crest both anteroventrally and posterodorsally (although the crest is slightly damaged in this region). It thus seems that the crest bifurcates to enclose the foramen for the facial nerve, as described for *Panphagia* (Martinez *et al*., 2012b). This morphology is also observed in *Plateosaurus* (MB.R. 5586-1, AMNH 6810), *Melanorosaurus* (NMQR 1551)*, Adeopapposaurus, Thecodontosaurus,* and in the sauropod *Spinophorosaurus nigerensis* Remes *et al*., 2009 (Knoll *et al*., 2012).

In SMNS 12667, the aperture of the facial nerve on the medial side of the prootic is circular, with a diameter of approximately 5 mm, but its shape and size may be slightly distorted, given the poor preservation of the medial surface of the bone (see Appendix for this chapter). After leaving the brain, the facial nerve of dinosaurs becomes sub-divided and exhibits two distinct rami, the hyomandibular and palatine rami (Galton, 1985; Sampson & Witmer, 2007). In SMNS 12667, there are two foramina on the lateral side of the prootic, which probably represents separate exits

for the two distinct rami of the facial nerve. One of these is visible on the lateral side of the prootic at the otosphenoidal crest posteroventral to the trigeminal foramen, and probably represents the passage of the hyomandibular ramus of the facial nerve (Galton, 1985). This foramen has an elliptical shape, 6 mm long from the posterodorsal to the anteroventral limit and it is 3 mm wide at its mid-lenght, although these values have quite certainly been exaggerated by breakage. According to Galton (1985), this ramus in *Plateosaurus* turns posterodorsally after passing through the external aperture of the foramen. Based on the CT-Scan data it is possible to trace the initial way of the hyomandibular ramus in SMNS 12667. As in *Plateosaurus,* the nerve turns posteriorly and then runs posterodorsally along the otosphenoidal crest. The second branch of the facial nerve, the palatine ramus, runs anteroventrally and joins the internal carotid artery below the dorsal lamina of the parabasisphenoid, with both entering the vidian canal together (Galton, 1985). In SMNS 12667, the second opening for the facial nerve is a circular aperture (3-4 mm diameter) located at the posterodorsal corner of the anterior tympanic recess, separated from the foramen of the hyomandibular ramus by a thin crest that encloses the latter posteroventrally. This opening probably represents the passage for the palatine ramus, as the CT data shows that both foramina converge on the same medial aperture within the prootic. An aperture in this area, at the posterodorsal corner of the anterior tympanic recess, is not present in *Plateosaurus* and *Panphagia*. In these taxa, there is a single lateral opening for cranial nerve VII. A similar condition as in SMNS 12667 is probably present in *Coloradisaurus*. The region of the anterior tympanic recess is not very well preserved in the braincase of *Coloradisaurus,* but a foramen was probably present at the dorsoventral corner of this structure (pers. obs). The presence of this foramen was also mentioned by Apaldetti *et al*. (2014: fig. 6B), but these authors interpreted it as

the vidian canal. However, this opening is probably not related to the vidian canal in *Coloradisaurus*, as the foramen for the passage of the carotid is usually located anteroventrally in the anterior tympanic recess. Likewise, Gow (1990) noted a small foramen in a juvenile braincase of *Massospondylus* posteroventral to the foramen for the facial nerve, which he interpreted as the passage of a blood vessel. However, the position of this foramen closely corresponds to that for the palatine ramus of the facial nerve in SMNS 12667, as Gow (1990: 60) notes that this foramen is separated from the facial foramen by a small crest underneath the latter, which he termed "*crista subfacialis*". Thus, we regard this foramen as a probable separate exit for the palatine branch of the nerve in *Massospondylus*. Interestingly, Gow noted that such a foramen is not present in adult braincases of *Massospondylus*, indicating the possibility of ontogenetic variation in this character.

Otoccipital

According to Sampson & Witmer (2007), the exoccipital and opisthotic are completely fused in dinosaurs, forming a single element for which they used the name ottoccipital, which is the term adopted here. In SMNS 12667, both otoccipitals are preserved, although the right element, which is only visible with CT-Scan, is considerably damaged (Fig. 5.2). The left element is visible in the matrix, but additional details of its morphology are shown by CT-Scan data. The description herein is solely based on the left otoccipital (Figs. 5.6, 5.7, 5.8).
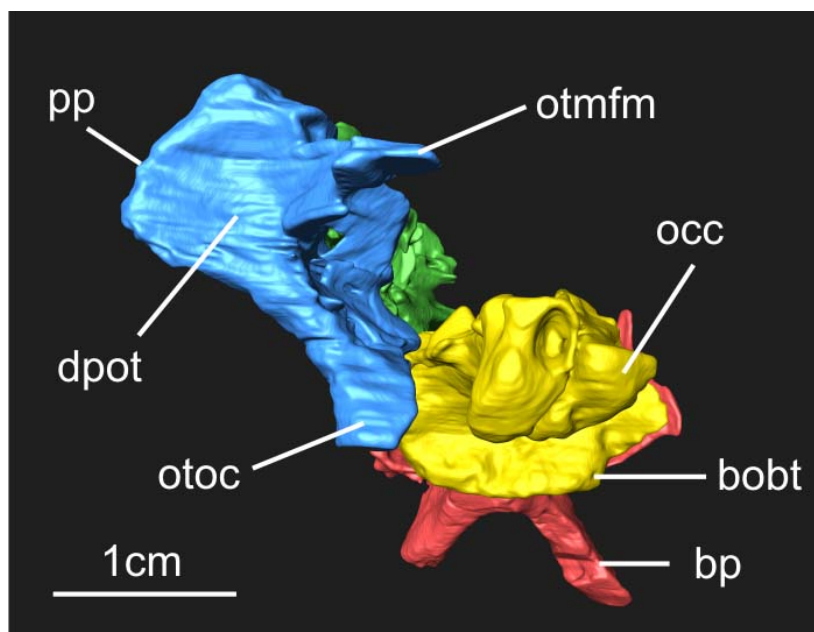
Figure 5.8: Posterior view of the braincase of the SMSN – 12667 specimen of *Efraasia minor* (right otoccipital is excluded due to the poor preservation and higher level of displacement of the element). Abbreviations: **bobt** – basioccipital component of the basal tubera; **bp** – basipterigoyd process; **dpot** – depression in the posterior portion of the otoccipital; **occ** – occipital condyle; **otoc** – otoccipital contribution to the occipital condyle; **otmfm** – otoccipital contribution to the margin of the foramem magnum; **pp**: proximal portion of the left paroccipital process.

The otoccipital of dinosaurs usually contacts most of the bones of the braincase, including the supraoccipital medially, the parabasisphenoid anteroventrally, the basioccipital posteroventrally, and the prootic anterodorsally (Galton, 1985; Sampson & Witmer, 2007). In SMNS 12667, the otoccipital is completely disarticulated from other bones, except for the contact with the prootic, with the latter overlapping the former anterolaterally at the base of the paroccipital process (Figs. 5.2, 5.7). Structures that are associated with the otoccipital, being formed exclusively by it or in conjunction with other bones, are the paroccipital process, the occipital condyle, the foramen magnum, the anterior and posterior

foramina between the exoccipital pillar and the fenestra ovalis, and the fenestra ovalis.

As mentioned above, the otoccipital forms the laterodorsal portion of the occipital condyle (Fig. 5.8). This part of the otoccipital is developed as a pyramidal posterior projection at the posteromedioventral edge of the bone (Figs. 5.6, 5.8). Laterally, the projection has a total extension of 8 mm from its posterior to its anterior tip, the latter here delimited as the ventral margin for the posterior foramen for the hypoglossal nerve. The ventromedial portion of this pyramidal projection contacts the basioccipital at the occipital condyle, and also forms part of the posterolateral surface of the floor of the braincase (Fig. 5.2). This contribution of the otoccipital to the floor of the braincase is similar to the condition observed in other sauropodomorphs (e.g. *Plateosaurus*, *Coloradisaurus*, and *Massospondylus*). Dorsal to the pyramidal projection, the medial side of the otoccipital forms the lateral and part of the dorsal margins of the foramen magnum (Fig. 5.8). In occipital view, the surface of the otoccipital bordering the foramen extends dorsolaterally from the ventral limit of the foramen magnum to a point where it curves medially and assumes a dorsomedial orientation. This change in the orientation occurs approximately at the mid-height of the foramen magnum, at the same dorsoventral level where the ventral limit of the proximal base of the paroccipital is located laterally. Furthermore, the portion of the otoccipital bordering the dorsal half of the foramen magnum projects slightly further posteriorly than the portion of the bone in the ventral half of the border. The exact contribution of the otoccipital to the dorsal margin of the foramen magnum, and consequently the supraoccipital contribution to it, cannot be determined precisely. In *Coloradisaurus*, *Thecodontosaurus*, *Plateosaurus*, and *Adeopapposaurus*, the contribution of the supraoccipital in the dorsal margin of the foramen magnum is

greater than that by the otoccipital. A different morphology is observed in *Melanorosaurus,* which has a reduced contribution of the supraoccipital to the border of the foramen magnum (less than one third of the dorsal border). In SMNS 12667, the condition probably differed from *Melanorosaurus,* being more similar to that of the other sauropodomorphs mentioned above, given the extent of the medial projection of the otoccipital in the region corresponding to the dorsal border of the foramen magnum (Fig. 5.8). The total height of the foramen magnum is difficult to establish because of the dislocation of the elements and incompleteness of the dorsal margin. Based on the morphology of the otoccipital and basioccipital, the foramen had a total height of c. 15 mm, which is about three times greater than the height of the occipital condyle (Fig. 5.8).

In occipital view, the otoccipital forms a rectangular to sub-quadrangular surface that projects dorsolaterally and slightly posteriorly lateral to the dorsal half of the foramen magnum (Fig. 5.8). This surface is slightly depressed at its center, so that it is medioventrally-dorsolaterally concave. This morphology was also observed in this region in all other sauropodomorph taxa studied. The ventromedial limit of the rectangular surface is confluent with the pyramidal posterior projection described above. Laterally, the contact between these two parts is formed by a 2 to 3 mm thick, rounded ridge that anteriorly forms the posterior border for the posterior opening of the hypoglossal nerve (XII) and the metotic foramen. The dorsolateral limit of the rectangular concave surface represents the base of the paroccipital process. However, only the proximal-most part of the paroccipital process is preserved in SMNS 12667 (Fig. 5.8), which does not allow the recognition of any further details of this structure.

In sauropodomorphs, as in dinosaurs generally, several cranial foramina are partially or completely enclosed by the otoccipital (Galton, 1985; Sampson & Witmer,

2007). On the lateral side of the otoccipital of SMNS 12667, two smaller posteroventrally placed foramina and two larger (Fig. 5.9) dorsally and more anteriorly placed openings are placed in a lateral depression on the bone below the paroccipital process, which corresponds to the paracondylar fossa in theropods (e.g. Bever *et al*., 2013). The two most ventral and posterior foramina represent openings for the hypoglossal nerve (XII), and are completely enclosed by the otocipital (Figs. 5.6, 5.7, 5.9). All non-sauropodan sauropodomorph taxa we observed (e.g. *Adeopapposaurus, Coloradisaurus, Massospondylus, Melanorosaurus, Plateosaurus, Thecodontosaurus*) also have two openings for the hypoglossal nerve. In Sauropoda this condition is not present in all members, and some taxa show a single opening for cranial nerve XII (e.g. Paulina-Carabajal *et al.,* 2014). In SMNS 12667, the external aperture of the posterior foramen for the hypoglossal nerve is elliptical, 5 mm tall, and 3 mm wide at its mid-length. The anterior foramen is circular and considerably smaller than the posterior one, with a diameter of approximately 1.5 mm. The same pattern in the relative size of these openings, with the posterior being larger than the anterior one, is observed in other non-sauropodan sauropodomorphs. One aspect that varies is the relative position of the ventral margin of these openings. In SMNS 12667 and *Thecodontosaurus,* the ventral margin of both foramina are aligned horizontally, whereas in taxa such as *Adeopapposaurus, Plateosaurus* and *Melanorosaurus,* the ventral margin of the anterior foramen is located ventral to the ventral margin of the posterior foramen.
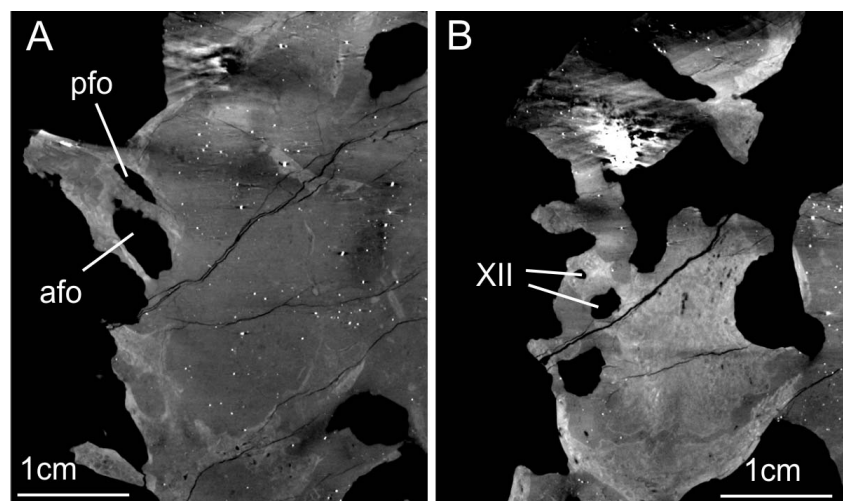
Figure 5.9: X-ray slices obtained from the CT-Scan procedure showing cranial opening in the braincase of the specimen SMNS - 12667 of *Efraasia minor*. A – anterior and posterior foramina in the left otoccipital between the exoccipital pillar and the fenestra ovalis. B – the two foramina for the cranial nerve XII (hypoglossal). Abbreviations: **afo** – anterior foramen of the otoccipital between the exoccipital pillar and the fenestra ovalis; p**fo** – posterior foramen of the otoccipital between the exoccipital pillar and the fenestra ovalis; **XII** – foramina for the hypoglossal nerve.

Dorsal and anterodorsal to the foramina for the hypoglossal nerve, there are two other foramina completelly enclosed by the otoccipital (Figs. 5.6, 5.7, 5.9). In their description of the braincase, Galton & Bakker (1985) considered the posterior of these foramina as the *foramen lacerum*, and the anterior one as the *foramen jugularis*. According to these authors, the former is the opening related to cranial nerves IX-XI, whereas the latter represents the opening for the jugular vein. Based on previous studies on archosaur braincases (e.g. Bellairs & Kamal, 1981; Walker, 1990; Gower & Webber, 1998; Sampson & Witmer, 2007; Sobral *et al.,* 2012), we come to a different interpretation (see discussion below). In this study we name the posterior foramen as the posterior foramen between the exoccipital pillar and the fenestra ovalis, whereas the anterior foramen is here treated as the anterior foramen between the exoccipital pillar and the fenestra ovalis (see discussion below).

We here consider the name *foramen lacerum posterior* (= *foramen jugularis*; Orliac, 2009) as inappropriate because this opening might not represent the path of the jugular vein (see discussion below). The aperture of this posterior foramen in the medial portion of the otoccipital is about two to three times the size of the aperture of the posterior foramen for the hypoglossal nerve (Figs. 5.6, 5.7). The aperture is located in the posterodorsal corner of the lateral margin of the otoccipital, ventral to the proximal portion of the paroccipital process. Laterally, the aperture has a more elliptical shape, with a length of 6 mm from the posterodorsal to the anteroventral margin, and a width of 2 mm at its widest portion. Anteriorly, a bony strut (we prefer to do not use any specific name for this strut, as for example, prevagal strut or metotic strut - see more in the discussion below) separates the posterior and anterior foramen. In lateral view, the strut is about 3mm and 2 mm wide in its dorsal and ventral portion, respectively. Although the lateral surface of the bony strut is depressed even below the level of the paracondylar fossa around the openings for the hypoglossal nerve, it extends laterally dorsally to become confluent with the dorsolateral surface of the prootic, ventral to the portion of the otoccipital overlapped by the prootic and the proximal portion of the parocipital process. Its ventral limit is located 3 mm more medially in relation to the external openings for the hypoglossal nerve.

We here the term anterior foramen of the otoccipital between the exoccipital pillar and the fenestra ovalis preferable to *foramen jugularis* (Galton, 1985), since this opening does not represent the foramen for the passage of the jugular vein (see discussion below). This anterior foramen (Fig. 5.6) is posterodorsally defined by the bony strut separating it from the posterior foramen described above. Anteriorly, it is defined by a ventral process of the otoccipital. The total length of this foramen from its posterodorsal margin to the anteroventral limit cannot be determined because

the ventral margin is not preserved. However, this foramen is considerably larger than the other three foramina within the otoccipital. As in other dinosaurs, a ventral process (Fig. 5.7) of the otocipital extends from the basis of the paroccipital process posterodorsally to the contact with the parabasisphenoid anteroventrally (Sampson & Witmer, 2007). It marks the separation between the anterior foramen and the fenestra ovalis anteriorly. This process has been also named the *crista interfenestralis* (see Sampson & Witmer, 2007), but we prefer to avoid this term because it has been used to name the process separating the fenestra ovalis from the fenestra pseudorotunda, which might not be the case in SMNS 12667 (see discussion below). In SMNS, this crest is developed as a lateromedially expanded sheet of bone. The lateral margin of this sheet is 1 mm wide, whereas medially its width is c. 5 mm ventrally and c. 3 mm dorsally.

Anterior to the ventral process of the otoccipital is located the fenestra ovalis (= *fenestra vestibuli*; Fig. 5.7). In contrast to the other cranial openings described above, the fenestra ovalis is not completely enclosed by the otoccipital, but is anteriorly bordered by the prootic (Fig. 5.6). The anterodorsal margin of this foramen is defined by the otoshpenoidal crest of the prootic, as described above. Ventrally, the opening of the fenestra ovalis reaches the posterior portion of the parabasisphenoid, but this part is slightly dislocated from its original position in SMNS 12667. The fenestra ovalis is an elongated foramen with an ellyptical shape. The total length of this foramen from the anteroventral to the posterodorsal margin is approximately 14 mm, with a maximum width of 5 mm.

Supraoccipital

The supraoccipital is partially preserved and visible only in anteroventral view (Fig. 5.10). CT-Scan shows that the posterodorsal margin of the bone is damaged so that it is impossible to observe any detail of its morphology. As in most non-sauropodan sauropodomorphs, the supraoccipital was strongly inclined anterodorsally, so that the dorsal part of the occiput faced posterodorsally.
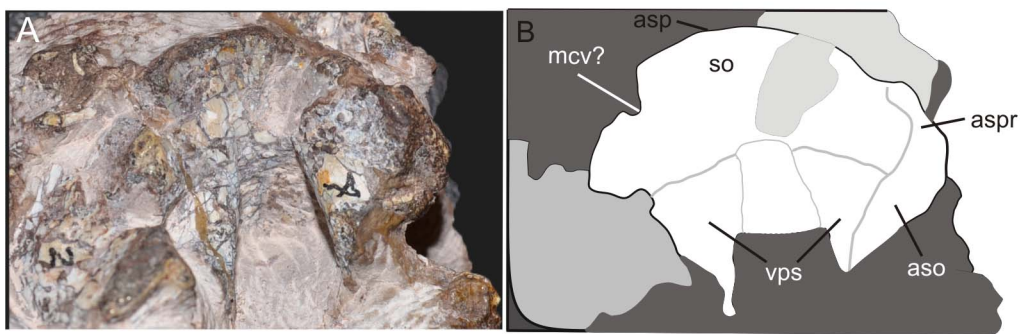
Figure 5.10: A – Anteroventral view of the supraoccipital of the specimen SMNS – 12667 of *Efraasia minor*. B – Schematic drawing of A. Abbreviations: **aso** – articulation surface with the otoccipital; **asp** – articulation surface with the parietal; **aspr** – articulation surface with the prootic; **mcv** – notch for the mid-cerebral vein; **so** – supraocipital; **vps** – ventral projection of the ventral surface of the supraoccipital.

In previous phylogenetic data matrices (Yates, 2007b; Apaldetti *et al*., 2014; McPhee *et al*., 2014, 2015), the supraoccipital of *Efraasia* has been treated as being wider than high as in other sauropodomorphs, such as *Thecodontosaurus*, *Panphagia*, and *Pantydraco*, but in contrast to the condition of *Coloradisaurus* and *Plateosaurus*, in which the supraoccipital is as high as wide. Based on the preserved and visible part of the supraoccipital in SMNS 12667, this bone has a maximum width of 25 mm. The height of the preserved supraoccipital is 18 mm. However, a part of the posteroventral portion of the supraoccipital, including the surface that probably formed part of the

border of the foramen magnum, is missing (Fig. 5.10). It is thus not possible to establish the condition in SMNS 12667 with certainty.

The supraoccipital forms a narrow, tunnel-like roof of the endocranial cavity posteriorly between robust ventral projetions laterally (Fig. 5.10). Anterior to the projections, the supraoccipital expands both laterally and dorsally, up to a dorsally widely arched and laterally slightly concave margin that would have contacted the parietal wings. On the right side of the anterodorsal margin there is a notch that most probably represents the path of the mid-cerebral vein towards its posterior exit, as in *Panphagia* (Martinez *et al.,* 2012b). This area is poorly preserved on the left side of the supraoccipital, but at least a small, matrix-filled incision is present here in the same position. Anteroventral to the incision in the margin, a large recess is found on the medial side of the supraoccipital on either side, which probably housed the posterior venous sinus associated with the mid-cerebral vein. Sauropodomorphs show some variation regarding the path of this vein in the supraoccipital. In some taxa, such as *Coloradisaurus* and *Plateosaurus*, the foramen for the vein is completely enclosed by the supraoccipital. In *Efraasia*, the anterior margin of the supraoccipital would have contacted the parietals, so the mid-cerebral vein would have exited the braincase between the supraoccipital and the ventral margin of the parietal wings.

It is here worth mentioning the variation in the nomenclature adopted in different studies on sauropodomorph braincases regarding the vein associated to the foramen or notch in the supraoccipital (in case the vein passes between the supraoccipital and parietal). In the original description of *Panphagia*, Martinez & Alcober (2009) identified the notch in the supraoccipital as the path for *vena capitis dorsalis*, which is the same term adopoted in Apaldetti *et al.* (2014) to refer to the vein associated to the foramen in the supraoccipital of *Coloradisaurus*. Posteriorly,

Martinez *et al.* (2012) refers to the notch of *Panphagia* as the path for the external occipital vein. Still, Yates (2007) label the foramen in the supraoccipital as the path for the mid-cerebral vein (*vena cerebralis media*).

According to Sampson & Witmer (2007), a foramen in the anteromedial portion of the supraoccipital of the theropod *Majungasaurus* Depéret, 1896 is related to the posterior exit of the mid-cerebral vein, which becomes the external occipital vein after exiting the skull. Still according to the authors, the exit of the *vena capitis dorsalis* is located at the juncture between parietal, laterosphenoids, and possibly the prootic, lateral to the exit of the mid-cerebral vein. Thus, as the foramen in the supraoccipital of sauropodomorphs such as *Plateosaurus* and *Coloradisaurus* is located in the same position of the foramen described for *Majungasaurus* in Sampson & Witmer (2007), we here consider the foramen or notch in the supraoccipital of sauropodomorphs as associated to the mid-cerebral vein (or external occipital vein), as previously identified by Yates (2007) and Martinez *et al.* (2012).

Posteroventrally, the ventral margin of the supraoccipital would have contacted the otoccipital posteriorly, and the prootics anteriorly (Fig. 5.10). The ventral projections are 11 mm long dorsoventrally, 9 mm thick lateromedially, and have a preserved anteroposterior length of 9 mm. The anteroventral surface of the supraoccipital between the ventral projections formed the posterodorsal portion of the internal cavity of the braincase, including the dorsal margin of the foramen magnum in the posterior limit of the bone. The surface between these two projections is concave. Anteriorly, the surface between the projections is 5 mm wide, but as the projections diverge laterally at the posteroventral end of the bone, the surface widens to 8 mm at the preserved posterior end.

Laterosphenoid

The left laterosphenoid is preserved (Fig. 5.11), but has been displaced from its original connections to other bones of the braincase (Figs. 5.2, 5.6A). As in other dinosaurs, the laterosphenoid would have contacted the prootic posteroventrally, the parietal and, possibly the frontal dorsally, and the postorbital dorsolaterally. The laterosphenoid might furthermore have contacted an orbitosphenoid anteriorly, as it is the case in *Plateosaurus* (Galton, 1985), and the parabasisphenoid ventrally.
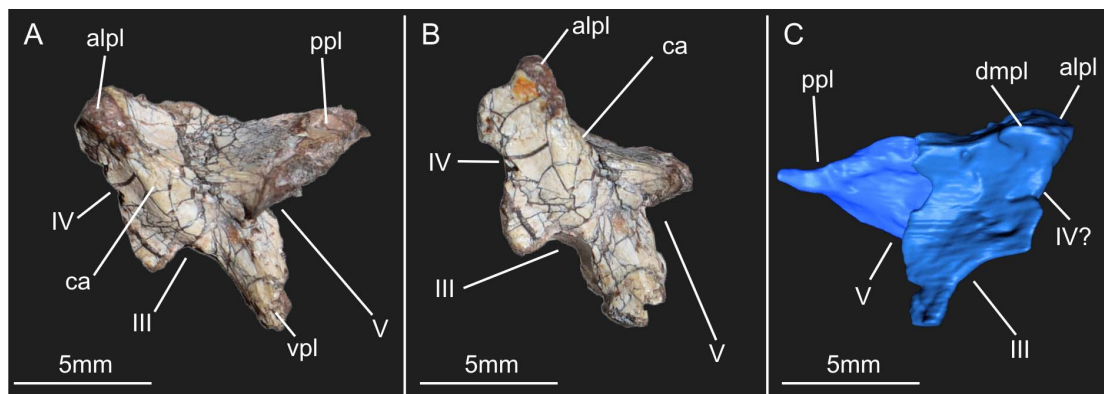
Figure 5.11: Left laterosphenoid of the specimen SMNS – 12667 of *Efraasia minor* in lateral (A), anterolateral (B), and, medial (C) views. Abbreviations: **alpl** – anterolateral process of the laterosphenoid; **ca** – crista antotica; **dmpl** – dorsomedial process of the laterosphenoid; **pbsp** – parabasisphenoid process; **pop** – postorbital process; **ppl** – posterior process of the laterosphenoid; **prop** – prootic process; **vpl** – ventral process of the laterosphenoid; **III** – path of the cranial nerve III (oculomotor); **IV** – path of the cranial nerve IV (trochlear); **V** – path of the cranial nerve V (trigeminal).

The laterosphenoid seems to be somewhat incomplete and is mainly exposed in anterior and lateral view (Fig. 5.11). The bone formed the anterior and anterolateral wall of the braincase and can be subdivided into an anterior and a lateral surface, which meet at an angle of approximately 90°. An anterolateral process (= the postorbital process of Prieto-Marquez & Norell, 2011) extends from the dorsal part of the junction of these two surfaces and would have possibly contacted the postorbital

laterally. The extremity of the process with the articular facet for the postorbital seems to be missing, however. As preserved, this process is relatively short in SMNS 12667, being about one fourth of the total anteroposterior length of the laterosphenoid. This is also the condition in *Massospondylus,* whereas *Plateosaurus* (Prieto-Marquez & Norell, 2011) has an anterolateral process that is slender and with a length corresponding to half of the length of the laterosphenoid in lateral view. In how far the condition in *Efraasia* might be owed to the missing portion of the process cannot be established. As it is the case in *Massospondylus* (Gow, 1990), the laterosphenoid of SMNS 12667 is longer anteroposteriorly than wide transversely. In lateral view, the laterosphenoid is triangular to trapezoidal in outline, becoming higher anteriorly. The dorsal part of the laterosphenoid is considerably concave anteroposteriorly especially dorsally where it turns into the anterolateral process. In this area, the lateral side curves gradually into the posterior side of the anterolateral process. Anteriorly, it is separated from the anterior side by a low, but well-defined crista antotica (Madsen *et al.*, 1995), which separates the orbital cavity anteriorly from the adductor chamber posteriorly (Sampson & Witmer, 2007). Towards the anterior end of the laterosphenoid as seen in lateral view, there is a slender, roughly triangular ventral process (= the parabasisphenoid process of Prieto-Marquéz & Norell, 2011) with a slightly concave posterior margin; this margin most probably represents the anterior border of the trigeminal foramen. This process widens slightly ventrally, where it would have contacted the anterior portion of the prootic and eventually the parabasisphenoid, at the region of the preotic pendant. It is dorsally overhung by the lateroventral extension of the dorsal part of the laterosphenoid, resulting in a short, longitudinal, ventrally open channel anterior to the trigeminal foramen. Galton & Bakker (1985: fig. 2) interpreted this channel as conducting a

branch of the mid-cerebral vein. However, in other dinosaurs that show such a channel or a groove anterior to the trigeminal foramen, this is usually interpreted as the passage of the ophthalmic branch of the trigeminal nerve (V_1; e.g. Sampson & Witmer, 2007; Sobral *et al*., 2012), and we consider this the more likely interpretation here as well.

In anterior view (Fig. 5.11), the laterosphenoid is narrow ventrally, but gradually expands dorsally towards the anterolateral process. In articulation with the rest of the braincase, the anterior surface of the laterosphenoid would have faced slightly anteroventrally. A large indentation is present in its medial rim just dorsal to the level of the overhanging lateral shelf. This indentation is higher than wide and becomes slightly wider dorsally. Galton & Bakker (1985) identified this opening as the foramen for the optic nerve, II (see also Prieto-Marquez & Norell, 2011, for the same interpretation in *Plateosaurus*). However, in dinosaurs in which the orbitosphenoid is preserved, this nerve usually exits the braincase through this bone (e.g. Gow, 1990; Currie & Zhao, 1993; Sampson & Witmer, 2007), and thus this opening is probably for the passage of the oculomotor nerve (III), as interpreted by Gow (1990) in *Massosopondylus*. At the dorsal margin of the anterior surface of the laterosphenoid, a wider, but lower second indentation is present medially. As noted by Galton & Bakker (1985), this opening represents the passage of the fourth (trochlear) cranial nerve.

Based on CT-Scan data it is possible to examine the medial surface of the laterosphenoid (Fig. 5.11). Athough the medial surface of the bone is not well preserved, some details can be observed. In SMNS 12667, the medial surface of the main body of the laterosphenoid (excluding the processes) is concave, being deeper around the center of this region. This is similar to the condition in other non-

sauropodan sauropodomorphs with laterosphenoids visible in medial view, such as *Plateosaurus* (AMNH 6810) and *Massospondylus*. Based on comparisons with these two taxa, a small protuberance located at the level of the proximal portion of the anterolateral process of SMNS 12667 corresponds to the proximal portion of a dorsomedial process (= the frontal process of Prieto-Marquez & Norell, 2011). Prieto-Marquez & Norell (2011: fig. 26C) indicated the path of cranial nerve IV as being immediately ventral to this dorsomedial process. However, in SMNS 12667 there is a notch at the anterior margin of the laterosphenoid, followed by a concave surface on the medial side, which might correspond to the path of cranial nerve IV. If this indeed represents the path for the trochlear nerve, this nerve would be more ventrally located in relation to the dorsomedial process in SMNS 12667 than it is in *Plateosaurus* (as indicated by Prieto-Marquez & Norell, 2011).

5.5. DISCUSSION

The discussion is divided into two main sections. First we discuss morphological aspects of the braincase of sauropodomorphs. This part of the discussion deals with the interpretation of soft tissues associated with two foramina located in the otoccipital of sauropodomorphs, here treated as the anterior and posterior metotic foramina. Another morphological trait discussed here is the presence of an unossified gap between the parabasisphenoid, basioccipital, and the otoccipital in the braincase of sauropodomorphs. In the second section of the discussion we provide an analysis of the evolution of non-neosauropodan sauropodomorph braincases from a comparative perspective. For this, a phylogenetic framework in which to trace the evolutionary history of each particular trait is necessary. The topology used here is based on a numerical analysis using a dataset that is modified from the recent study of

McPhee *et al.* (2015), focusing on non-neosauropodan sauropodomorph relationships. In the course of our study we identified problematic aspects in phylogenetic characters representing braincase anatomy that have been used in phylogenetic studies of sauropodomorphs. The problematic aspects are mainly related to character definition, which does not accurately represent the morphology observed in the specimens, and the scoring of taxa in the matrix. Accordingly, we discuss some of the phylogenetic characters related to braincase anatomy that are present in the matrix, and also new characters proposed in this study, the phylogenetic history of which is also discussed here (see Appendix I for more details).

CONSIDERATIONS ON THE MORPHOLOGY OF THE BRAINCASE OF SAUROPODOMORPHS

The division of the metotic fissure and the course of the jugular vein

Our survey of the literature indicates that previous studies of braincases of sauropodomorphs (e.g. Galton, 1985; Galton & Bakker, 1985; Benton *et al.,* 2000; Yates, 2007b) probably misidentified the soft tissues associated with the two foramina in the otoccipital located between the exoccipital pillar and the fenestra ovalis. Very detailed explanations regarding the development of the metotic fissure in archosaurs and the presence of two foramina between the exoccipital pillar and the fenestra ovalis have been provided in the literature (Gower & Weber, 1998; Gower, 2002, Sampson & Witmer, 2007; Sobral *et al.,* 2012). These have implications for the exit route of cranial nerve X (vagus nerve) and the posterior cephalic vein (= internal jugular vein of some authors; Gower, 2002; Sobral *et al.,* 2012), and also for the development of a secondary tympanic membrane (Gower & Weber, 1998; Sampson

& Witmer, 2007), the latter being related to a refinement of the auditory system (Müller & Tsuji, 2007; Sobral, 2014). A brief overview is presented here in order to clarify our point regarding the nature of the two foramina in the otoccipital of sauropodomorph dinosaurs.

According to Gower & Weber (1998), the metotic fissure is a gap present during embryonic stages, which is positioned between the otic capsule and the basicranium of the chondocranium (see also Bellairs & Kamal, 1981 and Rieppel, 1985). During the embryonic stage, cranial nerves X and XI and usually the posterior cephalic vein pass through the metotic fissure. During ontogeny, this structure can then persist as a single opening, or can become subdivided by a prevagal strut *sensu* Gower & Weber (1998). In the first case, the single opening of adults should be referred to as the metotic foramen, and represents the opening for cranial nerves IX to XI and possibly the posterior cephalic vein. If the metotic fissure becomes subdivided, the anterior opening should be referred to as the fenestra pseudorotunda (= fenestra cochleae in Sampson & Witmer, 2007), whereas Gower & Weber (1998) suggest to use the term vagal foramen for the posterior opening, which has variously also been called the jugular foramen. Cranial nerve X and XI and, possibly, the posterior cephalic vein pass through this posterior foramen in adults. The path of cranial nerve IX is more plastic among archosaurs, and this nerve can exit the internal cavity through different paths (Sobral *et al.*, 2012). Likewise, whereas the vagal nerve (X) always seems to pass through this posterior foramen (when present), the course of the posterior cephalic vein is more variable, and this vessel might exit the braincase through this foramen or the foramen magnum (see Gower & Weber, 1998; Gower, 2002, Sampson & Witmer, 2007). In those taxa in which the fissura metotica becomes divided, the anterior opening, the fenestra pseudorotunda, represents the lateral

opening of the recessus scalae tympani and is covered by a secondary tympanic membrane (see also Rieppel, 1985; Sampson & Witmer, 2007).

Although the presence of a divided metotic fissure (i.e. the presence of a fenestra pseudorotunda and a vagal foramen in adults – see Sampson & Witmer, 2007) is observed in both major clades of extant archosaurs (Crocodylia and Aves), it might be better explained as independent acquisitions in the pseudosuchian and avemetatarsalian lineages (Gower & Weber, 1998). In Dinosauria, the division of the metotic fissure, with the presence of a fenestra pseudorotunda and a vagal foramen, might be present among members of three main lineages of dinosaurs (Ornithischia, Sauropodomorpha, Theropoda); however it is still debatable if this represents a symplesiomorphy retained from dinosauriform ancestors or independent acquisition in the different groups (Sobral, 2014).

Gower (2002) furthermore noted the presence of an additional foramen posterodorsal to the metotic foramen in the non-crocodylomorphan pseudosuchian *Batrachotomus* Gower, 1999 and *Postosuchus* Chatterjee, 1985. This foramen in *Batrachotomus* is associated with a venal sinus on the interior of the braincase, and was thus interpreted as a separate opening for the posterior cephalic vein only (Gower, 2002). Thus, according to Gower (2002), *Batrachotomus* and *Postosuchus* do not have a divided metotic foramen in a fenestra pseudorotunda and a vagal foramen (i.e. there is no formation of a secondary tympanic membrane).

In respect to sauropodomorphs, earlier interpretations (see e.g. Galton, 1985; Galton & Bakker, 1985) of the soft tissues associated with the foramina here treated as anterior and posterior foramina of the otoccipital between the exoccipital pillar and the fenestra ovalis differ from that suggested by Gower & Webber (1998) and Gower (2002) for archosaurs in general. In the original description of the braincase of SMNS

12667, Galton & Bakker (1985) interpreted the anterior foramen as the *foramen jugularis*, through which the internal jugular vein would pass. According to the authors of that study, cranial nerves IX-XI would exit through the posterior foramen, which they called *foramen lacerum* posterior. This nomenclature was followed in subsequent studies on the braincase of sauropodomorphs (e.g. Benton *et al.*, 2000; Yates, 2007b). A first problem of this nomenclature adopted by Galton & Bakker (1985) is that the term *foramen lacerum posterior* is equivalent to the term *foramen jugularis* (Orliac, 2009), which is the name the authors used to refer to the anterior foramen.

Furthermore, the interpretation of Galton & Bakker (1985), identifying the anterior foramen (their *foramen jugularis*) as the path of the jugular vein, is problematic. In cases where a divided metotic foramen is present, the posterior cephalic vein (internal jugular vein in Galton & Bakker, 1985) may either pass through the foramen magnum, as reported for lepidosaurs and crocodiles (see Gower, 2002; Sobral *et al.*, 2012), or this vein passes through the posterior one of the two foramina, the vagal foramen. In the latter case, if the posterior foramen is relatively small, this might be an indication that the vein drained mainly into the occipital sinus, as proposed for abelisaurids in Sampson & Witmer (2007). As explained by Bellairs & Kamal (1981), a vein passes through the metotic fissure in embryonic stages of reptiles. However this vein disappears during ontogeny and then the posterior cephalic vein of adults leaves the skull through the foramen magnum in lepidosaurs and at least some crocodiles. On the other hand, in cases where the metotic foramen is undivided (i.e. there is no formation of a fenestra pseudorotunda, which is covered by a secondary tympanic membrane, and a vagal foramen), but there is an additional

foramen at the level of the exoccipital pillar, this foramen might represent the path for the posterior cephalic vein (Gower, 2002).

Given the scenario explained above, it would thus be highly unusual that the posterior cephalic vein passes through the anterior opening, as proposed by Janensch (1935), followed by Galton (1985), Galton & Bakker (1985), and subsequent studies on the braincase of sauropodomorphs (e.g. Yates, 2007b; Martinez, 2009; Apaldetti *et al.,* 2014). According to our survey in the literature, there are two possible scenarios regarding the path of the posterior cephalic vein and the nature of the two foramina of SMNS 12667, and thus for other non-sauropodan sauropodomorphs. One scenario is that our anterior foramen corresponds to the fenestra pseudorotunda (*sensu* Gower & Weber, 1998) and that it was covered by a secondary tympanic membrane (Gower & Weber, 1998; Sampson & Witmer, 2007). In this case, our posterior foramen would be equivalent to the vagal foramen (*sensu* Gower & Weber, 1998). Given the reduced size of this foramen, it probably represented the path for the vagus nerve, but not for the posterior cephalic vein, which would pass through the foramen magnum (Sampson & Witmer, 2007). The second scenario is that SMNS 12667 has an undivided metotic foramen (*sensu* Gower & Weber, 1998), and our posterior foramen actually corresponds to the path of the posterior cephalic vein, as argued for some other archosaurs (Gower, 2002). In the latter case, one possibility is that the undivided metotic foramen seen in sauropods is related to a configuration in which the posterior cephalic vein leaves the braincase through the foramen magnum, as in many lepidosaurs and crocodiles.

The presence of an unossified gap in sauropodomorph braincases

The term unossified gap has been used in braincase studies to refer to unossified areas of the braincase that remain cartilagenous throughout life, whereas the braincase usually ossifies extensively in reptiles (Gower & Sennikov, 1996; Gower & Weber, 1998). Unossified gaps in different regions of the chondrocranium and presenting different morphologies were recognized in the braincase of diapsids (Gower & Weber, 1998). In the context of non-archosaur archosauriform and non-crocodylomorph pseudosuchian braincases, the presence of such structures has received great attention in previous studies (Gower & Sennikov, 1996; Gower, 2002; Gower & Nesbitt, 2006; Nesbitt, 2011; Sookias *et al.*, 2014). In these forms, an unossified gap occurs between the components of the basioccipital and parabasisphenoid that form the basal tubera and at the ventral end of the ventral ramus of the otoccipital, which separates the fenestra ovalis from the posterior foramen in the otoccipital (Gower & Sennikov, 1996; Gower & Weber, 1998).

Some of the sauropodomorph braincases we analysed also exhibit an unossified area (Fig. 5.12) that is topologically equivalent to the unossified gap (sensu Gower & Webber, 1998, Gower, 2002) of some non-archosaurian archosauriforms and non-crocodylomorph pseudosuchians. This structure is also present in *Adeopapposaurus*, *Unaysaurus, Massospondylus, Melanorosaurus, Plateosaurus, Leyesaurus,* and *Thecodontosaurus* (already pointed out by Benton *et al.*, 2000). Above we discussed the significance of the junction between the parabasisphenoind and basioccipital as a possible indicator of the level of the maturity of the individual.
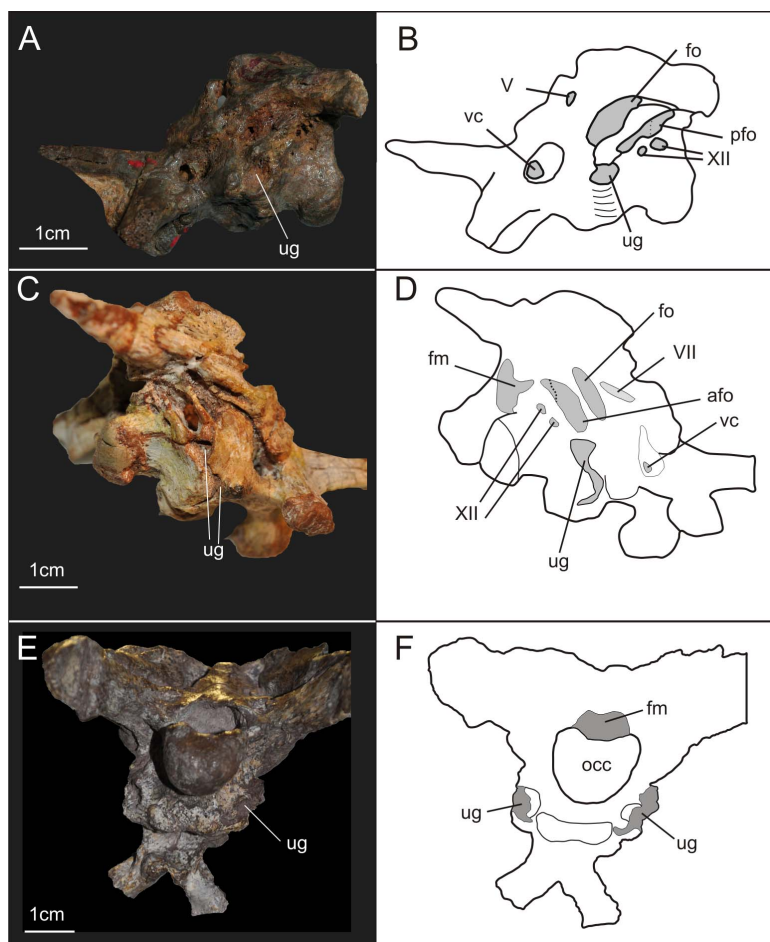
Figure 5.12: Posterolateral view of the braincases of the specimens YPM 2192 of *Thecodontosaurus antiquus* (A and B) and PVSJ 568 of *Adeopapposaurus mognai* (C and D), and posteroventral view of the braincase of the specimen SMNS – 13200 of *Plateosaurus* (E and F) illustrating the presence of an unossified gap in sauropodomorph braincases. Abbreviations: **afo** – anterior foramen of the otoccipital between the exoccipital pillar and the fenestra ovalis; **fm** – foramen magnum; **fo** – fenestra ovalis; **occ** – occipital condyle; **pfo** – posterior foramen of the otoccipital between the exoccipital pillar and the fenestra ovalis; **ug** – unossified gap; **vc** – vidian canal; **V** – foramen for the trigeminal nerve; **VII** – foramen for the facial nerve; **XII** – foramina for the hypoglossal nerve.

Nevertheless, even in braincases of presumed adult individuals (*Plateosaurus, Melanorosaurus, Massospondylus, Thecodontosaurus, Leyesaurus*) in which the basioccipital and parabasisphenoid are firmly attached to each other, an unossified gap is still present between basioccipital, parabasisphenoid and otoccipital. Finally, we do not think that the existence of an unossified gap in the braincase of non-sauropodan sauropodomorphs can be attributed to preservation or sampling bias,

given that we analysed most of the non-sauropodan sauropodomorph taxa that have braincase elements preserved first-hand (Table 1).

PHYLOGENETIC ANALYSIS

Recent phylogenetic analyses (e.g. Martinez, 2009; Apaldetti *et al*., 2012, 2014; McPhee *et al*., 2014, 2015; Otero *et al*., 2015) focused on non-neosauropodan sauropodomorph relationships mostly represent extensions of two data matrices, those of Yates (2007b) and Upchurch *et al*. (2007). These matrices differ slightly in taxa composition and characters, and the results of both shows some disagreements regarding the arrangement of the classic "prosauropods" (see Galton & Upchurch, 2004; Sereno, 2007a). Results of Yates (2007b), and of the analyses derived from his data matrix (e.g. Otero & Pol, 2013; Apaldetti *et al*., 2014; McPhee *et al*., 2014, 2015; Otero *et al*., 2015), exhibit the majority of these taxa as a series of consecutive sister-groups of Sauropoda. On the other hand, the results of Upchurch *et al*. (2007) and subsequent analyses extending this dataset (e.g. Martinez 2009; one of the analyses presented in Apaldetti *et al*. 2011) have found taxa such as Plateosauridae and Massospondylidae ("the core prosauropods" – Sereno, 2007a) forming a monophyletic Prosauropoda (but see Yates *et al*., 2010).

Nevertheless, the data matrices presented by Upchurch *et al*. (2007) and Yates (2007b) include almost the same set of phylogenetic characters related to braincase anatomy. The only difference between the set of characters is character 64 used by Upchurch *et al*. (2007) – "Ossification of the extremity of the basal tubera: complete, so that the basioccipital and parabasisphenoid form a single rugose tuber (0); unossified, with the basioccipital forming a ventrally facing platform of unfinished

bone that abuts a similarly unfinished caudally facing wall of the parabasisphenoid (1)". This character was originally proposed by Yates & Kitching (2003), but was later excluded in Yates (2007b) and subsequent analyses based on it. This character obviously describes the presence of an unossified gap (Gower & Sennikov, 1996; Gower & Weber, 1998; Gower, 2002) between the basioccipital, parabasisphenoid, and otoccipital in the braincase of sauropodomorphs discussed above.

We revised the phylogenetic characters related to braincase anatomy used in McPhee *et al.* (2015), which, in turn, represents one of the most recent versions of the data matrix based on Yates (2007b). It is worth mentioning that characters of McPhee *et al.* (2015) that are related to the braincase anatomy have no modification in relation to the way they are presented in Yates (2007b), also the case for previous studies using an extended version of this dataset (e.g. Yates *et al.* 2010; Pol *et al.* 2011; Apaldetti *et al.* 2014; Otero *et al.* 2015). The revision resulted in the recognition of problematic issues regarding character definition and character scoring. Accordingly, we here propose modifications of character definitions and/or in the character states attributed to some taxa. Following revision and the addition of new characters, a phylogenetic analysis was carried out using TNT (Goloboff *et al.*, 2008) under the following parameters: random seed 0; 10 000 replicates; hold 10; TBR (tree bi-section reconnection) for branch swapping. The analysis recovered a total of 144 MPT's (most parsimonious trees), 1248 steps long. We used the prunnelsen command of TNT (Goloboff & Szumik, 2015) in order to identify unstable taxa in the analysis. This procedure identifies *Blikanasaurus* as an unstable OTU (Operational Taxonomic Unit) in this analysis. A reduced strict consensus tree (Fig. 5.13) excluding *Blikanasaurus* was used as the framework to analyse aspects of the evolution of the braincase in the sauropodomorph lineage.
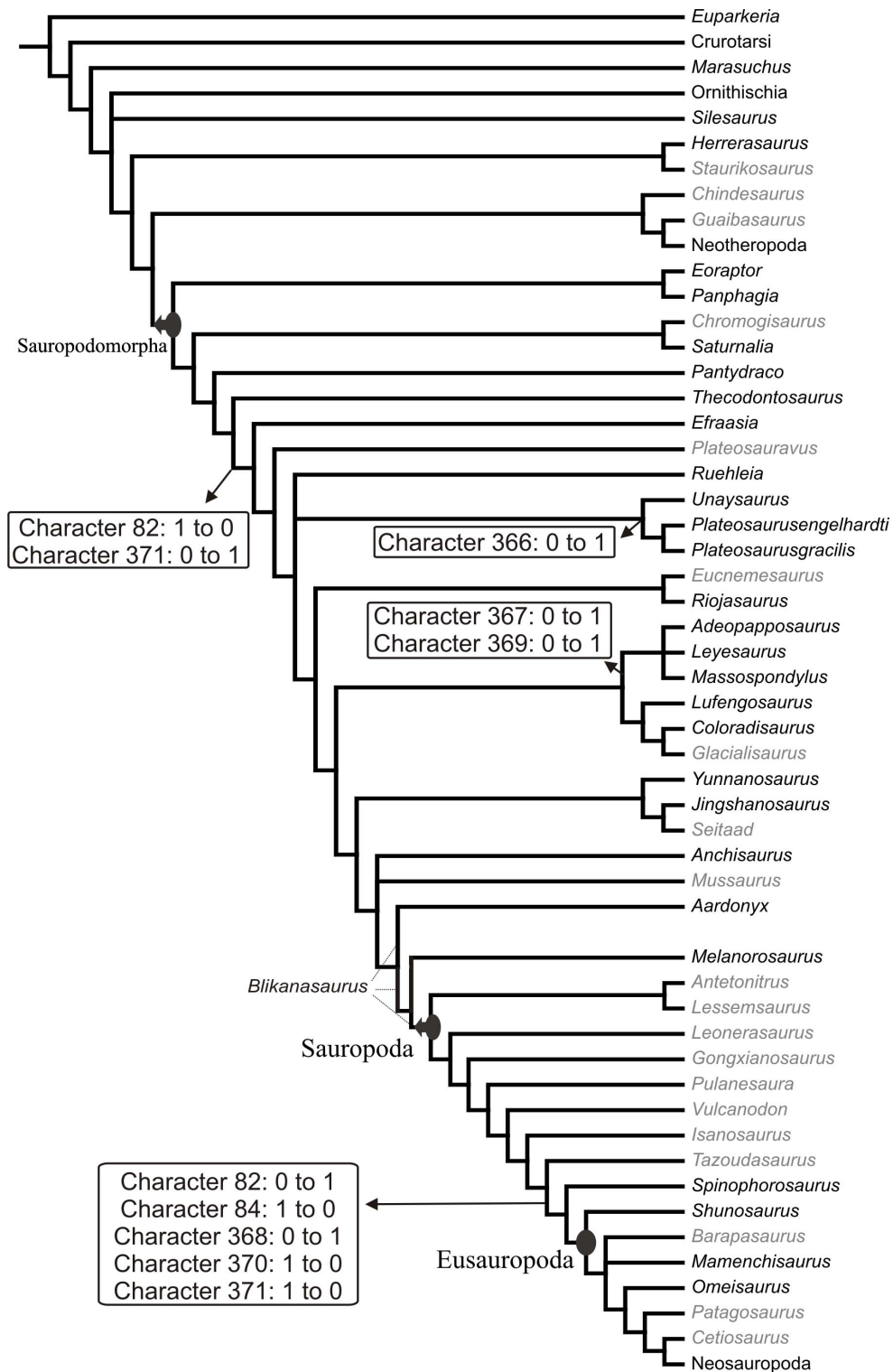
Figure 5.13: Strict consensus tree of the 144 MPT's recovered in the phylogenetic analysis. Taxa names written in black indicate that at least one character related to the braincase anatomy could be scored in the data matrix for that taxon.

Despite the substantial modifications in the data matrix (see Appendix I), the results of our analysis agree with that of McPhee *et al*. (2015). The reduced consensus tree is well resolved (more than 90% of the nodes). The classical "prosauropods" are found paraphyletic in relation to Sauropoda. Nevertheless, some less inclusive groups are found among this assemblage of taxa. Our results confirm the affinity of *Unaysaurus* to *Plateosaurus,* with both taxa forming Plateosauridae. Our reduced consensus tree also depicts a monophyletic Massospondylidae (Fig. 13), which are found more closely related to sauropods than to plateosaurids. Finally, the non-eusaropodan sauropods are majorly found as consecutive sister-group of successively less inclusive clades containing the eusauropods.

In the following discussion of braincase characters, numbers follow those in the dataset of our analysis; however, these are the same as those in the data matrices of McPhee *et al*. (2015) and previous analyses (e.g. Pol *et al*., 2011; Apaldetti *et al*., 2014, McPhee *et al*., 2014; Otero *et al*., 2015), using an expanded version of the Yates (2007b) matrix, except for the new characters proposed here.

REVISON OF PREVIOUS CHARACTERS AND NEW CHARACTERS RELATED TO BRAINCASE ANATOMY

Deep septum in the interbasipterygoid space VS deep subsellar and basisphenoid recesses – Character 85 of this study and of Yates (2007b)

This character was previously defined as: "Deep septum spanning the interbasipterygoid space: absent (0) or present (1)". The evolution of this trait was recently discussed by Apaldetti *et al*. (2014). In their study these authors considered

five OTUs (Operational Taxonomic Unit) to have the state "1": *Anchisaurus,*

Coloradisaurus, Efraasia, Plateosaurus, and *Riojasaurus incertus* Bonaparte, 1967.

In the course of our study, we found anatomical variation regarding the morphology

of the "septum" among taxa scored with state '1'. Furthermore, we were unable to

identify anatomical congruence to clearly distinguish these taxa coded with state '1'

from those coded with state '0', as some of the taxa coded '0' have a morphology that

matches the morphology of taxa coded with state '1'. This problem stems from the

lack of a clear statement about the nature of the septum and what really represents the

interbasipterygoid space.

The basipterygoid processes arise from the ventral surface of the main body of

the parabasisphenoid anteriorly, and their bases are connected to the ventrolateral

edge of the cultriform process by a curved lamina. The median space between the

anterior and posterior limits of left and right basipterygoid processes is the region of

the subsellar recess (*sensu* Witmer, 1997). In taxa that have a deep subsellar and also

a deep basisphenoid recesses, there is a transverse wall or septum of bone spanning

between the bases of the basipterygoid processes that separates these two recesses.

This is the case e.g. in *Coloradisaurus* (see Apaldetti *et al.*, 2014: Fig. 6c),

Riojasaurus, and *Anchisaurus* (see Fedak & Galton, 2007: Fig. 6a). This morphology

is more obvious in theropods, in which both recesses are typically better developed

than in sauropodomorphs [the septum is treated as the interbasipterygoideal lamina of

the basisphenoid in Witmer & Ridgely, (2010); or basisphenoid web in Bakker *et al.*,

(2004) and Rauhut (2004)]. However, in contrast to *Coloradisaurus, Riojasaurus,* and

Anchisaurus, the other two taxa scored with state '1', *Efraasia* and *Plateosaurus,*

have a much more shallow basisphenoid recess. In this case, there is no septum in

these taxa, as the bone spanning between the basipterygoid processes only forms the

posterior wall of the subsellar recess. What has probably been treated as a septum in these two taxa is thus the posterior margin of the deep subsellar recess. Therefore, it is clear that there is a difference in the morphology of taxa coded with state '1'. Whereas *Riojasaurus*, *Coloradisaurus*, and *Anchisaurus*, have a vertical sheet of bone between the subsellar and basisphenoid recesses, *Efraasia* and *Plateosaurus* do not possess such a structure because they do not possess a deep basisphenoid recess. Thus, it seems that what has been coded as the presence of a deep septum between the interbasipterygoid process is actually related to the depth of the subsellar recess.

Furthermore, we also found problematic aspects for taxa that were coded as '0' that should be considered. *Leyesaurus* exhibits a morphology that strongly resembles that of *Efraasia*, in having a deep subsellar recess but a shallow basisphenoid recess. However, whereas *Efraasia* is coded as '1', *Leyesaurus* is coded as '0'. In addition, a structure similar to that described by Fedak & Galton (2007: fig. 6a) as a ridge (i.e. septum) between the basipterygoid processes in *Anchisaurus* is clearly present in *Eoraptor* (see Sereno *et al*., 2012: fig. 29), but the latter was coded with state '0'. Finally, neotheropods usually have well defined subsellar and basisphenoid recesses (Witmer, 1997; Rauhut, 2004), and, as a consequence, they also have a deep septum in the interbasipterygoid space. However, the OTU Neotheropoda was also coded with state '0' in all previous analyses using an updated version of Yates (2007b) matrix.

The differences between our interpretations and those of previous studies when coding this character could be attributed to the implicit subjectivity of the word "deep", used in the character definition. However, as shown by the example of *Efraasia* and *Leyesaurus* described above, this problem may also arise from different interpretations of what constitutes a septum spanning the interbasipterygoid space.

Although neither *Efraasia* nor *Leyesaurus* do possess a septum, the deep subsellar recess was misinterpreted as a septum in the former, but not in the latter.

Here we propose a modification of the definition of character 85 (Fig. 5.14) in order to avoid subjectivity and try to minimize conflicts in coding in future studies. Thus, the character is here defined as: *subsellar recess: maximum width equal or greater than the dorsoventral height (0); maximum width smaller than the dorsoventral height (1)*.

The results of our analysis show that the presence of a subsellar recess state '1' occurs in all taxa belonging to the clade containing *Efraasia* and Neosauropoda (Fig. 5.14). The only sauropodomorpha scored with state '0' in the data matrix was *Pantydraco*, whereas *Massospondylus* was scored with states 0 and 1. For this taxon, state '0' was observed in the specimen SAM PK K1314 (Fig. 5.14a), whereas the specimen BP 1 5241 exhibits a deep subsellar recess, conforming to the morphology of state '1'. Thus, although the recess is not as developed as the subsellar recess of some theropod taxa (Witmer, 1997), it is clear that a similar structure is also present and considerably developed in Sauropodomorpha, but was not mentioned in previous studies.
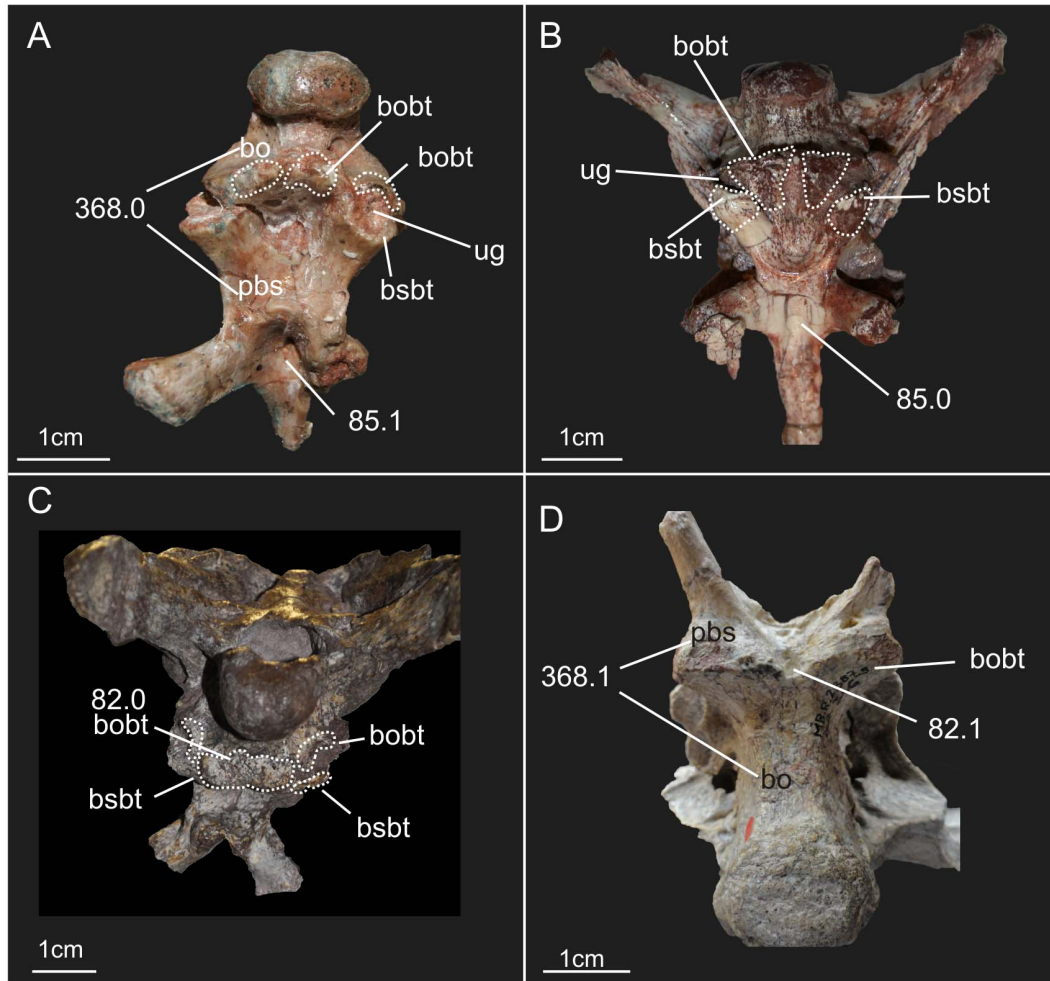
Figure 5.14: Braincases of four different sauropodomorphs illustrating the distinct morphologies associated with character states of characters 85, 82, and 368 (number after point indicates the respective character state). A – specimen UFSM 11069 of *Unaysaurus* (ventral view); B – specimen SAM-PK-K1314 of *Massospondylus* (ventral view); C – specimen SMNS 13200 of *Plateosaurus* (posteroventral view); D – specimen MB.R.2387.3, an indeterminate Sauropoda (posteroventral view – antero-posterior axis is inverted in relation to other braincases in the figures). Abbreviations: **bo** – basioccipital; **bobt** – basioccipital component of the basal tubera; **bsbt** – basisphenoidal component of the basal tubera; **pbs** – parabasisphenoid; **ug** – unossified gap.

*The anterior limit of the subsellar recess – **new character** (366 of this study)*

Here we propose a new character, related to the lamina (e.g. in the case of *Efraasia* and *Coloradisaurus*) or ridge (e.g. in the case of *Plateosaurus* and *Massospondylus*) that extends from the basipterygoid process onto the ventral surface of the cultriform

process of the parasphenoid. As detailed above in the description of the parabasisphenoid, the extension of these ridges on the cultriform process of the parasphenoid converge medially in some taxa, whereas in others, as in *Efraasia,* the extension of the ridges extend parallel to each other until they fade away into the cultriform process distally. When these ridges converge medially, the subsellar recess has a marked anterior end, which is triangular in shape in ventral view. When the ridges do not converge medially, the anterior limit of the subsellar recess is not well marked, with its ventral margin being confluent with the ventral margin of the cultriform process (Fig. 5.15).
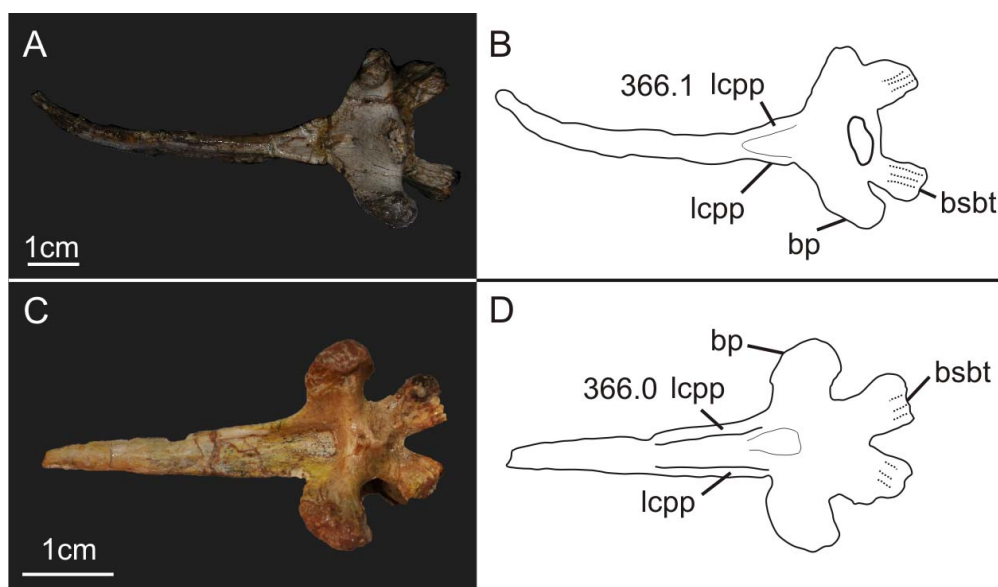
Figure 5.15: Ventral view of the parabasisphenoid of the specimens AMNH 6810 of *Plateosaurus engelhardti* (A and B) and PVSJ 568 of *Adeopapposaurus mognai* showing the two different morphologies associated with character states of character 366 (number after point indicates the respective character state) in sauropodomorphs. Abbreviations: **bp** – basipterygoid process; **bsbt** – basisphenoidal component of the basal tubera; **lcpp** – lamina on the cultriform process of the parabasisphenoid.

The new character (number 366 in the character list) is proposed as follows:

laminae/ridges extending from the basipterygoid process onto the parasphenoid

rostrum: *extend parallel untill they fade into the ventral margin of the cultriform process (0); converge anteromedially on the ventral surface of the cultriform process (1)*. Character state '0' is scored for e.g., *Efraasia,* and *Massospondylus*. Character state '1' is scored for e.g., *Plateosaurus*, and *Melanorosaurus* (undescribed specimen NM QR 1551 - Jay Nair, *pers. comm.*).

This character was only scored for nine of the OTUs within Sauropodomorpha in this study. Our results indicate two independent events of a modification from state '0' to '1', one in the branch leading to the clade including *Plateosaurus* and *Unaysaurus* (Plateosauridae) and the other at the branch leading to *Melanorosaurus*.

The relative position of the components of the basal tubera – Character 82 of this study and of Yates (2007b)

Romer (1956) defined the basal tubera as structures present in the region of the basisphenoid and basioccipital contact related to the attachment of hypaxial musculature, with the contribution of each bone varying among groups. More recently, Snively & Russell (2007) have shown that in the case of living archosaurs, the majority of the surface consisting of the occipital plate and the posterior region of the basisphenoid represent areas for the attachment of neck musculature (e.g. *m. rectus capitis ventralis, m. longissimus capitis*). It has long been recognised that the basal tubera of sauropodomorphs have a basioccipital and a parabasisphenoid component (see e.g. Yates, 2010), and the relative position of the basal tubera components of each one of the two bones was translated into a phylogenetic character for the group. Character 82 of Yates (2007b) was thus defined as: "shape of basal tuberae: knob-like, with basisphenoidal component rostral to basioccipital component

(0), or forming a transverse ridge, with the basisphenoidal component lateral to the basioccipital component (1)".

Problematic aspects of this character were identified in the course of our analyses of sauropodomorph braincase materials. The first is related to the morphology described by each of the character states. *Efraasia* (SMNS 12667) is scored in previous data matrices as having state '1', and matches the morphology described by the character state as possessing a transverse ridge (see Figs. 5.2, 5.4). However, in *Efraasia,* the transverse ridge is actually formed by the basioccipital component of the tubera only. In other taxa, such as *Coloradisaurus, Massospondylus* and *Melanorosaurus,* part of the basioccipital component is also medial to the basisphenoid components, but in these taxa the basioccipital components are not entirely connected to form a ridge (see e.g. Apaldetti *et al.,* 2014; and Fig. 5.14), but are separated by a shallow recess, which results in a knob-like aspect for the structure. It thus does not correspond to the ridge-like shape as described in character state '1'. On the other hand, in contrast to this discontinuous and knob-like appearance of the basal tubera in these forms, some neosauropods exhibit a laminar basioccipital component of the basal tubera. In these taxa, the basioccipital forms has a laminar aspect that connects to the posterolateral projections of the parabasisphenoid, where the tubera are located (Fig. 5.14 – see also Tschopp *et al.,* 2015). This laminar morphology of the basioccipital component of the basal tubera is also observed in other archosaurs (Gower, 2002; Nesbitt, 2011). Thus, even if the basioccipital component of the basal tubera is located posterior to the basisphenoidal one, we could not recognise a knob-like morphology as predicted by character state '0'. Removing the statement regarding the shape of the basioccipital component does not suffice, as this character has a second problematic aspect.

In the way the character is defined, it is implied that the basioccipital components of the basal tubera are either medially or posteriorly located in relation to the basisphenoid component, excluding a morphology in which both possibilities are present (Fig. 5.14). Yates (2010) already discussed that the basioccipital component is not entirely posteriorly or medially located in relation to the basisphenoid component, and recommended that the scoring for the character should be based on where the major portion of the former structure is positioned. However, Yates (2010) did not take into account the entire set of structures that together correspond to the basioccipital component of the basal tubera in some sauropodomorphs. Taxa such as *Adeopapposaurus, Melanorosaurus, Pantydraco, Plateosaurus,* and *Unaysaurus* exhibit multiple protuberances in the basioccipital that can be considered as different basioccipital components of the tubera when previous definitions of the term are applied (Romer, 1956; Snively & Russell, 2007). These taxa posses protuberances on the medial surface of the basioccipital, which are medially (or posteriorly) located in relation to the posterolateral projections of the parabasisphenoid that form the component of the tubera of this bone, and also protuberances located on the lateral surface of the basioccipital, posterior to the basisphenoid component of the tubera (Fig. 5.14). Therefore, it is not possible to establish which portion of the structure forms the majority of the basioccipital tubera, as suggested by Yates (2010).

After our survey of the literature (see *e.g.* Tschopp *et al.,* 2015), together with first-hand analysis of sauropod specimens, we could not recognise any sauropod taxa (if *Melanorosaurus* is not included in the group) that has part of the basioccipital component of the basal tubera (either a knob or a ridge-like structure) medially located in relation to the basisphenoidal component, as observed in non-sauropodan taxa, such as *Efraasia*. It is very likely that this was the variation intended to be

captured in character state '2' of character 84 of Yates (2007): "… with the basal tuberae being separated by a deep caudally opening U-shaped fossa" – see below. The left and right portion of the basal tuberae of sauropods correspond to two well defined anchorage surfaces for muscle attachments, either globular or box-like, as defined in Tschopp *et al*. (2015 – see character 82 of that study), that are separate by a U/V shaped fossa.

To incorporate this variation in the morphology of the basal tubera into information for the phylogenetic analysis focusing on non-eusauropodan sauropodomorphs, a modified version of character 82 is proposed as follows: *"Basioccipital component of the basal tubera, medial component in relation to the parabasisphenoidal components: present (0); absent (1)"*.

Our results indicate a single event within Sauropodomorpha in which a transformation from state '0' to state '1' occurred, at the branch leading to Sauropoda. It is here important to mention that the medial component of the basioccipital basal tubera is located posterior to the anterior projection of the bone treated in character 84 (see below). Thus, we consider both characters as independent.

The variation regarding the morphology of the basioccipital component of the basal tubera is probably related to differences in the neck musculature among taxa. Snively & Russell (1997) demonstrated differences in muscle numbers and their corresponding points of insertion in the braincases of birds and crocodiles. For the former, the authors indicate a single muscle inserting on the tuberosities of the basioccipital, the *m. rectus capitis ventralis,* also present in crocodiles. However, crocodiles have a second muscle that also inserts on basioccipital tuberosities, the *m. longissimus capitis*. It is beyond the scope of this work to provide any statement regarding the homology of the insertion areas of muscles in sauropodomorphs with

those of birds or crocodiles, but future studies might show that the variation seen in the development of the basal tubera in different groups of archosaurs might reflect differences in neck musculature.

*Junction of the parabasisphenoid and basioccipital – **new character** (84 of this study)*
Character 84 of Yates (2007b) was defined as: "ridge formed along the junction of the parabasisphenoid and the basioccipital, between the basal tuberae: present with a smooth rostral face (0), present with a median fossa on the rostral face (1), or absent with the basal tuberae being separated by a deep caudally opening U-shaped fossa (2)".

A first problem to be considered here is related to the character locator (*sensu* Sereno, 2007b) – *along the junction of the parabasisphenoid and basioccipital, between the basal tuberae*. The ventral surface of the parabasisphenoid of sauropodomorphs, such as *Efraasia, Pantydraco* and *Plateosaurus,* all coded as having a ridge along the junction between basioccipital and parabasisphenoid, has two posterolateral projections that form the basal tubera component of this bone at their distal ends (see Figs. 5.4, 5.14). In these taxa, the posterior margin of the parabasisphenoid has a "V/U" shape in ventral view (Fig. 5.16) and the basioccipital exhibits an median anterior projection, which forms the contact with the parabasisphenoid in this region (see basioccipital description). For these taxa, previously coded with '0' or '1' (see e.g. Yates, 2007b), no ridge was observed at the junction of the parabasisphenoid and the basioccipital, either in this region or laterally. Based on an examination of the scoring for this character in the data matrix of Yates (2007b), we suppose that what was possibly coded as a ridge is in fact part of the basioccipital portion of the tubera that is medially located in relation to the

basisphenoid component (see description of the basioccipital and Figs. 5.4, 5.16). All taxa scored with state '0' or '1' (ridge present) in character 84, are also scored with state "1" for character 82 (basioccipital component medially located; see discussion above). On the other hand, taxa scored as '2' (ridge absent) have state '0' for character 82 (basioccipital component posteriorly located). The only exception is *Pantydraco,* which was coded with state 0 for both characters. However, first hand analysis of the material showed that *Pantydraco* clearly has a part of the basioccipital component of the basal tubera medially located in relation to the basisphenoid tubera, and this component was probably regarded as a ridge. Further evidence that the basioccipital component of the basal tubera was treated as a ridge in the junction between the basioccipital and the parabasisphenoid is that early interpretations of the contact between these two bones assumed a linear contact at the level of the basal tubera (see e.g. Galton & Bakker, 1985 - fig. 4).

Given the problems detailed here, we propose the exclusion of character 84 of (Yates, 2007b) and a new character 84 that accounts for the details of the junction between the parabasisphenoid and basioccipital (see Fig. 5.16). The character is thus proposed as follows: *basioccipital - parabasisphenoid junction on the ventral surface of the bones: straight line (0); U/V shaped (1).* We considered the morphology in which the anterior portion of the basioccipital projects anteriorly between two posterolateral projections of the parabasisphenoid as U/V shaped – in this case, the posterolateral projections of the parabasisphenoid are separated from each other by a significant portion of the basioccipital. Character state '0' is scored for OTUs such as Neosauropoda. Character state '1' is scored for OTUs such as *Efraasia* and *Pantydraco*.
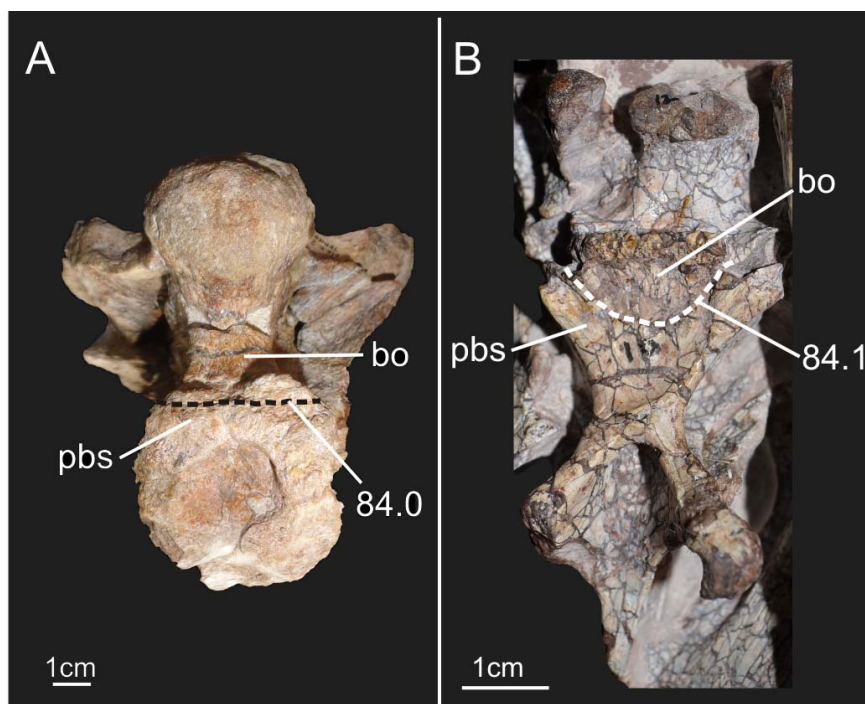
Figure 5.16: Ventral view of braincases of two specimens of sauropodomorphs illustrating the two different morphologies associated with character states of character 84 (number after point indicates the respective character state). A – specimen MB.R.2386 of the neosauropod *Tornieria;* B – specimen SMNS 12667 of *Efraasia*. The dashed lines mark the suture between the parabasisphenoid and basioccipital. Abbreviations: **bo** – basioccipital; **pbs** – parabasisphenoid.

The results of our analysis show that, in Sauropodomorpha, all non-sauropodan sauropodomorphs exhibit state '1', which is symplesiomorphic for these taxa (state '1' is found among other early dinosaurs and non-dinosaurian dinosauriforms, but the non-archosaurian archosauriform *Euparkeria* was treated as having state '0'). There was a single modification from state '1' to '0' within the sauropodomorph clade, which happened at the branch leading to Neosauropoda. Nevertheless, it is important to emphasize that we did not score the taxa *Spinophorosaurus*, *Mamenchisaurus* Young, 1954, and *Shunosaurus lii* Dong *et al.* 1983 in our analysis because we did not analyse the braincase materials first-hand, and the contact between the basioccipital and parabasisphenoid has not been described in detail for these taxa.

Thus, it is possible that the modifications in the contact between the parabasisphenoid and basioccipital happened earlier in the evolution of Sauropodomorpha.

The exit of the mid-cerebral vein in the lateral surface of the braincase – character 80 of this study and of Yates (2007b)

The mid-cerebral vein pierces the endocranial cavity on the lateral surface of the braincase and exits it through a foramen in the occiput (Galton, 1985; Sampson & Witmer, 2007). In sauropodomorphs, the foramen for the posterior exit of the mid-cerebral vein (sometimes called the external occipital vein; Sampson & Witmer, 2007) leaves the cavity on the occipital surface of the skull and can be enclosed solely by the supraoccipital or have its borders formed by the supraoccipital and parietal as discussed above. This difference in the exit route is used as a phylogenetic character (character 73 of Yates, 2007b). Likewise, the exit of the vein on the lateral surface of the braincase is also variable and has also been used as a phylogenetic character. Character 80 of Yates (2007b) has been stated as: "Exit of the mid-cerebral vein: through trigeminal foramen (0) or through a separate foramen anterodorsal to trigeminal foramen (1)".

This character was proposed by Rauhut (2003) in an analysis of the phylogenetic relationships of theropod dinosaurs. However, it is necessary to make a small modification to this character in the context of a phylogenetic analysis focusing on sauropodomorph dinosaurs. The problem with this character is related to the location of the foramen for the mid-cerebral vein as stated in character state '1'. In contrast to the description of this character state, in taxa such as *Efraasia* and *Plateosaurus* the separate (or partially separate) foramen for the mid-cerebral vein is located posterodorsal to the trigeminal foramen. However, the morphology of

Efraasia (Fig. 5.6) and *Plateosaurus* is not the only condition present among sauropodomorphs. *Shunosaurus* presents a separate foramen for the mid-cerebral vein that is located anterodorsal to the trigeminal foramen (Chatterjee & Zheng, 2002), as described by the character state originally.

Thus, we propose a subtle modification in the statement of character 80, with the modified version as follows: *Exit of the mid-cerebral vein: through trigeminal foramen (0) or through a separate foramen (1).* With this modification we intend to avoid misinterpretation in future studies while coding this character as the position of the separate for the mid-cerebral vein varies among taxa. Character state '0' is scored in e.g., *Coloradisaurus*, whereas character state '1' is scored for OTUs such as *Plateosaurus* and *Shunosaurus*.

In the context of our analysis, the only sauropodomorph to exhibit state '0' is *Coloradisaurus*.

*Orientation of the basipterygoid process – **new character** (367 of this study)*

The different orientations of the basipterygoid processes were used as character states of phylogenetic characters in previous studies of archosaurs and dinosaurs (e.g. Wilson, 2002; Nesbitt 2011; Butler *et al.*, 2008; Bittencourt *et al.*, 2014). Here we also propose to use this variation as a phylogenetic character in the context of non-eusauropodan sauropodomorphs. As detailed in the comparative description of the basipterygoid processes, there is some variation regarding their orientation in distinct sauropodomorph taxa. However, some considerations should be made in order to avoid confusion when coding this character.

Orienting the braincase can be difficult because it is not always the case that the braincase is found entirely preserved and associated with the rest of the skull. For

sauropodomorphs outside Sauropoda, one possibility might be to use the orientation of the foramen magnum as a landmark to determine the orientation of the braincase. In non-neosauropodan sauropodomorph taxa, the foramen magnum typically faces posteriorly when the braincase is seen in lateral view. However, among sauropodomorphs, a different condition is observed in taxa within the Neosauropoda clade, such as diplodocoids (Salgado, 1999), in which the foramen magnum faces posteroventrally. Thus, in order to make this character more adequate in the context of analysis of sauropodomorph taxa, we use the angle between the basipterygoid processes and the cultriform process of the parasphenoid as a proxy for this character. It is worth mentioning that Wilson (2002) used the angle between the basipterygoid processes in order to capture the variation in the orientation of these structures. Despite agreeing with the approach adopted in Wilson (2002), we decided to analyse the angle formed between the basipterygoid process and the cultriform process of the parabasisphenoid, because, as part of the parabasisphenoid, these structures are more commonly found in articulation than are the basipterygoid process and the skull roof (i.e. frontals and parietals). For example, SMNS 12667 has anteroventrally projected basipetrygoid processes, exhibiting an acute angle between these structures and the parasphenoid rostrum. On the other hand, *Plateosaurus* has ventrally/posteroventrally projected basipterygoid processes, and the angle between these structures and the cultriform process is obtuse.

New character (number 367 in the characters list) is thus proposed as follows: *angle between basipterygoid process and cultriform process of the parabasisphenoid: < 90 degress (0); 90 degress (1); > 90 degrees (2)*. Character state '0' is scored e.g. for *Efraasia*, state '1' is scored for e.g. *Thecodontosaurus,* and state '2' is scored for e.g. *Plateosaurus*.

Our analysis shows a transformation from state '0' to '1' in the branch leading to the clade including *Leyesaurus, Massospondylus,* and *Adeopapposaurus*. This represents further evidence that these taxa form a clade within Massospondylidae (e.g. Apaldetti *et al.,* 2014; Otero *et al.,* 2015). Tracing this character in the phylogeny shows that there are multiple transformations within Sauropodomorpha, but, as shown for the clade including *Leyesaurus, Massospondylus,* and *Adeopapposaurus,* this character may be important in establishing smaller sub-clades within Sauropodomorpha in future works.

*Relative length of the parabasisphenoid – **new character** (368 of this study)*

Sauropods exhibit an anteroposteriorly short parabasisphenoid in comparison to "prosauropod" taxa. The relative length of the parabasisphenoid was used as a phylogenetic character in other studies of archosaurs (char. 56 in Rauhut, 2003; char. 53 in Nesbitt 2011; and char. 51 in Bittencourt *et al.,* 2014). We took a different approach than that adopted in previous studies in order to quantify and translate this variation into a phylogenetic character. The new character (number 368 in the character list) is proposed as follows*: length of the parabasisphenoid (from the proximal limit of the basipterygoid process to the basisphenoidal component of the basal tubera) in relation to the length of the basioccipital (from the basioccipital component of the basal tubera to the posterior limit of the condyle): longer or equal (0); shorter (1)*. Character state '0' is scored for many non-sauropodan sauropodomorphs, such as *Efraasia, Plateosaurus,* and *Massospondylus,* whereas state '1' is scored for Neosauropoda (e.g. *Giraffatitan, Dicraeosaurus, Tornieria*).

As noted above, the parasphenoid and basisphenoid are fused in dinosaurs into a single element, the parabasisphenoid (Sampson & Witmer, 2007). Thus, we used the

basipterygoid processes as the markers of the anterior limit of the parabasisphenoid. Regarding the basioccipital, we decided to use the medial component of the basioccipital basal tubera in order to mark an anterior limit, as some taxa do not have the anterior triangular projection of the basioccipital described above. In taxa that do exhibit such a projection, the basioccipital component of the basal tubera is located in the posterior limit of it. Thus, the area posterior to the basal tubera is topologically congruent for taxa with or without the anterior projection.

Characters that are based on two structures that can vary might be problematic (see e.g. Simões *et al.*, 2016), but we believe that this ratio represents the notable reduction of the parabasisphenoid observed in Eusauropoda rather well. Indeed, state '1' is found only in members of Neosauropoda (represented by a single terminal taxon in this analysis), and *Spinophorosaurus*.

Notch in the posterodorsal margin in the lateral surface of the parabasisphenoid –
new character *(369 of this study)*

After first hand analysis of specimens of *Massospondylus* and *Adeopapposaurus*, we found that both taxa have a notch in the posterodorsal margin of the lateral portion of the parabasisphenoid, right below the fenestra ovalis in lateral view (Fig. 5.17; see also Martinez, 2009: fig. 10 C). Here we propose a new character related to the presence/absence of this notch in the parabasisphenoid (obs. despite recognising this notch, we did not find any indication of a soft-tissue structure that might be associated with it in the literature).

New character (number 369 in the list of characters) is proposed as follows: *"Notch in the posterodorsal margin of the lateral portion of the parabasisphenoid:*

absent (0); present (1). State '0' is scored for e.g. *Efraasia* and *Plateosaurus*, whereas state '1' is scored for *Adeopapposaurus* and *Massospondylus*.

The presence of the notch in the parabasisphenoid has only been observed in *Adeopapposaurus* and *Massospondylus*, and thus represents further evidence that these taxa form a clade within Massospondylidae. It is worth mentioning that the parabasisphenoid of *Leyesaurus* (a member of the clade containing *Massospondylus* and *Adeopapposaurus*) is incomplete, and this OTU was coded with '?' in our analysis.
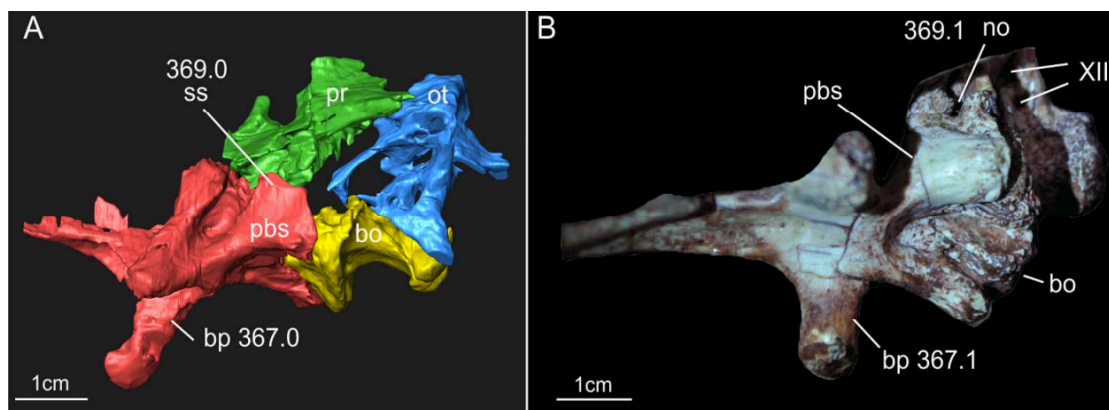
Figure 5.17: Lateroventral view of the braincases of the specimens SMNS – 12667 of *Efraasia minor* (A – virtual reconstruction) and SAM-PK-K1314 of *Massospondylus carinatus* illustrating different morphologies associated with character states of characters 367 and 369 (number after point indicates the respective character state). Abbreviations: **bo** – basioccipital; **bp** – basipterygoid process **no** – notch; **ot** – otoccipital; **pbs** – parabasisphenoid; **pr** – prootic; **ss** – smooth surface; **XII** – foramina for the hypoglossal nerve.

*Divided/undivided metotic fissure – **new character** (370 of this study)*

Following from the discussion of the subdivision of the metotic fissure presented above, we here propose a new character to account for this variation in sauropodomorphs. The new character (number 370 in the list of characters) is proposed as: "*Number of foramina in the otoccipital between the exoccipital pillar*

(excluding the foramina for the hypoglossal nerve) posteriorly and fenestra ovalis anteriorly: one (0), two (1)". Character state '0' is scored for e.g. *Plateosaurus*. Character state '1' is scored for *Efraasia*, among others.

The presence of two foramina in this region of the ottocipital is observed in all non-sauropodan sauropodomorph OTUs, except for *Plateosaurus*. Regarding *Thecodontosaurus*, Benton *et al*. (2000) report a morphology that would be similar to that in *Massospondylus* in Gow (1990) and *Plateosaurus* in Galton (1985). However, these taxa differ in morphology. The specimen of *Massospondylus* (BPI 1 5231) analysed by Gow (1990) has two foramina that correspond to the two foramina seen in *Efraasia*. Regarding *Plateosaurus*, there is only a sub-division in the metotic foramen of the specimens, with a smaller opening forming a notch at the posterodorsal edge of the metotic foramen (Galton, 1985; Prieto-Marquez & Norell, 2011). Thus, *Plateosaurus* is the only OTU belonging to Sauropodomorpha but not to Sauropoda that was scored with state '0' in our analysis.

Regarding sauropods, no evidence of the presence of two foramina is observed in the taxa for which information is available, including *Shunosaurus* (Chatterjee & Zheng, 2002), *Giraffatitan, Dicraeosaurus, Spinophorosaurus* (Knoll *et al*., 2012), *Apatosaurus* Marsh, 1877 (Balanoff *et al*., 2010), and an indeterminate titanosaurian (Sues et al. 2015). In the context of our analyses, a change to a condition of a single foramen in Sauropodomorpha happens at the branch leading to the clade containing *Shunosaurus* and Neosauropoda. However, stating the presence of a single foramen for the whole Neosauropoda clade may be misleading because, as neosauropods are not the focus of our study, we did not conduct an extensive review of all the braincase materials preserved in this clade (see Table 1).

*Presence/absence of an unossified gap – **new character** (371 of this study)*

New character (number 371 in the list of characters) is proposed as follows: "*Unossified gap between the basioccipital and basisphenoidal component of the basal tubera and ventral ramus of the opistothic: absent (0); present (1)*". Character state '0' is scored for OTUs such as Neosauropoda and *Saturnalia*. Character state '1' is scored for OTUs such as *Thecodontosaurus* and *Plateosaurus* (Fig. 5.12). Gower (2002) and Nesbitt (2011) already discussed the relation of the unossified gap and the cochlear recess. However, the character we proposed here does not deal with the morphology of this recess, but only with the presence and absence of the gap.

In our analysis, the only taxon within Sauropodomorpha but outside Sauropoda that exhibits state '0' is *Saturnalia*. All other sauropodomorph OTUs outside Sauropoda that we analysed first hand and that were scored for this character have an unossified gap between the basioccipital, parabasisphenoid, and otoccipital. In *Efraasia minor* it seems likely that such a gap was present (as pointed out by Galton & Bakker, 1985), although this cannot be said with certainty due to displacement of elements. In the left side of the braincase, for example, the gap between the basal tubera of the basisphenoid and the basioccipital is much bigger than that between the basioccipital and parabasisphenoid medially. Nevertheless, a secure statement requires material in which this region is better preserved. On the other hand, we did not find any evidence for the presence of such a gap in the sauropods analysed for this study.

Braincase evolution in Sauropodomorpha

For some of the phylogenetic characters related to the anatomy of the braincase, our results demonstrate that non-sauropodan sauropodomorphs exhibit a condition that is

distinct from that observed in sauropod taxa present in our analysis, namely: a basioccipital component of the basal tubera composed of multiple protuberances including a protuberance medially located in relation to the basisphenoidal component of the tubera, main body of the parabasisphenoid that is relatively longer than the basioccipital, the presence of two foramina in the otoccipital between the exoccipital pillar and the fenestra valis, the presence of an unossified gap, the U/V shape contact between parabasisphenoid and basiocipital, the presence of an unossified gap). Some of these characters (e.g. the proportion of the main body of the parabasisphenoid in comparison to the basioccipital; the type of contact between the basioccipital and the parabasisphenoid) represent the plesiomorphic condition and thus highlight that the anatomy of the Sauropoda is unique among Sauropodomorpha, and strongly deviates from the anatomy of taxa outside this clade. Others (e.g. the morphology of the basal tuberae, the presence of an unossified gap) are apomorphic when compared to sauropodomorph outgroups and might thus be seen as supporting the monophyly of the non-sauropodan sauropodomorphs. However, the paraphyletic array of these taxa is strongly supported by postcranial characters, which override the cranial similarities in the current analysis.

We conducted exploratory phylogenetic analyses in order to test the hypothesis of a monophyletic "Prosauropoda" using our dataset. One constrained analysis indicates that 66 additional steps are necessary in order to recover a monophyletic "Prosauropoda" including all the non-sauropodan sauropodomorphs of our analysis, similar to the arrangement found in Benton *et al*. (2000) and Galton & Upchurch (2004). On the other hand, only 20 additional steps are necessary to obtain a monophyletic "Prosauropoda" including the same taxa found within this clade in Barrett & Upchurch (2007), the "core prosauropods", which do not include taxa such

as *Saturnalia* and *Thecodontosaurus*. Thus, even with some braincase characters indicating the monophyly of all non-sauropodan sauropodomorphs, this scenario is much less unlikely than a scenario of a less inclusive "Prosauropoda", for which we found no additional evidence based on the braincase anatomy.

It is here worth discussing the results of our analysis in the context of the different definitions already proposed for Sauropoda. The first phylogenetic definition for Sauropoda based on results of a numerical analysis of a data matrix was presented by Salgado *et al.* (1997), which defined the group as the least inclusive clade including *Vulcanodon* Raath, 1972 and Eusauropoda. An additional definition was proposed by Yates (2007 – the definition adopted here), which defined Sauropoda as the least inclusive clade that includes *Saltasaurus loricatus* (Bonaparte & Powell, 1980) but not *Melanorosaurus readi*. In this context, our statement that most of the character states observed in sauropods differ from the character states of the non-sauropodan sauropodomorphs holds true when either the definition of Salgado *et al.* (1997) or the one of Yates (2007a) is applied (see Fig. 5.13). However, Wilson & Sereno (1998) also proposed a phylogenetic definition for Sauropoda, which consider the group as including all sauropodomorphs closer to *Saltasaurus* than to *Plateosaurus*. In the context of this definition, a series of transformations related to the characters discussed above would still happen within Sauropoda. However, the presence of taxa such as massospondylids and *Anchisaurus* in Sauropoda would indicate that some members of Sauropoda have braincase morphology mostly similar to the one of the non-sauropodan representatives. Nevertheless, one aspect of the definition of Wilson & Sereno (1998) should be taken into account. It was proposed at a time when some studies (e.g. Galton, 1990, Sereno, 1999) were finding support for a monophyletic "Prosauropoda" including plateosaurids and massospondylids.

However, in the context of the most recent analysis of sauropodomorphs, which shows that even the "core prosauropods" (including massospondylids) do not form a monophyletic group that excludes sauropods, the definition of Sauropoda proposed by Wilson & Sereno (1998) fell into disuse (see e.g. McPhee *et al.* 2015).

Finally, there is a lack of braincase materials and/or of detailed descriptions (the only exception being *Spinophorosaurus*) of this structure in taxa more closely related to Neosauropoda than to *Melanorosaurus* (here considered as the sister group of Sauropoda). This hampers the reconstruction of the character transformations at the base of Sauropoda at the moment. Thus, only with the description and/or discovery of additional braincase materials will it be possible to achieve a detailed scenario of the anatomical transformations in the braincase anatomy of taxa within Sauropoda (i.e. if the anatomical modifications happened at the branch leading to Sauropoda or in less inclusive subclades of this clade).

5.6. CONCLUSIONS

Braincase anatomy still plays a minor role in descriptive works of sauropodomorphs, with this structure usually being much less detailed than other parts of the skull or postcranium. Here we supplement the original work of Galton & Bakker (1985) on the braincase of *Efraasia minor*, and carry out a comparative description in order to illustrate morphological variation in sauropodomorphs.

The usually short description of the braincase probably also had an impact on the use of characters related to this complex structure formed by multiple elements in phylogenetic analyses, and may have led to the problematic aspects of the characters used in previous analysis discussed above. For example, the braincase (including

frontals and parietals, elements that are also part of the skull roof) was only represented by 13 characters out of 365 in the matrix of McPhee et al. (2015). In this study, we propose seven new characters related to the anatomy of the braincase. We further highlight some issues that we consider as problematic when coding phylogenetic characters related to braincase anatomy in a data matrix for Sauropodomorpha. Setting aside the problems with the term in general and the distinction between characters and character states (see Forey & Kitching, 2000), phylogenetic characters represents our translation of the observable morphological variation into the basic units of a cladistic analysis (Freudenstein, 2005). As our explanation of the evolutionary history of a group or even only single morphological traits is based on a phylogenetic hypothesis, proper definition of the phylogenetic characters is crucial, as our hypothesis ultimately rely on these characters (Rieppel & Kearney, 2007; Simões et al., 2016). Trying to clarify the criteria used when formulating these fundamental units is a way of avoiding problems of interpretations that can cause, for example, conflicts in coding or inability to recognize the transformation series proposed for such a character. With this contribution, we therefore intend to clarify aspects of phylogenetic characters related to the anatomy of braincase in sauropodomorphs as an attempt to minimize differences in interpretations in future studies. Nevertheless, our points and suggestions are not definitive, and will certainly be subject to changes in future studies that provide more data on this complex structure.

Finally, our study indicates that the braincase anatomy of sauropods is a result of modifications that happened within this clade, or along the branch directly leading to it. This contrasts with the evolution of other parts of the organisms. As mentioned above, it has been demonstrated that the peculiar anatomy of sauropods is

a result of modifications that took place earlier in the evolutionary history of Sauropodomorpha. In this case, two factors need to be taken into account. One is the current inability to translate existent transitional morphologies in the braincase anatomy among "prosauropod" lineages into phylogenetic characters. Another factor is the relatively small number of non-sauropodan sauropodiformes with braincases preserved or described.

5.8. REFERENCES

Apaldetti C, Martinez RN, Alcober OA, Pol D. 2011. A New Basal Sauropodomorph (Dinosauria: Saurischia) from Quebrada del Barro Formation (Marayes-El Carrizal Basin), Northwestern Argentina. *PLoS ONE* 6 (11): e26964.

Apaldetti C, Pol D, Yates A. 2012. The postcranial anatomy of *Coloradisaurus brevis* (Dinosauria: Sauropodomorpha) from the late Triassic of Argentina and its phylogenetic implications. *Palaeontology* 56(2): 277–301.

Apaldetti C, Martinez RN, Pol D, Souter T. 2014. Redescription of the skull of *Coloradisaurus brevis* (Dinosauria, Sauropodomorpha) from the Late Triassic Los Colorados Formation of the Ischigualasto-Villa Union Basin, Northwestern Argentina. *Journal of Vertebrate Paleontology* 34(5): 1113–1132.

Bakker RT, Williams M, Currie PJ. 1988. *Nanotyrannus*, a new genus of pygmy tyrannosaur, from the latest Cretaceous of Montana. *Hunteria* 1: 1–30.

Balanoff AM, Bever GS, Ikejiri T. 2010. The braincase of *Apatosaurus* (Dinosauria: Sauropoda) based on computed tomography of a new specimen with comments on variation and evolution in Sauropod Neuroanatomy. *American Museum Novitates* 3677: 1–29.

Barrett PM. 2009. A new basal sauropodomorph dinosaur from the Upper Elliot Formation (Lower Jurassic) of South Africa. *Journal of Vertebrate Paleontology* 29(4): 1032-1045.

Barrett PM, Upchurch P. 2007. The evolution of feeding mechanisms in early sauropodomorph dinosaurs. *Special Papers in Palaeontology* 77: 91–112.

Baumel JJ. 1993. Systema Cardiovasculare. In: Baumel JJ, King AS, Breazile JE, Evans HE, Berge JVC, eds. *Handbook of Avian Anatomy: Nomina Anatomica Avium*, 2nd edition. Publications of the Nuttall Ornithological Club 23, pp. 407 – 475.

Bellairs AA, Kamal AM. 1981. The chondrocranium and the development of the skull in recent reptiles. In: Gans C, ed. *Biology of the Reptilia. vol. 11, Morphology F*. New York: Academic Press, 1–263.

Benton MJ, Juul L, Storrs GW, Galton PM. 2000. Anatomy and systematics of the prosauropod dinosaur Thecodontosaurus antiquus from the Late Triassic of Southwest England. *Journal of Vertebrate Paleontology* 20: 77–108.

Bever GS, Brusatte SL, Carr TD, Xu X, Balanoff AM, Norell MA. 2013. The braincase anatomy of the Late Cretaceous dinosaur Alioramus (Theropoda: Tyrannosauroidea). *Bulletin of the American Museum of Natural History* 376:1–72.

Bittencourt JS, Arcucci AB, Marsicano CA, Langer MC. 2014. Osteology of the Middle Triassic archosaur Lewisuchus admixtus Romer (Chañares Formation, Argentina), its inclusivity, and relationships amongst early dinosauromorphs. Journal of Systematic Palaeontology 13(3): 189–219.

Bonaparte JF. 1967. Dos nuevas "faunas" de reptiels triásicos de Argentina. *Ameghiniana* 10(1): 89–102.

Bonaparte JF. 1978. *Coloradia brevis* n. g. et n. sp. (Saurischia–Prosauropoda), dinosaurio Plateosauridae de la Formacion Los Colorados, Triasico Superior de La Rioja, Argentina. *Ameghiniana*. 15 (3–4): 327–332.

Bonaparte JF, Powell JE. 1980. A continental assemblage of tetrapods from the Upper Cretaceous beds of El Brete, northwestern Argentina (Sauropoda-Coelurosauria-Carnosauria-Aves). *Mémoires de la Société Géologique de France, Nouvelle Série* 139: 19–28.

Bonnan MF, Senter P. 2007. Were the basal sauropodomorph dinosaurs *Plateosaurus* and *Massospondylus* habitual quadrupeds? In: Barrett PM, Batten DJ, eds. *Evolution and palaeobiology of early sauropodomorph dinosaurs. Special Papers in Palaeontology*, 77. pp. 139–135.

Broom R. 1913. Note on Mesosuchus Browni, Watson, and on a new South African Triassic pseudosuchian (*Euparkeria capensis*). *Records of the Albany Museum* 2: S394–396.

Brusatte SL, Benton MJ, Desojo JB, Langer MC. 2010. The higher-level phylogeny of Archosauria (Tetrapoda: Diapsida). *Journal of Systematic Palaeontology*. 8(1): 3–47.

Butler RJ, Upchurch P, Norman DB. 2008. The phylogeny of ornithischian dinosaurs. *Journal of Systematic Palaeontology* 6(1): 1–40.

Cabreira SF, Kellner AWA, Dias-da-Silva S, Silva LR, Bronzati M, Marsola JCA, Müller RT, Bittencourt JS, Batista BJ, Raugust T, Carrilho R, Brodt A, Langer MC. In press. A unique Late Triassic dinosauromorph assemblage reveals dinosaur ancestral anatomy and diet. *Current Biology*

Carrano MT, Benson RBJ, Sampson SD. 2012. The phylogeny of Tetanurae (Dinosauria:Theropoda). *Journal of Systematic Paleontology* 10(2): 211-230.

Chatterjee S. 1985. *Postosuchus*, a new Thecodontian reptile from the Triassic of Texas and the origin of Tyrannosaurs. *Philosophical Transactions of the Royal Society of London, Series B, Biological Sciences* 309 (1139): 395–460.

Chatterjee S, Zheng Z. 2002. Cranial anatomy of *Shunosaurus*, a basal sauropod dinosaur from the Middle Jurassic of China. *Zoological Journal of the Linnean Society* 136: 145–169.

Chure DJ, Madsen JH Jr. 1996. Variation in aspects of the tympanic pneumatic system in a population of *Allosaurus fragilis* from the Morrison Formation (Upper Jurassic). *Journal of Vertebrate Paleontology* 16: 573–577.

Chure DJ, Madsen JH Jr. 1998. An unusual braincase (? *Stokesosaurus clevelandi*) from the Cleveland-Lloyd Dinosaur Quarry, Utah (Morrison Formation; Late Jurassic). *Journal of Vertebrate Paleontology* 18: 115–125.

Crompton AW, Charig AJ. 1962. A new ornithischian from the Upper Triassic of South Africa. *Nature* 196: 1074–1077.

Currie PJ. 1997. Braincase anatomy. In: Currie PJ, Padian K, eds. *Encyclopedia of dinosaurs*. San Diego: Academic Press, pp. 81–85.

Currie PJ, Zhao X-J. 1993. A new troodontid (Dinosauria, Theropoda) braincase from the Dinosaur Park Formation (Campanian) of Alberta. *Canadian Journal of Earth Sciences* 30(10): 2231-2247.

Depéret C. 1896. Note sur les Dinosauriens Sauropodes et Théropodes du Crétacé supérieur de Madagascar. *Bulletin de la Société Géologique de France* 21: 176–194.

Dong Z, Zhou S, Zhang Y. 1983. Dinosaurs from the Jurassic of Sichuan. *Palaeontologica Sinica, New Series C* 162(23): 1–136.

Dzik J. 2003. A beaked herbivorous archosaur with dinosaur affinities from the early Late Triassic of Poland. *Journal of Vertebrate Paleontology* 23: 556–574.

Evans DC, Reisz RR, Dupuls K. 2007. A juvenile *Parasaurolophus* (Ornithischia: Hadrosauridae) braincase from Dinosaur Provincial Park, Alberta, with comments on crest ontogeny in the genus. *Journal of Vertebrate Palaeontology* 27(3): 642–650.

Evans DC, Bavington R, Campione NE. 2009. An unusual hadrosaurid braincase from the Dinosaur Park Formation and the biostratigraphy of *Parasaurolophus* (Ornithischia: Lambeosaurinae) from southern Alberta. *Canadian Journal of Earth Sciences* 46(11): 791–800.

Ezcurra MD. 2010. A new early dinosaur (Saurischia: Sauropodomorpha) from the Late Triassic of Argentina: a reassessment of dinosaur origin and phylogeny. *Journal of Systematic Palaeontology* 8(3): 371-425.

Fedak TJ, Galton PM 2007. New information on the braincase and skull of *Anchisaurus polyzelus* (Lower Jurassic, Connecticut, USA; Saurischia: Sauropodomorpha): implications for sauropodomorph systematics. In: Barrett PM, Batten DJ, eds. *Evolution and palaeobiology of early sauropodomorph dinosaurs*. *Special Papers* in *Palaeontology*, 77. pp. 245–260.

Fraas E. 1908. Dinosaurierfunde in Ostafrika. *Jahreshefte des Vereins für Vaterländische Naturkunde in Württemberg* 64: 84-86

Fraas E. 1913. Die neusten Dinoraurierfunde der schwäbischen Trias. *Die Naturwissenchaften I,* 45: 1097-1100.

Forey P, Kitching I. 2000. Experiments in coding multistate characters. In: Scotland RW, Pennington RT, eds. *Homology and systematics: coding characters for phylogenetic analysis*. London: Taylor & Francis, 54–80.

Freudenstein JV. 2005. Characters, States and Homology. *Systematic Biology* 54: 965–973.

Galton PM. 1973. On the anatomy and relationships of *Efraasia diagnostic* (Huene) n.gen., a prosauropod dinosaur (Reptilia: Saurischia) from the Upper Triassic of Germany. *Paläontologische Zeitschrift* 47: 229–255.

Galton PM. 1984. Cranial anatomy of the prosauropod dinosaur *Plateosaurus* from the Knollenmergel (Middle Keuper, Upper Triassic) of Germany. I. Two complete skulls from Trossingen/Württ, with comments on the diet. *Geologica et Palaeontologica* 18: 139–171.

Galton PM. 1985. Cranial anatomy of the prosauropod dinosaur *Sellosaurus gracilis* from the Middle Stubensandstein (Upper Triassic) of Nördwürttemberg, West Germany. *Stuttgarter Beiträge zur Naturkunde B* 116: 1–29.

Galton PM, Bakker RT. 1985. The cranial anatomy of the prosauropod dinosaur "*Efraasia diagnostica*", a juvenile individual of *Sellosaurus gracilis* from the Upper Triassic of Nordwürttemberg, West Germany. *Stuttgarter Beiträge zur Naturkunde B* 117: 1–15

Galton PM, Kermack D. 2010. The anatomy of *Pantydraco caducus*, a very basal sauropodomorph dinosaur trom the Rhaetian (Upper Triassic) of South Wales, UK. *Revue de Paléobiologie* 29(2): 341-404.

Galton PM, Upchurch P. 2004. Prosauropoda. In: Weishampel DB, Dodson P, Osmólska H, eds. *The Dinosauria, second edition*. Berkley: University of California Pres. pp. 232–258

Galton PM, Yates AM, Kermack DM. 2007. *Pantydraco* n. gen. for *Thecodontosaurus caducus* Yates, 2003, a basal sauropodomorph dinosaur from the Upper Triassic or Lower Jurassic of South Wales, UK. *Neues Jahrbuch für Geologie und Paläontologie Abhandlungen* 243(1): 119–125

Goloboff PA, Farris JS, Nixon KC. 2008. TNT, a free program for phylogenetic analysis. *Cladistics* 24: 1–13.

Goloboff PA, Szumik CA. 2015. Identifying unstable taxa: Efficient implementation of triplet-based measures of stability, and comparison with Phyutility and RogueNaRok. *Molecular Phylogenetics and Evolution* 88: 93-104.

Gow CE. 1990. Morphology and growth of the *Massospondylus* braincase (Dinosauria, Prosauropoda). *Paleontologia Africana* 27: 59–75.

Gower DJ. 1999. Cranial osteology of a new Rauisuchian Archosaur from the Middle Triassic of southern Germany. *Stuttgarter Beiträge zur Naturkunde B* 280: 1–9.

Gower DJ. 2002. Braincase evolution in suchian archosaurs (Reptilia: Diapsida): evidence from the rauisuchian *Batrachotomus kupferzellensis*. *Zoological Journal of the Linnean Society* 136: 49–76.

Gower DJ, Sennikov AG. 1996. Morphology and phylogenetic informativeness of early archosaur braincases. *Palaeontology* 39: 883–906.

Gower DJ, Nesbitt SJ. 2006. The braincase of *Arizonasaurus babbitti* – further evidence for the non-monophyly of "rauisuchian" archosaurs. *Journal of Vertebrate Paleontology* 26: 79–87.

Gower DJ, Weber E. 1998. The braincase of *Euparkeria*, and the evolutionary relationships of avialans and crocodilians. *Biological Reviews* 73: 367–411.

Haughton SH. 1924. The fauna and stratigraphy of the Stormberg Series. *Annals of the South African Museum* 12: 323–497

Hitchcock EJr. 1865. A supplement to the ichnology of New England. Boston: Wright and Potter, 90 p.

Hopson JA. 1979. Paleoneurology. In: Gans C, Northcut RG, Ulinski P, eds. *Biology of the Reptilia*. New York: Academic press. pp 39–146.

Hopson JA. 1980. Relative brain size in dinosaurs: implications for dinosaurian endothermy. In: Thomas RDK, Olson EC, eds. *A cold look at the warm blooded dinosaurs*. Washington, DC: American Association for the Advancement of Science. pp. 287–210

Huene F von. 1908. Die Dinosaurier der europäischen Triasformation, mit Berücksichtigung der ausser–europäischen Vorkomnisse (part). *Geologie und Paläontologie Abhandlungen* 6(1, suppl.): 345–419.

Huene F von. 1932. Die fossile Reptil-Ordnung Saurischia, ihre Entwicklung und Geschichte. *Monographien zur Geologie und Paläontologie* 4: 1–361.

Janensch W. 1914. Übersicht über der Wirbeltierfauna der Tendaguru-Schichten nebst einer kurzen Charakterisierung der neu aufgeführten Arten von Sauropoden. *Archiv für Biontologie* 3(1): 81–110.

Janensch W. 1936. Uber Bahnen von Hirnvenen bei Saurischiern und Ornithischiern, sowie einigen anderen fossilien und rezenten Reptilien. *Palaeontologische Zeitschrift* 18:181–198.

Knoll F, Witmer LM, Ortega F, Ridgely RC, Schwarz-Wings D. 2012. The braincase of the basal Sauropod dinosaur *Spinophorosaurus* and 3D reconstructions of the cranial endocast and inner ear. *Plos One* 7(1): e30060.

Kurzanov SM. 1976. Brain-case structure in the carnosaur *Itemirus* N. gen. and some aspects of the cranial anatomy of dinosaurs. *Paleontological Journal* 1976: 361–369.

Langer MC, Abdala F, Richter M, Benton MJ. 1999. A sauropodomorph dinosaur from the Upper Triassic (Carnian) of southern Brazil. *Earth & Planetary Sciences* 329: 511–517.

Lautenschlager S, Rayfield EJ, Altangerel P, Zanno LE, Witmer LM. 2012 The Endocranial Anatomy of Therizinosauria and Its Implications for Sensory and Cognitive Function. *PLoS ONE*. 7(12): e52289.

Leal LA, Azevedo SAK, Kellner AAW, da Rosa AAS. 2004. A new early dinosaur (Sauropodomorpha) from the Caturrita Formation (Late Triassic), Paraná Basin, Brazil. *Zootaxa* 690: 1–24.

Madsen Jr JH, Welles SP. 2000. *Ceratosaurus* (Dinosauria, Theropoda), a revised osteology. *Utah Geological Survey Miscellaneous Publications* MP-00–2: 1–80.

Marsh, O.C. 1877. New order of extinct Reptilia (Stegosauria) from the Jurassic of the Rocky Mountains. *American Journal of Science* 14: 513–514.

Martinez RN. 2009. *Adeopapposaurus mognai*, gen. et sp. nov. (Dinosauria: Sauropodomorpha), with comments on adaptations of basal Sauropodomorpha. *Journal of Vertebrate Paleontology* 29: 142–164.

Martinez RN, Alcober OA. 2009. A Basal Sauropodomorph (Dinosauria: Saurischia) from the Ischigualasto Formation (Triassic, Carnian) and the Early Evolution of Sauropodomorpha. *PLoS ONE* 4(2): e4397.

Martinez RN, Apaldetti C, Pol D. 2012a. Basal Sauropodomorphs from the Ischigualasto Formation. *Journal of Vertebrate Paleontology* 32(suppl. 6): 51–69.

Martinez RN, Haro JA, Apaldetti C. 2012b. Braincase of *Panphagia protos* (Dinosauria, Sauropodomorpha). *Journal of Vertebrate Paleontology* 32(suppl. 1): 70–82.

McPhee BW, Yates AM, Choiniere JN, Abdala F. 2014. The complete anatomy and phylogenetic relationships of *Antetonitrus longiceps* (Sauropodiformes, Dinosauria): implications for the origins of Sauropoda. *Zoological Journal of the Linnean Society* 171: 151–205.

McPhee BW, Bonnan MF, Yates AM, Neveling J, Choiniere JN. 2015. A new basal sauropod from the pre-Toarcian Jurassic of South Africa: evidence of niche-partitioning at the sauropodomorph-sauropod boundary? *Scientific Reports* 5: 13224.

Meyer H von. 1837. Briefliche Mitteilung an Prof. Bronn über *Plateosaurus engelhardti*. *Neues Jahrbuch für Mineralogie, Geognosie, Geologie und Petrefakten-Kunde* 1837: 316.

Müller J, Tsuji LA. 2007. Impedance-matching hearing in Paleozoic reptiles: evidence of advanced sensory perception at an early stage of amniote evolution. *PLoS ONE* 2(9): e889.

Müller J, Sterly J, Anquetin J. 2011 Carotid circulation in amniotes and its implications for turtle relationships. *Neues Jahrbuch für Paläontologie-Abhandlungen* 261(3): 289–297.

Nesbitt SJ. 2011. The early evolution of archosaurs: relationships and the origin of the major clades. *Bulletin of the American Museum of Natural History* 352: 1–292.

O'Donoghue CH. 1920. The blood vascular system of the tuatara, Sphenodon punctatus. *Philosophical Transactions of the Royal Society of London Series, B* 210: 175–252.

Orliac MJ. 2009. The differentiation of bunodont Listriodontinae (Mammalia, Suidae) of Africa: new data from Kalodirr and Moruorot, Kenya. *Zoological Journal of the Linnean Society* 157: 653-678.

Otero A, Pol D. 2013. Postcranial anatomy and phylogenetic relationships of Mussaurus patagonicus (Dinosauria, Sauropodomorpha). *Journal of Vertebrate Paleontology* 33: 1138–1168.

Otero A, Krupandan E, Pol D, Chinsamy A, Choiniere J. 2015. A new basal sauropodiform from South Africa and the phylogenetic relationships of basal sauropodomorphs. *Zoological Journal of the Linnean Society* 174: 589–634.

Owen R. 1854. Descriptive catalogue of the Fossil organic remains of Reptilia and Pisces contained in the Museum of the Royal College of Surgeons of England. London: Taylor & Francis, 213 p.

Parrish JM. 2005. The origins of high browsing and the effects of phylogeny and scaling on neck length in sauropodomorphs. In: Carrano MT, Gaudin TJ, Blob RW, Wible JR, eds. *Amniote paleobiology: perspectives on the evolution of mammals, birds, and reptiles*. Chicago: University of Chicago Press. pp. 201–223.

Paulina-Carabajal A. 2011. The braincase anatomy of *Carnotaurus sastrei* (Theropoda, Abelisauridae) from the Upper Cretaceous of Patagonia. *Journal of Vertebrate Paleontology* 31(2): 378–386.

Paulina-Carabajal A, Carballido JL, Currie PJ. 2014. Braincase, neuroanatomy, and neck posture of *Amargasaurus cazaui* (Sauropoda, Dicraeosauridae) and its implications for understanding head posture in sauropods. *Journal of Vertebrate Palaeontology* 34(4): 870–882.

Pol D, Garrido A, Cerda IA. 2011. A new sauropodomorh dinosaur from the Early Jurassic of Patagonia and the origin and evolution of the Sauropod-type sacrum. *Plos ONE* 6(1): e14572

Pol D, Rauhut OWM, Lecuona A, Leardi JM, Xu X, Clark JM. 2013. A new fossil from the Jurassic of Patagonia reveals the early basicranial evolution and the origins of Crocodyliformes. *Biological Reviews* 88: 862–872.

Prieto-Márquez A, Norell MA. 2011. Redescription of a nearly complete skull of *Plateosaurus* (Dinosauria: Sauropodomorpha) from the Late Triassic of Trossingen (Germany). *American Museum Novitates* 3727: 1–58.

Raath MA. 1972. Fossil vertebrate studies in Rhodesia: a new dinosaur (Reptilia, Saurischia) from near the Triassic-Jurassic boundary. *Arnoldia* 5: 1– 4.

Rauhut OWM. 2003. The interrelationships and evolution of basal theropod dinosaurs. *Special Papers in Palaeontology* 69: 1–213.

Rauhut OWM. 2004. Braincase structure of the Middle Jurassic theropod dinosaur *Piatnitzkysaurus*. *Canadian Journal of Earth Sciences* 41: 1109–1122.

Rauhut OWM. 2014. New observations on the skull of *Archaeopteryx*. *Paläontologische Zeitschrift* 88(2): 211–221.

Rauhut OWM, Fechner R, Remes K, Moser K. 2011. How to get big in the Mesozoic: the evolution of the sauropodomorph body plan. In: Klein N, Remes K, Sander PM, eds. *Biology of the sauropod dinosaurs: understanding the life of giants*. Bloomington and Indianapolis, Indiana University Press. pp. 119–149.

Remes K, Ortega F, Fierro I, Joger U, Kosma R, Marín Ferrer JM. 2009. A New Basal Sauropod Dinosaur from the Middle Jurassic of Niger and the Early Evolution of Sauropoda. *PLoS ONE* 4(9): e6924.

Rieppel O. 1985. The recessus scalae tympani and its bearing on the classification of reptiles. Journal of Herpetology, 19(3): 373–384.

Rieppel O, Kearney M. 2007. The poverty of taxonomic characters. *Biology and Phylosophy* 22: 95113.

Riley H, Stutchbury S. 1836. A description of various fossil remains of three distinct saurian animals discovered in the autumn of 1834, in the Magnesian Conglomerate on Durdham Down, near Bristol. *Proceedings of the Geological Society of London* 2:397–399.

Romer AS. 1956. Osteology of the Reptiles. Chicago: University of Chicago Press Chicago, 772 p.

Rowe TB, Sues H-D, Reisz RR. 2011. Dispersal and diversity in the earliest North American sauropodomorph dinosaurs, with a description of a new taxon. *Proceedings of the Royal Society -B* 278: 1044–1053.

Salgado L. 1999. The macroevolution of the Diplodocimorpha (Dinosauria; Sauropoda): a developmental model. *Ameghiniana* 36: 203–216

Salgado L, Coria RA, Calvo JO. 1997. Evolution of titanosaurid sauropods. I. Phylogenetic analysis based on the postcranial evidence. *Ameghiniana* 34: 3–32.

Sampson SD, Witmer LM. 2007. Craniofacial anatomy of *Majungasaurus crenatissimus* (Theropoda: Abelisauridae) from the Late Cretaceous of Madagascar. *Journal of Vertebrate Paleontology* 27: 32–102.

Sereno PC. 1999. The evolution of dinosaurs. *Science* 284: 2137–2147.

Sereno PC. 2007a. Basal Sauropodomorpha: Historical and recent phylogenetic hypotheses, with comments on *Ammosaurus major* (Marsh, 1889). In: Barrett PM, Batten DJ, eds. *Evolution and palaeobiology of early sauropodomorph dinosaurs*. *Special Papers* in *Palaeontology*, 77. pp. 261–289.

Sereno PC. 2007b. Logical basis for morphological characters in phylogenetics. *Cladistics* 23: 565–587.

Sereno PC, Forster CA, Rogers RR, Moneta AM. 1993. Primitive dinosaur skeleton from Argentina and the early evolution of the Dinosauria. *Nature* 361: 64–66.

Sereno PC, Wilson JA, Witmer LM, Whitlock JA, Maga A, Ide O, Rowe T. 2007. Structural Extremes in a Cretaceous Dinosaur. *PLoS ONE* 2(11): e1230.

Sereno PC, Martinez RN, Alcober OA. 2012. Osteology of *Eoraptor lunensis* (Dinosauria, Sauropodomorpha). *Journal of Vertebrate Paleontology*. 32(suppl. 6): 83–179.

Simões TR, Caldwell MW, Palci A, Nydam Rl. 2016. Giant taxon-character matrices: quality of character constructions remains critical regardless of size. *Cladistics* 1-22 (published online).

Snively E, Russell AP. 2007. Functional morphology of neck musculature in the Tyrannosauridae (Dinosauria, Theropoda) as determined via a hierarchical inferential approach. *Zoological Journal of the Linnean Society*, 151: 759–808.

Sobral G. 2014. The evolutionary origins of Impedance-Matching hearing in Archosauria. Unplished PhD Thesis. Lebenswissenschaftlichen Fakultät der Humboldt–Universität zu Berlin. 245 p.

Sobral G, Hipsley CA, Müller J. 2012. Braincase redescription of Dysalotosaurus lettowvorbecki (Dinosauria, Ornithopoda) based on computed tomography. *Journal of Vertebrate Paleontology* 32:1090–1102.

Sobral G, Sookias RB, Bhullar B-AS, Smith R, Butler RJ, Müller J. 2016. New information on the braincase and inner ear of *Euparkeria capensis* Broom: implications or diapsid and archosaur evolution. *Royal Society Open Science*, 3:160072.

Sookias RB, Sennikov AG, Gower DJ, Butler RJ. 2014. The monophyly of Euparkeriidae (Reptilia: Archosauriformes) and the origins of Archosauria: a

revision of *Dorosuchus neoetus* from the Mid-Triassic of Russia. *Palaeontology* 57(6): 1177–1202.

Sues H-D, Averianov A, Ridgely RR, Witmer LM. 2015. Titanosauria (Dinosauria, Sauropoda) from the Upper Cretaceous (Turonian) Bissekty Formation of Uzbekistan. *Journal of Vertebrate Paleontology* e889145.

Upchurch P, Barrett PM. 2000. The evolution of sauropod feeding mechanisms. In: Sues H-D, ed. *Evolution of herbivory in terrestrial vertebrates: perspectives from the fossil record*. Cambridge: Cambridge University Press. pp 79-122.

Upchurch P, Barrett PM, Dodson P. 2004. Sauropoda. In: Weishampel DB, Dodson P, Osmolska H, eds. *The Dinosauria 2nd Edition*. Berkeley: University of California Press pp. 259–322.

Upchurch P, Barrett PM, Galton PM. 2007 A phylogenetic analysis of basal sauropodomorph relationships: implications for the origin of sauropod dinosaurs. In: Barrett PM, Batten DJ, eds. *Evolution and Palaeobiology of Early Sauropodomorph Dinosaurs*. *Special Papers in Palaeontology* 77. pp 57–90.

Virchow H. 1919. Atlas und Epistropheus bei den Schildkröten. *Sitzungsberichte der Gesellschaft Naturforschender Freunde zu Berlin*. 1919(8): 303–332.

Walker AD. 1990. A revision of Sphenosuchus acutus Haughton, a crocodylomorph reptile from the Elliott Formation (Late Triassic or Early Jurassic) of South Africa. *Philosophical Transactions of the Royal Society of London B* 330: 1–120.

Wilkinson M. 1995. A comparison of two methods of character construction. *Cladistics* 11: 297–308.

Wilson JA. 2005. Overview of sauropod phylogeny and evolution. In Curry Rogers KA, Wilson JA, eds. *The Sauropods: Evolution and Paleobiology*, Berkeley: University of California Press. pp. 15–49.

Witmer LM. 1997. Craniofacial air sinus systems. In: Currie PJ, Padian K, eds. *Encyclopedia of dinosaurs*. San Diego, California: Academic Press. pp. 151–159.

Witmer LM, Ridgely RC. 2009. New Insights Into the brain, braincase, and ear region of Tyrannosaurs (Dinosauria, Theropoda), with implications for sensory organization and behaviour. *The Anatomical Record* 292:1266–1296.

Witmer LM, Ridgely RC. 2010. The Cleveland tyrannosaur skull (Nanotyrannus or Tyrannosaurus): new findings based on CT scanning, with special reference to the braincase. *Kirtlandia* 57: 61–81.

Yates AM. 2003. The species taxonomy of the sauropodomorph dinosaurs from the Löwenstein Formation (Norian, Late Triassic) of Germany. *Palaeontology* 46(2): 317–337.

Yates AM. 2004. *Anchisaurus polyzelus* (Hitchcock): The smallest known sauropod dinosaur and the evolution of gigantism amongst sauropodomorph dinosaurs. *Postilla* 230: 1–58.

Yates AM. 2007a. Solving a dinosaurian puzzle: the identity of *Aliwalia rex* Galton. *Historical Biology* 19(1): 93–123.

Yates AM. 2007b. The first complete skull of the Triassic dinosaur M*elanorosaurus* Haughton (Sauropodomorpha: Anchisauria). In: Barrett PM, Batten DJ, eds. *Evolution and Palaeobiology of Early Sauropodomorph Dinosaurs*. *Special Papers in Palaeontology* 77. pp 9–55.

Yates AM. 2010. A revision of the problematic sauropodomorph dinosaurs from Manchester, Connecticut and the status of *Anchisaurus* Marsh. *Palaeontology* 53(4): 739–752.

Yates AM, Kitching JW. 2003. The earliest known sauropod dinosaur and the first steps towards sauropod locomotion. *Proceedings of the Royal Society of London B* 270: 1753–1758.

Yates AM, Bonnan MF, Nevelling J, Chinsamy A, Blackbeard MG. 2010. A new transitional sauropodomorph dinosaur from the Early Jurassic of South Africa and the evolution of sauropod feeding and quadrupedalism. *Proceedings of the Royal Society of London B* 277: 787–794.

Young CC. 1954. On a new sauropod from Yiping, Szechuan, China. *Palaeontologia sinica* 4: 481–514.

CHAPTER 6

Rapid transformation in the braincase of sauropod dinosaurs: implications for the early evolution of gigantism

Authors: Mario Bronzati, Roger Benson, Oliver W. M. Rauhut[1,2]

Author contributions:

M.B. and R.B. conceptualized the study; **M.B.** segmented the CT-Scan data; **M.B.** compiled the data matrix; **M.B.** performed the phylogenetic analysis; R.B. performed the discrete character-taxon matrices analyses; **M.B., R.B.** and O.W.M.R. analysed the results; **All authors** wrote the manuscript.

Chapter 6

Rapid transformation in the braincase of sauropod dinosaurs: implications for the early evolution of gigantism

Mario Bronzati[1,2,*], Roger Benson[3], Oliver W. M. Rauhut[1,2]

[1] Bayerische Staatssammlung für Paläontologie und Geologie, Richard-Wagner-Straße 10, 80333 Munich, Germany.

[2] Ludwig-Maximilians-Universität, Richard-Wagner-Straße 10, 80333 Munich, Germany.

[3] University of Oxford, Department of Earth Sciences, South Parks Road, OX1 3AN, Oxford, United Kingdom.

6.1. Abstract

Sauropod dinosaurs were quadrupedal herbivores with a highly specialised body plan that attained the largest masses of any terrestrial vertebrates. Recent discoveries have shown that key traits associated with sauropods gigantism appeared in a stepwise fashion during the Late Triassic and Early Jurassic. Here, we investigate the evolutionary transformation of the sauropodomorph braincase using discrete anatomical characters, prompted by the reanalysis of a Middle Jurassic (Bathonian) sauropod braincase from England, the Oxford Braincase. Sauropod braincases are highly distinct, and occupy a different region of morphospace in relation to their evolutionary relatives. The shift in the morphology is in great part related to

transformations in areas corresponding to surface attachments of craniocervical musculature, and our data are so far an indicative of a linked evolution between neck elongation and transformation in the braincase anatomy. Furthermore, skull reduction in the Late Triassic and Middle Jurassic are associated with the moments of neck elongation, indicating that the 'head and neck' cascade of gigantism was activated more than once in the evolutionary history of Sauropodomorpha, and likely had an impact in the differential survival of sauropodomorph lineages in the Early-Middle Jurassic. The endocast of the Oxford Braincase also allows an investigation of the soft-tissues associated to the braincase. The endocast exhibit many similarities with the one of the close relative and contemporaneous *Spinophorosaurus*, such as the presence of a dural venous sinus of the hindbrain, the absence of a secondary tympanic membrane, and a flocculus of the cerebellum that does not project into the space between the semi-circular canals. The latter is likely a simplesiomorphy of sauropods, rather than a derived condition of the group. However, the lack of more quantitative data on the braincase of non-sauropodan sauropodomorphs still hampers a more detailed investigation regarding the transformations associated to the low encephalization quotients of sauropod dinosaurs.

6.2. Introduction

Sauropodomorphs are one of the three main dinosaur clades that likely diverged in the Middle Triassic (Lloyd *et al.*, 2016), but with oldest fossils known from Late Triassic (Carnian – c.230 Ma) rocks of South America (Langer *et al.*, 2010). They include Sauropoda, which originated in the Late Triassic (c. 210 Ma) or Early Jurassic (c. 180 Ma) and survived until the Cretaceous/Paleogene (c. 66 Ma) mass extinction (Wilson, 2005; McPhee et al. 2015). Sauropods were quadrupedal herbivores that exhibit a

characteristic body plan (Bates *et al.,* 2016) with an elongated neck and tail in combination with a reduced skull and typically gigantic size of c. 30 m in length and up to 90 tonnes (Mazetta et al. 2004; Benson et al. 2014). Furthermore, the neuroanatomy of sauropods also deviates from other dinosaurs, with sauropods exhibiting the lowest encephalization quotients among members of all dinosaurs (Hopson, 1977). In other words, sauropods had small brains. Even without the statistical support of modern approaches (e. g. Lloyd, 2016), it is clear that sauropod anatomy was highly distinct from that of earlier sauropodomorphs: the earliest sauropodomorphs were small (c. 1.5m in length and weighing less than 50 kg), probably bipedal and faunivorous/omnivorous (Langer et al. 2010; Cabreira *et al.,* 2016). Subsequent anatomical transformations occurred across the skeleton, in an apparently stepwise fashion as evidenced by the Late Triassic/Early Jurassic fossil record (e.g. Barrett & Upchurch 2007; Bonnan & Yates 2007; Yates et al 2010; Pol et al. 2011; McPhee et al. 2014, 2015; Otero et al. 2015). Ultimately, these structural changes were part of an evolutionary cascade that led to the evolution of gigantism, crucial for the evolutionary success of sauropods during the Jurassic and Cretaceous (Sander, 2013). A key question is whether these transformations occurred through the steady accumulation of anatomical changes at rates comparable to 'background' evolution, or whether they evolved rapidly compared to other changes involved in the origins of Sauropoda.

Here we explore the evolution of the braincase (including the posterior portion of the skull roof) of Sauropodomorpha. Although vertebrate braincases have sometimes been regarded as anatomically conservative, with more phylogenetic than functional signal (e.g. Gow 1975; Coria & Currie 2002; though see Gower & Sennikov 1996; Rauhut 2007), the braincase may in fact be under strong functional

constraints as it bears multiple sites for the attachment of craniocervical musculatures (Romer, 1956) and houses important soft tissues such as the brain and the inner ear (Witmer *et al.*, 2003). Our study is prompted by the reanalysis of a Middle Jurassic (Bathonian) braincase from England (OUMNH J13596 – hereafter Oxford braincase) based on CT-Scan data. The specimen has previously been assigned to Sauropoda, and tentatively referred to *Cetiosaurus* Owen, 1841 (Galton & Knoll, 2006). We support this identification using phylogenetic analysis, which shows that the Oxford braincase belonged to Sauropoda, and is thus among the oldest sauropod braincases known so far. The anatomical study of the Oxford Braincase alongside the phylogenetic analysis presented here backs up an investigation seeking patterns of morphological transformations and their evolutionary implications for the evolution of gigantism in Sauropodomorpha.

6.3. Material and Methods

(a) Systematic terminology

Here we follow the definitions proposed by Galton & Upchurch (2004) for Sauropodomorpha "all taxa more closely related to *Saltasaurus* than Theropoda", and the definition of Yates (2007b) for Sauropoda "all taxa more closely related to *Saltasaurus* than to *Melanorosaurus*".

(b) Virtual preparation of the Oxford Braincase

As reported by Galton & Knoll (2006), existing information on the OUMNH J13596 (Fig. 6.1) indicates that it most probably comes from the *"Cetiosaurus* quarries". These are located near Oxfordshire (England), and are part of the White Limestone Formation (*Procerites hodsoni* Ammonite Zone), which is Middle Jurassic (Upper

Bathonian – c. 168 Ma) in age (Palmer, 1979; Wyatt, 1997). OUMNH J13596 is a partially preserved braincase consisting of parts of the basioccipital and parabasisphenoid, parietals, laterosphenoids, prootics, supraoccipital and otoccipital. High resolution computed tomography was used to visualise the morphology of the braincase and internal cavities that housed associated soft tissues. Segmentation was conducted using the software Amira (version 6.0.1, Visage Imaging, Berlin, Germany).

(c) Phylogenetic analysis

To test the affinities of the Oxford braincase, we conducted a phylogenetic analysis using a modified version of the data matrix presented in Chapter 5; which consists of an expanded version of the dataset of Yates (2007a) and subsequent studies focusing on non-neosauropodan sauropodomorphs (e.g. McPhee *et al.*, 2014, 2015). Changes in the matrix (see ESM) of Chapter 4 comprise the addition of 4 new characters, and also the inclusion of Oxford braincase as an Operational Taxonomic Unit (OTU). The analysis was conducted in the software TNT (Goloboff et al. 2008) using an heuristic search with the following specifications: 5 000 replicates of Wagner Trees, hold 10, TBR (tree bi-section and reconnection) for branch swapping, and collapse of zero length branches according to "rule 1" of TNT.

(d) Discrete character-taxon matrix analysis

Principal co-ordinates analyses (PCoA) implemented in the R package Claddis (Lloyd, 2016) were used to investigate morphospace occupation and rates of evolution of the braincase anatomy of sauropodomorphs. Both analyses have a discrete character-taxon matrix as primary data, and the estimation of evolutionary

rates requires a phylogeny with branch lengths as a framework (reviewed by Lloyd, 2016). Characters used in these analyses consist only of those related to the braincase anatomy (29 out of the 379 in the matrix for the phylogenetic analysis – see ESM).

Our PCoA was conducted using the pairwise matrix of Gower distances for braincase characters between taxa in the matrix. To ameliorate problems of non-comparability, which occur when a pair of taxa have no characters scored other than missing data in common, we screened taxa for inclusion in the PCoA based on the presence of less than 50% missing data in total. In other words, only taxa with at least 50% of braincase character scored other than missing data were included in this analysis (27 taxa out of 59 in total).

Our evolutionary rates analyses were conducted across a subset of 100 MPTs recovered by our phylogenetic analysis, rather than on a single consensus topology. This allowed us to determine the influence of phylogenetic uncertainty on our results. We also added five neosauropod taxa of the Middle and Late Jurassic to the matrix in order to avoid the loss of information by representing a diverse clade as a single terminal taxon. To achieve this, we replaced the single terminal "Neosauropoda" in our set of MPTs with two alternative topologies of a clade of five taxa: (1) (*Jobaria* , ((*Camarasaurus supremus*, *Giraffatitan*), (*Tornieria*, *Dicraeosaurus sattleri*))); (2) ((*Jobaria*, (*Camarasaurus supremus*, *Giraffatitan*)), (*Tornieria*, *Dicraeosaurus sattleri*)). These two alternative topologies take into account the uncertainty regarding the position of *Jobaria* (e.g. Sereno *et al*., 1999; Upchurch *et al*., 2004; Sander *et al*., 2011), which is either found within Macronaria (here represented by *Camarasaurus supremus* and *Giraffatitan brancai*), or as the sister group of Neosauropoda, which includes Macronaria and Diplodocoidea (here represented by *Tornieria* and *Dicraeosaurus*).

Trees were time-scaled by enforcing a minimum branch length ('mbl') of 1 Ma using the timePaleoPhy() function of the R package paleotree (Bapst, date). We conducted two sets of analyses, one using the full set of MPTs, allowing a Late Triassic/Early Jurassic split of the Oxford Braincase from other sauropods. This is a very unlikely scenario because it implies hitherto undetected survival of a Triassic-diverging sauropodomorph lineage in the Middle Jurassic. Nevertheless, it cannot be ruled out based on character evidence because of the paucity of Triassic sauropodomorph braincases so far discovered. In the second set of analyses, we constrained the position the Oxford Braincase to belong to *Cetiosaurus* [(the only sauropod identified from the locality where the braincase comes from – Galton & Knoll, 2006)], and therefore to be nested in the less inclusive clade containing *Spinophorosaurus* and the eusauropods. This clade currently includes all Middle Jurassic and younger sauropodomorphs (see also Results 3b).

Evolutionary rates were estimated using the DiscreteCharacterRate() function of the R package Claddis (Lloyd date), including only those taxa for which at least 50% of braincase characters were scored, assessing the evolutionary rates for individual branches that attained p-values of 0.05 of lower.

6.4. Results

(a) Osteology and soft tissue anatomy of the Oxford braincase

The computed tomography data allowed us to produce a detailed virtual model of the braincase and associated cavities representing soft tissue structures (Fig. 6.1). These include the inner ear, cranial nerves, blood vessels, and parts of the brain. A more detailed osteological description has already been provided by Galton & Knoll

(2006), and only specific and novel aspects are discussed here. The parietals are anteroposteriorly short, and in dorsal view the supratemporal region of the skull is longer transversely than anteroposteriorly (Fig. 6.1). The same configuration is observed for the supratemporal fenestra, with a longer transversal axis. In dorsal view, the posterodorsal surface of the skull is horizontally aligned, an aspect given by the transverse orientation of the paroccipital process. This is the typical condition of sauropods, whereas non-sauropodan sauropodomorphs have a paroccipital processes that project posterolaterally (Galton, 1985; Yates, 2007a). We recognise no clear indication of a bony bar dividing the foramen in the otoccipital posterior to the fenestra ovalis and anterior to the hypoglossal nerve as hypothesized by Galton & Knoll (2006, figs. 3c,d). Thus, the aperture is here regarded as the metotic foramen (*sensu* Gower & Weber, 1998 – see discussion below). The otosphenoidal crest is configures as a low ridge, which has its posterodorsal limit located at the proximal portion of the paroccipital process, and the anteroventral limit at the anterodorsal portion of the parabasisphenoid. An otosphenoidal crest configured as a low-ridge is typical of non-sauropod sauropodomorphs (Chapter 5), whereas some sauropods, especially diplodocoids, exhibit a more pronounced crest with a posterolateral projection that obscures part of the fenestra ovalis in lateral view (Janensch, 1935; Tschopp *et al.*, 2015).

The positions of the cranial nerves (Fig. 6.1) follow the typical pattern observed in sauropods and other dinosaurs (see e.g. Witmer et al. 2008; Balanoff et al. 2010; Paulina-Carabajal, 2012; Knoll et al. 2012). The trigeminal nerve (cranial nerve V) exits the endocranial cavity through a foramen located anteroventral to the anterior semi-circular canal of the inner ear. Dorsal to the trigeminal foramen, an additional foramen corresponds to the ventrolateral exit of the mid-cerebral vein. Sauropods

typically exhibit independent formina for the vein and the trigeminal nerve in this region of the braincase (e.g. Balanoff *et al.,* 2010; Knoll *et al.,* 2012; Paulina-Carabajal, 2012). The mid-cerebral vein also has a dorsal component that exits the braincase at the level of the occipital plate of the skull (Sampson & Witmer, 2007), but it was only possible to reconstruct its anteroventral path on the lateral surface of the Oxford braincase (Fig. 6.1).
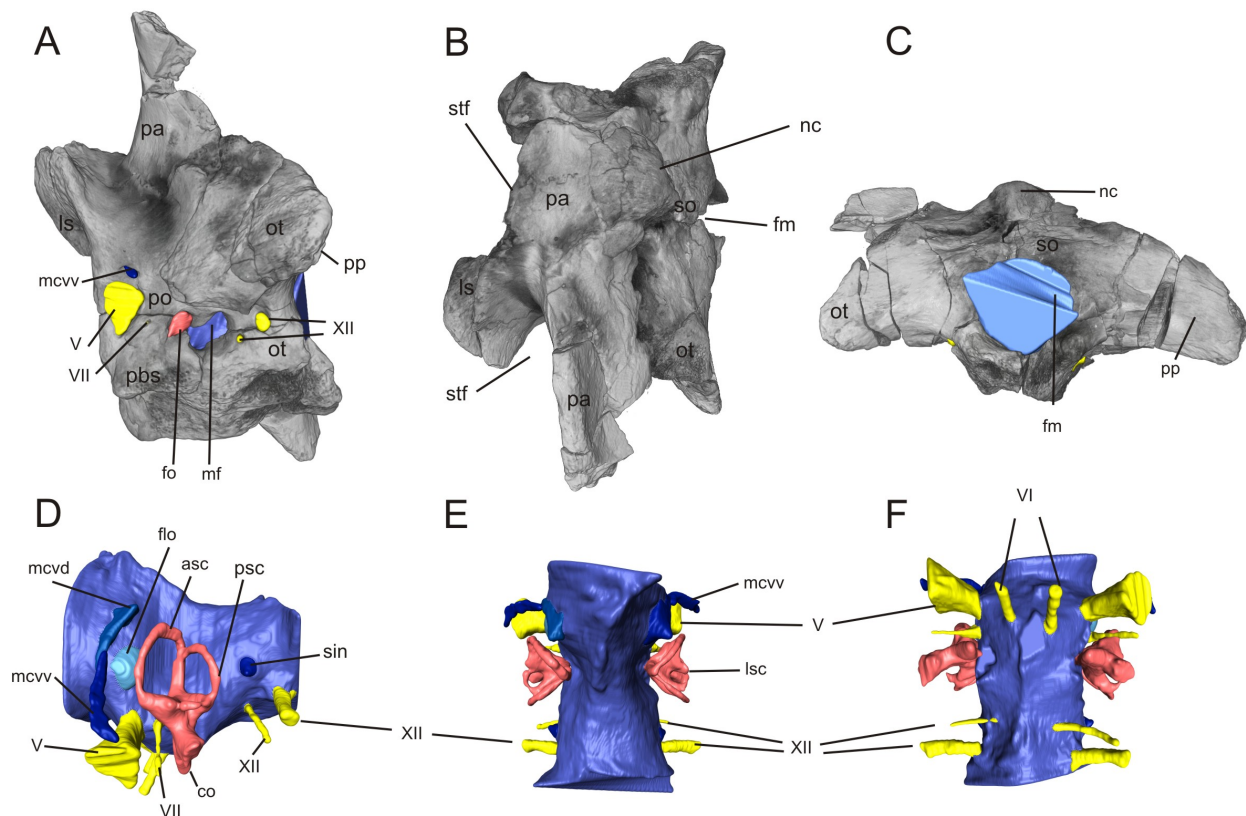
Figure 6.1: Braincase of the Oxford Braincase (OUMNH J13596) in left lateral (A), dorsal (B), and posterior (C) views. Segmented endocast of the Oxford Braincase in left lateral (C), dorsal (E), and ventral (F) views. Abbreviations: asc – anterior semi-circular canal of the inner ear; co – cochleae; flo – flocculus of the cerebellum; fm – foramen magnum; fo – fenestra ovalis; ls – laterosphenoid; lsc – lateral semi-circular canal of the inner ear; mcvd – dorsal ramus of the mid-cerebral vein; mcvv – ventral ramus of the mid-cerebral vein; mf – metotic foramen; nc – nuchal crest; ot – otoccipital; pa – parietal; pbs – parabasisphenoid; po – prootic; pp – paroccipital process; psc – posterior semi-circular canal of the inner ear; sin – dural sinus of the hindbrain; so – supraoccipital; stf – supratemporal fenestra; V – trigeminal nerve; VI – abducens nerve; VII – facial nerve; XII – hypoglossal nerve.

A low protuberance posterior to the point of confluence of the dorsal and ventral rami of the mid-cerebral vein is here identified as the floccular lobe of the cerebellum. As typical of sauropod dinosaurs (Witmer *et al.*, 2008; Paulina-Carabajal, 2012), in the Oxford Braincase this structure does not project into the space between the semi-circular canals of the inner ear. The facial nerve (VII) exits the brain posterior to the trigeminal foramen, and ventral to the anterior and lateral semi-circular canals of the inner ear. A pair of apertures in the anteroventral portion of the braincase, at approximately the same anteroposterior level of the opening for the facial nerve laterally, corresponds to the exits of the abducens nerve (VI). The hypoglossal nerve (XII) has two main branches that exit the braincase through separate apertures (Fig. 6.1). This condition is observed in all non-sauropod sauropodomorphs, and also reported for other Middle Jurassic sauropods such as *Spinophorosaurus* (Knoll *et al.*, 2012) and *Shunosaurus* (Chaterjee & Zheng, 2002). Differently, the presence of a single ramus for the hypoglossal nerve was reported for taxa such as *Diplodocus* (see Balanoff *et al.*, 2010) and *Amargasaurus* (Paulina-Carabajal *et al.*, 2014). Additionally, the presence of a third ramus of the hypoglossal has been hypothesized for *Apatosaurus* (Balanoff *et al.*, 2010). A protuberance on the posterior portion, dorsal to the hypoglossal nerves, of the endocast of the Oxford Braincase is here interpreted as the blind dural venous sinus of the hindbrain, which is topologically equivalent to the one reported for the Middle Jurassic neosauropod *Spinophorosaurus* (Knoll *et al.*, 2012).

The anterior semi-circular canal (ASC) of the inner ear has the greatest diameter of the three semi-circular canals, similar to the condition of other dinosaurs (see e.g. Witmer et al. 2008; Knoll et al. 2012; Lautenschlager *et al.*, 2012; Paulina-Carabajal *et al.*, 2016). The morphology of the ASC of the Oxford braincase (Fig. 6.1)

resembles that of *Spinophorosaurus* and *Giraffatitan*, with a maximum length that is approximately the same of the length of the vestibule of the inner ear. In contrast, *Nigersaurus* (Sereno *et al.*, 2011) has an ASC with a maximum length smaller than that of the vestibule, and taxa such as *Camarasaurus* and *Jainosaurus* have a more reduced ASC, with a total length of less than half of the length of the vestibule (see reconstructions in Knoll et al. 2012).

(b) Phylogenetic analysis

Our phylogenetic analysis (Fig. 6.2) indicates that the Oxford braincase is more closely related to Neosauropoda than to *Melanorosaurus*. Characters (see Appendix). Characters that support placement of the Oxford Braincase within this clade are: supratemporal fenestra with a transverse axis longer than the anteroposterior one (character 59), flat occiput in dorsal view (character 78), and the presence of an undivided metotic foramen (character 370). Additional braincase features that are common to all sauropods included in our analysis consist of: depth of the parietal wing greater than the depth of the foramen magnum (character. 72); a linear parabasisphenoid/basioccipital junction in the ventral surface of the braincase (character 84); lack of a medial component of the basioccipital basal tubera (character 82); basioccipital relatively longer than the parabasisphenoid (character 368); an undivided metotic foramen (character 370); the absence of an unossified gap between the basioccipital and basisphenoidal component of the basal tubera and ventral ramus of the opistothic (character 371). It is worth stressing out that distinct morphologies might be present in other Late Jurassic and Cretaceous sauropods, which exhibit great variation in the braincase anatomy (Tschopp *et al.*, 2015), but these are not captured by our phylogenetic analysis which focus on non-neosauropodan sauropodomorphs.
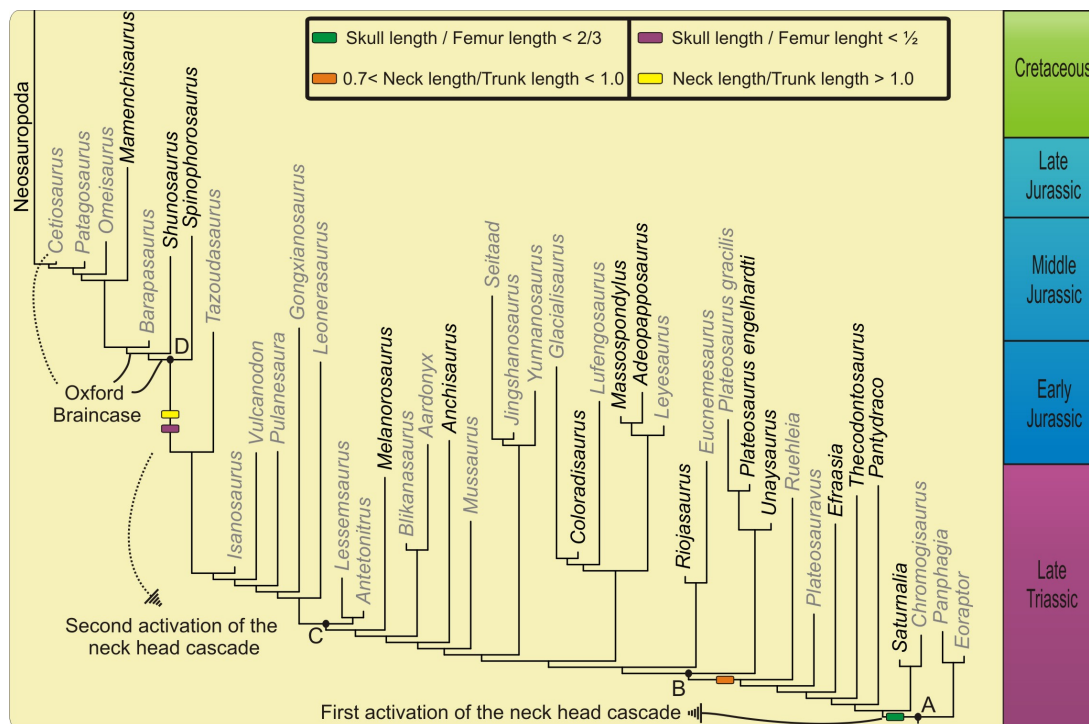
Figure 6.2: Reduced strict consensus tree of the phylogenetic analysis calibrated against geological time, and moments of the activation of the 'head and neck' cascade. Taxa with the name written in black correspond to those included in the discrete character-taxon matrices analyses.

The PCRPrune command of TNT (Goloboff & Szumik, 2015) was used to generate a reduced strict consensus tree depicting the alternative position of the unstable OTUs (Fig. 6.2). The Oxford Braincase is identified as one of the unstable OTUs of our analysis (see ESM). The different positions occupied by the Oxford Braincase in the MPT's are within the less inclusive clade including *Antetonitrus* and Neosauropoda, or as the sister group of this clade. In our topology, this clade is equivalent to Sauropoda as defined by Yates (2007b), which excludes *Melanorosaurus* of the group. It is worth stressing out one aspect of the multiple alternative positions of the Oxford Braincase recovered in the analysis in TNT. The

position of this OTU as the sister group or within the minimal clade defined by node C, which contains *Antetonitrus* and Neosauropoda, is supported by a set of morphological characters, as mentioned above. However, the alternative positions (see ESM) between nodes C and D (see Fig. 6.2) occur because taxa within this paraphyletic array lack braincase material preserved, so the distinct trees are equally optimal because all other taxa in this region of the tree are scored with missing data for braincase characters.

(c) Discrete character-taxon matrix analyses

In the principal coordinate analysis (Fig. 6.3), when the variation in PCo 1 (27,5%) is plotted against PCo2 (7,9%) and PCo3 (5,1%) it is possible to observe that the braincase of sauropods occupies a different region of the morphospace in relation to the one occupied by other sauropodomorphs and related sister groups, with no overlap between them.

Analyses of rates of character evolution using the full set of MPT's, without enforcing the position of the Oxford Braincase, return a fast rate of evolution of discrete characters in 59 out of the 100 trees. Of these, 34 (approximately 50%) found high rates leading to the clade including all the Middle Jurassic and younger sauropods (the minimal clade including *Spinophorosaurus* and neosauropods), but excluding the Oxford Braincase. Using the set of MPT's where the position of the Oxford Braincase was constrained as the one occupied by *Cetiosaurus* in the original phylogenetic analysis, a fast rate of evolution in the branch leading to the Middle Jurassic sauropods is recovered in 91 of the 100 trees (see ESM). The clade in this case corresponds to the minimal clade including *Spinophorosaurus* and Neosauropoda. Note that this second option (the Oxford braincase belongs to

Cetiosaurus) is much more likely than the first option (the Oxford braincase represents an early-diverging lineage from the Triassic) for reasons discussed above.
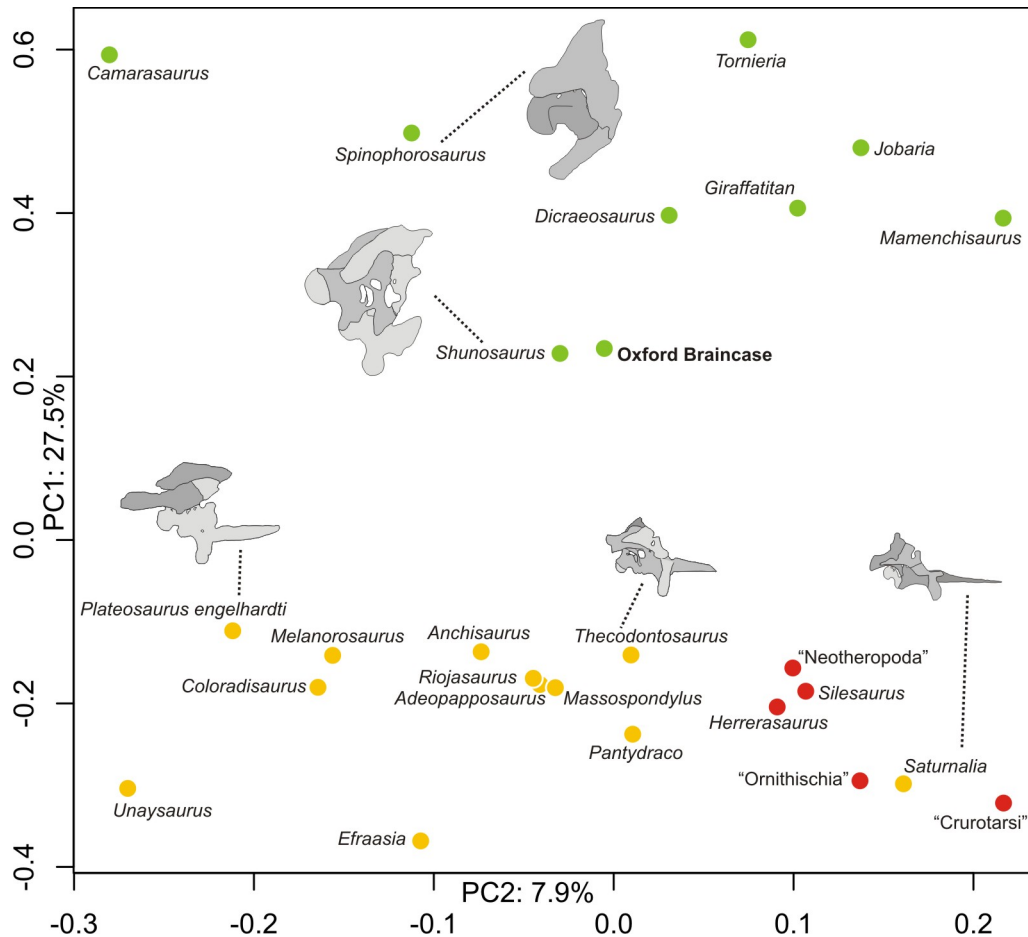
Figure 6.3: Results of the principal coordinate analysis with the variation in PCo 1 plotted against PCo2. Taxa with the name in yellow correspond to non-sauropodan sauropodomorphs, in green to sauropods, and in red to other archosaurs.

6.5. Discussion

(a) Braincase anatomy

In their description of the Oxford braincase, Galton & Knoll (2006) hypothesized the presence of a bony strut dividing the foramen here interpreted as the metotic foramen. If the metotic foramen was truly divided, it implies that the bony strut dividing it was broken on both sides (see Galton & Knoll, 2006). However, a bony strut is present in

non-sauropod sauropodomorphs such as *Massospondylus, Melanorosaurus, Efraasia* (e.g. Yates, 2007a; Chapter 5), which have braincases that are smaller and less robust than the Oxford Braincase. Thus a breakage on both sides of the Oxford specimen seems unlikely, especially because all the bony struts dividing other foramina are preserved on both sides, such as the one between the fenestra ovalis and the metotic foramen. Thus, our interpretation is that the Oxford Braincase has a single foramen, similar to the condition observed in early sauropods of the Middle Jurassic such as *Spinophorosaurus* (Knoll *et al*., 2012) and *Shunosaurus* (Chaterjee & Zheng, 2002). Differently, non-sauropodan sauropodomorphs, with the exception of *Plateosaurus* (see Prieto-Marquez & Norell, 2011), exhibit a pair of foramina (Chapter 5).

Briefly, there are two alternative hypotheses regarding the nature of the pair of foramina of non-sauropodan sauropodomorphs (Chapter 5; Balanoff *et al*., 2010). One possibility is that they represent the fenestra pseudorotunda (anterior opening), which is covered by a secondary tympanic membrane, and a vagal foramen (posterior opening) for the passage of the vagus nerve and possibly the posterior cephalic vein (e.g. Sampson & Witmer, 2007; Sobral et al. 2012). An alternative scenario is that there is no division of the metotic foramen and hence the formation of a secondary tympanic membrane (i.e. absence of a fenestra pseudorotunda). In this sense, there is a metotic foramen (anterior opening) and the additional foramen (posterior foramen) is the result of further ossification resulting in a separate opening for the posterior cephalic vein dorsally (Gower, 2002). If the latter is true, the presence of a single foramen in sauropods indicate that the posterior cephalic vein simply exited the braincase laterally, together with cranial nerve X; or, that the cephalic vein of sauropods possibly exited the braincase through the foramen magnum as reported for some lepidosaurs (Bellairs & Kamal, 1981), especially because of the small size of

the posterodorsal opening (Balanoff *et al*., 2010Chapter 5). However, if the former is true (i.e. the anterior foramen is homologous to the fenestra pseudorotunda of birds and crocodiles), it indicates that sauropods did not have a pressure relief window (Clack & Allin, 2004), the fenestra pseudorotunda (Gower & Weber, 1998). It is also worth mentioning that the additional foramen in *Apatosaurus* has been interpreted as the passage for a third ramus of the hypoglossal nerve (Balanoff *et al*., 2010), showing that the soft-tissue identification in sauropodomorphs is still a debatable topic.

(b) Rates of evolution in the braincase anatomy of sauropodomorphs

The recovery of a fast rate of evolution in c. 60% of the trees when the Oxford Braincase is not constrained in the position of *Cetiosaurus* is a moderate indicator of rapid transformation in braincase anatomy of Middle Jurassic sauropods. However, in this subset of MPT's, most trees recover the Oxford Braincase as the sister group of *Antetonitrus* + *Lessemsaurus*, the sister-group of the minimal clade including *Antetonitrus* and Neosauropoda, the sister-group of the minimal clade including *Leonerasaurus* and Neosauropoda. As mentioned above, this is a very unlikely scenario because this would imply a still undetected survival of a Triassic-diverging sauropodomorph lineage in the Middle Jurassic. Furthermore, in this configuration, optimization of braincase characters at the branch leading to the clade including Middle Jurassic sauropods is more ambiguous because of the high percentage of missing data for the Oxford Braincase. Only six of the thirteen characters undergoing transformation in the branches associated to the Middle Jurassic sauropods are scored for this taxon.

On the other hand, if the Oxford Braincase simply belongs to *Cetiosaurus*, a sauropod of which other bones are known from the same locality (Galton & Knoll 2006), character optimization at the branch leading to the clade of the Middle Jurassic sauropods is improved (i.e. fewer states are optimised ambiguously). In this configuration of the tree, *Spinophorosaurus* is the sister group of all the other sauropods (i.e. those with more than 50% of characters of braincase scored in the matrix), and nine of the thirteen characters undergoing transformation in the branches associated to the Middle Jurassic sauropods are scored for this taxon. In this arrangement, fast rates are recovered for the branching leading to these Middle Jurassic taxa in more than 90% of the tress. Accordingly, transformations in the braincase anatomy of sauropods are thus better understood as a result of a rapid evolution rather than transformations within the range of 'background' rates over a long time.

(c) Linked evolution of the neck and braincase in early sauropods

The complete shift in morphospace occupation (Fig. 6.3) indicated out by our PCoA analyses shows that braincase osteology of sauropods significantly differs from that of their non-sauropodan relatives. Furthermore, the transformations shaping the braincase of Middle Jurassic sauropods occurred at a fast rate when compared to background rates of evolution. Here we demonstrate that these results can be understood as part of major transformations of the craniocervical complex of sauropods, which are related to further neck elongation in the lineage.

Besides housing the brain and other sensory organs (Romer, 1976), the braincase also bears multiple attachment sites for muscles of the masticatory apparatus and of the craniocervical complex (Snively & Russell, 2007; Button et al.

2014, 2016). A series of transformations in the braincase anatomy detected by our analysis correspond to changes in the morphology of sites for the anchorage of neck muscles, with the majority of them occurring at the branch leading to the minimal clade including *Spinophorosaurus* and neosauropods (node D). These are: an increase in the depth of the occipital wing of the parietal (attachment surface of *m. splenius capitis*), change in the orientation of the paroccipital process of the otoccipital from a posterolateral to a lateral orientation in dorsal view (attachment surface of *m. longissimus capitis superficialis*), elongated basioccipital (attachment surface of *m. rectus capitis dorsalis, m. rectus capitis ventralis*), and, change from a U- or V-shaped to a linear contact of the basioccipital and the parabasisphenoid at the region of the basal tuberae (attachment surface of *m. rectus capitis dorsalis, m. rectus capitis ventralis*).

Sauropodomorphs possessing these characters states belong to the sauropod clade delimited by node D in (Fig. 6.2), which is the clade for which the fast rate of transformation in braincase anatomy was recovered. Those members of this clade that are known from more complete materials exhibit proportionally long necks in relation to their trunks (see Table 1). On the other hand, other sauropodomorphs have proportionally shorter necks, with a trunk that is longer than the neck (Rauhut *et al.*, 2011). Our findings are consistent with a scenario in which further elongation of the neck in sauropods not only involved a series of modification in vertebral morphology, such as pneumatisation and elongation (e.g. Wedel *et al.*, 2000; Wedel & Sanders, 2002; Wedel, 2005; Wedel, 2007), but was also accompanied by modifications in the anchor points of neck muscles in the braincase.

Support for this hypothesis is complicated because of difficulties constraining the precise timing of transformations of the sauropod braincase due to the paucity of

these elements. The lack of fairly complete specimens, or even the total absence of braincases and axial series, is the case for all sauropodomorphs between node C and D (see e.g. Pol & Powell, 2007; Pol *et al.*, 2011; McPhee *et al.*, 2014, 2015). Nevertheless, our observations so far are an indicative of a linked evolution of the elongated neck with transformation of the braincase in Middle Jurassic sauropods belonging to clade delimited by node D; but it is not yet possible to determine the directionality of the causal relation between changes to these anatomical compartments (elongation of the neck <–> modification in the region of neck musculature attachment in the braincase).

(d) Multiple activations of the 'head and neck' cascade

The gigantism of sauropod dinosaurs is related to a series of evolutionary cascades leading to an increase in body size; among them is the so-called "head and neck" cascade (Sander, 2013). As neck length is biomechanically constrained by skull size, the reduction of the skull in the Late Triassic has been considered as having reduced the moment of force exerted by the head on the neck (Rauhut *et al.* 2011). Indeed, the reduction of the skull (cranial length < 2/3 of femoral length) occurs at the branch leading to the minimal clade including *Saturnalia tupiniquim* and neosauropods, suggesting that this transformation took place in the Carnian (Late Triassic – c. 230 Ma; Langer *et al.*, 2010). The neck length of *S. tupiniquim,* with a cranial/femoral length ratio of c. 0.64, accounts for c. 0.55-0.60 of the trunk length. This represents just a slight elongation in the neck when compared with the possible sauropodomorph *Eoraptor lunensis* (neck length/trunk length – c. 0.50-0.55) also from the Carnian, which does not exhibit a reduced skull (cranial length/femoral length – c. 0.80). However, a more marked cervical elongation (neck/trunk length ratio > 0,7) is

recovered at the branch leading to the minimal clade including *Plateosaurus* and sauropods (node B). *Plateosaurus,* with a cranial/femoral length ratio of c. 0.57, has a trunk/neck ratio of c. 0.75 (Rauhut *et al.,* 2011). This increase in neck length in the Norian (the age of clade delimited by node B) is an indicator that the reduction of the skull in the Carnian triggered the "head and neck" cascade for the first time in Sauropodomorpha evolution. An increase in body-mass is also observed in the minimal clade including *Plateosaurus* and sauropods. Carnian representatives such as *Saturnalia* and *Eoraptor* are small and with a body mass not exceeding 50kg (Benson et al. 2014). On the other hand, *Plateosaurus* attained body masses of c. 910 kg (Benson et al. 2014), at least one order of magnitude bigger than its older counterparts. Yet, estimates for other non-sauropodan sauropodomorph indicate that these animals could attain body masses up to c. 2300 kg, as is the case of *Lufengosaurus* (Benson *et al*., 2014).

In spite of the neck elongation in the Late Triassic, the Middle Jurassic sauropods of the clade delimited by node D have necks that are proportionally much longer than those of other sauropodomorphs (Rauhut *et al*., 2011). Patterns of morphological transformation in the skull of sauropodomorphs are congruent with a further activation of the "head and neck" cascade in the Jurassic, but this time encompassing only sauropods (node D in Fig. 6.2). The Middle Jurassic taxa *Shunosaurus* and *Mamenchisaurus* have a cranial/femoral length ratio of 0,43 (Ouyang & Ye, 2002; Rauhut *et al*., 2011), and 0,35 (Zhang, 1988; Rauhut *et al*., 2011), respectively. In our phylogenetic analysis, this reduction can be linked to a change in the orientation of the longest axis of the supratemporal fenestra from a transversal to horizontal plane (character 59), also firstly detected in in the branch leading to the clade delimited by node D (this clade include *Spinophorosaurus*, but

the total length of the skull is not possible to be determined for this taxon). Furthermore, whereas *Shunosaurus* and *Mamenchisaurus* already exhibit necks longer than the trunks, all the other sauropodomorphs outside the clade delimited by node D known from more complete materials exhibit the inverse relation (Rauhut *et al.*, 2011). Increases in body mass predicted in the "head and neck" cascade are also observed. Body mass of *Shunosaurus* are estimated in c. 6300 kg and body mass estimations for different species of *Mamenchisaurus* range from c. 6200 kg to c. 18000 kg (Benson *et al.*, 2014). These values are greater than the maximal value of body mass estimated for a sauropodomorph outside clade delimited by node D, c. 5600 kg for *Antetonitrus* (Benson *et al.*, 2014). Yet, even if body mass inferior to the ones of *Antetonitrus* are estimated for taxa within clade D (e.g. neosauropods such as *Amargasaurus* and *Europasaurus*), the biggest mass values estimated among sauropods are for those with a neck longer than the trunk, such as *Brachiosaurus* and *Argentinosaurus* (see Benson *et al.*, 2014 for body mass estimates).

Finally, the Early-Middle Jurassic boundary (c. 175 Ma) is a key period in the evolution of Sauropodomorpha. Whereas non-sauropodan lineages disappeared by the end of the Early Jurassic/early Middle Jurassic, sauropodan lineages that originated in the late Early Jurassic/early Middle Jurassic remained as important component of terrestrial faunas until the Cretaceous/Paleogene (c. 66 Ma) mass extinction (Wilson. 2005). It has been argued that a longer neck provides greater access to food resources, and also diminishes the amount of energy spent during food intake (Sander, 2013). In this context, the reactivation of the 'head and neck' cascade encompassing only sauropods, and hence the presence of a longer neck in these animals, was probably one of the factors behind the differential survival of sauropodomorph lineages in the Jurassic, the time when non-sauropodan sauropodomorphs became extinct.

6.6. Conclusions

When transformations in the sauropodomorph lineage are traced in a cladogram (Fig. 6.2), it is possible to observe that a first moment of neck elongation in the Norian (clade B) was preceded by the skull reduction in the Carnian (clade A). However, no significant shift in the braincase anatomy could be detected at this period. On the other hand, our data indicates that the abrupt evolutionary shift (Figs. 6.2 and 6.3) in braincase anatomy happens concomitantly with further neck elongation (i.e. necks longer than the trunks), at the branch leading to the clade delimited by node D (Fig. 6.2). However, given the data for the braincase and axial series of the taxa within the array between nodes C and D (Fig. 6.2) so far available, it is not possible to determine the directionality of the causal relation between changes to these anatomical compartments.

The moments of neck elongation in sauropodomorph evolutionary history (i.e. activation of the 'head and neck' cascade) can be linked to reduction of the skull (Fig 6.2), indicating that the 'head and neck' cascade (Sander, 2013) was activated more than once during the evolution of Sauropodomorpha. Furthermore, the increase in body mass predicted by the cascade can also be detected at the branch leading to the clades where the anatomical transformations occur. As greater body mass increases the amount of energy obtained in the context of a fully herbivore diet and provide more protection against predators (Sander, 2013), independent activations of each of the multiple cascades of gigantism can potentially explain the difference in survival among sauropodomorph lineages during the history of the group; such as the disappearance of the non-sauropodan lineages in the Early-Middle Jurassic boundary.

Finally, if the transformations in braincase osteology of sauropodomorphs are now possible to be traced in relative detail, the same is not true for the soft-tissues

associated to this structure, which still suffers from the lack of more detailed analysis. One problem is the small number of taxa for which the endocast is known and/or have been described. Nevertheless, new data (Chapter 3) show that one of the most studied (but still not fully explained) transformations in the brain of sauropodomorphs, the reduction of the flocculus, preceded the origin of Sauropoda. This emphasize that tracing anatomical transformation in non-sauropodan lineages is crucial to understand the early evolution of the gigantic sauropods.

6.7. Acknowledgements

6.8. References

Balanoff AM, Bever GS, Ikejiri T. 2010. The braincase of *Apatosaurus* (Dinosauria: Sauropoda) based on computed tomography of a new specimen with comments on variation and evolution in Sauropod Neuroanatomy. *American Museum Novitates*. 3677, 1-29.

Barrett PM, Upchurch P. 2007. The evolution of feeding mechanisms in early sauropodomorph dinosaurs. *Special Papers in Palaeontology,* 77, 91–112.

Bates KT, Mannion PD, Falkingham PL, Brusatte SL, Hutchinson JR, Otero A, Sellers WI, Sullivan C, Stevens KA, Allen V. 2016. Temporal and phylogenetic evolution of the sauropod dinosaur body plan. *Royal Society Open Science,* 3, 15063

Bellairs AA, Kamal AM. 1981. The chondrocranium and the development of the skull in recent reptiles. In (ed. C Gans) *Biology of the Reptilia. vol. 11, Morphology F*. Academic Press, New York, pp. 1–263.

Benson RBJ, Campione NE, Carrano MT, Mannion PD, Sullivan C, Upchurch P, et al. 2014. Rates of Dinosaur Body Mass Evolution Indicate 170 Million Years of Sustained Ecological Innovation on the Avian Stem Lineage. *PLoS Biology*, 12(5), e1001853.

Bonnan MF, Yates AM. 2007. A new description of the forelimb of the basal sauropodomorph *Melanorosaurus*: implications for the evolution of pronation, manus shape and quadrupedalism in sauropod dinosaurs. *Special Papers in Palaeontology*, 77, 157-168.

Button DJ, Rayfield ER, Barrett PM. 2014. Cranial biomechanics underpins high sauropod diversity in resource-poor environments. *Proceedings of the Royal Society B*, 281, 20142114.

Button DJ, Barrett PM, Rayfield EJ. 2016. Comparative cranial myology and biomechanics of *Plateosaurus* and *Camarasaurus* and evolution of the sauropod feeding apparatus. *Palaeontology*, 59(6), 887-913.

Cabreira SF, Kellner AWA, Dias-da-Silva S, Silva LR, Bronzati M, Marsola JCA, Müller RT, Bittencourt JS, Batista BJ, Raugust T, Carrilho R, Brodt A, Langer MC. 2016. A unique Late Triassic dinosauromorph assemblage reveals dinosaur ancestral anatomy and diet. *Current Biology*, 26(22), 3090-3095.

Carballido JA, Salgado L, Pol D, Canudo JI, Garrido A. 2012. A new basal rebbachisaurid (Sauropoda, Diplodocoidea) from the Early Cretaceous of the Neuquén Basin; evolution and biogeography of the group. *Historical Biology*, 24(6), 631-654.

Chatterjee S, Zheng, Z. 2002. Cranial anatomy of *Shunosaurus*, a basal sauropod dinosaur from the Middle Jurassic of China. *Zoological Journal of the Linnean Society*, 136, 145-169.

Clack JA, Allin E. 2004. The Evolution of Single- and Multiple-Ossicle Ear in Fishes and Tetrapods. In (eds. GA Manley, AN Popper, RR Fay) *Evolution of the Vertebrate Auditory System*. Springer, New York, pp. 128-163.

Coria RR, Currie PJ. 2002. The braincase of *Giganotosaurus carolinii* (Dinosauria: Theropoda) from the Upper Cretaceous of Argentina. *Journal of Vertebrate Palaeontology*, 22(4), 802-811.

Galton PM, Knoll F. 2006. A saurischian dinosaur braincase from the Middle Jurassic (Bathonian) near Oxford, England: from the theropod *Megalosaurus* or the sauropod *Cetiosaurus*? *Geological Magazine*, 143, 905 – 921.

Goloboff PA, Farris JS, Nixon KC. 2008. TNT, a free program for phylogenetic analysis. *Cladistics*, 24, 1-13.

Goloboff PA, Szumik CA. 2015. Identifying unstable taxa: Efficient implementation of triplet-based measures of stability, and comparison with Phyutility and RogueNaRok. *Molecular Phylogeny and Evolution*, 88, 93-104.

Gow CE. 1975. The morphology and relationships of Youngina capensis Broom and *Prolacerta broomi* Parrington. *Palaeontologia Africana*, 18, 89-131.

Gower DJ. 2002. Braincase evolution in suchian archosaurs (Reptilia: Diapsida): evidence from the rauisuchian *Batrachotomus kupferzellensis*. *Zoological Journal of the Linnean Society,* 136, 49–76.

Gower DJ, Sennikov AG. 1996. Morphology and phylogenetic informativeness of early archosaur braincases. *Palaeontology,* 39(4), 883-906.

Gower DJ, Weber E. 1998. The braincase of *Euparkeria*, and the evolutionary relationships of avialans and crocodilians. *Biological Reviews*, 73, 367–411.

Janensch W. 1935. Die Schädel der Sauropoden *Brachiosaurus*, *Barosaurus* und *Dicraeosaurus* aus den Tendaguru-Schichten Deutsch-Ostafrikas. *Palaeontographica*, *Supplement* 7, 1(2),147-298.

Knoll F, Witmer LM, Ortega F, Ridgely RC, Schwarz-Wings D. 2012. The braincase of the basal Sauropod dinosaur *Spinophorosaurus* and 3D reconstructions of the cranial endocast and inner ear. *PlosOne*, 7(1), e30060.

Langer MC. 2003. The pelvic and hindlimb anatomy of the stem-sauropodomorph *Saturnalia tupiniquim* (Late Triassic, Brazil). *Paleobios*, 23, 1-40.

Langer MC, França MAG, Gabriel S. 2007. The pectoral girdle and forelimb anatomy of the stem-sauropodomorph *Saturnalia tupiniquim* (Upper Triassic, Brazil). *Special Papers in Palaeontology*, 77, 113-137.

Langer MC, Ezcurra MD, Bittencourt JS, Novas FE. 2010. The origin and early evolution of dinosaurs. *Biological Reviews,* 85, 55-110.

Lautenschlager S, Rayfield EJ, Altangerel P, Zanno LE, Witmer LM. 2012. The Endocranial Anatomy of Therizinosauria and Its Implications for Sensory and Cognitive Function. *PLoS ONE,* 7(12), e52289.

Lloyd GT. 2016. Estimating morphological diversity and tempo with discrete character-taxon matrices: implementation, challenges, progress, and future directions. *Biological Journals of the Linnean Society,* 118(1), 131-151.

Lloyd GT, Bapst DW, Friedman M, Davis KE. 2016. Probabilistic divergence time estimation without branch lengths: dating the origins of dinosaurs, avian flight and crown birds. *Biology Letters,* 12, 20160609.

Mazzetta GM, Christianssen P, Farina RA. 2004. Giants and bizarres: body size of some Southern American Cretaceous dinosaurs. *Historical Biology,* 16, 1-13.

McPhee BW, Yates AM, Choiniere JN, Abdala F. 2014. The complete anatomy and phylogenetic relationships of *Antetonitrus longiceps* (Sauropodiformes, Dinosauria): implications for the origins of Sauropoda. *Zoological Journal of the Linnean Society,* 171, 151-205.

McPhee BW, Bonnan MF, Yates AM, Neveling J, Choiniere JN. 2015. A new basal sauropod from the pre-Toarcian Jurassic of South Africa: evidence of niche-partitioning at the sauropodomorph-sauropod boundary?. *Scientific Reports,* 5, 13224.

Otero A, Krupandan E, Pol D, Chinsamy A, Choiniere J, 2015. A new basal sauropodiform from South Africa and the phylogenetic relationships of basal sauropodomorphs. *Zoological Journal of the Linnean Society,* 174 (3), 589–634.

Ouyang H, Ye Y. 2002. The First Mamenchisaurian Skeleton with Complete Skull, *Mamenchisaurus youngi.* Sichuan Science and Technology Press, Chengdu.

Palmer TJ. 1979. The Hampen Marly and White Limestone formations: Florida type carbonate lagoons in the Jurassic of central England. *Palaeontology,* 22, 189–228.

Paulina-Carabajal A. 2012. Neuroanatomy of titanosaurid dinosaurs from the Upper Cretaceous of Patagonia, with comments on endocranial variability within Sauropoda. *Anatomical Record,* 295(12), 2141-2156.

Paulina-Carabajal A, Carballido JL, Currie PJ. 2014. Braincase, neuroanatomy and neck posture of *Amargasaurus cazaui* (Sauropoda: Dicraeosauridae) and its implications for understanding head posture in sauropods. *Journal of Vertebrate Paleontology,* 34, 870–882.

Paulina-Carabajal A, Lee Y-N, Jacobs LL. 2016- Endocranial Morphology of the Primitive Nodosaurid Dinosaur *Pawpawsaurus campbelli* from the Early Cretaceous of North America. *PLoS ONE*, 11(3), e0150845.

Preuschoft H, Hohn B, Stoinski S, Witzel U. 2011. Why so huge? Biomechanical reasons for the acquisition of large size in sauropods and theropods. In (eds. N Klein, K Remes, CT Gee, PM Sander). *Biology of the sauropod dinosaurs: Understanding the life of giants.* Indiana University Press, Bloomington, pp. 197-218.

Prieto-Márquez A, Norell MA. 2011. Redescription of a nearly complete skull of *Plateosaurus* (Dinosauria: Sauropodomorpha) from the Late Triassic of Trossingen (Germany). *American Museum Novitates,* 3727, 1–58.

Pol D, Garrido A, Cerda IA. 2011. A new sauropodomorh dinosaur from the Early Jurassic of Patagonia and the origin and evolution of the Sauropod-type sacrum. *Plos ONE,* 6(1), e14572.

Pol D, Powell JE, 2007. New information on *Lessemsaurus sauropoides* (Dinosauria: Sauropodomorpha) from the Upper Triassic of Argentina. *Special Papers in Palaeontology,* 77, 223–243.

Rauhut OWM. 2007. The myth of the conservative character: braincase characters in theropod phylogenies. *Hallesches Jahrbuch für Geowissenschaften, Beiheft,* 23, 51-54.

Rauhut OWM, Fechner R, Remes K, Reis K. 2011. How to get big in the Mesozoic: the evolution of the sauropodomorph body plan. . In (eds. N Klein, K Remes, CT Gee, PM Sander). *Biology of the sauropod dinosaurs: Understanding the life of giants.* Indiana University Press, Bloomington, pp. 119-149.

Romer AS. 1956. Osteology of the Reptiles. University of Chicago Press, Chicago, 772 pp.

Salgado L, Coria RA, Calvo JO. (1997). Evolution of titanosaurid sauropods. I. Phylogenetic analysis based on the postcranial evidence. *Ameghiniana,* 34, 3–32.

Sampson SD, Witmer LM. 2007. Craniofacial anatomy of *Majungasaurus crenatissimus* (Theropoda: Abelisauridae) from the Late Cretaceous of Madagascar. *Journal of Vertebrate Paleontology,* 27, 32–102.

Sander PM. et al. 2011. Biology of the sauropod dinosaurs: the evolution of gigantism. *Biological Reviews*, 86, 117-155.

Sander PM. 2013. An Evolutionary Cascade Model for Sauropod Dinosaur Gigantism - Overview, Update and Tests. *PLoS ONE,* 8(10), e78573.

Sereno PC, Beck AL, Dutheil DB, Larsson HCE, Lyon GH,Moussa B, Sadleir RW, Sidor CA, Varricchio DJ, Wilson GP, Wilson JA. 1999. Cretaceous sauropods from the Sahara and the uneven rates of skeletal evolution among dinosaurs. *Science,* 286, 1342-1347.

Sereno PC, Wilson JA, Witmer LM, Whitlock JA, Maga A, Ide O, Rowe T. (2011) Structural extremes in a Cretaceous dinosaur. *PLoS One,* 2, e1230.

Snively E, Russell AP. 2007. Functional morphology of neck musculature in the Tyrannosauridae (Dinosauria, Theropoda) as determined via a hierarchical inferential approach. *Zoological Journal of the Linnean Society,* 151, 759–808.

Sobral G, Hipsley CA, Müller J. 2012. Braincase redescription of Dysalotosaurus lettowvorbecki (Dinosauria, Ornithopoda) based on computed tomography. *Journal of Vertebrate Paleontology,* 32, 1090–1102.

Tschopp E, Mateus O, Benson RBJ. 2015. A specimen-level phylogenetic analysis and taxonomic revision of Diplodocidae (Dinosauria, Sauropoda). *PeerJ,* 3, e857.

Upchurch P, Barrett PM, Dodson P. 2004. Sauropoda. In (eds. DB Weishampel, P Dodson, H Osmolska). *The Dinosauria (2nd Edition).* University of California Press, Berkely, pp. 259–322

Wedel MJ. 2005. Postcranial skeletal pneumaticity in sauropods and its implications for mass estimates. In (eds. JA Wilson, K Curry Rogers*) The sauropods: evolution and paleobiology.* University of California Press, Berkeley, pp. 201-228

Wedel MJ. 2007. What pneumaticity tells us about 'Prosauropods', and vice versa. *Special papers in Palaeontology,* 77, 207-222.

Wedel MJ, Sanders RK. 2002. Osteological correlates of cervical musculature in Aves and Sauropoda (Dinosauria: Saurischia), with comments on the cervical ribs of Apatosaurus. *PaleoBios,* 22(3), 1-6

Wedel MJ, Cifelli RL, Sanders RK. 2000b. Osteology, paleobiology, and relationships of the sauropod dinosaur Sauroposeidon. *Acta Palaeontologica Polonica,* 45, 343-388

Wilson JA. 2005. Overview of sauropod phylogeny and evolution. In (eds. JA Wilson, K Curry Rogers*) The sauropods: evolution and paleobiology.* University of California Press, Berkeley, pp. 15-49.

Witmer LM, Ridgely RC. 2009. New insights into brain, braincase, and ear region of tyranossaurs (Dinosauria: Theropoda), with implicaions for sensory organization and behaviour. *The Anatomical Record*, 292, 1266-1296.

Witmer LM, Ridgely RC, Dufeau DL, Semones MC. 2008. Using CT to peer into the past: 3D visualization of the brain and ear regions of birds, crocodiles, and nonavian dinosaurs. In (eds. H Endo, R Frey). *Anatomical imaging: towards a new morphology*. Springer-Verlag, Tokyo, pp. 67–87.

Witzel U, Preuschoft H. 2005. Finite-element model construction for the virtual synthesis of the skulls in vertebrates: case study of Diplodocus. *Anatomical Record*, 283, 391–401.

Wyatt RJ. 1997. A correlation of the Bathonian (Middle Jurassic) succession between Bath and Burford, and its relation to that near Oxford. *Proceedings of the Geologists' Association*, 107, 299-322.

Yates AM. 2007a. The first complete skull of the Triassic dinosaur *Melanorosaurus* Haughton (Sauropodomorpha: Anchisauria). *Special Papers in Palaeontology*, 77, 1-56.

Yates AM. 2007b. Solving a dinosaurian puzzle: the identity of *Aliwalia rex* Galton. *Historical Biology*, 1, 93-123.

Yates AM, Bonnan MF, Nevelling J, Chinsamy A, Blackbeard MG. 2010. A new transitional sauropodomorph dinosaur from the Early Jurassic of South Africa and the evolution of sauropod feeding and quadrupedalism. *Proceedings of the Royal Society of London B*, 277(1682), 787-794.

Zhang Y. 1988. The Middle Jurassic Dinosaur Fauna from Dashanpu, Zigong, Sichuan: Sauropod Dinosaurs. Vol. 1, Shunosaurus. Sichuan Publishing House of Science and Technology, Chengdu.

CHAPTER 7

Should the terms 'basal taxon' and 'transitional taxon' be extinguished from cladistic studies with extinct organisms?

Chapter re-submitted to *Palaeontologia Electronica* after the first round of peer-review as: Should the terms 'basal taxon' and 'transitional taxon' be extinguished from cladistic studies with extinct organisms?. Manuscript number: MS# 735.

Author contributions:

Research design: **Mario Bronzati.**

Mario Bronzati wrote the chapter.

<div align="right">

Chapter 7

</div>

Should the terms 'basal taxon' and 'transitional taxon' be extinguished from cladistic studies with extinct organisms?

Mario Bronzati

Bayerische Staatssammlung für Paläontologie und Geologie. Richard–Wagner–Str. 10, 80333, Munich, Germany.

Department of Earth and Enviromental Sciences, Ludwig–Maximilians–Universität, Richard–Wagner–Str. 10, 80333, Munich, Germany.

7.1. ABSTRACT

The terms basal and transitional have been widely adopted to designate the condition or nature of taxa in a phylogenetic context. Because they are taken as informative, some authors might even use these terms in an attempt to enhance the perceived value of a particular fossil discovery. Nevertheless, basal and transitional are most of the times erroneously or inconsistently applied, or are redundant to the arguments or quality of a scientific work and/or condition of taxa. In some cases, they can lead to the idea that the evolution of a lineage happened toward a specific group, in a mode of teleological reasoning. Here I illustrate problematic issues that can arise from this varied use of both terms. Finally, it is shown how statements that are in accordance with the cladistic method can substitute both terms in order to avoid pointless or misleading information.

7.2. PLAIN LANGUAGE SUMMARY

One of the main challenges of the scientific community is to adopt a consistent nomenclature that is congruent with the scientific method and at the same time also understandable for people outside the scientific community. When reporting the discovery of a new fossil, some scientists might attempt to use enhanced language in order to make their research more attractive to journals, and also externally for science communication activities, particularly regarding the mainstream media in which perceived attractiveness is a key factor in uptake and reporting of discoveries. However, there are cases on which the terminology employed for such reports is inconsistent with the theoretical basis of methods employed in the research. A special problem in the field of palaeontology is the adoption of specific terms that can confuse non-scientific readers in relation to the mechanisms of the evolutionary process, with potentially negative implications for public understanding of this research. Terms like 'basal taxon' and 'transitional form', widely adopted in the field of vertebrate palaeontology (Google Scholar found 2270 hits for "basal taxon", 141 for "transitional taxon", and 1980 "transitional form" & palaeontology – search on 06 March 2017), can be replaced by a language that avoids communicating information that is potentially misleading to non-specialists, and in a manner that is valid and consistent with the scientific method.

7.3. INTRODUCTION

The terms 'basal taxon/form' (e.g. Martinez et al., 2011; Sues et al., 2011; Xu et al., 2014) and 'transitional taxon/form' (e.g. Daeschler et al., 2006; Longrich et al., 2012; Pinheiro et al., 2016) have been widely adopted in cladistic studies in vertebrate palaeontology. These terms are taken as informative, and sometimes applied in an

attempt to increase the putative impact of research when communicating the importance of specimens or taxa. For example, "*Coniophis* therefore represents a transitional snake, combining a snake–like body and a lizard–like head" (Longrich et al., 2012); "new discoveries of transitional fossils such as *Tiktaalik* make the distinction between fish and the earliest tetrapods increasingly difficult to draw" (Daeschler et al., 2006); "*Teyujagua paradoxa*, transitional in morphology between archosauriforms and more primitive reptiles" (Pinheiro et al., 2016); "the result of analysis of that second matrix places *Chongmingia* as the most basal bird other than the iconic 'Urvogel' *Archaeopteryx* (Wang et al., 2016); "despite its basal position in early avian evolution, the advanced features of the pectoral girdle and the carpal trochlea of the carpometacarpus of *Jeholornis* indicate the capability of powerful flight" (Zhou and Zhang 2002); represent only some of several uses of the terms in order to tentatively capture the phylogenetic context of particular taxa. As such, it can be seen that these are often highly attractive expressions to journals and for broader science communication activities. However, their employment in the scientific literature appears to be inconsistent, and often applied with insufficient rationale.

'Tree thinking' has been much debated in the literature often regarding extant taxa (e.g. Krell and Cranston, 2004; Baum et al., 2005; Crisp and Cook, 2005; Omland et al., 2008: Zachos, 2016), but the lack of studies dealing with the question of extinct taxa might explain the persistence of incorrect terminology application in the field of palaeontology. Here, I use the example of the sauropodomorph dinosaurs to better illustrate how the terms 'basal' and 'transitional' have been variably applied in the field of vertebrate palaeontology. In this context, it is explained what taxa have been referred to as 'basal' sauropodomorphs and why they have often been called

'transitional' in this regard. Finally, it is discussed if the application of these terms makes sense in phylogenetic studies of other groups.

What are the so-called 'basal' sauropodomorphs?

Sauropodomorpha, one of the three main established dinosaur lineages (Langer et al., 2010), has a fossil record extending from the Late Triassic (Carnian) till the K/Pg mass extinction event. The earliest representatives (Carnian – c. 230 Ma) of Sauropodomorpha are probably bipedal (or facultatively bipedal), omnivorous and faunivorous (Cabreira et al., 2016), and small–bodied, not reaching more than 2 m in length (Langer et al., 2010). On the other hand, the sauropods are the largest terrestrial animals that have ever inhabited the Earth (Sander et al., 2011), and their long necks, quadrupedal stance and gigantic body size represents a very distinct morphological body plan in comparison to the earliest sauropodomorphs.

'Prosauropoda' was once thought to be a monophyletic group encompassing Late Triassic and Early to Middle Jurassic sauropodomorphs, and the sister group of Sauropoda (Galton and Upchurch 2004). However, more recent studies have pointed out that the most likely scenario concerning the evolution of the Sauropodomorpha lineage is that the classical 'prosauropods' represent a paraphyletic assemblage of taxa in relation to Sauropoda (see Peyre de Fabrègues et al., 2015 for historical discussion on this issue). This paraphyletic condition of 'Prosauropoda' is the root cause of the association of the term 'basal' sauropodomorph to refer to sauropodomorph taxa that fall outside of the main Sauropoda clade (Otero and Salgado, 2015). This is probably due to the consequential interpretation of non-sauropod sauropodomorphs as being closer to the root of Sauropodomorpha than sauropods.

'Basal sauropodomorphs' as transitional forms

The recognition of 'Prosauropoda' (i.e. 'basal sauropodomorphs') as paraphyletic in relation to sauropods triggered the idea that these taxa were therefore transitional forms with respect to the Sauropodomorpha lineage (Gauthier 1986). For instance, Sereno (1989) argued against this transitional view not because of problems related to the term itself (see the discussion in that study), but because the results of his analysis depicted 'Prosauropoda' as the sister–group of Sauropoda. This probably reflects the problem of visualising cladograms as ladders of progress (Zachos, 2016), and the use of transitional in these cases might be the result of something visual, but has no evolutionary significance. The resulting topologies of phylogenetic analyses are usually represented by ladderized (pectinate) trees (i.e. a tree which has the species–poor sister group always represented in the same side of a dichotomy). In the case of sauropodomorphs, the 'basal' sauropodomorphs are typically represented in the left/up side of the tree and taxa, and taxa nested within Sauropoda are presented on the right/down side of the tree (see Figure 7.1). Furthermore, discoveries of non-sauropodan sauropodomorphs exhibiting morphologies once thought to be exclusive of sauropods contributes to postulations that these animals are transitional between early sauropodomorphs from the Carnian and later sauropods (e.g. Yates et al., 2010; McPhee et al., 2015).
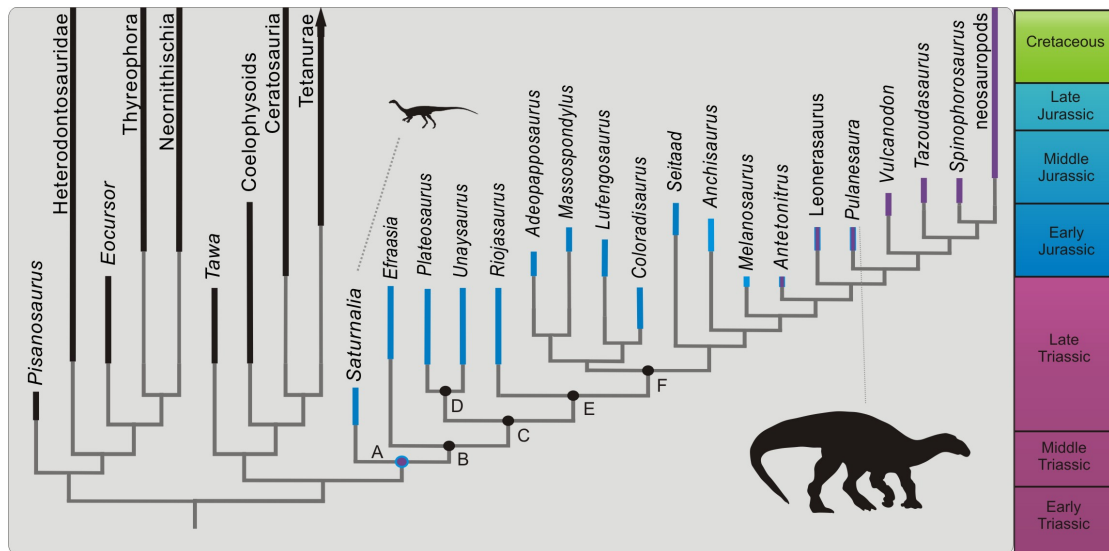
Figure 7.1: Simplified cladogram showing the relationships of the three main lineages of dinosaurs with focus on Sauropodomorpha. Letters A - E are related to clades treated in the main text. The assumed ages for the taxa of the tree are represented by rectangles thicker than other branches. Cladogenetic events (dichotomies) are not calibrated against geological time. Ornithischia is represented by the following taxa: *Pisanosaurus*, Heterodontosauridae, *Eocursor*, Thyreophora, Neornithischia. Theropoda is represented by the following taxa: *Tawa*, coelophysoids, Ceratosauria, Tetanurae. All other taxa represent Sauropodomorpha (here following the definition of Galton & Upchurch, 2004). Sauropoda (here following the definition of Salgado *et al.*, 1997) is represented by *Vulcanodon, Tazoudasaurus, Spinophorosaurus,* Neosauropoda.

7.4. DISCUSSION

Palaeontology and Neontology: where are the differences?

Previous neontological studies (Krell and Cranston, 2004; Crisp and Cook, 2005; Zachos, 2016) have emphasized that all OTUs of a cladogram containing solely living taxa are equally far away from the root, because they all co-exist in the same time. But what about the relationship between time and 'basal forms' in the context of a cladrogram that contains extinct taxa? The y-axis of a cladogram has time as a component (Hennig, 1965; Zachos 2016) once a root is assigned to it (Brower and de Pinna, 2012). In this way, using the phylogeny of Figure 7.1 it is correct to state that

the node A is 'closer' to the base than the node B, as it is older. It is also possible to state that the branches leading to nodes D and E originated at the same age. However, the taxa descending from the node A in both sides of the tree have specific ages assigned to them (note that these are the minimum ages; and that the minimum age can change if an older fossil referred to a particular taxon is found). In the specific case of *Saturnalia* and *Efraasia,* the former is older than the latter. So, if time is the unit assigned to the y-axis, *Saturnalia* is closer to the basis than *Efraasia* (*Saturnalia* is 'basal' to *Efraasia*). *Coloradisaurus* is also 'closer' to node F, than are other taxa within the clade delimited by this node. But this statement is only related to the age of fossils and not to positions in the tree. Even if *Saturnalia* were recovered among sauropods in a hypothetical analysis it would still be older, and then closer to the root, than *Efraasia*.

Regarding the age of taxa, one possibility to refer to a particular assemblage is to use terms such as 'early' or 'late'. For example, this has been done for dinosaurs as a whole, with the term 'early dinosaurs' being used to refer to the oldest representatives of the lineage (e.g. Langer and Benton, 2006). However, as there are no pre-defined boundaries for these terms, the best approach might be to always use a specific time frame, or to use terms like 'early' and 'late' in an explicit comparative framework. Some possibilities include 'the Carnian sauropodomorph *Saturnalia* and *Buriolestes* have teeth with small serrations, whereas later sauropodomorphs such as *Efraasia* and *Plateosaurus* exhibit coarser denticles'; and 'differently from the gigantic sauropods, the earliest sauropodomorphs from the Carnian were small animals'. The usage of such a framework will avoid any ambiguity between scientists, and will also benefit the clarity of communication to non-scientific audiences by explicitly incorporating the concept of time in the evolutionary process (see below). It

is however important to stress out that taxa from the same period of time (e.g. Carnian, Middle Jurassic, Cenozoic) do not necessarily compose a monophyletic group, and therefore comparisons using time as a reference for an assemblage of taxa should be aware of the limitations of the term. Yet, in a cladogram containing extinct taxa, the oldest taxon is not necessarily associated to the oldest cladogenetic events of the tree, and therefore 'basal taxon' and early taxon cannot be always interchangeably used.

'Basal' sauropodomorphs *versus* non-sauropodan sauropodomorphs

As observed by Otero and Salgado (2015), the term 'basal sauropodomorphs' has been widely used interchangeably with 'non-sauropodan sauropodomorphs' in the published research literature. At first glance, applying the term in such a way seems to be a good alternative, as the phylogenetic context is clearly defined. Indeed, it might seem semantically easier to refer to a taxon as a 'basal sauropodomorph' instead of a non-sauropod sauropodomorph, and as shown both are often used interchangeably. Nevertheless, even if researchers think that these terms are clear, different people certainly have different assumptions of what a 'basal' taxon is. For instance, is a 'basal' sauropodomorph a non-sauropodiform (i.e. a clade within Sauropodomorpha that includes Sauropoda) sauropodomorph or a non-sauropodan sauropodomorph? Furthermore, the use of 'basal', in this context, is inaccurate. As 'basal' is a relative term regarding the base of the tree, this in turn corresponds to the root of rooted trees (Krell and Cranston 2004; Crisp and Cook 2005), and it is erroneous to use it here to mean *not belonging to a clade*.

How should the 'basal forms' be treated in this case? When the term 'basal' is used to refer to a paraphyletic assemblage of taxa (as 'basal sauropodomorphs'), there might not actually be a single correct way to refer to it – it is also important to stress

here that we cannot give formal taxonomic recognition to 'prosauropods' or non-sauropodan sauropodomorphs, simply because they are not monophyletic (Schmidt-Lebuhn, 2012). In this way, referring to these assemblages of taxa can be done as, for example, "all the non-sauropodan sauropodomorph lineages vanished before the end of the Middle Jurassic", or "so far, no fossils of non-sauropodan sauropodomorph lineages have been discovered in Mongolia". This nomenclature has value in that it defines bounds for the phylogenetic context of all the monophyletic clades (separately, not as an unit) within one particular region of the tree, and therefore should be used instead of terms like 'basal', which can even carry misleading assumptions (see below the discussion regarding basal taxa and plesiomorphic character states). This is already the case for dinosaurs (see e.g. Lloyd et al., 2008), as the most common way now to refer to the famous extinct relatives of birds is to call them 'non–avian dinosaurs'. A desirable aspect of this terminology instead of the term 'basal' is that it precisely describes the hierarchical system advocated in phylogenetics (Hennig, 1966), and is probably clearer for communication with non-specialists.

Basal taxa are closer to the root of the tree: but how to measure it?

The idea of basal taxa is probably related to an assumption that basal forms are 'close' to the root of the tree, or, to the node corresponding to the group being dealt with (e.g. Langer et al., 2010; Martinez et al., 2011; Wang et al., 2016). In the case of sauropodomorph dinosaurs, one can argue that some 'prosauropods' are 'closer' to the node corresponding to Sauropodomorpha, and therefore in this case they are regarded as 'basal sauropodomorphs'. This association between proximity to the root and basal forms has even led authors to consider some taxa as the most basal representative of Sauropodomorpha (e.g. Langer et al., 2010; Cabreira et al., 2016).

The most likely scenario here is that authors assume that the number of nodes between a taxon and the root (or clade of interest) gives a 'measurement' of how basal it is. However, a single example can demonstrate how problematic (or pointless) this approach is. In the topology of Figure 7.1, there is no node *between Saturnalia* and the node encompassing all the sauropodomorphs used as terminal taxa (i.e. node A of figure 7.1), and, there is one node (i.e. node B of Figure 7.1) between node A and *Efraasia*. Nevertheless, if two new taxa are included in a different analysis, and these two taxa are found to be closer to *Saturnalia* than to *Efraasia* (Figure 7.2), there can be two nodes between *Saturnalia* and the node of the clade containing all the sauropodomorphs (node C of Figure 7.2), whereas only one between node C and *Efraasia* (Figure 7.2). In the latter case, using the number of nodes to calculate how basal a taxon is, *Efraasia* would be considered 'more basal' than *Saturnalia*, even with *Efraasia* belonging to a less-inclusive clade with later sauropodomorphs (including sauropods) that does not include *Saturnalia*.

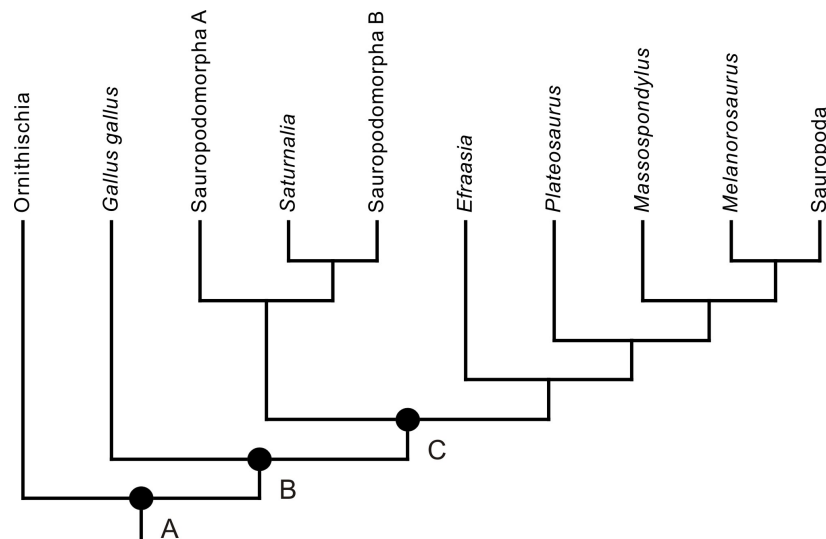**Figure 7.2:** Simplified version of the cladogram of Figure 7.1 showing the relationships of the three main lineages of dinosaurs with focus on Sauropodomorpha. 'Sauropodomorpha A' and 'Sauropodomorpha B' represent two hypothetical taxa that are more closely related to *Saturnalia* than to Sauropoda. Ornithischia is represented by a single terminal taxon and Theropoda is represented by the living bird *Gallus gallus*.

The number of nodes between a terminal taxon and the root of the tree does not tell us how far it is from the root (i.e. if it is a basal taxon or not). The number of nodes can be related, among other things, to the diversity of a clade. More cladogenetic events (i.e. more nodes) mean more speciation and more diversity (Tarver and Donoghue, 2011), and therefore tell us more about evolutionary mode than phylogenetic status. The number of nodes can also be related to the ingroup sampling. For example, in a cladogram where theropods are represented solely by a living bird alongside with all the ornithischians and sauropodomorphs known so far (see Figure 7.2), the living bird *Gallus gallus* (the red junglefowl) would be only a few nodes away from the base of the clade encompassing all the dinosaurs (node A). In this case, we would hope that no one would suggest that the bird is a 'basal' dinosaur or a 'basal' saurischian based on the number of intervening nodes to the root. Finally, the existence of a branch leading to taxa (or to a taxon) that are much younger than its sister group can mean, among other things, that there are still unknown taxa that are more closely related to the taxa (or taxon) descending from this branch than to any other one in the tree; or that the ingroup is not well sampled (as in the case of the living bird representing theropods).

The discussion regarding the number of nodes and the 'apparent' distance to the root can also be used to discuss aspects of another term that has been applied in studies dealing with extinct taxa, early divergent (e.g. Zanno et al., 2015; Griffin & Nesbitt, 2016). As the term implies, it is typically applied to refer to lineages that apparently diverged earlier in relation to the others depicted in a cladogram. Using the example of the cladogram in Figure 7.2, in the context of the clade defined by node A, *Gallus gallus* could be interpreted as having diverged earlier than *Saturnalia* because there are fewer nodes between *Gallus gallus* and node A, than there are nodes between

Saturnalia and node A. Nevertheless, this interpretation is problematic. Firstly, it compares things that are not comparable phylogenetically. Comparisons only apply to sister-groups (Crisp & Cook, 2005; Zachos, 2016), and in this case, *the lineage containing *Gallus gallus* but not sauropodomorphs* diverged at the same time of the *lineage containing all the sauropodomorphs*, which in turn includes *Saturnalia*. Yet, the cladogram also indicates that *the lineage containing *Gallus gallus* but not sauropodomorphs* diverged from *the lineage containing all the sauropodomorphs* earlier than *the lineage containing *Saturnalia,* Sauropodomorpha A and Sauropodomorpha B, but not the other sauropodomorphs* diverged from *the lineage containing all the other sauropodomorphs but not *Saturnalia**. However, *the taxon *Gallus gallus** **did not** diverge early than *the taxon *Saturnalia**. Time of divergence is only associated to the age of the taxa, but not to their relative position in the cladogram.

Other aspects of the usage of the term 'basal' have already been addressed in other publications in the context of living species (Krell and Cranston 2004; Crisp and Cook 2005; Zachos 2016). As mentioned in these studies, it is not terminal taxa (or OTUs – Operational Taxonomical Units) that can be 'more basal' in relation to other terminal taxa, but the nodes (i.e. hypothetical ancestors) of the tree in relation to other nodes (Crisp and Cook 2005, Zachos, 2016). Thus, in the tree topology (Figure 7.1), it is the node corresponding to the ancestor of the less inclusive clade including *Saturnalia* and neosauropods (node A) that is basal in relation to the node representing the ancestor of the less inclusive clade containing *Efraasia* and neosauropods (node B). *Saturnalia* is not a basal sauropodomorph in relation to *Efraasia,* neither even in relation to Sauropoda, and nor is *Saturnalia* the basal most taxon of Sauropodomorpha because of its position in the cladogram. Still, *Saturnalia*

and *Efraasia* are consecutive sister-groups of less inclusive clades within Sauropodomorpha, clade B (node B and all species descending from it) and clade C (node C and all species descending from it), respectively. The clade D (node D and all species descending from it) is not more basal than the clade F (node F and all species descending from it). Moreover, clades defined by nodes C and D are not sister-groups, and therefore no direct comparison can be made between them alone in terms of relationships between each other (Hennig, 1966). This is important to stress because many authors claim that basal is related to something graphical instead of evolutionary or phylogenetic (see also Crisp & Cook, 2005). The resulting tree is an arrangement of organisms in a phylogenetic (or hierarchical) system of progressively less/more inclusive clades and its respective sister groups (Hennig, 1966). Thus, enunciating relationships in the basis of a sister group relationship is the proper way to describe phylogenetic relationships in a cladogram (Zachos, 2016). For instance, the most 'basal' taxon is actually the sister group of all other taxa within that lineage; 'basal lineages' are consecutive sister groups of progressively less inclusive clades.

Do 'basal' taxa have more plesiomorphic traits?

The idea of 'basal' taxon can be accompanied by the false notion that the 'most basal taxon' exhibits less apomorphic character states than the other taxa (see e.g. Crisp & Cook, 2005). However, despite the possibility of having such scenario, it is not true for all the cases. This can be demonstrated using the example of Figure 7.3. A single most parsimonious tree (MPT) is found when the data matrix is analysed using parsimony. Using the notion of basal as discussed above, one could argue that Taxon A is the 'basal most' taxon of clade X. Nevertheless, in the context of clade X, taxon A has six apomorphic traits, whereas taxon B has two, and taxa C-F have four each.

Thus, B-F are more closely related to each other than to A because they share more apomorphies among them than any of them shares with A, but not because A has less apomorphies in the context of the clade including A-F.

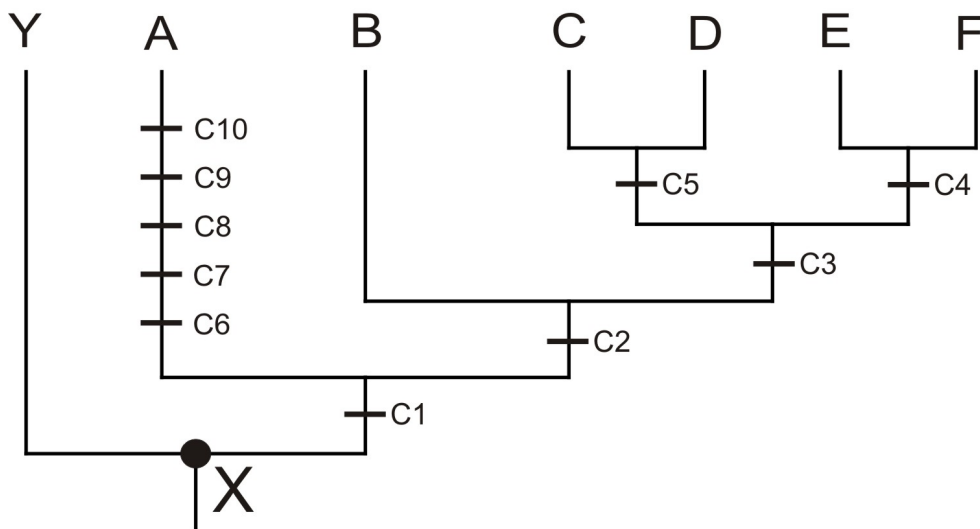|	C1	C2	C3	C4	C5	C6	C7	C8	C9	C10
Taxon Y	0	0	0	0	0	0	0	0	0	0
Taxon A	1	0	0	0	0	1	1	1	1	1
Taxon B	1	1	0	0	0	0	0	0	0	0
Taxon C	1	1	1	0	1	0	0	0	0	0
Taxon D	1	1	1	0	1	0	0	0	0	0
Taxon E	1	1	1	1	0	0	0	0	0	0
Taxon F	1	1	1	1	0	0	0	0	0	0

Figure 7.3: Hypothetical data matrix and the most parsimonious tree obtained when it is analysed using parsimony.

Transitional taxa: a linear way of thinking about evolution?

The first question that probably comes to the mind after reading a sentence such as "*a new transitional taxon is here presented*" is: transitional between what? After all, this way of thinking makes no sense in the theoretical basis of biological evolution as understood nowadays because evolution has no goal (Laland et al., 2015). It also has no basis in a cladistic paradigm because trees are branching diagrams (Hennig, 1966), not ladders of progress (Zachos, 2016).

Two resulting lineages of a cladogenetic event (if dichotomous) exhibit similar character states for some of the characters, but each has a combination of plesiomorphic and apomorphic traits not observed in any other. It is important to stress out that the absence of autapomorphies in taxa B (Figure 7.3) does not indicate that it is transitional between A and C-F. Firstly, this might be just a reflex of the lack of ability to translate different morphologies into phylogenetic characters. Furthermore, the study of living species shows us that even if there is no recognisable morphological difference between, they can differ in the genetic level. Using sauropodomorphs to illustrate that, we can consider taxa E-F as sauropods, and taxa A-D as non-sauropodan sauropodomorphs (Figure 7.3). This shows that some characteristics of non-sauropodan lineages (characters 6-10) are not present in sauropods. Thus, despite sharing some common ancestors, part of the evolutionary history of each lineage is independent from the others. In this way, figure 7.3 highlights the problem of visualizing trees as ladders of progress because there is no directed evolution to a specific part of the cladogram. Diversification of lineages is a process through time with unpredictable paths. As a result, there is no stepwise evolution leading to any particular *bauplan*.

For Sauropodomorpha, the presence of some of the features found in all sauropods in other lineages outside the Sauropoda clade do not tell us that the non-sauropodan sauropodomorphs are transitional between the ancestor of Saruopodomorpha and sauropods. It only tells us that the evolution of these characters happened in a step-wise and/or mosaic fashion on the evolutionary history of the group. Any terminal taxon (OTU) possesses a combination of apomorphic and plesiomorphic character states in the context of a particular phylogenetic analysis and considering a particular root (Nixon and Carpenter, 1983). In cladistic analyses, the MPTs are those that have the smaller number of *ad–hoc* hypothesis (i.e. homoplasies), which means that they are the ones with less character–state changes (Farris 1983; Nixon and Carpenter, 2012). Thus, what the tree topology tells us is that a taxon is more closely related to a second taxon (its sister taxon), a conclusion derived from the observation that they share more apomorphies (synapomorphies) between them than in relation to all other sampled taxa.

If there are no transitional taxa, is there an evolutionary process?

One might argue that the term 'transitional' is important in order to communicate with non-scientific audiences, or to be used to combat anti-evolutionary rhetoric. Indeed, it might not be trivial for people outside the scientific field of phylogenetics to comprehend that *Tiktaalik* (Daeschler et al., 2006) shares more apomorphies with tetrapods than it shares with the lungfishes (i.e. Dipnoi). However, if we treat *Tiktaalik* as a transitional form between lungfishes and tetrapods, we do imply that the evolutionary goal of the Sarcopterygii lineage was to 'produce' a tetrapod (i.e. that evolution is a directional process leading to a specific morphology). This is clearly a case in which a wrong concept of evolution is not solely caused by the way scientific

knowledge is transmitted to a general audience, but a case when scientists themselves probably created the misconception. This is often observed in discussions dealing with human evolution, with *Homo sapiens* being treated as the final evolutionary product of a lineage (sometimes even the final product of all the living beings), and our close relatives treated in a stepwise fashion as our ancestors (see Crisp and Cook 2005; Zachos 2016). We know that we are just one of the many branches of the evolutionary history of all the living forms of the planet. In this way, elevating human beings as a special way of life can have negative consequences, and distort or confound our understanding of our very own origins (Nee, 2005; Montgomery 2012).

The current biodiversity is the result of distinct rates of diversification and extinctions through geological time (e.g. Benton and Emerson, 2007; Meredith et al., 2011; Tarver and Donoghue 2011). Due to the extinction of some lineages, some of the living animals may seem alien in relation to their closest relatives because of the great morphological disparity between them. This is, for example, the case for cetaceans (dolphins, porpoises and whales). From a first glance, it might be difficult to conceive a close phylogenetic relationship between a blue whale and a hippopotamus or a cow, or even that a cow is more closely related to a blue whale than it is to a horse (see Meredith et al., 2011). However, the fossil record clearly shows the existence of animals with a mix of 'cow– and whale–like' features (Thewissen et al., 2009). These animals with a mosaic of features have been constantly called 'the transitional forms' or 'ancestor forms' (e.g. Yates et al., 2010). As demonstrated above, this is wrong and misleading, as those extinct taxa are in reality neither.

Time is probably the most important 'factor' in the field of palaeontology (and also in Cladistics – see Hennig, 1965). It is known that observations on the current

biodiversity, or in the diversity of fossils from a single point in geological time, without taking temporal contexts into account, will provide an incomplete understanding of life (Benton and Emerson, 2007; Tarver and Donoghue 2011). After all, biological evolution happens through time (Laland et al., 2015), and therefore it is a dimension that cannot be ignored. The fossil record gives us an estimative of when a group originated and/or went extinct, when evolutionary events such as diversification occurred, when 'key' morphological features may have first appeared, and, mostly important, the timing of a transformation series. In this sense, rather than using the idea of 'transitional taxa', we can show the morphological evolution across geological time, and the important role that fossils play in that. A new fossil can exhibit a particular combination of features that helps us bridging the morphological 'gaps'. The fossil record is full of taxa such as *Pakicetus*, *Ambulocetus*, *Rodhocetus*, and *Basilosaurus*, animals which possess 'cow -and whale-like traits' (Thewissen and Williams, 2002). Likewise, *Eosinopteryx*, *Anchiornis*, *Archaeopteryx* are examples in the dinosaur lineage (e.g. Foth et al., 2014); *Odontochelys* and *Proganochelys* examples in the turtle lineage (Li et al., 2008); *Panderichthys*, *Tiktaalik*, *Acanthostega*, *Ichthyostega* examples in the tetrapodomorph lineage (Friedman & Brazeau, 2010); comprising just a few examples of taxa that help us trace the evolution of important vertebrate lineages in more detail. Finally, if evolution is regarded as change through time (Laland et al., 2015), then tracing the history of morphological transformations in a cladogram clearly demonstrates the existence of an evolutionary process.

7.5. Practical Guidelines

Based on the issues discussed above, some practical guidelines are presented here that should help to alleviate any misuse or ambiguity regarding what are commonly but incorrectly regarded as 'transitional' or 'basal' taxa.

- Describe relationships on the basis of sister-group relationships and/or following the hierarchical pattern of cladograms: *the new mammal presented here is the sister taxon of all other therians* (rather than: the 'most basal' Theria); *our analysis indicates that the new taxon belongs to Dinosauriformes but outside Dinosauria* (rather than: a new basal dinosauriform).

- 'Basal' also introduces ambiguity in communication among scientists. For instance, is a 'basal' theropod a non-avian theropod or a non-tetanuran theropod; or is a 'basal' sauropodomorph a non-sauropodan sauropodomorph or a non-sauropodiform sauropodomorph. Thus, define boundaries in order to avoid ambiguity: *non-sauropodan sauropodomorphs, non-avian dinosaurs, non-tetrapodan tetrapodomorphs.*

- Taxa have a unique combination of plesiomorphic and apomorphic character states. Thus, present a new taxon showing how it can help scientists bridging the 'gaps' of the fossil record, but not as a 'transitional taxon' or as 'transitional in morphology': *the new taxon shows a mosaic of features in relation to those found in tetrapods and other sarcopterygians* (rather than: the new transitional tetrapodomorph).

- There is no direction in the evolution. One group might be the best-known and most studied group of a certain lineage, but this does not postulate them as the 'final product' of that lineage: *the biomechanical analysis indicates that the*

new sauropodomorph was a facultative bipedal animal, but its unique combination of plesiomorphic and apomorphic features of the limbs and axial skeleton helps to explain the acquisition of the traits related to the quadrupedal stance of sauropods (rather than: the new taxon shows that the evolution of sauropodomorphs was driven by the acquisition of characters related to a fully quadrupedal stance).

7.6. CONCLUSIONS

Problematic issues related to the usage of the term 'basal' in studies dealing with living taxa have been widely demonstrated (Crisp and Cook, 2005; Zachos, 2016), and here it is further shown that 'basal', as well as the term 'transitional', has also been inconsistently applied in cladistics studies with extinct taxa. Scientific papers typically represent the primary data that will be later integrated into the knowledge base of a broader audience. Thus, the avoidance of misusing terms and being more clear and explicit as to their definition is a way to diminish problems in communication when transmitting science to those outside the professional scientific community, or even to researchers from the same particular scientific field. Finally, we do not need to use terms that are inaccurate and/or pointless (e.g. a new basal dinosaur, the most basal bird, a new transitional whale) in order to make fossil discoveries more attractive to journals or to the media. Fossils with a mosaic of features and which help us to fill the gaps in our knowledge on the evolution of a group are already interesting enough without embellishing their phylogenetic status.

7.7. ACKNOWLEDGEMENTS

7.8. REFERENCES

Baum DA, Smith SD, Donovan, SSS. 2005. The tree thinking challenge. *Science*, 310, 979-980.

Benton MJ, Emerson BC. 2007. How did life become so diverse? The dynamics of diversification according to the fossil record and molecular phylogenetics. *Palaeontology*, 50, 23-40.

Brower AVZ, de Pinna MC. C. 2012. Homology and errors. *Cladistics*, 28, 529-538.

Cabreira SF, Kellner AWA, Dias-da-Silva S, Silva LR, Bronzati M, Marsola JCA, Müller RT, Bittencourt JS, Batista BJ, Raugust T, Carrilho R, Brodt A, Langer MC. 2016. A unique Late Triassic dinosauromorph assemblage reveals dinosaur ancestral anatomy and diet. *Current Biology*, 26(22), 3090-3095.

Crisp MD, Cook LG. 2005. Do early branching lineages signify ancestral traits? *Trends in Ecology and Evolution*, 20(3), 123-128.

Daeschler EB, Shubin NH, Jenkins JrFA. 2006. A Devonian tetrapod–like fish and the evolution of the tetrapod body plan. *Nature*, 440, 757-763.

Farris JS. 1983. The logical basis of phylogenetic analysis. In (Eds. NI Platnick, VA Funk) *Advances in Cladistics Vol. 2*. Columbia University Press, New York, pp. 7-36

Foth C, Tischlinger H, Rauhut OWM. 2014. New specimen of *Archaeopteryx* provides insights into the evolution of pennaceous feathers. *Nature,* 511, 79-82.

Friedman M, Brazeau D. 2010. Sequences, stratigraphy and scenarios: what can we say about the fossil record of the earliest tetrapods? *Proceedings of the Royal Society B,* 278, 432-439.

Galton PM, Upchurch P. 2004. Prosauropoda. In (Eds. DB Weishampel, P Dodson, H Osmólska) *The Dinosauria, second edition.* University of California Press, Berkley, pp. 232-258.

Gauthier J. 1986. Saurischian monophyly and the origin of birds. *Memoirs of the California Academy of Sciences*, 8, 1-55.

Hennig W. 1965. Phylogenetic systematics. *Annual Review of Entomology,* 10, 97-116.

Hennig W. 1966. Phylogenetic systematics. University of Illinois Press, Urbana.

Krell FT, Cranston PS. 2004. Which side of the tree is more basal? *Systematic Entomology,* 29, 279-281.

Laland KN, Uller T, Feldman MW, Sterelny K, Müller GB, Moczek A, Jablonka E, Odling–Smee J. 2015. The extended evolutionary synthesis: its structure, assumptions and predictions. *Proceedings of the Royal Society Biological Sciences,* 282: 20151019

Langer MC, Benton MJ. 2006. Early dinosaurs: a phylogenetic study. *Journal of Systematic Palaeontology,* 4, 309-358.

Langer MC, Ezcurra MD, Bittencourt JS, Novas FE. 2010. The origin and early evolution of dinosaurs. *Biological Reviews,* 85, 55-110.

Li C, Wu X-C, Rieppel O, Wang LT, Zhao LJ. 2008. An ancestral turtle from the Late Triassic of southwestern China. *Nature,* 456, 497-501.

Lloyd GT, Davis KE, Pisani D, Tarver JE, Ruta M, Sakamoto M, Hone DWW, Jennings R, Benton MJ. 2008. Dinosaurs and the Cretaceous Terrestrial Revolution. *Proceedings of the Royal Society Biological Sciences,* 275, 2483-2490.

Longrich NR, Bhullar B–AS, Gauthier JA. 2012. A transitional snake from the Late Cretaceous Period of North America. *Nature,* 488, 205-208.

Martinez RN, Sereno PC, Alcober OA, Colombi CE, Renne PR, Montanez IP, Currie BS. 2011. A basal dinosaur from the Dawn of the Dinosaur Era in Southwestern Pangaea. *Science,* 331, 206-210.

McPhee BW, Yates AM, Choiniere JN, Abdala F. 2014. The complete anatomy and phylogenetic relationships of *Antetonitrus longiceps* (Sauropodiformes, Dinosauria): implications for the origins of Sauropoda. *Zoological Journal of the Linnean Society,* 171, 151-205.

Meredith RW, Janecka JE, Gatesy J, et al. 2011. Impacts of the Cretaceous Terrestrial Revolution and KPg Extinction on Mammal Diversification. *Science,* 334, 521-524.

Montgomery DR. 2012. The evolution of creationism. *GSA Today,* 22, 4-9.

Nee S. 2005. The great chain of being. *Nature,* 435, 429.

Nixon KC, Carpenter JM. 1993. On outgroups. *Cladistics*, 9(4), 413-426.

Nixon KC, Carpenter JM. 2011. On homology. *Cladistics*, 28(2), 160-169.

Omland KE, Cook LG, Crisp MD. 2008. Tree thinking for all biology: the problem with reading phylogenies as ladders of progress. *Bioessays*, 30(9), 854-867.

Otero A, Salgado L. 2015. El registro de Sauropodomorpha (Dinosauria) de la Argentina. *Publicación Electrónica de la Asociación Paleontológica Argentina*. 15(1), 69-89.

Pinheiro FL, Franca MAG, Lacerda MB, Butler RJ, Schultz CL. 2016. An exceptional fossil skull from South America and the origins of the archosauriform radiation. *Scientific Reports*, 6, 22817.

Peyre de Fabrègues C, Allain R, Barriel V. 2015. Root causes of phylogenetic incongruence observed within basal sauropodomorph interrelationships. *Zoological Journal of the Linnean Society*, 175(3), 569-586.

Sander PM, Christian A, Clauss M, Fechner R, Gee CT, Griebeler EM, Gunga HC, Hummel J, Mallison H, Perry S, Preuschoft H, Rauhut OWM, Remes K, Tütken T, Wings O, Witzel U. 2010. Biology of the sauropod dinosaurs: the evolution of gigantism. *Biological Reviews*, 86, 117-155.

Salgado L, Coria RA, Calvo JO. 2010. Evolution of titanosaurid sauropods. I: Phylogenetic analysis based on the postcranial evidence. *Ameghiniana*, 34(1), 3-32.

Schmidt-Lebuhn AN. 2012. Fallacies and false premises—a critical assessment of the arguments for the recognition of paraphyletic taxa in botany. *Cladistics*, 28(2), 174-187.

Sereno PC. 1989. Prosauropod monophyly and basal sauropodomorph phylogeny. *Journal of Vertebrate Palaeontology*, 9(suppl. 3), 38A.

Sues H–D, Nesbitt SJ, Berman DS, Henrici AC. 2011. A late–surviving basal theropod dinosaur from the latest Triassic of North America. *Proceedings of the Royal Society Biological Sciences*, 278, 3459-3464.

Tarver JE, Donoghue PC. 2011. The trouble with topology: Phylogenies without fossils provide a revisionist perspective of evolutionary history in topological analyses of diversity. *Systematic Biology*, 60(5), 700-712.

Thewissen JGM, Cooper LN, George JC, Bajpai S. 2009. From land to Water: The origin of Whales, Dolphins, and Porpoises. *Evolution: Education and Outreach*, 2, 272-288.

Wang M, Wang X, Wang Y, Zhou Z. 2016. A new basal bird from China with implications for morphological diversity in early birds. *Scientific Reports*, 6: 19700.

Xu X, Norell MA, Kuang X, Wang X, Zhao Q, Jia C. 2014. Basal tyrannosauroids from China and evidence for protofeathers in tyranossauroids. *Nature*, 431, 680-684.

Yates AM, Bonnan MF, Nevelling J, Chinsamy A, Blackbeard MG. 2010. A new transitional sauropodomorph dinosaur from the Early Jurassic of South Africa

and the evolution of sauropod feeding and quadrupedalism. *Proceedings of the Royal Society Biological Sciences*, 277, 787-794.

Zachos FE. 2016. Tree thinking and species delimitation: Guidelines for taxonomy and phylogenetic terminology. *Mammalian Biology,* 81, 185-188.

Zhou Z, Zhang F. 2002. A long–tailed, seed–eating bird from the Early Cretaceous of China. *Nature*, 418, 405-409.

Chapter 8

Conclusions

- The phylogeny of early dinosauromorphs is still on dispute (Langer, 2014; Cabreira *et al.,* 2016). The lack of consensus regarding the interrelationships of Late Triassic forms still hampers a more definitive statement regarding the ancestral diet of Dinosauria. Nevertheless, the discovery of *Buriolestes schultzi* revealed a new scenario regarding the early evolution of dinosaurs' diet. The tooth morphology of *B. schultzi* indicates that it was a faunivore animal. Thus, given its phylogenetic position as the sister-group of Sauropodomorpha, the current data indicate that faunivory corresponds to the ancestral condition of Saurischia, and also of its two main sub-lineages, Theropoda and Sauropodomorpha (Cabreira *et al.*, 2016 – Chapter 2).

- The endocast of the sauropodomorph *Saturnalia tupiniquim* from the Late Triassic of Brazil is described based on CT-Scan data (Chapter 3). This is the first time that the neurological soft-tissues were reconstructed for one of the oldest dinosaurs known, enabling an analysis of the feeding behaviour of *S. tupiniquim* based on hard and soft cranial tissues. Its tooth morphology resembles that of the faunivorous *Buriolestes schultzi,* not showing the features correlated to a herbivorous diet, as seen in later sauropodomorphs, such as *Efraasia minor* and *Plateosaurus*. Furhtermore,

the reconstructed cranial soft tissues of *S. tupiniquim* provide additional evidence that early sauropodomorphs had a predatory behaviour.

▪ The Late Triassic sauropodomorph fossil record shows carnivorous (*Buriolestes schultzi*) and omnivorous (e.g. *Saturnalia tupiniquim, Eoraptor lunensis, Panphagia protos*) taxa sharing the terrestrial ecosystems of southwest Pangaea during the Carnian. The transition to a fully herbivorous diet still during the Triassic lacks direct evidence from the fossil record; tooth morphology of taxa such as *Plateosaurus engelhardti, Pantydraco caducus*, and *Efraasia minor* are still compatible with an omnivorous diet. In addition, most non-sauropodan sauropodomorphs closely related to Sauropoda, and early sauropod taxa are known from incomplete materials, hampering inferences on their diet. In this context, a fully herbivorous diet is probably associated with a fully quadrupedal stance (loss of grasping hands) and the increase in body size (enhanced absorption of nutrients during digestion), all appearing together during the Early Jurassic, with the anatomical traits related to this habit continuing to diversify along the next steps of sauropod evolution (Barrett & Upchurch, 2007; Sander *et al.*, 2011).

▪ The transition from a faunivorous to a herbivorous diet in Sauropodomorpha also involved neurological modifications, such as the reduction of the flocculus, already observed in taxa belonging to the less inclusive clade containing *Plateosaurus* and sauropods (Chapter 3). Therefore, the small flocculus of most sauropodomorphs is understood as a vestigial structure, retained in a reduced version from the bipedal, predatory early sauropodomorphs. The loss of neurological traits related to an efficient predation occurred together with the first steps toward body

size increase in the lineage, in a scenario that preceded the later acquisition of quadrupedalism and a fully herbivorous diet.

▪ Head reduction certainly played an important role in sauropodomorph evolution, triggering the evolutionary 'head and neck' cascade that led to the unusual sauropod body plan and, ultimately, their gigantism (Sander, 2013). Therefore, the small skull of faunivorous early sauropodomorphs can be seen as a case of exaptation, which constrained the evolution of the highly efficient plant-eating strategy of sauropods (Chapter 3). The first activation of the cascade happened in the Norian, after the skull reduction (skull length < two thirds of femoral length) in the Carnian. The Norian and Rhaetian, the last stages of the Late Triassic, also witnessed a first moment of body mass and neck length increase in sauropodomorphs. The analysis of sauropodomorph braincases indicate an additional activation of the 'head and neck' cascade in the Middle Jurassic, after a second moment of skull reduction (skull length < half of the femoral length) at the branch leading to eusauropods. Differently from what is detected for the Late Triassic, the neck elongation that followed the skull reduction in the Middle Jurassic was also accompanied by a drastic transformation in the braincase bones that bears attachment sites for the neck musculature. Statistical comparison of evolutionary rates indicates that these major anatomical modifications occurred in a short time interval, indicating rapid morphological transformation. This second activation of the neck and head cascade is so far understood as one of the factors of the differential survival of sauropodomorph lineages in the Early/Middle Jurassic: the extinction of all the non-sauropodan lineages and the diversification of neosauropods (Chapter 6).

- The comparative study of the braincase osteology of *Saturnalia tupiniquim* and *Efraasia minor* provided a solid basis for the revision of the braincase characters used in data matrices focused on early dinosaurs and non-neosauropodan sauropodomorphs (Chapters 4 and 5). This study revealed problems with some of the phylogenetic characters previously adopted, which did not accurately reflect the morphological variation observed among taxa within the ingroup. Besides proposing modified version of previously used characters, new characters related to the braincase anatomy were also proposed and used to investigate the phylogenetic relationships of sauropodomorph dinosaurs. The phylogenetic analyses presented here indicate that a paraphyletic condition of non-sauropodan sauropodomorphs in relation to Sauropoda is a much stronger hypothesis in relation to a monophyletic 'Prosauropoda' (Chapter 5).

- The paraphyletic condition of 'Prosauropoda' does not indicate that these taxa were transitional between sauropodomorph ancestors and Sauropoda (Chapter 7). Nevertheless, the studies conducted for this thesis reinforce the importance of the studies on 'prosauropods' in order to understand the origin and early evolution of Sauropoda.

Future directions

Despite recent discoveries, only a consensus regarding the phylogenetic relationships of early dinosauriforms will provide a clearer scenario regarding the evolution of dinosaurs' anatomy and biology. New fossils will probably bring important information for such, but a revision of phylogenetic characters used in previous matrices is probably the best starting point.

"The incompleteness of the fossil record" is one of the most used sentence in conclusion sections of works on vertebrate palaeontology. As this thesis is one of those, I cannot leave it out. The incompleteness of the Early Jurassic fossil record of Sauropodomorpha, so far restricted to incomplete and fragmentary taxa, is the biggest challenge to our understanding of the origins and early evolution of sauropod dinosaurs. In this case, new fossils will certainly help us to understand all the transformations that enabled sauropods to reach the biggest sizes among all the terrestrial vertebrates.

The incompleteness of the fossil record, however, is not a big problem to study the evolution of the non-sauropodan lineages of Sauropodomorpha. But, the small number of endocasts for taxa of these lineages hampers tracing the evolution of the brain soft-tissues in more details. In this sense, Computed Tomography will certainly enable future works to show the modifications in the brain anatomy of sauropodomorphs in a more comprehensive manner, revisiting the implications for the palaeobiology as discussed here.

References

Barrett PM, Upchurch P. 2007. The evolution of feeding mechanisms in early sauropodomorph dinosaurs. *Special Papers in Palaeontology*, 77, 91–112.

Cabreira SF, *et al*. 2016. A unique Late Triassic dinosauromorph assemblage reveals dinosaur ancestral anatomy and diet. *Current Biology*, 26(22), 3090-3095.

Langer MC. 2014. The origins of Dinosauria: Much ado about nothing. *Palaeontology*, 57, 469-478.

Sander PM. 2013. An Evolutionary Cascade Model for Sauropod Dinosaur Gigantism - Overview, Update and Tests. *PLoS ONE,* 8(10), e78573.

Sander, P.M. et al., 2011. Biology of the sauropod dinosaurs: the evolution of gigantism. *Biological Reviews*, 86: 117-155.

Appendix of

Braincase anatomy in non-neosauropodan sauropodomorphs:

evolutionary and functional aspects

By

Mario Bronzati Filho

APPENDIX - CHAPTER 2

Institutional abbreviations

BP - Bernard Price Institute for Palaeontological Research, University of the Witwatersrand, Johannesburg, South Africa; GPIT – Institut und Museum für Geologie und Paläontologie, Universität Tübingen, Tübingen, Germany; ULBRA - Museu de Ciências Naturais, Universidade Luterana do Brasil, Canoas, Brazil.

Details of the Phylogenetic Analysis

In order to determine the affinities of *Ixalerpeton polesinensis* and *Buriolestes schultzi*, we scored both taxa (based on ULBRA-PVT059 and PVT280, respectively) in a novel data matrix composed of early dinosauromorphs. The matrix is a modified version of that published by [1], with additional information (basically extra morphological characters) gathered from various other sources, notably [2-55]. The taxon-character matrix consists of 43 terminal taxa and 256 morphological characters. The Ingroup includes all Triassic dinosauromorphs known to date from more than fragmentary remains (except for various uncontroversial sauropodomorphs such as *Atetonitrus*, *Blikanasaurus*, *Coloradisaurus*, *Ruehleia*, *Eucnemesaurus*, *Lessemsaurus*, *Melanorosaurus*, *Plateosauravus*, *Riojasaurus*, *Thecodontosaurus*, and *Unaysaurus*), plus some Early Jurassic members of both Theropoda and Ornithischia. The morphological characters are all variable (except if explicitly mentioned; character 48 below) within the group of interest, i.e., Dinosauromorpha not consensually nested within Ornithischia, Sauropodomorpha, or Theropoda. This means that the data-matrix does not include characters that are invariable within the Ingroup (i.e. all taxa of the analyses except for *Euparkeria capensis*) even if they potentially unite/diagnose the Ingroup. In addition, we defined three subsets of terminal taxa (but did not constrain them as clades for the analysis) that, based on most previous studies, consensually nest within the three major dinosaur groups; i.e. *Eocursor parvus*, *Heterodontosaurus tucki*, *Lesothosaurus diagnosticus*, and *Scutellosaurus lawleri* within Ornithischia [56]; *Efraasia minor*, *Pantydraco caducus*, and *Plateosaurus engelhardti* within Sauropodomorpha [57]; and *Coelophysis bauri*, *Dilophosaurus wetherilli*, *Liliensternus liliensterni*, "Petrified Forest theropod", *Syntarsus kayentakatae*, *S. rhodesiensis*, and *Zupaysaurus ruggieri* within Theropoda [45]. As for the Ingroup, after testing all characters (from the above mentioned data-sets) that possibly vary within the terminal taxa included in the present phylogenetic analysis,

we chose not to include in our data-matrix those that vary only within each of those subsets, or that unite/diagnose one of them: e.g., a character scored as "0" for *Efraasia minor*, *Pantydraco caducus*, and *Plateosaurus engelhardti*, but as "1" for all other taxa, or a character scored differently only for two of those three taxa within the data-matrix. With this procedure we intent to narrow down the efforts into the aspects that form the core of this study, avoiding the inflation of data with characters that, to the present knowledge, represent variation that do not help unravelling the basic phylogenetic patterns of early dinosaurs radiation. Only three (*Daemonosaurus chauliodus* and the two species of *Dromomeron*) of the 43 terminal taxa were not analysed first hand by either MCL, MB, JCAM, or JSB.

The character-taxon matrix was analysed in TNT 1.1 [58]. All but two of the 33 multistate characters were treaded as additive (see "ORDERED" in the list below). Search for the most parsimonious trees (MPTs) was conducted via 'Traditional search' (RAS + TBR), with the following options: random seed = 0; 5,000 replicates; hold = 10; collapse of "zero-length" branches, according to rule 1 of TNT; root was placed between *Euparkeria capensis* and Dinosauromorpha. The heuristic search resulted in 36 MPTs of 846 steps (Consistency Index = 0. 347518; Retention Index = 0. 636364; Rescaled Consistency Index = 0. 221148). We further explored the information on the data-matrix by excluding the highly fragmentary *Saltopus elginensis* from the analysis. A search with the same original parameters resulted in 18 MPTs of 841 steps, but the relation amongst the other taxa remained exactly the same as that found in the original analysis (including *S. elginensis*).

The results confirm previously suggested hypotheses of relationship, stress points of disagreement among earlier studies, and also recover clades not identified before. The main relationship patterns are:

- Dinosauromorpha is composed of Lagerpetidae and Dinosauriformes.
- Lagerpetidae is composed of *Lagerpeton*, *Ixalerpeton*, and *Dromomeron*.
- *Ixalerpeton* and *Dromomeron* are sister taxa.
- Dinosauriformes includes *Marasuchus* and a clade with all other members of the group.
- *Saltopus*, *Lewisuchus*, and *Pseudolagosuchus* form a polytomy with Dinosauria.
- Dinosauria of composed f the Saurischia and Orithischia lineages.
- *Asilisaurus* is the sister group of all the other ornithischians, including Silesauridae.
- Silesauridae is composed of *Eucoelophysis*, *Silesaurus*, *Sacisaurus*, and *Diodorus*.

- Silesauridae is the sister-clade of the group composed of broadly accepted ornithischians.

- Herrerasauria is the sister group to all other saurischian dinosaurs.

- Herrerasauridae is composed of *Staurikosaurus*, *Herrerasaurus*, and *Sanjuansaurus*.

- *Herrerasaurus* and *Sanjuansaurus* are sister taxa.

- *Tawa* and *Chindesaurus* are sister taxa.

- *Guaibasaurus*, *Eodromaeus*, *Tawa+Chindesaurus*, and *Daemonosaurus* are saurischians belonging neither to Theropoda nor to Sauropodomorpha (i.e. non-Eusaurischia).

- Eusaurischia is composed of the theropod and sauromopodorph branches.

- *Buriolestes* is the sister group of all other sauropodomorphs.

- *Eoraptor* is the sister group of all other sauropodomorphs with the exception of *Buriolestes*.

- *Pampadromaeus* is the sister group of *Panphagia, Saturnalia+Chromogisaurus*, and all other sauropodomorphs.

Comments on clade support and the diagnosis of Dinosauria

Some of the clades are very badly supported by the statistics provided: Bootstrap (1,000 replicates) and Bremer support (Figure S1). This is particularly the case of the Dinosauria clade and those along the non-Eusaurischia saurischian branch. Although unattractive, this result is expected given the controversies that surround phylogenetic studies of early dinosaurs. This issue has been raised by recent reviews of the dinosaur radiation [60-61], where it becomes clear that more data (fossil specimens and phylogenetic characters) and detailed analyses are needed to unravel early dinosaur phylogeny. Some of these new data has been provided here, but unfortunately it was not enough to enforce a well-supported phylogenetic arrangement, and the position of various Triassic forms, as silesaurids and herrerasaurs, among dinosauriformes remain poorly constrained. Again, this mirror their shifting positions among different phylogenetic proposals [e.g. 1-5, 9-10, 45-46, 54-55], most of which have been compiled into the character-taxon matrix provided here (see below). Indeed, this study represents one of the attempts to overcome the recognized [62] problem of non-overlap of characters among early dinosaur phylogenetic data-sets. As such, the compiling of conflictual data from different studies potentially increases the amount of characters with homoplastic distribution of states, leading to less supported phylogenetic hypothesis. Indeed, it is symptomatic that better scrutinized taxonomic groups and anatomical parts accumulate more conflictual phylogenetic data [61]. As such, the debated value of

resampling methods apart [63], the low support of the phylogeny proposed here may be understood not as much as a problem, but as a necessary step towards a more comprehensive understanding of early dinosaur phylogeny. Finally, the evidence that higher levels of support is no guaranty of more reliable phylogenetic hypotheses is that, in the case of early dinosaurs, such greater support is commonly found in studies with highly dissimilar results, all of which cannot be obviously correct.
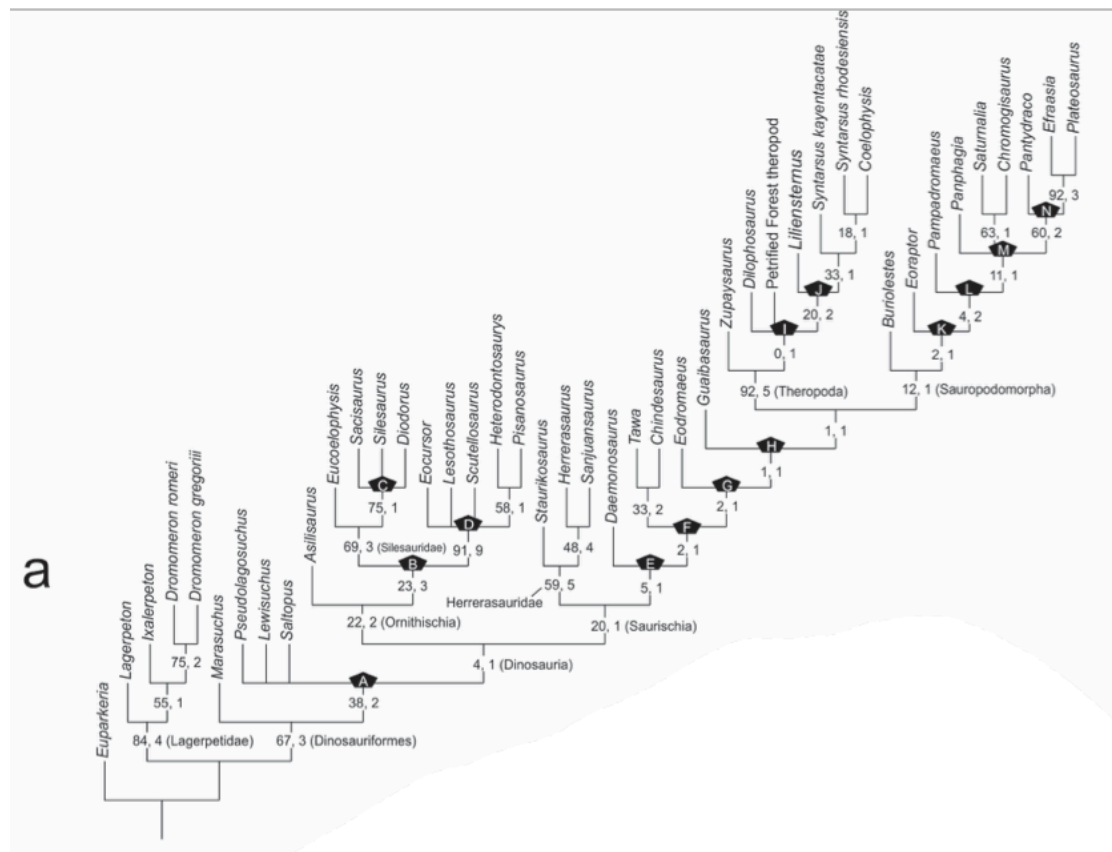
Figure S1: Phylogenetic position of *Ixalerpeton polesinensis* and *Buriolestes schultzi*. a. Strict consensus of the 36 MPTs found in the analysis performed here. Bootstrap (1,000 replicates) and Bremer support (to the right) values indicated for each node.

One of the unorthodox, although previously proposed [64], hypotheses of relationships identified here is the nesting of Silesauridae within Ornithischia. This leads to a rather different view of dinosaur inclusivity, deserving some further discussion. It has been already stated [61], that the practice of identifying diagnostic anatomical traits for major groups such as Dinosauria is very often of limited value in light of new discoveries and phylogenetic scenarios. In spite of that, we compiled below the list of potential synapomorphies identified in the present analysis of Dinosauria inclusive of Silesauridae:

- Distal margin of the trunk vertebrae neural spines less than twice the craniocaudal length of the base;

- Scapular blade longer than tree times its distal width *;

- Pubic pair significantly narrower (mediolaterally) distally than proximally * †;

- Ligament sulcus forms a medial excavation in the proximal surface of the femur *;

- Femur with a craniolateral tuber in the proximal portion *;

- Tibia with a craniolaterally arching cnemial crest *;

- Proximal articular facet for fibula accounts for less than 0.3 of the astragalus transverse width * †.

Various of the above traits are not present in all early dinosaurs included in the phylogenetic analysis conducted here (marked * above) and fewer of them are also seen among some non-dinosaur dinosauromorphs (marked † above). Both patterns highlight the high levels of homoplasy seen in early dinosaur character evolution. Indeed, their status as strict diagnostic traits (i.e. those that you need to find in a given taxon/specimen in order to assign it to a more inclusive group) must be seen with extreme caution.

Character list
Each character of the list below is followed (under brackets) by a reference to the first author that (to our knowledge) employed a similar morphological character in the context of early dinosaur phylogeny.

1. Skull; length (Gauthier, 1986):
    0, longer than two thirds of the femoral (or estimate of its) length;
    1, shorter than, or subequal to, two thirds of the femoral (or estimate of its) length.
2. Premaxilla; rostrodorsal process (Nesbitt, 2011):
    0, shorter than the craniocaudal length of the premaxillary body;
    1, longer than, or subequal to, the craniocaudal length of the premaxillary body.
3. Premaxilla; caudodorsal process (Gauthier, 1986) ORDERED:
    0, extends caudally between nasal and maxilla;
    1, restricted to the ventral-caudal margin of the external naris;
    2, restricted to the ventral margin of the external naris.
4. Skull; premaxilla (caudodorsal process) nasal (cranioventral process) contact (Yates, 2003) ORDERED:
    0, broad sutured contact;
    1, point contact;
    2, no contact.
5. Premaxilla; narial fossa at the rostroventral corner of the naris (Sereno, 1999):
    0, absent or shallow;
    1, deep.
6. Skull; alveolar margin of the premaxilla-maxilla articulation (Gauthier, 1986) ORDERED:
    0, continuous/straight;

1, arched;

2, deeply arched (arch deeper than its distance to the external naris).

7. Skull; subnarial foramen (Benton & Clark 1988):

0, absent;

1, present.

8. Premaxilla; caudomedial process (Rauhut 2003):

0, absent;

1, present.

9. Maxilla; facial portion, rostral to the rostral edge of external antorbital fenestra (Nesbitt, 2011):

0, shorter than caudal portion;

1, equal in length or longer than portion caudal to the rostral edge of fenestra.

10. Maxilla; buccal emargination separated from the ventral margin of the antorbital fossa (Butler 2005):

0, absent;

1, present.

11. Maxilla; rostrodorsal margin, except for the rostromedial process (Yates, 2003) ORDERED:

0, straight;

1, slightly concave;

2, with a strong inflection at the base of the ascending ramus.

12. Maxilla; ventral margin of the antorbital fossa (Nesbitt, 2011):

0, smooth (continuous to the more ventral area);

1, elevated relative to the ventral surface (sharp longitudinal ridge present).

13. Maxilla; antorbital fossa, rostrocaudal extension of its medial wall (Langer, 2004):

0, extends onto the whole ventral border of the internal antorbital fenestra;

1, does not reach the caudoventral edge of the internal antorbital fenestra.

14. Maxilla; antorbital fossa, lateral surface of its medial wall, close to the base of the ascending process (Rauhut 2003):

0, smooth; or with subcircular or oval blind pockets;

1, with one or more foramen or fenestra sized perforations.

15. Maxilla; surface ventral to the external antorbital fenestra, except for the articulation area with the lacrimal (Nesbitt, 2011):

0, significantly deeper (more than 50%) rostrally than caudally;

1, approximately the same depth trougtout.

16. Nasal; caudolateral process (Yates, 2003):

0, does not envelop part of the rostral ramus of the lacrimal;

1, envelops part of the rostral ramus of the lacrimal.

17. Nasal; contribution to the antorbital fossa (Sereno et al, 1994):

0, does not form part of the dorsal border of the antorbital fossa;

1, forms part of the dorsal border of the antorbital fossa.

18. Nasal; rostroventral process width (Yates, 2007):

0, equally broad or narrower than the rostrodorsal process at the basal portion;

1, wider than the rostrodorsal process at the basal portion.

19. Lacrimal; shape (Sereno, 1999):

0, does not fold over the caudodorsal part of the antorbital fenestra;

1, fold over the caudodorsal part of the antorbital fenestra.

20. Lacrimal; height (Rauhut, 2003):

0, significantly less than the height of the orbit and usually fails to reach the ventral margin of the orbit;

1, as high as the orbit and contacts the jugal at the level of the ventral margin of the orbit.

21. Lacrimal; dorsal exposure (Yates, 2003):
    0, exposed in dorsal view;
    1, dorsal portion of the lacrimal does not reach the skull dorsal surface.

22. Squamosal; ventral process (Yates, 2003):
    0, wider than one quarter of its length;
    1, narrower than one quarter of its length.

23. Squamosal; ventral process contribution to laterotemporal fenestra (Bittencourt et al. 2014):
    0, more than half of the caudal margin of the laterotemporal fenestra;
    1, less than half of the caudal margin of the laterotemporal fenestra.

24. Postorbital bar (Nesbitt, 2011):
    0, composed by both the jugal and postorbital in nearly equal proportions;
    1, composed mostly by the postorbital.

25. Postorbital; rostral process (Ezcurra 2006):
    0, equal to or longer than the caudal process;
    1, shorter than the caudal process.

26. Jugal; long axis of the body (Nesbitt, 2011):
    0, nearly horizontal to the alveolar margin of the maxilla;
    1, oblique to the alveolar margin of the maxilla.

27. Jugal; rostral and caudal rami ventral margin (new):
    0, straight or forming an angle of more than 180°;
    1, forming angle of less than 180°.

28. Jugal; rostral extent of the slot for the quadratojugal (Nesbitt, 2011):
    0, caudal to the caudal edge of the dorsal ramus of the jugal;
    1, rostral to the caudal edge of the dorsal ramus of the jugal.

29. Jugal; rostral process (Rauhut, 2003):
    0, participates in caudal edge of internal antorbital fenestra;
    1, excluded from the internal antorbital fenestra by the lacrimal or maxilla.

30. Jugal; forked caudal process (Tykoski & Rowe 2004):
    0, ventral tine longer than the dorsal one;
    1, dorsal tine longer or subequal than the ventral one

31. Jugal; longitudinal ridge on the lateral surface of the body (Nesbitt, 2011):
    0, absent;
    1, present.

32. Quadratojugal; dorsal ramus (Langer & Benton 2006):
    0, longer than the cranial ramus;
    1, equal or shorter than the cranial ramus.

33. Quadratojugal; angle between rostral and dorsal rami (Upchurch *et al*. 2007):
    0, about 90° or more;
    1, about 60° or lower.

34. Quadrate; ventral portion (Rauhut 2003):
    0, aligned to the long axis of the bone;
    1, caudaly displaced relative to the long axis of the bone.

35. Ectopterygoid; jugal process shape (Yates 2003):
    0, slightly curved;
    1, strongly curved and hook-shaped.

36. Parabasisphenoid; median recess (Nesbitt, 2011) ORDERED:

    0, absent;
    1, present as a shallow depression;
    2, present as a fossa.
37. Parabasisphenoid; caudal margin; outline in ventral view (new):
    0, flat (approaching basal tubera);
    1, excavated.
38. Opisthotic; paraoccipital process (Rauhut 2003):
    0, directed laterally or dorsolaterally;
    1, directed ventrolaterally.
39. Opisthotic; ventral ramus (Nesbitt, 2011):
0, extends further laterally or about the same as lateralmost edge of exoccipital in caudal view;
    1, covered by the lateralmost edge of exoccipital in caudal view.
40. Exoccipital; relative positions of the exits of the hypoglossal nerve XII (Nesbitt, 2011):
    0, aligned in a near rostrocaudally plane;
    1, aligned sub vertically.
41. Supraoccipital; rugose ridge on the craniolateral edges (Nesbitt, 2011):
    0, absent;
    1, present.
42. Foramen for trigeminal nerve and middle cerebral vein (Nesbitt, 2011):
    0, combined and undivided;
    1, fully or partially divided.
43. External narial fenestra length (Yates 2003):
    0, half or less than the orbit;
    1, more than half of the orbit.
44. External narial fenestra; rostral edge (Yates 2007):
    0, rostral or close to the midlength of the premaxillary body;
    1, closer to the maxilla articulation than to the rostral edge of the premaxilla.
45. Antorbital fenestra; length (Langer 2004):
    0, equal to or longer than the orbit;
    1, shorter than the orbit.
46. Laterotemporal fenestra; rostral edge (Yates 2003):
    0, caudal to the caudal edge of the orbit;
    1, rostral to the caudal edge of the orbit.
47. Supratemporal fossa/fenestra (Gauthier 1986):
    0, does no excavate the frontal bone;
    1, excavates the frontal bone.
48. Predentary bone (Sereno, 1986) *uninformative*:
    0, absent;
    1, present.
49. Lower jaw; rostral portion (Nesbitt, 2011):
    0, rounded;
    1, tapers to a sharp point.
50. Dentary; length versus height (Yates 2007):
    0, less than 0.2;
    1, more than 0.2.
51. Dentary; rostral tip, dorsal surface (Sereno 1999)
0, at nearly the same plane as the rest of the alveolar margin of the bone;
    1, ventrally inclined.
52. Dentary; extension of the caudoventral process (Smith et al. 2007):
    0, elongated, extends caudally to the caudodorsal process;

1, short, does not extend caudally to the caudodorsal process.

53. Dentary; coronoid process dorsally expanded (Sereno, 1986):
    0, absent;
    1, present.
54. Mandibular buccal emargination (Langer & Benton 2006):
    0, absent, lateral dentary surface smooth;
1, present, lateral dentary surface with a caudal crest bordering an emargination which encompasses half of the dentary width.
55. Splenial; milohyoyd foramen (Rauhut, 2003):
    0, absent;
    1, present.
56. Surangular; lateral surface (Tykoski & Rowe 2004):
    0, evenly convex;
    1, bears a prominent horizontal shelf.
57. Mandible; articular glenoid location (Gauthier, 1986):
    0, at the dorsal margin of the dentary;
    1, well ventral of the dorsal margin of the dentary.
58. Articular, retroarticular process (Yates 2003):
    0, shorter than the height of the mandible ventral to the glenoid;
    1, longer than the height of the mandible ventral to the glenoid.
59. Mandibular fenestra rostrocaudal length (Butler, 2005):
    0, more than maximum depth of dentary ramus;
    1, reduced, less than maximum depth of dentary ramus.
60. Premaxilla; teeth number (Nesbitt, 2011) ORDERED:
    0, three;
    1, four;
    2, five or more.
61. Premaxilla; tooth row (Tykoski & Rowe 2004):
    0, extends ventrally below the internal narial fenestra;
1, does not extend caudally farther than the cranial edge of the internal narial fenestra.
62. Maxilla; teeth number (Nesbitt et al. 2009) ORDERED:
    0, 15 or less;
    1, more than 15 but less than 20;
    2, 20 or more.
63. Teeth at the caudal half of maxilla/dentary; caudal edge (Nesbitt, 2011):
    0, concave or straight;
    1, convex.
64. Middle maxillary/dentary teeth; serrations (Irmis et al. 2007) ORDERED:
    0, small (c. 10 denticles per mm) forming right angles with the tooth margin;
    1, large (c. 5 denticles per mm) but mostly forming right angles with the tooth margin;
    2, larger forming oblique angles with the margin of the tooth.
65. Maxillary/dentary teeth; extensive planar wear facets across multiple teeth (Weishampel & Witmer 1990):
    0, absent;
    1, present.
66. Maxillary/dentary teeth; medial or lateral overlap of adjacent crowns (Sereno 1986):
    0, absent;
    1, present.
67. Maxillary/dentary teeth; some with moderately developed lingual expansion of crown cingulum (Sereno 1986):

0, absent;

1, present.

68. Maxillary/dentary teeth; crown shape (Sereno 1986):

0, apicobasally tall and blade like;

1, apicobasally short and subtriangular.

69. Middle maxillary/dentary teeth, distal margin (Sereno 1986):

0, never or subtly expanded at the base;

1, clearly expanded at the base.

70. Middle maxillary/dentary teeth; long axis (new):

0, caudaly curved;

1, straight.

71. Dentary teeth; number (Smith *et al.* 2007):

0, maximal of 25;

1, more than 25.

72. Dentary teeth; rostral portion of the bone (Kammerer *et al.* 2012):

0, teeth remain relatively same size throughout rostral portion of dentition;

1, teeth significantly decrease in size rostrally.

73. Dentary teeth; rostral portion of the bone, long axis (Kammerer *et al.* 2012):

0, vertical;

1, inclined rostrally.

74. Marginal teeth, crown shape in distal-medial view (Sereno 1986):

0, blade-like;

1, labiolingualy expanded.

75. Pterygoid teeth on palatal process (Rauhut, 2003):

0, present;

1, absent.

76. Axis; dorsal margin of the neural spine (Nesbitt, 2011):

0, expanded caudodorsally;

1, arcs dorsally where the cranial portion height is equivalent to the caudal height.

77. Axis; parapophysis development (Tykoski & Rowe 2004):

0, well developed;

1, reduced.

78. Axis; epipophysis on postzygapophysis (Rauhut, 2003):

0, absent;

1, present.

79. Cervical vertebrae 3-5, centrum length (Sereno 1991):

0, shorter or the same length as the mid dorsal;

1, longer than mid dorsal.

80. Cervical vertebrae; deep recesses on the cranial face of the neural arch lateral to the neural canal (Nesbitt, 2011):

0, absent;

1, present.

81. Third cervical vertebra; centrum length (Gauthier, 1986):

0, subequal to the axis centrum;

1, longer than the axis centrum.

82. Cervical vertebrae; neural spine shape (Yates, 2007):

0, not twice as long (at the midheight) as height;

1, at least twice at midheight as long as height.

83. Cranial cervical vertebrae, caudal chonos (Langer & Benton, 2006) ORDERED:

  0, absent
  1, as a shallow fossa;
  2, as a deep excavation with a lamina covering the rostral extent.
 84. Post-axial cranial cervical vertebrae; epipophyses (Gauthier, 1986):
  0, absent;
  1, present.
 85. Cervical vertebrae 6-9; epipophyses (Sereno et al., 1993):
  0, absent;
  1, present.
86. Cervical vertebrae; cranial portion of the centrum, pneumatic features/ pleurocoels (Holtz, 1994):
  0, absent;
  1, present.
 87. Cervical vertebrae; neural arch (Galton & Upchurch 2004):
0, neural arch (from the base of neural canal to the top of postzygapophysis) higher than caudal articular facet of the centrum;
  1, neural arch lower than caudal articular facet of the centrum.
 88. Cervical vertebrae; middle portion of the ventral keel (Nesbitt, 2011):
  0, dorsal to the ventralmost extent of the centrum rim;
  1, extends ventral to the centrum rims.
 89. Cervical ribs; length of relative to the centrum (Tykoski & Rowe 2004):
  0, no more than twice longer;
  1, at least twice longer.
 90. Presacral vertebrae; parapophysis position (Langer & Benton 2006):
  0, parapophyses do not contact centrum in vertebra caudal to the twelfth presacral;
  1, parapophyses contact centrum in vertebra caudal to the twelfth presacral.

91. Caudal cervical and/or dorsal vertebrae; hyposphene-hypantrum accessory articulations (Gauthier, 1986):
  0, absent;
  1, present.
 92. Trunk vertebrae; neural spine distal lateromedial expansion (Langer, 2004):
  0, absent;
  1, present
93. Trunk vertebrae; neural spine, distal craniocaudal length (Bittencourt et al. 2014):
  0, at least twice longer than the base;
  1, less than twice longer than the base.
 94. Trunk vertebrae; crest onto the lateral wall of caudal chonos (Yates 2004):
  0, absent;
  1, present.
 95. Caudal trunk centra; shape (Rauhut 2003):
  0, short, centra are significantly shorter than high;
  1, centra are approximately as long as high, longer than high.
 96. Trunk vertebrae; transverse process shape (Tykoski & Rowe 2004):
  0, subrectangular;
  1, subtriangular.
 97. Trunk vertebrae; infradiapophyseal fossa (Yates, 2007):
  0, absent;
  1, present.
 98. Sacral centra (Nesbitt, 2011):

0, separate;

1, co-ossified at the ventral edge.

99. Sacral vertebrae; incorporation of trunk vertebrae (Sereno et al. 1993):

0, free from the sacrum;

1, incorporated into the sacrum with ribs transverse processes articulating with the pelvis.

100. Sacral vertebrae, incorporation of caudal vertebrae (Galton, 1976):

0, free from the sacrum;

1, incorporated into the sacrum with ribs transverse processes articulating with the pelvis.

101. Number vertebra fully incorporated to the sacrum (Gauthier, 1986):

0, 2;

1, 3 or more.

102. Sacral ribs (Nesbitt 2011):

0, almost entirely restricted to a single sacral vertebra;

1, shared between two sacral vertebrae.

103. First primordial sacralvertebra; articular surface of the rib (Langer & Benton, 2006):

0, circular;

1, C-shaped in lateral view.

104. Sacral transverse process; development (Langer & Benton, 2006):

0, craniocaudally short not roofing the space between ribs;

1, craniocaudally long, roofing the space between ribs.

105. Sacral ribs depth (Langer & Benton, 2006):

0, as deep as half of the medial ilium depth;

1, deeper than half of the ilium depth.

106. Sacral rib and transverse process; lateral notch between elements (Bittencourt et al. 2014):

0, absent;

1, present.

107. First three caudal vertebrae; orientation of the neural spine (Langer & Benton, 2006):

0, caudally inclined;

1, vertical.

108. Middle caudal centra; length (Yates, 2003):

0, centra longer than twice the height of the cranial articular facet;

1, centra shorter than twice the height of the cranial articular facet.

109. Distal caudal vertebrae; prezygapophyses (Gauthier, 1986):

0, length is less than a quarter of the adjacent centrum;

1, elongated, more than a quarter of the adjacent centrum.

110. Scapula; cranial margin (Nesbitt 2011):

0, straight convex or partially concave;

1, markedly concave.

111. Scapula; blade height (Sereno, 1999):

0, less than 3 times distal width;

1, more than 3 times distal width.

112. Coracoid; caudal margin (Nesbitt, 2011):

0, continuous (subcircular in lateral view);

1, with notch ventral to the glenoid.

113. Coracoid; post glenoid process (Nesbitt, 2011):

0, absent or short;

1, extending caudal to glenoid.

114. Limbs; humerus+radius/femur+tibia length ratio (Gauthier, 1984):
0, more than 0.55;
1, less than 0.55.

115. Humerus; apex of deltopectoral crest, situated at a point corresponding to (Bakker & Galton, 1974) ORDERED:
0, about or less than 30% down the length of the humerus;
1, between 30% and 43% down the length of the humerus.
2, about or more than 43% down the length of the humerus.

116. Humerus; deltopectoral crest size (Yates, 2007):
0, low;
1, expanded.

117. Humerus; deltopectoral crest shape (Yates, 2007):
0, low rounded crest;
1, subtriangular, concave betwem apec and articulation;
2, subrectangular, convex/stragr between apex and articulation..

118. Limbs; humerus/femur length ratio (Novas, 1996):
0, humerus longer than or subequal to 0.6 of the length of the femur;
1, humerus shorter than 0.6 of the length of the femur.

119. Humerus; distal end width (Langer & Benton, 2006):
0, narrower or equal to 30% of humerus length;
1, wider than 30% of humerus length.

120. Humerus; shape in lateral view (Rauhut, 2003):
0, straight;
1, sigmoid.

121. Forelimb; humerus/radius length ratio (Langer & Benton, 2006):
0, radius longer than 80% of humerus length;
1, radius shorter than or suequal to 80% of humerus length.

122. Ulna; olecranon process (Wilson & Sereno 1998):
0, short;
1, enlarged and strongly striated.

123. Distal carpal 1; articulation (Rauhut, 2003) ORDERED:
0, does not articulate with metacarpal II;
1, articulates to metacarpal II.
2, caps metacarpal II.

124. Distal carpals; number of ossified elements (Sereno, 1999):
0, 5;
1, 4.

125. Medialmost distal carpal; size (Gauthier, 1986):
0, subequal other distal carpals;
1, significantly larger than other distal carpals.

126. Manus; length measured as the average length of digits I-III (Gauthier, 1986):
0, accounts for less than 0.4 of the total length of humerus plus radius;
1, more than 0.4 of the total length of humerus plus radius.

127. Metacarpals; proximal ends (Sereno & Wild, 1992):
0, overlap one another;
1, abut one another without overlapping.

128. Manus; ungual phalanges (Gauthier, 1986):
0, blunt unguals on at least digits II and III;
1, trenchant unguals on digits I to III.

129. Metacarpals II-III; extensor pits on distal/dorsal portion (Sereno et al. 1993):

0, absent or shallow;
1, deep.

130. Digit I; metacarpal/ungual phalanx length ratio (Sereno, 1999):
    0, metacarpal subequal or longer than ungual;
    1, metacarpal shorter than ungual.
131. Metacarpal I; width (at the middle of the shaft)/length ratio (Bakker & Galton, 1974):
    0, width less than 0.35 of the length of the bone;
    1, width more than 0.35 of the length of the bone.
132. Metacarpal I; distal condyles (Bakker & Galton, 1974):
    0, approximately aligned or slightly offset;
    1, lateral condyle strongly distally expanded relative to medial condyle.
133. Manual digit I; first phalanx, twisting of the transverse axis (Sereno, 1999):
    0, not twisted;
    1, twisted.
134. Manual digit I; first phalanx (Gauthier, 1986):
    0, not the longest non ungual phalanx of the manus;
    1, longest non ungual phalanx of the manus.
135. Manual unguals; digit I & II length ratio (Yates, 2007):
    0, ungual of digit II as long as or longer than that of I;
    1, ungual of digit II shorter than that of I.
136. Metacarpals; length ration between II and III (Gauthier, 1986):
    0, metacarpal II shorter than metacarpal III;
    1, metacarpal II equal to or longer than metacarpal III.
137. Manual digit II; pre-ungual phalanx and phalanx 1 length ratio (Rauhut 2003):
    0, pre-ungual phalanx equal or shorter;
    1, pre-ungual phalanx longer.
138. Metacarpals; width (at midlength) ratio between elements II & III (Rauhut 2003):
    0, equal;
    1, metacarpal III at least 30% narrower.
139. Manual digit IV; number of phalanges (Gauthier, 1986) ORDERED:
    0, 3 or more;
    1, 2;
    2, 1 or none.
140. Metacarpal IV; shaft width (Sereno et al. 1993):
    0, about the same width as that of metacarpals I-III;
    1, significantly narrower than that of metacarpals I-III.
141. Manual digit V; phalanges (Bakker & Galton, 1974):
    0, one or more phalanges;
    1, no phalanges.
142. Digit V (Bakker & Galton, 1974):
    0, present;
    1, absent.
143. Ilium; preacetabular ala, tip shape (Galton, 1976):
    0, pointed, with vertex projected cranially;
    1, rounded.
    2, squared.
144. Ilium; preacetabular ala length (Galton, 1976):
    0, does not extend cranial to the cranial margin of the pubic peduncle
    1, extends cranial to the cranial margin of the pubic peduncle.

145. Ilium; supraacetabular crest, position of thicker (lateromedially) portion (Yates 2003):
    0, at the center of the acetabulum;
    1, closer to pubic peduncle.
146. Ilium; supraacetabular crest, extension on pubic peduncle (Nesbitt et al. 2009):
    0, ends before the distal margin of the peduncle;
    1, extends along the peduncle length.
147. Ilium; fossa for the attachment of m. caudifemoralis brevis (Gauthier & Padian, 1985) ORDERED:
    0, absent;
    1, present as an embankment on the lateral side of the caudal portion of the ilium;
    2, present as a fossa on the ventral surface of postacetabular part of ilium.
148. Ilium; ventral margin of the acetabular wall (Bakker & Galton, 1974) ORDERED:
    0, convex;
    1, slightly concave, straight or slightly convex;
    2, markedly concave.

149. Ilium; acetabular antitrochanter (Sereno & Arcucci 1994a):
    0, absent or just a slightly planar surface;
    1, raised shelf.
150. Ilium; brevis fossa lateral wall (Smith et al. 2007):
    0, vertical;
    1, lateroventraly directed.
151. Ilium; pubic peduncle distal articulation (Smith et al. 2007):
    0, not expanded;
    1, expanded distally.
152. Ilium; ischiadic peduncle orientation in lateral view (Langer & Benton, 2006):
    0, mainly vertical;
    1, well expanded caudal to the cranial margin of the postacetabular embayment.
153. Ilium; strong pillar caudal to the preacetabular embayment (Nesbitt 2011):
    0, absent;
    1, present.
154. Ilium; dorsal margin shape (Gauthier, 1986):
    0, sigmoid;
    1, entirely convex.
155. Ilium; position of dorsal margin concavity (new):
    0, above the acetabulum;
    1, caudally displaved.
156. Ilium; maximum length of the postacetabular ala (Yates, 2007):
    0, shorter than or subequal to the space between the pre and postacetabular embayments;
    1, longer than the space between the pre and postacetabular embayments.
157. Ilium; pubic articulation orientation (Langer & Benton, 2006) ORDERED:
    0, ventral;
    1, cranioventral
    2, cranial.
158. Pubis length (Novas, 1996):
    0, less than 70% or equal of femoral length;
    1, more than 70% or more of femoral length.
159. Pubis orientation (Sereno, 1986):
    0, cranioventral;
    1, rotated caudoventrally to lie alongside the ischium (opisthopubic).
160. Pubis; distal end (Gauthier, 1986) ORDERED:

      0, unexpanded;

      1, expanded relative to the shaft

      2, expanded and at least twice the breadth of the pubic shaft (pubis boot).

161. Pubis; medial articulation of the pair (Tykoski 2005):

      0, complete, reaches the distal edge of the pubis;

      1, forms a medial hiatus on the distal portion (bevel).

162. Pubis; distal apron (Langer & Benton, 2006):

      0, straight;

      1, lateral portion flipped caudally.

163. Pubis; proximal portion (Nesbitt, 2011):

      0, articular surfaces with the ilium and the ischium continuous;

      1, articular surfaces with the ilium and the ischium separated by a gap.

164. Pubis; shaft in lateral view (Harris, 1998):

      0, cranially bowed;

      1, straight.

165. Pelvis; ischio-pubis contact (Benton & Clark, 1988):

      0, present and extended ventrally;

      1, present and reduced to a thin proximal contact.

166. Pubis; distal pubis mediolateral width (Galton, 1976):

      0, nearly as broad as proximal width of the bone;

      1, significantly narrower than proximal width of the bone.

167. Ischium; medial contact with antimere (Novas 1996):

      0, restricted to the ventral edge;

      1, more dorsaly extensive contact.

168. Ischium; dorsolateral sulcus (Yates, 2003):

      0, absent;

      1, present.

169. Ischium; outline of the distal portion (Sereno, 1999):

      0, thin, plate-like;

      1, rounded or elliptical;

      2, subtriangular.

170. Ischium; distal portion (Smith & Galton, 1990):

      0, unexpanded;

      1, expanded relative to the ischial shaft.

171. Ischium; proximal articular surfaces (Irmis et al. 2007) ORDERED:

      0, continuous ilium and pubis articular surfaces;

      1, ilium and pubis articular surfaces continuous but separated by a fossa;

      2, ilium and pubis articular surfaces separated by a non-articulating concave surface.

172. Ischium; length relative to the dorsal margin of the iliac blade minus the preacetabular ala (Nesbitt, 2011):

      0, about the same length or shorter;

      1, markedly longer.

173. Femur; proximal portion, craniomedial tuber (Gauthier, 1986) ORDERED:

      0, small, unprojected, rounded;

      1, small and angled (separated from the caudomedial by the lig sulcus);

      2, offset medially or caudally relative to the caudomedial tuber.

174. Femur; ligament sulcus (new):

      0, does not form a medial excavation in proximal view;

      1, forms a medial excavation in proximal view.

175. Femur; proximal portion, caudomedial tuber (Novas, 1996) ORDERED:

      0, present and largest of the proximal tubera.

1, small;

2, absent.

176. Femur; proximal portion, craniolateral tuber (Sereno & Arcucci, 1994a):

0, absent (the craniolateral face is flat or equally rounded);

1, present.

177. Femur; medial articular surface of the head in dorsal view (Nesbitt, 2011):

0, rounded;

1, flat/straight.

178. Femur; head, expansion/shaft transition (Sereno & Arcucci, 1994a) ORDERED:

0, smooth transition from the femoral shaft to the head;

1, kinked transition from the femoral shaft to the head;

2, kinked transition and expanded head.

179. Femur; head long axis angle to the distal intercondylar line (Benton & Clark, 1988) ORDERED:

0, 45° or more

1, 20-45°;

2, 0-20°.

180. Femur; head in medial and lateral views (Sereno & Arcucci, 1994a):

0, rounded;

1, hook shaped.

181. Femur; dorsolateral trochanter (Nesbitt, 2011):

0, absent;

1, present.

182. Femur; "lesser" trochanter (Bakker & Galton, 1974) ORDERED:

0, absent;

1, present and forms a steep margin with the shaft but is completely connected to it;

2, present and separated from the shaft by a marked cleft;

3; present and approaches the proximal articulation of the bone.

183. Femur; medial articular facet of the proximal portion in caudomedial view (Nesbitt, 2011):

0, rounded;

1, straight.

184. Femur; craniolateral surface of the femoral head (Sereno & Arcucci, 1994a):

0, smooth, featureless;

1, ventral emargination present.

185. Femur; "trochanteric shelf" (Gauthier, 1986):

0, absent;

1, present.

186. Femur; head, facies articularis antitrochanterica (Novas, 1996):

0, level with "greater trochanter";

1, ventrally descended.

187. Femur; "greater trochanter" shape (Sereno, 1999):

0, rounded;

1, angled.

188. Femur; transverse groove on proximal surface (Ezcurra, 2006):

0, absent;

1, present.

189. Femur; "lesser" trochanter, lateromedial position (Yates, 2007):

0, closer to the medial edge;

1, closer to the lateral margin.

190. Femur; fourth trochanter shape (Gauthier, 1986):

0, mound-like or subtle crest;

1, flange.

191. Femur; fourth trochanter; symmetry (Langer & Benton, 2006):

0, symmetrical, distal and proximal margins forming similar low angle slopes to the shaft;

1, asymmetrical, distal margin forming a steeper angle to the shaft.

192. Femur; bone wall. thickness at or near mid shaft (Nesbitt, 2011):

0, thickness diameter > 0.3;

1, thin, thickness diameter >0.2, <0.3.

193. Femur; distal condyles, extension of the caudal division (Nesbitt, 2011):

0, less than 1/4 the length of the shaft;

1, between 1/4 and 1/3 the length of the shaft.

194. Femur cranial surface of the distal portion (Nesbitt et al. 2009):

0, smooth;

1, distinct scar orientated mediolaterally.

195. Femur; crista tibiofibularis size/shape (Sereno & Arcucci, 1994a) ORDERED:

0, smaller in size to the lateral condyle;

1, larger or equal than the lateral condyle;

2, larger/equal and globular.

196. Femur; craniomedial corner of the distal end (Nesbitt *et al*. 2009):

0, rounded;

1, squared off near 90° or acute.

197. Femur; cranial margin in distal view (new):

0, concave;

1, straight or convex.

198. Hindlimb; tibia or fibula relative length to the femur (Gauthier, 1986):

0, femur longer or about the same length as the tibia/fibula;

1, tibia/fibula longer than femur.

199. Tibia; depth of the sulcus lateral to cnemial crest (Langer *et al*. 2011):

0, no deeper than 10% of the length of proximal surface of tibia;

1, more than 10% of the length of proximal surface of tibia.

200. Tibia; cnemial crest (Benton & Clark, 1988) ORDERED:

0, absent or just a slight bump;

1, present and straight;

2, present arcs craniolaterally.

201. Tibia; proximal portion, fibular condyle (Langer & Benton, 2006) ORDERED:

0, offset cranially from the medial condyle;

1, level with the medial condyle at its caudal border

2, displaced caudally.

202. Tibia lateral side of the proximal portion (Gauthier, 1986) ORDERED:

0, smooth or scared;

1, dorsoventrally oriented crest present,

2, well developed ridge.

203. Tibia; separation of the proximal condyles (Rauhut, 2003):

0, separated by a shallow notch;

1, separated by a deep groove.

204. Tibia; separation of the condyles in proximal view (new):

0, single notch/ groove;

1, two separated notches.

205. Tibia; distal portion, caudolateral flange (Novas, 1992) ORDERED:

0, absent;

    1, present;

    2, present and extends well lateral to the craniolateral corner.

206. Tibia; distal end, caudal margin shape (Irmis *et al*. 2007):

    0, straight or convex;

    1, concave.

207. Tibia; distal surface outline (Rauhut, 2003):

    0, rounded or subquadrangular (approximately as wide as long);

    1, mediolaterally expanded.

208. Tibia; distal portion; caudomedial surface (Nesbitt, 2011):

    0, rounded surface;

    1, distinct proximodistally oriented ridge present.

209. Tibia; distal portion, lateral side (Novas, 1996):

    0, smooth rounded;

    1, proximodistally oriented groove.

210. Tibia; distal surface, caudomedial notch (Yates, 2007):

    0, absent;

    1, present.

211. Tibia; astragalar articulation (Novas, 1996):

    0, tibia articulates with astragalus medially to the ascending process;

    1, tibia covers the medial and caudal portion of the dorsal surface of astragalus.

212. Astragalus; caudal margin, dorsally expanded process (Sereno & Arcucci, 1994):

    0, absent or poorly expanded;

    1, expanded into a distinct raised process caudal to ascending process.

213. Astragalus; proximal margin in caudal view (new):

    0, straight at the lateralmos portion;

    1, depressed at the lateralmost portion (with subtle raided margin medial to it).

214. Astragalus; cranial ascending process (Gauthier, 1986):

    0, absent;

    1, present.

215. Astragalus; tibial articulation caudal to the ascending process (Langer & Benton, 2006):

    0, continuous to the medial articulation surface;

1, markedly rimmed and elliptical fossa (separated by a ridge or step from the medial surface).

216. Astragalus; proximal articular facet for fibula (Langer & Benton, 2006) ORDERED:

    0, equal more than 0.3 of the transverse width of the bone;

    1, less than 0.3 of the transverse width of the bone;

    2, vertical (no horizontal platform).

217. Astragalus; caudal groove (Nesbitt, 2011):

    0, present;

    1, absent.

218. Astragalus; shape of the craniomedial margin (Yates, 2007):

    0, obtuse or forming a right angle;

    1, acute.

219. Astragalus; medial portion of the tibial facet (Benton, 1999):

    0, concave or flat;

    1, divided into caudomedial and craniolateral basins.

220. Astragalus; shape (new):

    0, more than 80% broad lateromedialy than craniocaudally;

    1, less than 80% broad craniocaudally than lateromedialy.

221. Astragalus; cranial margin (new):

    0, straight or concave;

    1, deeply excavated with a groove extending along the distal surface of the bone.

222. Astragalus; cranial ascending process, cranial margin (Langer, 2004) ORDERED:

    0, continuous to the cranial surface of the astragalar body;

    1, separated from the cranial surface of the astragalar body by an oblique slope.

    2, separated from the cranial surface of the astragalar body by a platform.

223. Astragalus; caudolateral process (new):

    0, continuous to the caudal margin of the bone;

    1, displaced cranially.

224. Astragalus-calcaneum; articulation (Sereno & Arcucci, 1994a):

    0, free;

    1, co-ossified.

225. Calcaneum; calcaneal tuber (Gauthier, 1986):

    0, present;

    1, absent.

226. Calcaneum; tibial articulation (Langer *et al*. 2011):

    0, absent;

    1, present.

227. Calcaneum; articular surface for the fibula (Novas, 1996):

    0, convex;

    1, concave.

228. Calcaneum; shape (Langer & Benton, 2006):

0, proximodistally compressed and subtriangular, with short caudal projection and medial processes;

    1, transversely compressed and subrectangular, reduced projection and processes.

229. Distal tarsal 3; articulation with metatarsus (Butler et al. 2008):

    0, articulates with metatarsal III only;

    1, articulates with metatarsal II and III.

230. Distal tarsal 4; caudal prong (Langer & Benton, 2006):

    0, blunt;

    1, pointed.

231. Distal tarsal 4; medial process (Nesbitt 2011):

    0, absent;

    1, distinct in the craniocaudal middle of the element.

232. Distal tarsal 4; proximal surface (Sereno & Arcucci, 1994a):

    0, flat;

    1, distinct proximally raised region on the caudal portion.

233. Metatarsus; maximum length (Benton, 1999):

    0, equal or shorter than 50% of tibial length;

    1, longer than 50% of tibial length.

234. Metatarsus; metatarsals I and II, articulation (Gauthier, 1986):

    0, Metatarsal I reaches the proximal surface of metatarsal II;

    1, Metatarsal I does not reach and attaches onto the medial side of metatarsal II.

235. Metatarsus; metatarsals II and IV; length relation (Gauthier, 1986):

    0, Metatarsal IV longer than metatarsal II;

    1, Metatarsal IV subequal or shorter than metatarsal II.

236. Metatarsal IV; distal articulation surface (Sereno, 1999):

    0, broader than deep to as broad as deep;

    1, deeper than broad.

237. Metatarsal IV; proximal portion (Sereno, 1999):

    0, narrow;

1, expanded, overlaping the cranial surface of metatarsal V.

238. Metatarsal IV; shape (Novas, 1996):
    0, straight;
    1, laterally curved at the distal end.

239. Metatarsus; metatarsals III and V; length relation (Carrano *et al*. 2002):
    0, Metatarsal V equal to or longer than 50% of metatarsal III;
    1, Metatarsal V shorter than 50% of metatarsal III.

240. Metatarsal V; proximal (Yates, 2003) ORDERED:
    0, unexpanded;
    1, expanded;
    2, expanded, with a width more than 30% the length of the bone.

241. Metatarsal V; distal tip (Gauthier, 1984):
    0, blunt and with phalanges;
    1, without phalanges and tapers to a point.

242. Osteoderms; dorsal to the vertebral column (Gauthier, 1984):
    0, absent;
    1, present.

243. Jugal; total length relation relative to that of the skull (new):
    0, more than 35%;
    1, 35% or less.

244. Jugal, caudal process; pecidel projecting the forking part of the bone caudally (new):
    0, presente;
    1, absent.

245. Jugal, caudal process; reaches the caudal margin of the ventral temporal fenestra (new):
    0, yes;
    1, no.

246. Premaxillary teeth, serration in the mesial margin (Rowe, 1989):
    0, present;
    1, absent.

247. Ilium, pubic peduncle, shape; width (craniocaudal) at mid-length vs total length (Galton, 1976):
    0, less than 0,5;
    1, 0,5 or more.

248. Ilium, pubic peduncle, position; angle of the long axis to that of the long axis of the iliac lamina (new) ORDERED:
0, less 45 degrees;   1, about 45 degrees;
    2, less 45 degrees.

249. Ilium, dorsal lamina; depth relative to the acetabulum (Makovicky & Sues, 1998):
0, shallow that two times;   1, two times deeper or more.

250. Postfrontal (Gauthier 1986):
    0, present;
    1, absent.

251. Postparietal (Jull 1994):
    0, present;
    1, absent.

252. Postemporal opening (Sereno & Novas 1994):
    0, present minimally as a fissure;
    1, absent.

253. Basipterygoid process, proximal part; angle to the proximal portion of the cultriform process (Butler et al. 2008):
   0, less than 90°;
   1, 90° or more than 90°.
254. Parabasisphenoid, foramina for entrance of cerebral branches of internal carotid artery into the braincase; position (Nesbitt, 2011):
   0, on the ventral surface;
   1, on the lateral surface.
255. Parabasisphenoid, lateral wall, caudoventral corner; semilunar depression, presence (Gower and Sennikov, 1996):
   0, present;
   1, absent.
256. Basipterygoid process, shape (new):
   0, rounded;
   1, mediolaterally compressed.

Details of the feeding habits inference.

The ancestral diet of dinosaurs is a topic of intense debates [3, 65-67]. One of the goals of this study is to revaluate previous hypotheses in the context of the current paradigm concerning the phylogenetic relationships of dinosaurs in the lights of new discoveries, such as those described in this study.

As it is impossible to analyse the behaviour of extinct taxa *in vivo,* their diet is inferred based on anatomical (i.e. form-function approach) and historical (e.g. Extant Phylogenetic Bracket) evidences (*sensu* [67]). For early dinosaurs, anatomical evidences of feeding behaviour come mainly from the study of tooth morphology [66]. Recently, [3] concluded that the acquisition of three different morphologies (i.e. character states) was significantly correlated with an inferred omnivore/herbivore diet, namely: large/coarse tooth serrations, mesiodistally expanded tooth crowns above the root in cheek teeth, and overlap of adjacent tooth crowns. Other morphologies such as subtriangular tooth crowns with moderately developed lingual expansion (=cingulum) were "weakly" correlated (i.e. only under Deltran optimization) to a omnivore/herbivore diet. Based on that study, we inferred the diet (faunivory or omnivory/herbivory) for all taxa examined in our study using the following parameter: only taxa exhibiting states '0' or '1' for character 64 and state '0' for characters 66-69 of the present analysis (see list above) were treated as faunivores, as state '2' of character 64 and '1' of characters 66-69 represent the morphologies typically associated to herbivory/omnivory.

Faunivory and omnivory/herbivory were then treated as states of a character (feeding behaviour) and scored for the taxa following the above mentioned criterion. The

software *Mesquite* [68] was employed to trace the evolution of this character and the ancestral states (states inferred for the nodes) were reconstructed using Parsimony methods – no optimization criteria (Acctran or Deltran) were applied (i.e. ambiguities were treated as such). Still, because of the lack of consensus in the distinct phylogenetic hypotheses presented recently (e.g. [3]; this study), analyses were conducted in alternative scenarios: 1 - in the phylogenetic hypothesis preferred here, ancestral diet is reconstructed as faunivory for both Dinosauria and Saurischia; 2 - in the phylogenetic hypothesis preferred here, but with silesaurids as the sister group to Dinosauria, ancestral diet is reconstructed as ambiguous for Dinosauria and as faunivory for Saurischia; 3 - in the phylogenetic hypothesis preferred here, but with silesaurids as the sister group to Dinosauria and *Lewisuchus admixtus* taking part on the earliest Silesauridae spit, ancestral diet is reconstructed as faunivory for both Dinosauria and Saurischia; 4 - in the phylogenetic hypothesis preferred here, but with Sauropodomorpha taking part on the earliest Saurischia split, ancestral diet is reconstructed as faunivory for both Dinosauria and Saurischia; 5 - in the phylogenetic hypothesis preferred here, but with Sauropodomorpha taking part on the earliest Saurischia split and silesaurids as the sister group to Dinosauria, ancestral diet is reconstructed as ambiguous for Dinosauria and as faunivory for Saurischia; 6 - in the phylogenetic hypothesis preferred here, but with Sauropodomorpha taking part on the earliest Saurischia split, silesaurids as the sister group to Dinosauria, and *Lewisuchus admixtus* taking part on the earliest Silesauridae split, ancestral diet is reconstructed as faunivory for both Dinosauria and Saurischia; 7 - in the phylogenetic hypothesis preferred here, but with *Buriolestes schultzi* as the sister-taxon to Eusaurischia, ancestral diet is reconstructed as faunivory for both Dinosauria and Saurischia; 8 - in the phylogenetic hypothesis preferred here, but with *Buriolestes schultzi* as the earliest diverging theropod, ancestral diet is also reconstructed as faunivory for both Dinosauria and Saurischia.

SUPPLEMENTAL REFERENCES FOR CHAPTER 2

1. Bittencourt, J. S., Arcucci, A. B., Marsicano, C. A., and Langer, M. C. (2014). Osteology of the Middle Triassic archosaur *Lewisuchus admixtus* Romer (Chañares Formation, Argentina), its inclusivity, and relationships among early dinosauromorphs. J. Syst. Palaeontol. 13, 189–219.
2. Irmis, R. B., Nesbitt, S. J., Padian, K., Smith, N. D., Turner, A. H., Woody, D, and Downs, A. (2007). A Late Triassic dinosauromorph assemblage from New Mexico and the rise of dinosaurs. Science 317, 358–361.
3. Nesbitt, S. J., Sidor, C. A., Irmis, R. B., Angielczyk, K. D., Smith, R.M.H., and Tsuji, L. A. (2010). Ecologically distinct dinosaurian sister-group shows early diversification of Ornithodira. Nature 464, 95–98.
4. Nesbitt, S. J. (2011). The early evolution of archosaurs: relationships and the origin of major clades. Bull. Am. Mus. Nat. Hist. 352, 1–292.

5. Langer, M. C., and Benton, M. J. (2006). Early dinosaurs: A phylogenetic study. J. Syst. Palaeontol. 4, 309–358.

6. Sereno, P. C., and Arcucci, A. B. (1994). Dinosaurian precursors from the Middle Triassic of Argentina: *Marasuchus lilloensis*, n. gen. J. Vert. Paleontol. 14, 53–73.

7. Sereno, P. C., and Arcucci, A. B. (1994). Dinosaurian precursors from the Middle Triassic of Argentina: *Lagerpeton chanarensis*. J. Vert. Paleontol. 13, 385–3991).

8. Rowe, T. (1989). A new species of the theropod dinosaur *Syntarsus* from the Early Jurassic Kayenta Formation of Arizona. J. Vert. Paleontol. 9, 125–36.

9. Yates, A. M. (2007). The first complete skull of the Triassic dinosaur *Melanorosaurus* Haughton (Sauropodomorpha:Anchisauria). Spec. Pap. Palaeontol. 77, 9–55.

10. Ezcurra, M. D. (2010). A new early dinosaur (Saurischia: Sauropodomorpha) from the Late Triassic of Argentina: a reassessment of dinosaur origin and phylogeny. J. Syst. Palaeontol. 8, 371-425.

11. Bakker, R. T., and Galton, P. M. (1974). Dinosaur monophyly and a new class of vertebrates. Nature 248, 168–172.

12. Gauthier, J. A. (1984). PhD thesis, University of California, Berkeley.

13. Gauthier, J. A. (1986). Saurischian monophyly and the origin of birds. Mem. Calif. Acad. Sci. 8,1–55.

14. Gauthier, J. A., and Padian, K. (1987). Phylogenetic, functional, and aerodynamic analyses of the origin of birds and their flight. In The Beginnings of Birds: Proceedings of the International Archaeopteryx Conference, M. K., Hecht, J. H. Ostrom, G. Viohl, P. Wellnhofer ed. (Eichstätt: Freunde des Juras-Museums), pp. 185–197.

15. Sereno, P. C. (1986). Phylogeny of the bird-hipped dinosaurs (Order Ornithischia). Natl. Geogr. Res. 2, 234–256.

16. Sereno, P. C. (1991). Basal archosaurs: phylogenetic relationships and functional implications. J. Vert. Paleont. 11.S4, 1–53.

17. Sereno, P. C. (1999). The evolution of dinosaurs. Science 284, 2137–2147.

18. Benton, M. J., and Clark, J. M. (1988). Archosaur phylogeny and the relationships of the Crocodylia. In The Phylogeny and Classification of the Tetrapods. Vol. 1: Amphibians and Reptiles, M. J. Benton ed. (Oxford: Clarendon Press), pp. 295–338.

19. Benton, M. J. (1990). Origin and interrelationships of dinosaurs. In The Dinosauria, D. B. Weishampel, P. Dodson, H. Osmolska, ed. (Berkeley: Univ. of California Press), pp. 11–30.

20. Benton, M. J. (1999). *Scleromochlus taylori* and the origin of dinosaurs and pterosaurs. Philos. Trans. R. Soc. Lond. B Biol. Sci. 354, 1423–1446

21. Galton, P. M. (1976). Prosauropod dinosaurs (Reptilia:Saurischia) of North America. Postilla 169, 1–98.

22. Rowe, T., and Gauthier J. A. (1990). Ceratosauria. In The Dinosauria, D. B. Weishampel, P. Dodson, H. Osmolska, ed. (Berkeley: Univ. of California Press), pp. 151–168.

23. Smith, D., and Galton, P. M. (1990). Osteology of *Archaeornithomimus asiaticus* (Upper Cretaceous, Iren Dabasu Formation, People's Republic of China). J. Vert. Paleont. 10, 255–265.

24. Novas, F. E. (1992). Phylogenetic relationships of the basal dinosaurs, the Herrerasauridae. Palaeontology 35, 51–62.

25. Novas, F. E. (1996). Dinosaur monophyly. J. Vert. Paleontol. 16, 723–741.

26. Sereno, P. C., and Wild, R. (1992). *Procompsognathus*: theropod,"thecodont" or both?. J. Vert. Paleont. 12, 435–458.

27. Sereno, P. C., Forster, C. A., Rogers, R. R., Monetta, A. M. (1993). Primitive dinosaur skeleton from Argentina and the early evolution of Dinosauria. Nature 361, 64–66.

28. Sereno, P. C., Wilson, J. A., Larsson, H. C. E., Dutheil, D. B., Sues, H.-D. (1994). Early Cretaceous dinosaurs from the Sahara. Science 265, 267–271.

29. Rauhut, O. W. M. (2003). The Interrelationships and Evolution of Basal Theropod Dinosaurs. Spec. Pap. Palaeontol. 69, 1–213.

30. Holtz, T. R. (1994). The phylogenetic position of the Tyrannosauridae: implications for theropod systematics. J. Paleontol. 68, 1100–1117.

31. Wilson, J. A., and Sereno, P. C. (1998). Early evolution and higher-level phylogeny of sauropod dinosaurs. J. Vert. Paleontol. 18.S2, 1–79.

32. Tykoski, R. (2005). PhD thesis, University of Texas, Austin.

33. Carrano, M. T., Sampson, S. D., and Forster, C. A. (2002). The osteology of *Masiakasaurus knopfleri*, a small abelisauroid (Dinosauria: Theropoda) from the Late Cretaceous of Madagascar. J. Vert. Paleontol. 22, 510–534.

34. Fraser, N. C., Padian, K., Walkden, G. M., and Davis, A. L. M. (2002). Basal dinosauriform remains from Britain and the diagnosis of the Dinosauria. Palaeontology 45, 79–95.

35. Galton, P. M., and Upchurch, P. (2004). Basal Sauropodomorpha-Prosauropoda. In The Dinosauria 2nd edn, D. B. Weishampel, P. Dodson, H. Osmolska. ed. (Berkeley: Univ. of California Press), pp. 232–258.

36. Langer, M. C. (2004). Basal saurischian. In The Dinosauria 2nd edn, D. B. Weishampel, P. Dodson, H. Osmolska. ed. (Berkeley: Univ. of California Press), pp. 25–46.

37. Yates, A. M. (2004). *Anchisaurus polyzelus* (Hitchcock): the smallest known Sauropod Dinosaur and the evolution of gigantism among Sauropodomorph Dinosaurs. Postilla 230, 1–58.

38. Yates, A. M., and Kitching, J. W. (2003). The earliest known sauropod dinosaur and the first steps towards sauropod locomotion. Proc. R. Soc. Lond. B Biol. Sci. 270, 1753–1758.

39. Butler, R. J. (2005). The 'fabrosaurid' ornithischian dinosaurs of the upper Elliot Formation (Lower Jurassic) of South Africa and Lesotho. Zool. J. Linn. Soc. 145, 175–218.

40. Ezcurra, M. D. (2006). A review of the systematic position of the dinosauriform archosaur *Eucoelophysis baldwini* Sullivan & Lucas, 1999 from the Upper Triassic of New Mexico, USA. Geodiversitas 28, 649–684.

41. Butler, R. J., Smith, R. M. H., Norman, D. B. (2007). A primitive ornithischian dinosaur from the Late Triassic of South Africa, and the early evolution and diversification of Ornithischia. Proc. R. Soc. Lond. B Biol. Sci. 274, 2041–2046.

42. Butler, R. J., Upchurch, P., Norman, D. B. (2008). The phylogeny of the ornithischian dinosaurs. J. Syst. Palaeontol. 6, 1–40.

43. Smith, N. D., Makovicky, P. J., Hammer, W. R., Currie, P. J. (2007). Osteology of *Cryolophosaurus ellioti* (Dinosauria: Theropoda) from the Early Jurassic of Antarctica and implications for early theropod evolution. Zool. J. Linn. Soc. 151, 377–421.

44. Upchurch, P., Barrett, P. M., Galton, P. M. (2007). A phylogenetic analysis of basal sauropodomorph relationships: Implications for the origin of sauropod dinosaurs. Spec. Pap. Paleontol. 77, 57–90.

45. Nesbitt, S. J., Smith, N. D., Irmis, R. B., Turner, A. H., Downs, A., Norell, M. A. (2009). A complete skeleton of a Late Triassic saurischian and the early evolution of dinosaurs. Science 326, 1530–1533.

46. Langer, M. C., Bittencourt, J. S. Schultz,C. L. (2011). A reassessment of the basal dinosaur *Guaibasaurus candelariensis*, from the Late Triassic Caturrita Formation of south Brazil. Earth Environ. Sci. Trans. R. Soc. Edinb. 101, 301–332.

47. Kammerer, C. F., Nesbitt, S. J., Shubin, N. H. (2012). The first silesaurid dinosauriform from the Late Triassic of Morocco. Acta Palaeontol. Pol. 57, 277–284.

48. Gower, D. J., and Sennikov, A. G. (1996). Morphology and phylogenetic informativeness or early archosaur braincases. Palaeontology 39, 883–906.

49. Harris, J. D. (1998). A Reanalysis of *Acrocanthosaurus atokensis*, its Phylogenetic Status, and Paleobiogeographic Implications, Based on a New Specimen from Texas. New Mexico Mus. Nat. Hist. Sci. Bull. 13, 1–175.

50. Juul, L. (1994). The phylogeny of basal archosaurs. Paleontol. Afr. 31, 1–38.

51. Makovicky, P. J., and Sues, H.-D. (1998). Anatomy and phylogenetic relationships of the theropod dinosaur *Microvenator celer* from the Lower Cretaceous of Montana. American Museum Novitates 3240, 1–27.

52. Tykoski, R. S., and Rowe, T. (2004). Ceratosauria. In The Dinosauria 2nd edn, D. B. Weishampel, P. Dodson, H. Osmolska. ed. (Berkeley: Univ. of California Press), pp. 47–70.

53. Weishampel, D. B., and Witmer, L. M. (2004). *Lesothosaurus*, *Pisanosaurus*, and *Technosaurus*. In The Dinosauria 2nd edn, D. B. Weishampel, P. Dodson, H. Osmolska. ed. (Berkeley: Univ. of California Press), pp. 416–425.

54. Sereno, P. C., and Novas, F. E. (1994).The skull and neck of the basal theropod *Herrerasaurus ischigualastensis*. J. Vert. Paleont, 13, 451–476.

55. Martinez, R., Sereno, P. C., Alcober, O. A., Colombi, C. E., Renne, P. R., Montañez, I. P., Currie, B. S. 2011. A basal dinosaur from the dawn of the dinosaur era in southwestern Pangaea. Science, 331, 206–210.

56. Godefroit, P., Sinitsa, S., Dhouailly, M. D., Bolotsky, Y. L., Sizov, A. V., McNamara, M. E. Benton, M. J., and Spagna, P. (2014). A Jurassic ornithischian dinosaur from Siberia with both feathers and scales. Science 345, 451–455.

57. McPhee, B. W., Yates, A. M., Choiniere, J., and Abdala, N. F. (2015). The complete anatomy and phylogenetic relationships of *Antetonitrus ingenipes* (Sauropodiformes, Dinosauria): implications for the origins of Sauropoda. Zool. J. Linn. Soc. 171, 151–205.

58. Goloboff, P. A., Farris, J. S., and Nixon, K. C. (2008). TNT, a free program for phylogenetic analysis. Cladistics 24, 774–786.

59. Bremer, K. (1994). Branch support and tree stability. Cladistics 10: 295–304.

60. Brusatte, S. L. Nesbitt, S. J., Irmis, R. B., Butler, R. J., Benton, M. J., Norell, M. A. (2010). The origin and early radiation of dinosaurs. Earth-Sci. Rev. 101, 68–100.

61. Langer, M. C. (2014). The origins of Dinosauria: Much ado about nothing. Palaeontol. 57, 469–478.

62. Sereno, P. C. (2007). The phylogenetic relationships of early dinosaurs: a comparative report. Hist. Biol. 19, 145–155.

63. Hillis, D. M., Bull, J. J. (1993). An empirical test of bootstrapping as a method for assessing confidence in phylogenetic analysis. Syst. Biol. 42, 182–192.

64. Langer, M. C., Ferigolo, J. (2013). The Late Triassic dinosauromorph *Sacisaurus agudoensis* (Caturrita Formation; Rio Grande do Sul, Brazil): anatomy and affinities. Geol. Soc. Spec. Publ. 379: 353–392

65. Sereno, P. C. (1997). The origin and evolution of dinosaurs. Annu. Rev. Earth Planet. Sci. 25, 435–489.

66. Barrett, P. M., Butler, R. J., and Nesbitt, S. J. (2010). The roles of herbivory and omnivory in early dinosaur evolution. Earth Environ. Sci. Trans. R. Soc. Edinb. 101, 383–396.

67. Barrett, P. M., and Rayfield, E. J. (2006). Ecological and evolutionary implications of dinosaur feeding behaviour. Trends Ecol. Evol. 21, 217–224,

68. Maddison, W. P., and Maddison, D.R. (2016). Mesquite: a modular system for evolutionary analysis. Version 3.10 http://mesquiteproject.org

APPENDIX - CHAPTER 3

1. Institutional abbreviations

AMNH, American Museum of Natural History, New York, USA; **GPIT**, Institut und Museum für Geologie und Paläontologie, Universität Tübingen, Tübingen, Germany; **MB**, Museum für Naturkunde, Berlin, Germany; **MCP**, Museu de Ciências e Tecnologia, Pontifícia Universidade Católica do Rio Grande do Sul, Porto Alegre, Brazil; **OUMNH**, Oxford University Museum of Natural History, Oxford, UK; **PVSJ**, Museo de Ciencias Naturales, San Juan, Argentina; **PULR**, Universidad Nacional de La Rioja, La Rioja, Argentina; **PVSJ**, Museo de Ciencias Naturales, San Juan, Argentina; **SAM**, Iziko South African Museum, Capetown, South Africa; **SMNS**, Staatliches Museum für Naturkunde, Stuttgart, Germany; **ULBRA-PV**, Museu de Ciências Naturais, Universidade Luterana do Brasil, Canoas.

2. Specimen MCP-3845-PV of *Saturnalia tupiniquim*

Saturnalia tupiniquim is known from three specimens: MCP 3844 (holotype) - 3846-PV (see Langer, 2003 for more details). The fossils come from the Carnian Santa Maria Formation, in southern Brazil, from a locality commonly known as Cerro da Alemoa or Waldsanga (53°45' W; 29°40' S). Langer et al. (1999) provided a very preliminary description of *S. tupiniquim*, but more detailed descriptions of the pelvic (Langer, 2003) and scapular (Langer et al. 2007) girdles and limbs were provided later. The braincase is only preserved in MCP-3845-PV (Figure S1), and was never studied in detail. Its full description is under preparation, and will be presented elsewhere.
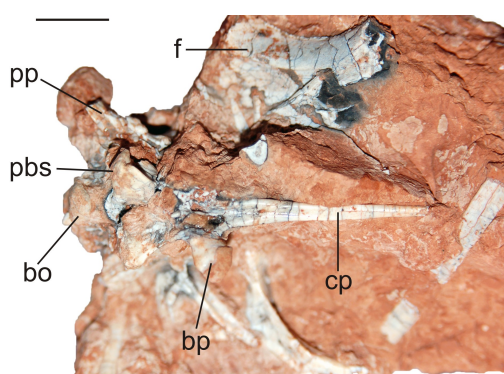

Figure S1: *Saturnalia tupiniquim* (MCP-3845-PV). Block containing the braincase and other skull elements. bo – basioccipital; bp – basipterygoid process; cp – cultriform process of the parabasisphenoid; f – frontal; pbs – parabasisphenoid; pp – paroccipital process of the otoccipital. (scale bar = 10mm)

The block containing the skull of MCP-3845-PV has multiple fractures, hampering its mechanical preparation. Computed tomography was, therefore, employed in order to access the braincase osteology of *Saturnalia tupiniquim* (Figure S2).
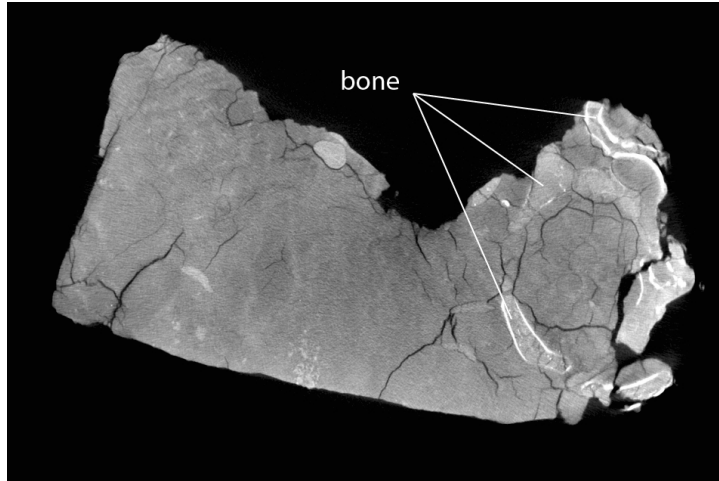

Figure S2: *Saturnalia tupiniquim* (MCP-3845-PV). Example of slice obtained from the Computed Tomographic. The contrast between bones and matrix allows a precise reconstruction of the osteology and soft-tissue anatomy of the braincase.

The CT-Scan data show that otoccipital (= exoccipital + opisthotic *sensu* Sampson & Witmer, 2007), parabasisphenoid, basioccipital, and supraoccipital are preserved in articulation inside the matrix (Figure S3), allowing a detailed reconstruction of the posterior portion of the endocranial cavity (see Main Document).

3. Skull length of *Saturnalia tupiniquim*

No complete and articulated skull is so far know for *Saturnalia tupiniquim*. Langer et al. (1999) originally estimated its skull size to be approximately 10 cm, based on the size of the dentary of MCP-3845-PV, but no detailed measurements or calculations were provided in that study. Here, the skull length of *S. tupiniquim* was estimated based on the length of the right frontal of MCP-3845-PV, which is entirely preserved inside the matrix (Figures S1 and S4). In addition, we also estimated the length of the mandible based on the dentary of this specimen (Figure S5). The calculations employed linear regressions (Figures S6 and S7), based on measurements of other Late Triassic and Early Jurassic dinosaurs known from more complete specimens, and the archosauriform *Euparkeria* (Table S1).
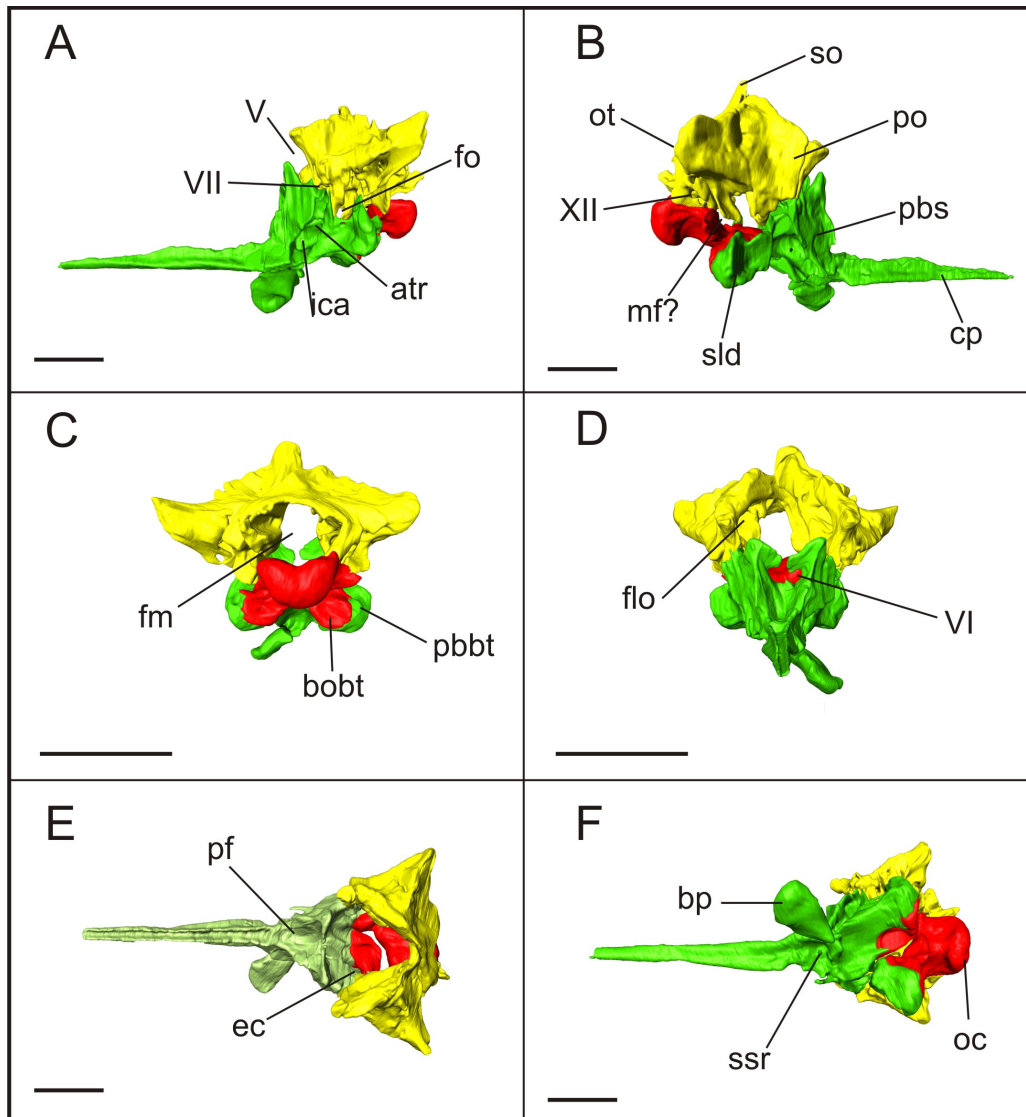
Figure S3: *Saturnalia tupiniquim* (MCP-3845-PV). Results of the braincase segmentation in left lateral (A), right lateral (B), occipital (C), anterior (D), dorsal (E), and ventral (F) views. atr – anterior tympanic recess; bobt - basioccipital component of the basal tubera; cp – cultriform process of the parabasisphenoid; ec – endocranial cavity; flo – flocculus of the cerebellum; fm – foramen magnum; fo – fenestra ovalis; ica – internal carotid artery; mf – metotic foramen; ot – otoccipital; pbbt – parabasisphenoid component of the basal tubera; pbs – parabasisphenoid; pf – pituitary fossa; po – prootic; sld – semi-lunar depression; so – supraoccipital; ssr – subsellar recess; V – trigeminal nerve; VI – abducens nerve; VII – facial nerve; XII – hypoglossal nerve. (scale bars = 10 mm).
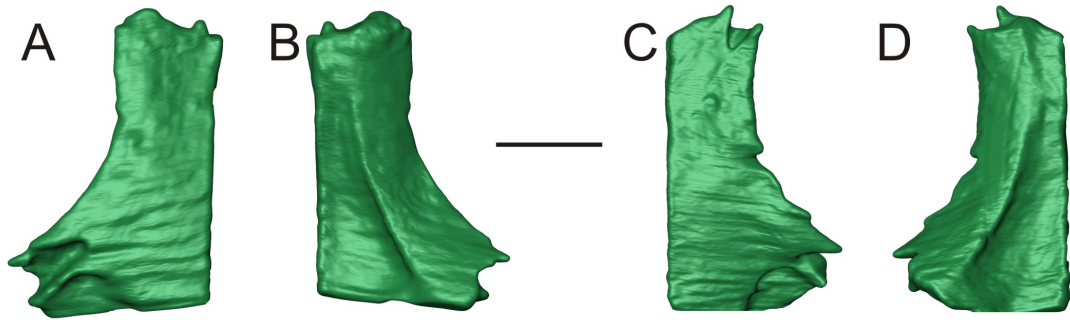
Figure S4: *Saturnalia tupiniquim* (MCP-3845-PV). Left frontal in dorsal (A) and ventral (B) views, and right frontal in dorsal (C) and ventral (D) views (scale bar = 10mm).

_____
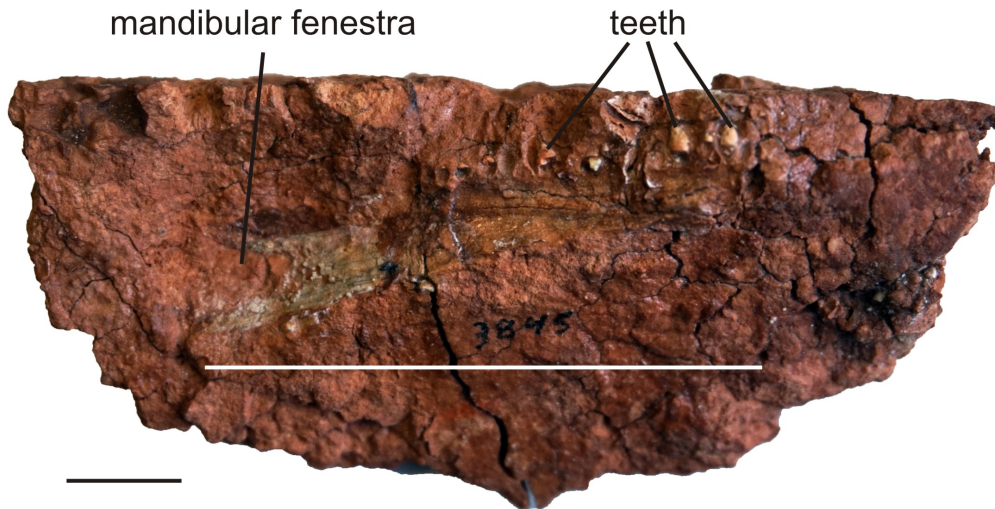
Figure S5: *Saturnalia tupiniquim* (MCP-3845-PV). Left dentary; white line indicates the entire length of the dentary, from its rostral edge to the tip of the posteroventral ramus, extending below mandibular fenestra. (scale bar – in black = 1cm)

Table S1: Frontal, skull, dentary, and mandible lengths of Late Triassic and Early Jurassic dinosaurs, plus the archosauriform *Euparkeria*. Values in red indicate estimated lengths for the skull and mandible of *Saturnalia tupiniquim* (MCP-3845-PV).

TAXON	SPECIMEN NUMBER	FRONTAL	SKULL	DENTARY	MANDIBLE
Saturnalia tupiniquim	MCP-3845-PV	29	97,0692	50	87,203
Adeopapposaurus mognai	PVSJ 610; PVSJ 568	47	160	87	166
Coelophysis bauri	Cast of AMNH FR 7224			144	215
Efraasia minor	SMNS 12668			113	160
Eocursor parvus	SAM-PK-K8025			43	73
Eoraptor lunensis	PVSJ 512	36	123	85	110
Euparkeria capensis	SAM-PK-5867	32	98	55	90
Herrerasaurus ischigualastensis	PVSJ 407	85	300	155	280
Heterodontosaurus tucki	SAM-PK-K1332	40	127	75	120
Massospondylus carinatus	SAM-PK-K1314	47	159	87	139
Panphagia protos	PVSJ 874			75	121
Plateosaurus	AMNH 6810	76	330	220	326
Riojasaurus incertus	PULR 056	76	250	160	240
Zupaysaurus rougieri	PULR 076	140	490	330	470

_____

$$y = 3.6716x - 9.8253$$
$$R^2 = 0.96953$$
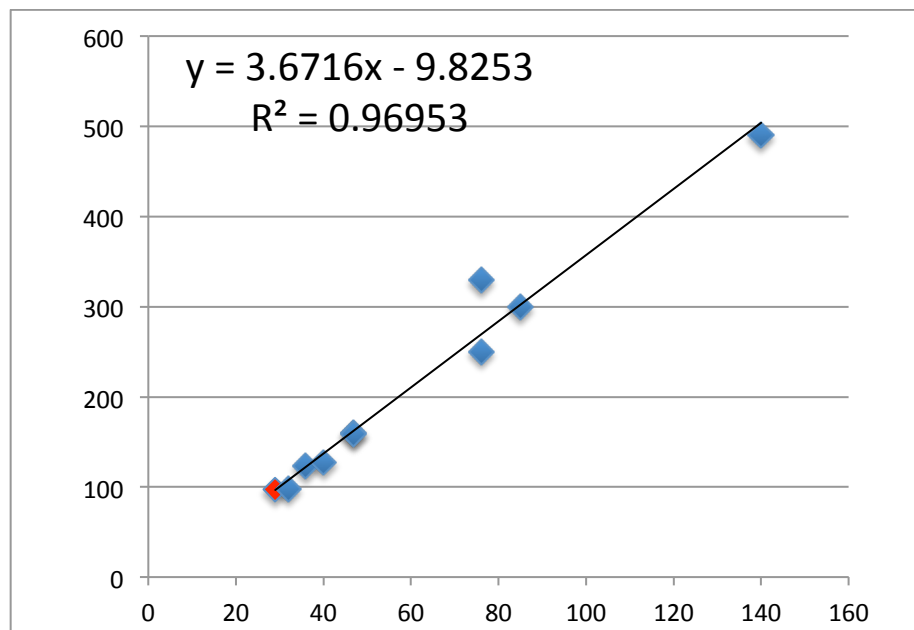
Figure S6: Linear regression used to estimate the total length of the skull of *Saturnalia tupiniquim* – see Table S1 for detailed measurements.

_____

y = 1.4064x + 16.85
R² = 0.97603
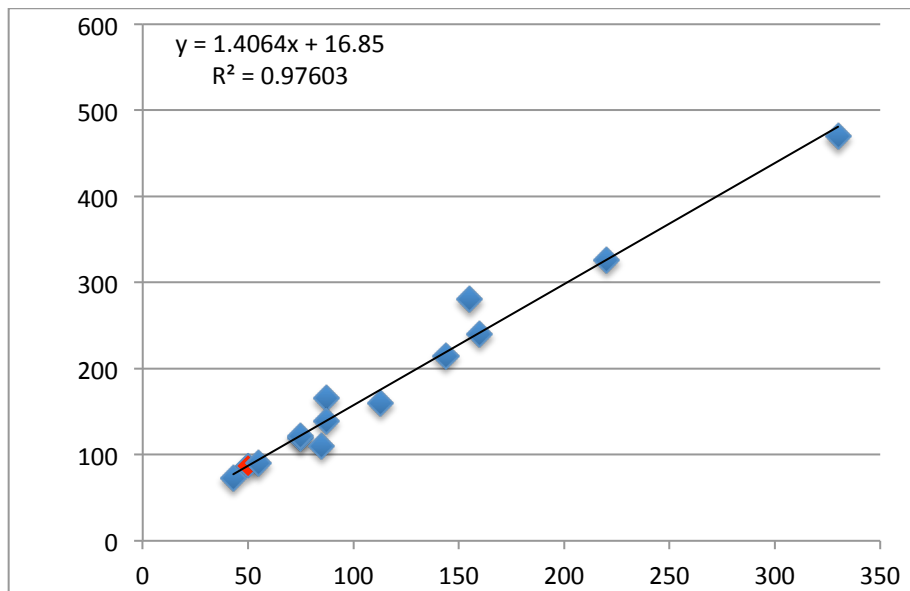
Figure S7: Linear regression used to estimate the total length of the mandible of *Saturnalia tupiniquim* – see Table S1 for detailed measurements.

Based on the linear regression including other taxa, the estimated skull length (c. 97 mm) of *Saturnalia tupiniquim* is compatible with its estimated mandible length (c. 87 mm); maximum skull length is c. 1.1 times longer than the maximum mandible length.

4. Dentition of *Saturnalia tupiniquim* and other sauropodomorphs

Inferences on the diet of the earliest dinosaurs have been made mostly based on their tooth morphology, on a form-function correlation approach (Barrett & Rayfield, 2006). Yet, a complete separation between an omnivore and a facultative herbivore diet is usually not possible solely on the basis of tooth morphology (Barrett, 2000; Barrett & Upchurch, 2007). Nevertheless, the earliest Sauropodomorpha exhibit tooth traits that are related to a carnivorous diet, which are not seen in later members of the lineage (Figure S8 - see Main text for details).
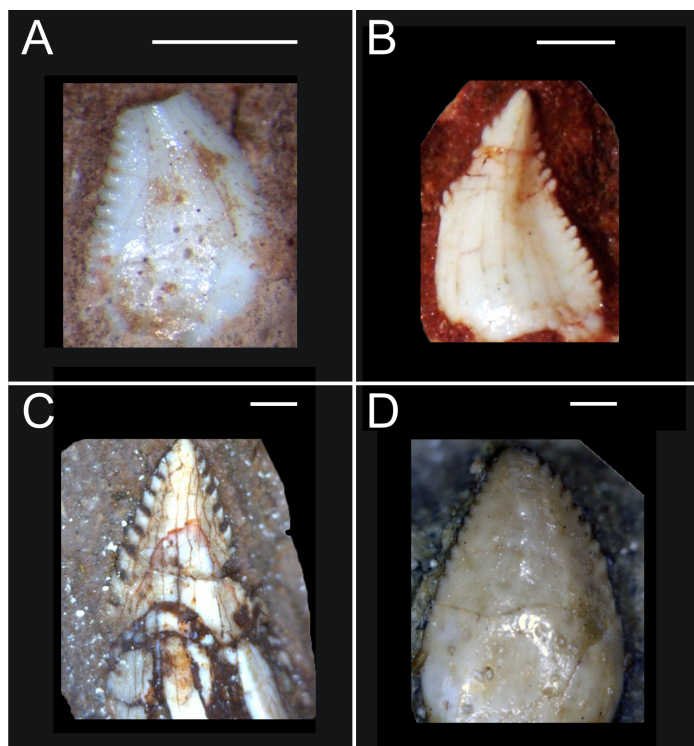
Figure S8: Mandibulary teeth of the sauropodomorph dinosaurs *Saturnalia tupiniquim* (A), *Pampadromaeus barbarenai* – ULBRA PVT 016 (B), *Efraasia minor* – SMNS 12684 (C); *Plateosaurus gracilis* – GPIT 18318a (D).

5. Neck morphology of *Saturnalia tupiniquim*

One paratype of *Saturnalia tupiniquim* (MCP-3845-PV) preserved 22 semi-articulated presacral vertebrae; the atlantal intercentrum, plus neural arch, and the caudalmost trunk vertebrae are missing. A conspicuous morphological transition between pre-sacral vertebrae 9 and 10, including a rectangular rather than parallelogram centrum shape and a larger area for the tuberculum attachment in the vertebra 10, suggests that *S. tupiniquim* has 9 "typical" cervical vertebrae (Figure S9). Indeed, the neck/trunk transition in early dinosaurs with more complete vertebral series available, e.g. *Eoraptor*, *Staurikosaurus*, *Coelophysis*, *Plateosaurus*, *Heterodontosaurus* (Santa Luca, 1980; Colbert, 1989; Galton and Upchurch, 2004; Bittencourt and Kellner, 2009; Rinehart, Lucas, Heckert, Spielmann and Celesky, 2009; Sereno, Martínez and Alcober, 2012), is positioned at presacrals 9 or 10. In the absence of further evidence concerning the exact transition point between the neck and trunk of *S. tupiniquim* (e.g. articulated ribs and scapular girdle), we estimated its neck length alternatively with 9 or 10 vertebrae. Except for *Heterodontosaurus*, the above-mentioned dinosaurs are thought to possess 15 trunk

("dorsal") vertebrae, which is assumed herein for *S. tupiniquim*. The presacral column of *S. tupiniquim* is thus reconstructed as having 24 or 25 vertebrae.

We estimated that the neck of *S. tupiniquim* accounts for c. 56-60% of the trunk (Tables S2–S3). This is slightly elongated if compared with early dinosauriforms such as *Marasuchus* and *Silesaurus* (Sereno and Arcucci, 1994; Piechowsky and Dzik, 2010), in which this proportion is not greater than 50%. In several early dinosaurs, e.g. *Eoraptor*, *Heterodontosaurus* (Santa Luca, 1980; Sereno et al., 2012), the neck/trunk relative length varies between 50–55%. A more significant cervical elongation is seen in early neotheropods, e.g. *Coelophysis* (88%), and firstly in *Plateosaurus* (75%) among sauropodomorphs (Rauhut, Fechner, Remes and Reis, 2011). The neck elongation in *S. tupiniquim* is intermediate between that of early saurischians and plateosaurians (i.e. members of the clade Plateosauria). The paucity of anatomical data for other early sauropodomorphs (i.e., *Panphagia*, *Pampadromaeus*, and *Chromogisaurus*), or even for taxa close to plateosaurians, hampers an accurate assessment of the initial pace of cervical elongation within sauropodomorphs. Yet, data gathered from *S. tupiniquim* alone indicates that a more conspicuous neck elongation was preceded by the relative shortening of the skull.

Table S2 – Ventral length (in mm) of the presacral centra of *Saturnalia tupiniquim* (MCP-3845-PV)

ps2*	ps3	ps4	ps5	ps6	ps7	ps8	ps9	ps10†	ps11	ps12
22	22.47	--	23.88	23.13	22.48	20.25	18.3	17.67	16.79	17.9

ps13	ps14	ps15	ps16	ps17	ps18	ps19	ps20	ps21	ps22	ps23
20.2	--	21.9	22.85	23.76	23.72	23.75	23.29	24.26	22.88	--

*Axis (including axial intercentrum)
†Last neck vertebra **or** first trunk vertebra
-- Incomplete centrum

Table S3 – Estimation of the neck and trunk length (in mm) of *Saturnalia tupiniquim* (MCP-3845-PV)

	Neck lenght (min.-max.)*	Trunk length (min.-max.)*	Neck-trunk ratio (min.-max)
9 neck vertebrae	**182.3–183.7**	**324.9–326.6**	**55.8–56.5%**
10 neck vertebrae	**199–200.4**	**330.1–331.8**	**60–60.7%**

*ps4 and ps14 estimated with basis on the adjacent vertebrae (min.-max.)
*atlas length corresponds to 1/3 of the axis
*values for the caudalmost presacrals are based on ps22.
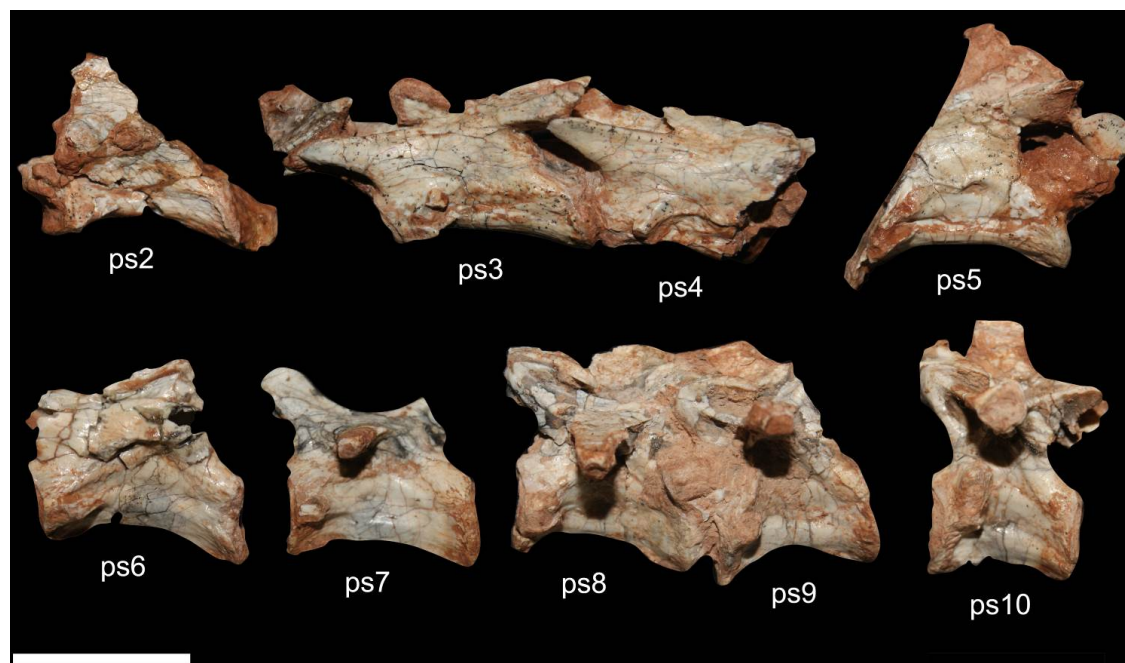
Figure S9 – *Saturnalia tupiniquim* (MCP-3845-PV), presacral vertebrae from 2 (axis) to 10. Scale bar = 20 mm.

SUPPLEMENTAL REFERENCES FOR CHAPTER 3

Barrett, P. M. 2000. Prosauropods and iguanas: speculation on the diets of extinct reptiles, In: (ed. H.-D. Sues) *Evolution of Herbivory in Terrestrial Vertebrates: Perspectives from the Fossil Record*. Cambridge University Press: Cambridge , pp. 42–78 .

Barrett, P. M., Upchurch, P. 2007. The evolution of feeding mechanisms in early sauropodomorph dinosaurs. *Special Papers in Palaeontology,* 77: 91–112.

Bittencourt, J. S. & Kellner, A. W. A. 2009. The anatomy and phylogenetic position of the Triassic dinosaur *Staurikosaurus pricei* Colbert, 1970. *Zootaxa*, 2079, 1–56.

Colbert, E. H. 1989. The Triassic dinosaur *Coelophysis*. Museum of Northern Arizona Bulletin, 57, 1–160.

Galton, P. M., Upchurch, P. 2004. Prosauropoda. In. (eds. D. B. Weishampel, P. Dodson and H. Osmólska) *The Dinosauria, second edition*University of California Press, Berkley. pp. 232–258

Langer, M. C., Abdala, F., Richter, M., Benton, M. J. 1999. A sauropodomorph dinosaur from the Upper Triassic (Carnian) of southern Brazil. *Earth & Planetary Sciences*, 329, 511-517.

Langer, M. C. 2003. The sacral and pelvic anatomy of the stem-sauropodomorph *Saturnalia tupiniquim* (Late Triassic, Brazil). *Paleobios* 23(2): 1–40.

Langer, M. C., França, M.A.G., & Gabriel, S. 2007. The pectoral girdle and forelimb anatomy of the stem sauropodomorph *Saturnalia tupiniquim* (Late Triassic, Brazil). In. (eds. P. M. Barrett and D. J. Batten) *Evolution and palaeobiology of early sauropodomorph dinosaurs. Special Papers in Palaeontology*, 77, 113–137.

Piechowsky, R. & Dzik, J. 2010. The axial skleton of Silesaurus opolensis. Journal of Vertebrate Paleontology, 30, 1127–1141.

Rauhut, O. W. M., Fechner, R., Remes, K. & Reis, K. 2011. How to get big in the Mesozoic: the evolution of the sauropodomorph body plan. Pp. 119-149 in N. Klein, K. Remes, C. T. Gee & M. Sander (eds) Biology of the sauropod dinosaurs: understanding the life of giants, Indiana University Press, Bloomington.

Rinehart, L. F., Lucas, S. G., Heckert, A. B., Spielmann, J. A. & Celesky, M. D. 2009. The paleobiology of Coelophysis bauri (Cope) from the Upper Triassic (Apchean Whitaker quarry, New Mexico), with detailed analysis of a single quarry block. Bulletin of the New Mexico Museum of Natural History and Science, 45, 1–260.

Sampson, S. D., Witmer, L. M. 2007. Craniofacial anatomy of *Majungasaurus crenatissimus* (Theropoda: Abelisauridae) from the Late Cretaceous of Madagascar. *Journal of Vertebrate Paleontology*, 27:32 – 102.

Santa Luca, A. P. 1980. The postcranial skeleton of Heterodontosaurus tucki (Reptilia, Ornithischia) from the Stormberg of South Africa. Annals of the South African Museum, 79, 159–211.

Sereno, P. C. & Arcucci, A. B. 1994. Dinosaurian precursors from the Middle Triassic of Argentina: Marasuchus lilloensis, n. gen. Journal of Vertebrate Paleontology, 14, 53–73.

Sereno, P. C., Martínez, R. N. & Alcober, O. 2012. Osteology of Eoraptor lunensis (Dinosauria, Sauropodomorpha). Journal of Vertebrate Paleontology, 32:sup 1, 83-179.

APPENDIX - CHAPTER 5

The characters used in the phylogenetic analyses represent a modified version of the dataset of McPhee *et al*. (2015), which in turn corresponds to an updated version of many previous works on Sauropodomorpha phylogeny (e.g. Yates, 2007b; Otero & Pol, 2013; Apaldetti *et al.,* 2014, McPhee *et al.,* 2014).

Characters 80, 82, 84 and 85 were modified (see main text) and rescored in the matrix. Characters 366-371 represent new characters proposed in this study - modified and new characters are highlighted in bold in the character list below. Character 365 was excluded from the analysis because we do not agree with the logical basis of the character (i.e. using only the total length of the femur instead of a relative measurement can be problematic, for example, because of ontogenetic variation). Character 86 was also excluded from the analysis because it lacks a more explicit definition (i.e. the depth of the parasphenoid rostrum varies anteriorly, but there is no specification in the character statement regarding where the measurements should be taken); and also because of problematic character scoring in previous analyses (i.e. many taxa that have only the ventral surface of the parasphenoid rostrum visible were coded for this character – e.g. *Coloradisaurus*, *Efraasia*). Additional modifications from the data matrix of McPhee *et al*. (2015) consists of rescoring the character 58 for all taxa, and, rescoring the character 74 for the taxa *Panphagia* and *Eoraptor* with "?".

Following McPhee *et al*. (2015), the following characters were set as additive (also followed by ORDERED in the characters list below): 8, 13, 19, 23, 40, 57, 69, 92, 102, 117, 121, 131, 144, 147, 149, 150, 157, 162, 167, 169, 170, 177, 207, 210, 225, 230, 237, 245, 255, 257, 270, 283, 304, 310, 318, 338, 351, 354, 356, 361, 365. A Nexus file with the data matrix is provided in the Supporting Information S2.

Characters List

1. Skull to femur ratio: greater than 0.6 (0); less than 0.6 (1).

2. Lateral plates appressed to the labial side of the premaxillary, maxillary and dentary teeth: absent (0); present (1).

3. Relative height of the rostrum at the posterior margin of the naris: more than 0.6 the height of the skull at the middle of the orbit (0); less than 0.6 the height of the skull at the middle of the orbit (1).

4. Foramen on the lateral surface of the premaxillary body: absent (0); present (1).

5. Distal end of the dorsal premaxillary process: tapered (0); transversely expanded (1).

6. Profile of premaxilla: convex (0); with an inflection at the base of the dorsal process (1).

7. Size and position of the posterolateral process of premaxilla: large and lateral to the anterior process of the maxilla (0); small and medial to the anterior process of the maxilla (1).

8. Relationship between posterolateral process of the premaxilla and the anteroventral process of the nasal: broad sutured contact (0); point contact (1); separated by maxilla (2). Ordered.

9. Posteromedial process of the premaxilla: absent (0); present (1)

10. Shape of the anteromedial process of the maxilla: narrow, elongated and projecting anterior to lateral premaxilla-maxilla suture (0); short, broad and level with lateral premaxilla-maxilla suture (1).

11. Development of external narial fossa: absent to weak (0); well-developed with sharp posterior and anteroventral rims (1).

12. Development of narial fossa on the anterior ramus of the maxilla: weak and orientated laterally to dorsolaterally (0); well-developed and forming a horizontal shelf (1).

13. Size and position of subnarial foramen: absent (0); small (no larger than adjacent maxillary neurovascular foramina) and positioned outside of narial fossa (1); large and on the rim of, or inside, the narial fossa (2). Ordered.

14. Shape of subnarial foramen: rounded (0); slot-shaped (1).

15. Maxillary contribution to the margin of the narial fossa: absent (0); present (1).

16. Diameter of external naris: less than 0.5 of the orbital diameter (0); greater than 0.5 of the orbital diameter.

17. Shape of the external naris (in adults): rounded (0); subtriangular with an acute posteroventral corner (1).

18. Level of the anterior margin of the external naris: anterior to the midlength of the premaxillary body (0); posterior to the midlength of the premaxillary body (1).

19. Level of the posterior margin of external naris: anterior to, or level with the premaxillamaxilla suture (0); posterior to the first maxillary alveolus (1); posterior to the midlength of the maxillary tooth row and the anterior margin of the antorbital fenestra (2). Ordered.

20. Dorsal profile of the snout: straight to gently convex (0); with a depression behind the naris (2).

21. Elongate median nasal depression: absent (0); present (1).

22. Width of anteroventral process of nasal at its base: less than the width of the anterodorsal process at its base (0); greater than the width of the anterodorsal process at its base (1).

23. Nasal relationship with dorsal margin of antorbital fossa: not contributing to the margin of the antorbital fossa (0); lateral margin overhangs the antorbital fossa and forms its dorsal margin (1); overhang extensive, obscuring the dorsal lachrymal-maxilla contact in lateral view (2). Ordered.

24. Pointed caudolateral process of the nasal overlapping the lachrymal: absent (0); present (1).

25. Anterior profile of the maxilla: slopes continuously towards the rostral tip (0); with a strong inflection at the base of the ascending ramus, creating a rostral ramus with parallel dorsal and ventral margins (1).

26. Length of rostral ramus of the maxilla: less than its dorsoventral depth (0); greater than its dorsoventral depth (1).

27. Shape of the main body of the maxilla: tapering posteriorly (0); dorsal and ventral margins parallel for most of their length (1).

28. Shape of the ascending ramus of the maxilla in lateral view: tapering dorsally (0); with an anteroposterior expansion at the dorsal end (1).

29. Rostrocaudal length of the antorbital fossa: greater than that of the orbit (0); less than that of the orbit (1).

30. Posteroventral extent of medial wall of antorbital fossa: reaching the anterior tip of the jugal (0); terminating anterior to the anterior tip of the jugal (1).

31. Development of the antorbital fossa on the ascending ramus of the maxilla: deeply impressed and delimited by a sharp, scarp-like rim (0); weakly impressed and delimited by a rounded rim or a change in slope (1).

32. Shape of the antorbital fossa: crescentic with a strongly concave posterior margin that is roughly parallel to the anterior margin of the antorbital fossa (0); subtriangular with a straight to gently concave posterior margin (1); antorbital fossa absent (2).

33. Size of the neurovascular foramen at the posterior end of the lateral maxillary row: not larger than the others (0); distinctly larger than the others in the row (1).

34. Direction that the neurovascular foramen at the posterior end of the lateral maxillary row opens: posteriorly (0); anteriorly, ventrally, or laterally (1).

35. Arrangement of lateral maxillary neurovascular foramina: linear (0); irregular (1).

36. Longitudinal ridge on the posterior lateral surface of the maxilla: absent (0); present (1).

37. Dorsal exposure of the lachrymal: present (0); absent (1).

38. Shape of the lachrymal: dorsoventrally short and blockshaped (0); dorsoventrally elongate and shaped like an inverted L (1).

39. Orientation of the lachrymal orbital margin: strongly sloping anterodorsally (0); erect and close to vertical (1).

40. Length of the anterior ramus of the lachrymal: greater than half the length of the ventral ramus (0); less than half the length of the ventral ramus (1); absent altogether (2). Ordered.

41. Web of bone spanning junction between anterior and ventral rami of lachrymal: absent and antorbital fossa laterally exposed (0); present, obscuring posterodorsal corner of antorbital fossa (1).

42. Extension of the antorbital fossa onto the ventral end of the lachrymal: present (0); absent (1).

43. Length of the posterior process of the prefrontal: short (0); elongated, so that total prefrontal length is equal to the anteroposterior diameter of the orbit (1).

44. Ventral process of prefrontal extending down the posteromedial side of the lachrymal: present (0); absent (1).

45. Maximum transverse width of the prefrontal: less than 0.25 of the skull width at that level (0); more than 0.25 of the skull width at that level (1).

46. Shape of the orbit: subcircular (0); ventrally constricted making the orbit subtriangular (1).

47. Slender anterior process of the frontal intruding between the prefrontal and the nasal: absent (0); present (1).

48. Jugal-lachrymal relationship: lachrymal overlapping lateral surface of jugal or abutting it dorsally (0); jugal overlapping lachrymal laterally (1).

49. Shape of the suborbital region of the jugal: an anteroposteriorly elongate bar (0); an anteroposteriorly shortened plate (1).

50. Jugal contribution to the antorbital fenestra: absent (0); present (1).

51. Dorsal process of the anterior jugal: present (0); absent (1).

52. Ratio of the minimum depth of the jugal below the orbit to the distance between the anterior end of the jugal and the anteroventral corner of the infratemporal fenestra: less than 0.2 (0); greater than 0.2 (1).

53. Transverse width of the ventral ramus of the postorbital: less than its anteroposterior width at midshaft (0); greater than its anteroposterior width at midshaft (1).

54. Shape of the dorsal margin of postorbital in lateral view: straight to gently curved (0); with a distinct embayment between the anterior and posterior dorsal processes (1).

55. Height of the postorbital rim of the orbit: flush with the posterior lateral process of the postorbital (0); raised so that it projects laterally to the posterior dorsal process (1).

56. Postfrontal bone: present (0); absent (1).

57. Position of the anterior margin of the infratemporal fenestra: behind the orbit (0); extends under the rear half of the orbit (1); extends as far forward as the midlength of the orbit (2). Ordered.

58. Frontal contribution to the supratemporal fenestra: present (0); absent (1).

59. Orientation of the long axis of the supratemporal fenestra: longitudinal (0); transverse (1).

60. Medial margin of supratemporal fossa: simple smooth curve (0); with a projection at the frontal/postorbital-parietal suture producing a scalloped margin (1).

61. Length of the quadratojugal ramus of the squamosal relative to the width at its base: less than four times its width (0); greater than four times its width (1).

62. Proportion of infratemporal fenestra bordered by squamosal: more than 0.5 of the depth of the infratemporal fenestra (0); less than 0.5 of the depth of the infratemporal fenestra (1).

63. Squamosal-quadratojugal contact: present (0); absent (1).

64. Angle of divergence between jugal and squamosal rami of quadratojugal: close to 90 degrees (0); close to parallel (1).

65. Length of jugal ramus of quadratojugal: no longer than the squamosal ramus (0); longer than the squamosal ramus (1).

66. Shape of the rostral end of the jugal ramus of the quadratojugal: tapered (0); dorsoventrally expanded (1).

67. Relationship of quadratojugal to jugal: jugal overlaps the lateral surface of the quadratojugal (0); quadratojugal overlaps the lateral surface of the jugal (1); quadratojugal sutures along the ventrolateral margin of the jugal (2).

68. Position of the quadrate foramen: on the quadrate-quadratojugal suture (0); deeply incised into, and partly encircled by, the quadrate (1); on the quadrate-squamosal suture, just below the quadrate head (2).

69. Shape of posterolateral margin of quadrate: sloping anterolaterally from posteromedial ridge (0); everted posteriorly creating a posteriorly facing fossa (1); posterior fossa deeply excavated, invading quadrate body (2). Ordered.

70. Exposure of the lateral surface of the quadrate head: absent, covered by lateral sheet of the squamosal (0); present (1).

71. Proportion of the length of the quadrate that is occupied by the pterygoid wing: at least 70 per cent (0); greater than 70 per cent (1).

72. Depth of the occipital wing of the parietal: less than 1.5 times the depth of the foramen magnum (0); more than 1.5 times the depth of the foramen magnum (1).

73. Position of foramina for mid-cerebral vein on occiput: between supraoccipital and parietal (0); on the supraoccipital (1).

74. Postparietal fenestra between supraoccipital and parietals: absent (0); present (1).

75. Shape of the supraoccipital: diamond-shaped, at least as high as wide (0); semilunate and wider than high (1).

76. Orientation of the supraoccipital plate: erect to gently sloping (0); strongly sloping forward so that the dorsal tip lies level with the basipterygoid processes (1).

77. Orientation of the paroccipital processes in occipital view: slightly dorsolaterally directed to horizontal (0); ventrolaterally directed (1).

78. Orientation of the paroccipital processes in dorsal view: posterolateral forming a Vshaped occiput (0); lateral forming a flat occiput (1)

79. Size of the post-temporal fenestra: large fenestra (0); a small hole that is much less than half the depth of the paroccipital process (1).

80. **Exit of the mid-cerebral vein: through trigeminal foramen (0) or through a separate foramen (1) (modified from Rauhut, 2003).**

81. Shape of the floor of the braincase in lateral view: relatively straight with the basal tuberae, basipterygoid processes and parasphenoid rostrum roughly aligned (0); bent with the basipterygoid processes and the parasphenoid rostrum below the level of the basioccipital condyle and the basal tuberae (1); bent with the basal tuberae lowered below the level of the basioccipital and the parasphenoid rostrum raised above it (2).

82. **Basioccipital component of the basal tubera, medial component in relation to the parabasisphenoidal component: present (0); absent (1). (Modified from Yates, 2007)**

83. Length of the basipterygoid processes (from the top of the parasphenoid to the tip of the process): less than the height of the braincase (from the top of the parasphenoid to the top of the supraoccipital) (0); greater than the height of the braincase (from the top of the parasphenoid to the top of the supraoccipital) (1).

84. **Basioccipital - basisphenoid junction on the ventral surface of the bones: straight line (0); U/V shaped (1) (This study)**

85. subsellar recess: maximum width equal or greater than the dorsoventral height (0); maximum width smaller than the dorsoventral height (1) (This study)

86. Dorsoventral depth of the parasphenoid rostrum: much less than (0), or about equal to (1), the trans- verse width (Yates, 2003a). **EXCLUDED**

87. Shape of jugal process of ectopterygoid: gently curved (0); strongly recurved and hooklike (1).

88. Pneumatic fossa on the ventral surface of the ectopterygoid: present (0); absent (1).

89. Relationship of the ectopterygoid to the pterygoid: ectopterygoid overlapping the ventral surface of the pterygoid (0); ectopterygoid overlapping the dorsal surface of the pterygoid (1).

90. Position of the maxillary articular surface of the palatine: along the lateral margin of the bone (0); at the end of a narrow anterolateral process due to the absence of the posterolateral process (1).

91. Centrally located tubercle on the ventral surface of palatine: absent (0); present (1).

92. Medial process of the pterygoid forming a hook around the basipterygoid process: absent (0); flat and blunt-ended (1); bent upward and pointed (2). Ordered.

93. Length of the vomers: less than 0.25 of the total skull length (0); more than 0.25 of the total skull length (1).

94. Position of jaw joint: no lower than the level of the dorsal margin of the dentary (0); depressed, well below this level (1).

95. Shape of upper jaws in ventral view: narrow with an acute rostral apex (0); broad and Ushaped (1).

96. Length of the external mandibular fenestra: more than 0.1 of the length of the mandible (0); less than 0.1 of the length of the mandible (1).

97. Caudal end of dentary tooth row medially inset with a thick lateral ridge on the dentary forming a buccal emargination : absent (0); present (1).

98. Height : length ratio of the dentary: less than 0.2; greater than 0.2 (1).

99. Orientation of the symphyseal end of the dentary: in line with the long axis of the dentary (0); strongly curved ventrally (1).

100. Position of first dentary tooth: adjacent to symphysis (0); inset one tooth's width from the symphysis (1).

101. Dorsoventral expansion at the symphyseal end of the dentary: absent (0); present (1).

102. Splenial foramen: absent (0); present and enclosed (1); present and open anteriorly (2). Ordered.

103. Splenial-angular joint: flattened sutured contact (0); synovial joint surface between tongue-like process of angular fitting in groove of the splenial (1).

104. A stout, triangular, medial process of the articular, behind the glenoid : present (0); absent (1).

105. Length of the retroarticular process: less than the depth of the mandible below the glenoid (0); greater than the depth of the mandible below the glenoid (2).

106. Strong medial embayment behind glenoid of the articular in dorsal view: absent (0); present (1).

107. Number of premaxillary teeth: four (0); more than four (1).

108. Number of dentary teeth (in adults): less than 18 (0); 18 or more (1).

109. Arrangement of teeth within the jaws: linearly placed, crowns not overlapping (0); imbricated with distal side of tooth overlapping mesial side of the succeeding tooth (1).

110. Orientation of the maxillary tooth crowns: erect (0); procumbent (1).

111. Orientation of the dentary tooth crowns: erect (0); procumbent (1).

112. Teeth with basally constricted crowns: absent (0); present (1).

113. Tooth-tooth occlusal wear facets : absent (0); present (1).

114. Mesial and distal serrations of the teeth: fine and set at right angles to the margin of the tooth (0); coarse and angled upwards at an angle of 45 degrees to the margin of the tooth (1).

115. Distribution of serrations on the maxillary and dentary teeth: present on both the mesial and distal carinae (0); absent on the posterior carinae (1); absent on both carinae (2).

116. Long axis of the tooth crowns distally recurved: present (0); absent (1).

117. Texture of the enamel surface: entirely smooth (0); finely wrinkled in some patches (1); extensively and coarsely wrinkled (2). Ordered.

118. Lingual concavities of the teeth: absent (0); present (1).

119. Longitudinal labial grooves on the teeth: absent (0); present (1).

120. Distribution of the serrations along the mesial and distal carinae of the tooth: extend along most of the length of the crown (0); restricted to the upper half of the crown (1).

121. Number of cervical vertebrae: eight or fewer (0); 9-10 (1); 12-13 (2); more than 13 (3). Ordered.

122. Shallow, dorsally facing fossa on the atlantal neurapophysis bordered by a dorsally everted lateral margin: absent (0); present (1).

123. Width of axial intercentrum: less than width of axial centrum (0); greater than width of axial centrum (1).

124. Position of axial prezygapophyses: on the anterolateral surface of the neural arch (0); mounted on anteriorly projecting pedicels (1).

125. Posterior margin of the axial postzygapophyses: overhang the axial centrum (0); flush with the caudal face of the axial centrum (1).

126. Length of the axial centrum: less than three times the height of the centrum (0); at least three times the height of the centrum (1).

127. Length of the anterior cervical centra (cervicals 3-5): no more than the length of the axial centrum (0); greater than the length of the axial centrum (1).

128. Length of middle to posterior cervical centra (cervical 6-8): no more than the length of the axial centrum (0); greater than the length of the axial centrum (1).

129. Dorsal excavation of the cervical parapophyses: absent (0); present (1).

130. Lateral compression of the anterior cervical vertebrae: centra are no higher than they are wide (0); are approximately 1.25 times higher than wide (1).

131. Relative elongation of the anterior cervical centra (cervical 3-5): lengths of the centra are less than 2.5 times the height of their anterior faces (0); lengths are 2.5-4 times the height of their anterior faces (1); the length of at least cervical 4 or 5 exceeds 4 times the anterior centrum height (2). Ordered.

132. Ventral keels on cranial cervical centra: present (0); absent (1).

133. Height of the mid cervical neural arches: no more than the height of the posterior centrum face (0); greater than the height of the posterior centrum face (1).

134. Cervical epipophyses on the dorsal surface of the postzygapophyses: absent (0); present on at least some cervical vertebrae (1).

135. Posterior ends of the anterior, postaxial epipophyses: with a free pointed tip (0); joined to the postzygapophysis along their entire length (1).

136. Shape of the epipophyses: tall ridges (0); flattened, horizontal plates (1).

137. Epipophyses overhanging the rear margin of the postzygapophyses: absent (0); present in at least some postaxial cervical vertebrae (1).

138. Anterior spur-like projections on mid-cervical neural spines: absent (0); present (1).

139. Shape of mid-cervical neural spines: less than twice as long as high (0); at least twice as long as high (1).

140. Shape of cervical rib shafts: short and posteroventrally directed (0); longer than the length of their centra and extending parallel to cervical column (1).

141. Position of the base of the cervical rib shaft: level with, or higher than the ventral margin of the cervical centrum (0); located below the ventral margin due to a ventrally extended parapophysis (1).

142. Postzygodiapophyseal lamina in cervical neural arches 4-8: present (0); absent (1).

143. Laminae of the cervical neural arches 4-8: well-developed tall laminae (0); weakly developed low ridges (1).

144. Shape of anterior centrum face in cervical centra: concave (0); flat (1); convex (2). Ordered.

145. Ventral surface of the centra in the cervicodorsal transition: transversely rounded (0); with longitudinal keels (1).

146. Number of vertebrae between cervicodorsal transition and primordial sacral vertebrae: 15-16 (0); no more than 14 (1).

147. Lateral surfaces of the dorsal centra: with at most vague, shallow depressions (0); with deep fossae that approach the midline (1); with invasive, sharp-rimmed pleurocoels (2). Ordered.

148. Oblique ridge dividing pleural fossa of cervical vertebrae: absent (0); present (1).

149. Laterally expanded tables at the midlength of the dorsal surface of the neural spines: absent in all vertebrae (0); present on the pectoral vertebrae (1); present on the pectoral and cervical vertebrae (2). Ordered.

150. Dorsal centra: entirely amphicoelous to amphiplatyan (1); first two dorsals are opisthocoelous (1); cranial half of dorsal column is opisthocoelous (2). Ordered.

151. Shape of the posterior dorsal centra: relatively elongated for their size (0); strongly axially compressed for their size (1).

152. Laminae bounding triangular infradiapophyseal fossae (chonae) on dorsal neural arches: absent (0); present (1).

153. Location of parapophysis in first two dorsals: at the anterior end of the centrum (0); located at the mid-length of the centrum, within the middle chonos (1).

154. Parapophyses of the dorsal column completely shift from the centrum to the neural arch: anterior to the thirteenth presacral vertebra (0); posterior to the thirteenth presacral vertebra (1).

155. Orientation of the transverse processes of the dorsal vertebrae: most horizontally directed (0); all upwardly directed (1).

156. Contribution of the paradiapophyseal lamina to the margin of the anterior chonos in mid-dorsal vertebrae: present (0); prevented by high placement of parapophysis (1).

157. Hyposphenes in the dorsal vertebrae: absent (0); present but less than the height of the neural canal (1); present and equal to the height of the neural canal (2). Ordered.

158. Prezygodiapophyseal lamina and associated anterior triangular fossa (anterior infradiapophyseal fossa): present on all dorsals (0); absent in mid-dorsals (1).

159. Anterior centroparapophyseal lamina in dorsal vertebrae: absent (0); present (1).

160. Prezygoparapophyseal lamina in dorsal vertebrae: absent (0); present (1).

161. Accessory lamina dividing posterior chonos from postzygapophysis: absent (0); present (1).

162. Pneumatic excavation of the dorsal neural arches: absent (0); equivocal (e.g., no more than depressions within the infradiapophyseal chambers) (1); sharp-rimmed subfossae or foramina clearly invading bone surface (2). Ordered.

163. Separation of lateral surfaces of anterior dorsal neural arches under transverse processes: widely spaced (0); only separated by a thin midline septum (1).

164. Height of dorsal neural arches, from neurocentral suture to level of zygapophyseal facets: much less than height of centrum (0); subequal to or greater than height of centrum (1).

165. Form of anterior surface of neural arch: simple centroprezygopophyseal ridge (0); broad anteriorly facing surface bounded laterally by centroprezygopophyseal lamina (1).

166. Shape of posterior dorsal neural canal: subcircular (0); slit-shaped (1).

167. Height of middle dorsal neural spines: less than the length of the base (0); higher than the length of the base but less than 1.5 times the length of the base (1); greater than 1.5 times the length of the base (2). Ordered.

168. Shape of anterior dorsal neural spines: lateral margins parallel in anterior view (0); transversely expanding towards dorsal end (2).

169. Cross-sectional shape of dorsal neural spines: transversely compressed (0); broad and triangular (1); square-shaped in posterior vertebrae (2). Ordered.

170. Spinodiapophyseal lamina on dorsal vertebrae: absent (0); present and separated from spinopostzygapophyseal lamina (1); present and joining spinopostzygapophyseal lamina to create a composite posterolateral spinal lamina (2). Ordered.

171. Well-developed, sheet-like suprapostzygapophyseal laminae: absent (0); present on at least the caudal dorsal vertebrae (2).

172. Shape of the spinopostzygapophyseal lamina in middle and posterior dorsal vertebrae: singular (0); bifurcated at its distal end

173. Shape of posterior margin of middle dorsal neural spines in lateral view: approximately straight (0); concave with a projecting posterodorsal corner (1).

174. Transversely expanded plate-like summits of posterior dorsal neural spines: absent (0); present (1).

175. Last presacral rib: free (0); fused to vertebra (1).

176. Sacral rib much narrower than the transverse process of the first primordial sacral vertebra (and dorsosacral if present) in dorsal view: absent (0); present (1).

177. Number of dorsosacral vertebrae: none (0); one (1); two (2). Ordered.

178. Caudosacral vertebra: absent (0); present (1).

179. Shape of the iliac articular facets of the first primordial sacral rib: singular (0); divided into dorsal and ventral facets separated by a non-articulating gap (1).

180. Deep, medially-directed pit excavating the surface of the non-articulating gap of the first primordial sacral rib: absent (0); present (1).

181. Depth of the iliac articular surface of the primordial sacrals: less than 0.75 of the depth of the ilium (0); greater than 0.75 of the depth of the ilium (1).

182. Sacral ribs contributing to the rim of the acetabulum: absent (0); present (1).

183. Posterior and anterior expansion of the transverse processes of the first and second primordial sacral vertebrae, respectively, partly roofing the intercostal space: absent (0); present (1).

184. Length of first caudal centrum: greater than its height (0); less than its height (1).

185. Position of postzygapophyses in proximal caudal vertebrae: protruding with an interpostzygapophyseal notch visible in dorsal view (0); placed on either side of the caudal end of the base of the neural spine without any interpostzygapophyseal notch (1).

186. A hyposphenal ridge on caudal vertebrae: absent (0); present (1).

187. Prezygadiapophyseal laminae on anterior caudals: absent (0); present (1).

188. Depth of the bases of the proximal caudal transverse processes: shallow, restricted to the neural arches (0); deep, extending from the centrum to the neural arch (1).

189. Position of last caudal vertebra with a protruding transverse process: distal to caudal 16 (0); proximal to caudal 16 (1).

190. Orientation of posterior margin of proximal caudal neural spines: sloping posterodorsally (0); vertical (1).

191. Longitudinal ventral sulcus on proximal and middle caudal vertebrae: present (0); absent (1).

192. Length of midcaudal centra: greater than twice the height of their anterior faces (0); less than twice the height of their anterior faces (1).

193. Cross-sectional shape of the distal caudal centra: oval with rounded lateral and ventral sides (0); square-shaped with flattened lateral and ventral sides (1).

194. Length of distal caudal prezygapophyses: short, not overlapping the preceding centrum by more than a quarter (0); long and overlapping the preceding the centrum by more than a quarter (1).

195. Shape of the terminal caudal vertebrae: unfused, size decreasing toward tip (0); expanded and fused to form a club-shaped tail (1).

196. 'Weaponized' dermal spikes on tail: absent (0); present (1).

197. Length of the longest chevron: less than twice the length of the preceding centrum (0); greater than twice the length of the preceding centrum (1).

198. Anteroventral process on distal chevrons: absent (0); present (1).

199. Mid-caudal chevrons with a ventral slit: absent (0); present (1).

200. Longitudinal ridge on the dorsal surface of the sterna plate: absent (0); present (1).

201. Craniocaudal length of the acromion process of the scapula: less than 1.5 times the minimum width of the scapula blade (0); greater than 1.5 times the minimum width of the scapula blade (1).

202. Minimum width of the scapula: greater than 20 per cent of its length (0); less than 20 per cent of its length (1).

203. Caudal margin of the acromion process of the scapula: rises from the blade at angle that is less than 65 degrees from the long axis of the scapula, at its steepest point (0); rises from the blade at angle that is greater than 65 degrees from the long axis of the scapula, at its steepest point (1).

204. Width of dorsal expansion of the scapula: less than the width of the ventral end of the scapula (0); equal to the width of the ventral end of the scapula (1).

205. Flat caudoventrally facing surface on the coracoids between glenoid and coracoid tubercle: absent (0); present (1).

206. Coracoid tubercle: present (0); absent (1).

207. Length of the humerus: less than 55 per cent of the length of the femur (0); 55-65 per cent of the length of the femur (1); 65-70 per cent of the length of the femur (2); more than 70 per cent of the length of the femur (3). Ordered.

208. Shape of the humeral head: weakly developed, rounded in anterior-posterior view but minimally expanded perpendicular to the latter axis (0); flat in anterior-posterior view

with only a slightly expanded lateral component (1); domed, being convex/hemispherical in anterior-posterior view with a strong lateral incursion onto the humeral shaft (2) (Unordered).

209. Shape of the deltopectoral crest: subtriangular (0); subrectangular (1).

210. Length of the deltopectoral crest of the humerus: less than 30 per cent of the length of the humerus (0); 30-50 per cent of the length of the humerus (1); greater than 50 per cent of the length of the humerus (2). Ordered.

211. Shape of the anterolateral margin of the deltopectoral crest of the humerus: straight (0); strongly sinuous (1).

212. Rugose pit centrally located on the lateral surface of the deltopectoral crest: absent (0); present (1).

213. Well-defined fossa on the distal flexor surface of the humerus: present (0); absent (1).

214. Transverse width of the distal humerus: less than 33 per cent of the length of the humerus (0); greater than 33 per cent of the length of the humerus (1).

215. Shape of the entepicondyle of the distal humerus: rounded process (0): with a flat distomedially facing surface bounded by a sharp proximal margin (1).

216. Length of the radius: greater than 80 per cent of the humerus (0); less than 80 per cent of the humerus (1).

217. Deep radial fossa, bounded by an anterolateral process, on proximal ulna: absent (0); present (1).

218. Olecranon process on proximal ulna: present (0); absent (1); greatly enlarged olecranon (2).

219. Maximum linear dimensions of the ulnare and radiale: exceed that of at least one of the first three distal carpals (0); less than any of the distal carpals (1).

220. Transverse width of the first distal carpal: less than 120 per cent of the transverse width of the second distal carpal (0); greater than 120 per cent of the transverse width of the second distal carpal (1).

221. Sulcus across the medial end of the first distal carpal:absent (0); present (1).

222. Lateral end of first distal carpal: abuts second distal carpal (0); overlaps second distal carpal (1).

223. Second distal carpal: completely covers the proximal end of the second metacarpal (0); does not completely cover the proximal end of the second metacarpal (1).

224. Ossification of the fifth distal carpal: present (0); absent (1).

225. Length of the manus: less than 38 per cent of the humerus + radius (0); 38-45 per cent of the humerus + radius (1); greater than 45 per cent of the humerus + radius (2). Ordered.

226. Shape of metacarpus: flattened to gently curved and spreading (0); a colonnade of subparallel metacarpals tightly curved into a U-shape (1).

227. Proximal width of first metacarpal: less than the proximal width of the second metacarpal (0); greater than the proximal width of the second metacarpal (1).

228. Minimum transverse shaft width of first metacarpal: less than twice the minimum transverse shaft width of second metacarpal (0); greater than twice the minimum transverse shaft width of second metacarpal (1).

229. Proximal end of first metacarpal: flush with other metacarpals (0); inset into the carpus (1).

230. Shape of the first metacarpal: proximal width less than 65 per cent of its length (0); proximal width 65-80 per cent of its length (1); proximal width 80-100 per cent of its length (2); greater than 100 per cent of its length (3). Ordered.

231. Strong asymmetry in the lateral and medial distal condyles of the first metacarpal: absent (0); present (1).

232. Deep distal extensor pits on the second and third metacarpals: absent (0); present (1).

233. Shape of the distal ends of second and third metacarpals: subrectangular in distal view (0); trapezoidal with flexor rims of distal collateral ligament pits flaring beyond extensor rims (1).

234. Shape of the fifth metacarpal: longer than wide at the proximal end with a flat proximal surface (0); almost as wide as it is long with a strongly convex proximal articulation surface (1).

235. Length of the fifth metacarpal: less than 75 per cent of the length of the third metacarpal (0); greater than 75 per cent of the length of the third metacarpal (1).

236. Length of manual digit one: less than the length of manual digit two (0); greater than the length of manual digit two (1).

237. Ventrolateral twisting of the transverse axis of the distal end of the first phalanx of manual digit one relative to its proximal end: absent (0); present but much less than 60 degrees (1); 60 degrees (2). Ordered.

238. Length of the first phalanx of manual digit one: less than the length of the first metacarpal (0); greater than the length of the first metacarpal (1).

239. Shape of the proximal articular surface of the first phalanx of manual digit one: rounded (0); with an embayment on the medial side (1).

240. Shape of the first phalanx of manual digit one: elongate and subcylindrical (0); strongly proximodistally compressed and wedge-shaped (1).

241. Length of the penultimate phalanx of manual digit two: less than the length of the second metacarpal (0); greater than the length of the second metacarpal (1).

242. Length of the penultimate phalanx of manual digit three: less than the length of the third metacarpal (0); greater than the length of the third metacarpal (1).

243. Shape of non-terminal phalanges of manual digits two and three: longer than wide (0); as long as wide (1).

244. Shape of the unguals of manual digits two and three: straight (0); strongly curved with tips projecting well below flexor margin of proximal articular surface (1).

245. Length of the ungual of manual digit two: greater than the length of the ungual of manual digit one (0); 75-100 per cent of the ungual of manual digit one (1); less than 75 per cent of the ungual of manual digit one (2); the ungual of manual digit two is absent (3). Ordered.

246. Phalangeal formula of manual digits two and three: three and four, respectively (0); with at least one phalanx missing from each digit (1).

247. Phalangeal formula of manual digits four and five: greater than 2-0, respectively (0); less than 2-0, respectively (1).

248. Strongly convex dorsal margin of the ilium: absent (0); present (1).

249. Cranial extent of preacetabular process of ilium: does not project further anterior than the anterior margin of the pubic peduncle (0); projects anterior to the cranial margin of the pubic peduncle (1).

250. Shape of the preacetabular process: blunt and rectangular (0); with a pointed, projecting anteroventral corner and a rounded dorsum (1).

251. Depth of the preacetabular process of the ilium: much less than the depth of the ilium above the acetabulum (0); subequal to the depth of the ilium above the acetabulum (1).

252. Length of preacetabular process of the ilium: less than twice its depth (0); greater than twice its depth (1).

253. Buttress between preacetabular process and the supraacetabular crest of the ilium: present (0); absent (1).

254. Medial wall of acetabulum: fully closing acetabulum with a triangular ventral process between the pubic and ischial peduncles (0); partially open acetabulum with a straight ventral margin between the peduncles (1); partially open acetabulum with a concave ventral margin between the peduncles (2); fully open acetabulum with medial ventral margin closely approximating lateral rim of acetabulum (3). Ordered.

255. Length of the pubic peduncle of the ilium: less than twice the anteroposterior width of its distal end (0); greater than twice the anteroposterior width of its distal end .

256. Caudally projecting 'heel' at the distal end of the ischial peduncle: absent (0); present (1).

257. Length of the ischial peduncle of the ilium: similar to pubic peduncle (0); much shorter than pubic peduncle (1); virtually absent so that the chord connecting the distal end of the pubic peduncle with the ischial articular surface contacts the postacetabular process (2). Ordered.

258. Length of the postacetabular process of the ilium: between 40 and 100 per cent of the distance between the pubic and ischial peduncles (0); less than 40 per cent of the distance between the pubic and ischial peduncles (1); more than 100 per cent of the distance between the pubic and ischial peduncles (2).

259. Well-developed brevis fossa with sharp margins on the ventral surface of the postacetabular process of the ilium: absent (0); present, ventrally facing (1); present, lateroventrally facing (2). 256; 3rd state (2)

260. Anterior end of ventrolateral ridge bounding brevis fossa: not connected to supracetabular crest (0); joining supracetabular crest (1). 261. Shape of the caudal margin of the postacetabular process of the ilium: rounded to bluntly pointed (0); square ended (1); with a pointed ventral corner and a rounded caudodorsal margin (2). 262. Width of the conjoined pubes: less than 75 per cent of their length (0); greater than 75 per cent of their length (1).

263. Pubic tubercle on the lateral surface of the proximal pubis: present (0); absent (1).

264. Proximal anterior profile of pubis: anterior margin of pubic apron smoothly confluent with anterior margin of iliac pedicel (0); iliac pedicel set anterior to the pubic apron creating a prominent inflection in the proximal anterior profile of the pubis (1).

265. Minimum transverse width of the pubic apron: much more than 40 per cent of the width across the iliac peduncles of the ilium (0); less than 40 per cent of the width across the iliac peduncles of the ilium (1).

266. Position of the obturator foramen of the pubis: at least partially occluded by the iliac pedicel in anterior view (0); completely visible in anterior view (1).

267. Lateral margins of the pubic apron in anterior view: straight (0); concave (1).

268. Orientation of distal third of the blades of the pubic apron: confluent with the proximal part of the pubic apron (0); twisted posterolaterally relative to proximal section so that the anterior surface turns to face laterally (1).

269. Orientation of the entire blades of the pubic apron: transverse (0); twisted posteromedially (1).

270. Craniocaudal expansion of the distal pubis: absent (0); less than 15 per cent of the length of the pubis (1); greater than 15 per cent of the length of the pubis (2). Ordered.

271. Notch separating posteroventral end of the ischial obturator plate from the ischial shaft: present (0); absent (1).

272. Elongate interischial fenestra: absent (0); present (1).

273. Longitudinal dorsolateral sulcus on proximal ischium: absent (0); present (1).

274. Shape of distal ischium: broad and plate-like, not distinct from obturator region (0); with a discrete rod-like distal shaft (1).

275. Length of ischium: less than that of the pubis (0); greater than that of the pubis (1).

276. Ischial component of acetabular rim: larger than the pubic component (0); equal to the pubic component (1)

277. Shape of the transverse section of the ischial shaft: ovoid to subrectangular (0); triangular (1).

278. Orientation of the long axes of the transverse section of the distal ischia: meet at an angle (0); are coplanar (1).

279. Depth of the transverse section of the ischial shaft: much less than the transverse width of the section (0); at least as great as the transverse width of the section (1).

280. Distal ischial expansion: absent (0); present (1).

281. Transverse width of the conjoined distal ischial expansions: greater than their sagittal depth (0); less than their sagittal depth (1).

282. Length of the hindlimb: greater than the length of the trunk (0); less than the length of the trunk (1).

283. Longitudinal axis of the femur in lateral view: strongly bent with an offset between the proximal and distal axes greater than 15 degrees (0); weakly bent with an offset of less than 10 degrees (1); straight (2). Ordered.

284. Shape of the cross-section of the mid-shaft of the femur: subcircular (0); strongly elliptical with the long axis orientated mediolaterally (1).

285. Angle between the long axis of the femoral head and the transverse axis of the distal femur: about 30 degrees (0); close to 0 degrees (1).

286. Shape of femoral head: roughly rectangular in profile with a sharp medial distal corner (0); roughly hemispherical with no sharp medial distal corner (1). This character only applies to taxa with a medially, or anteromedially protruding femoral head. It does not apply to outgroup taxa (Euparkeria or Crurotarsi) with proximally directed femoral heads and is coded as unknown in these taxa.

287. Posterior proximal tubercle on femur: well-developed (0); indistinct to absent (1).

288. Shape of the lesser trochanter: small rounded tubercle (0); proximodistally orientated, elongate ridge (1); absent (2).

289. Position of proximal tip of lesser trochanter: level with the femoral head (0); distal to the femoral head (1).

290. Projection of the lesser trochanter: just a scar upon the femoral surface (0); a raised process (1).

291. Transverse ridge extending laterally from the lesser trochanter: absent (0); present (1).

292. Height of the lesser trochanter in cross section: less than its basal width (0); at least as high as its basal width (1).

293. Position of the lesser trochanter in anterior view: near the centre of the anterior face of the femoral shaft (0); close to the lateral margin of the femoral shaft (1).

294. Visibility of the lesser trochanter in posterior view: not visible (0); visible (1).

295. Height of the fourth trochanter: a low rugose ridge (0); a tall crest (1).

296. Position of the fourth trochanter along the length of the femur: in the proximal half (0); straddling the midpoint (1).

297. Symmetry of the profile of the fourth trochanter of the femur: subsymmetrical without a sharp distal corner (0); asymmetrical with a steeper distal slope than the proximal slope and a distinct distal corner (1).

298. Shape of the profile of the fourth trochanter of the femur: rounded (0); subrectangular (1).

299. Position of fourth trochanter along the mediolateral axis of the femur: centrally located (0); on the medial margin (1).

300. Extensor depression on anterior surface of the distal end of the femur: absent (0); present (1).

301. Size of the medial condyle of the distal femur: subequal to the fibular + lateral condyles (0); larger than the fibular + lateral condyles (1).

302. Well-developed tibiofibular crest on distal femur: absent (0); present (1).

303. Distal surface of tibiofibular crest: as deep anteroposteriorly as wide mediolaterally or deeper (0); wider mediolaterally than deep anteroposteriorly (1).

304. Tibia:femur length ratio: greater than 1.0 (0); between 0.6 and 1.0 (1); less than 0.6 (2). Ordered.

305. Orientation of cnemial crest: projects anteriorly to anterolaterally (0); projecting laterally (1).

306. Paramarginal ridge on lateral surface of cnemial crest: absent (0); present (1).

307. Position of the tallest point of the cnemial crest: close to the proximal end of the crest (0); about half-way along the length of the crest, creating an anterodorsally sloping proximal margin of the crest (1).

308. Proximal end of tibia with a flange of bone that contacts the fibula: absent (0): present (1).

309. Position of the posterior end of the fibular condyle on the proximal articular surface tibia: anterior to the posterior margin of the proximal articular surface (0); level with the posterior margin of the proximal articularsurface (1).

310. Shape of the proximal articular surface of the tibia: transverse width subequal to anteroposterior length (0); transverse width between 0.6 and 0.9 times anteroposterior length (1); anteroposterior length twice the transverse width or higher (2). Ordered.

311. Transverse width of the distal tibia: subequal to its craniocaudal length (0); greater than its craniocaudal length (1).

312. Anteroposterior width of the lateral side of the distal articular surface of the tibia: as wide as the anteroposterior width of the medial side (0); narrower than the anteroposterior width of the medial side (1).

313. Relationship of the posterolateral process of the distal end of the tibia with the fibula: not flaring laterally and not making significant contact with the fibula (0); flaring laterally and backing the fibula (1).

314. Shape of the distal articular end of the tibia in distal view: ovoid (0); subrectangular (1).

315. Shape of the anteromedial corner of the distal articular surface of the tibia: forming a right angle (0); forming an acute angle (1).

316. Position of the lateral margin of descending caudoventral process of the distal end of the tibia: protrudes laterally at least as far as the anterolateral corner of the distal tibia (0); set well back from the anterolateralcorner of the distal tibia (1).

317. A triangular rugose area on the medial side of the fibula: absent (0); present (1).

318. Transverse width of the midshaft of the fibula: greater than 0.75 of the transverse width of the midshaft of the tibia (0); between 0.5 and 0.75 of the transverse width of the midshaft of the tibia (1); less than 0.5 of thetransverse width of the midshaft of the tibia (2). Ordered.

319. Position of fibula trochanter: on anterior surface of fibula (0); laterally facing (1); anteriorly facing but with strong lateral bulge (2).

320. Depth of the medial end of the astragalar body in cranial view: roughly equal to the lateral end (0); much shallower creating a wedge-shaped astragalar body (1).

321. Shape of the posteromedial margin of the astragalus in dorsal view: forming a moderately sharp corner of a subrectangular astragalus (0); evenly rounded without formation of a caudomedial corner (1).

322. Dorsally facing horizontal shelf forming part of the fibular facet of the astragalus: present (0); absent with a largely vertical fibular facet (1).

323. Pyramidal dorsal process on the posteromedial corner of the astragalus: absent (0); present (1).

324. Shape of the ascending process of the astragalus: anteroposteriorly deeper than transversely wide (0); transversely wider than anteroposteriorly deep (1).

325. Posterior extent of ascending process of the astragalus: positioned anteriorly upon the astragalus (0); close to the posterior margin of the astragalus (1).

326. Sharp medial margin around the depression posterior to the ascending process of the astragalus: absent (0); present (1).

327. Buttress dividing posterior fossa of astragalus and supporting ascending process: absent (0); present (1).

328. Vascular foramina set in a fossa at the base of the ascending process of the astragalus: present (0); absent (1).

329. Distal articular surface of astragalus: relatively flat or weakly convex (0); extremely convex and roller-shaped (1).

330. Transverse width of the calcaneum: greater than 30 per cent of the transverse width of the astragalus (0); less than 30 per cent of the transverse width of the astragalus (1).

331. Lateral surface of calcaneum: simple (0); with a fossa (1).

332. Medial peg of calcaneum fitting into astragalus: present, even if rudimentary (0); absent (1).

333. Calcaneal tuber: large and well developed (0); highly reduced to absent (1).

334. Shape of posteromedial heel of distal tarsal four (lateral distal tarsal): proximodistally deepest part of the bone (0); no deeper than the rest of the bone (1).

335. Shape of posteromedial process of distal tarsal four in proximal view: rounded (0); pointed (1).

336. Ossified distal tarsals: present (0); absent (1).

337. Proximal width of the first metatarsal: less than the proximal width of the second metatarsal (0); at least as great as the proximal width of the second metatarsal (1).

338. Size of first metatarsal: maximum proximal breadth less than 0.4 times its proximodistal length (0); maximum proximal breadth between 0.4 and 0.7 times its proximodistal length (1); maximum proximal breadth greater than 0.7times its proximodistal length (2). Ordered.

339. Orientation of proximal articular surface of metatarsal one: horizontal (0); sloping proximolaterally relative to the long axis of the bone (1).

340. Shaft of metatarsal I: closely appressed to metatarsal II throughout its length (0); only closely appressed proximally, with a space between metatarsals I and II distally (1).

341. Orientation of the transverse axis of the distal end of metatarsal one: horizontal (0); angled proximomedially (1).

342. Shape of the medial margin of the proximal surface of the second metatarsal: straight (0); concave (1).

343. Shape of the lateral margin of the proximal surface of the second metatarsal: straight (0); concave (1).

344. Projection of ventral flange on proximal surface of second metatarsal: neither corner appreciably more developed than the other (0); laterally flaring (1); medially flaring (2).

345. Well-developed facet on proximolateral corner of plantar ventrolateral flange of mt II for articulation with medial distal tarsal: absent (0); present (1).

346. Length of the third metatarsal: greater than 40 per cent of the length of the tibia (0); less than 40 per cent of the length of the tibia (1).

347. Proximal outline of metatarsal III: subtriangular with acute or rounded posterior border (0); subtrapezoidal, with posterior border broadly exposed in plantar view (1).

348. Minimum transverse shaft diameters of third and fourth metatarsals: greater than 60 per cent of the minimum transverse shaft diameter of the second metatarsal (0); less than 60 per cent of the minimum transverse shaft diameter ofthe second metatarsal (1).

349. Transverse width of the proximal end of the fourth metatarsal: less than twice the anteroposterior depth of the proximal end (0); at least twice the anteroposterior depth of the proximal end (1).

350. Angle formed by the anterior and anteromedial borders of metatarsal IV: obtuse (0); right angle, or acute (1).

351. Transverse width of the proximal end of the fifth metatarsal: less than 25 percent of the length of the fifth metatarsal (0); between 30 and 49 percent of the length of the fifth metatarsa (1); greater than 50 percent of the length of the fifth metatarsal(2). Ordered.

352. Transverse width of distal articular surface of metatarsal four in distal view: greater than the anteroposterior depth (0); less than the anteroposterior depth (1).

353. Pedal digit five: reduced, non-weight bearing (0); large (fifth metatarsal at least 70 per cent of fourth metatarsal), robust and weight bearing (1).

354. Length of non-terminal pedal phalanges: all longer than wide (0); proximalmost phalanges longer than wide while more distal phalanges are as wide as long (1); all nonterminal phalanges are as wide, if not wider, than long (2).Ordered.

355. Length of the first phalanx of pedal digit one: greater than the length of the ungual of pedal digit one (0); less than the length of the ungual of pedal digit one (1).

356. Length of the ungual of pedal digit one: less than at least some non-terminal phalanges (0); longer than all non-terminal phalanges but shorter than first metatarsal (1); longer than the first metatarsal (2). Ordered.

357. Shape of the ungual of pedal digit one: shallow, pointed, with convex sides and a broad ventral surface (0); deep, abruptly tapering, with flattened sides and a narrow ventral surface (1).

358. Shape of proximal articular surface of pedal unguals: proximally facing, visible on medial and lateral sides (0); proximomedially facing and visible only in medial view, causing medial deflection of pedal unguals in articulation (1).

359. Penultimate phalanges of pedal digits two and three: well-developed (0); reduced discshaped elements if they are ossified at all (1).

360. Shape of the unguals of pedal digits two and three: dorsoventrally deep with a proximal articulating surface that is at least as deep as it is wide (0); dorsoventrally flattened with a proximal articulating surface that is wider than deep (1).

361. Length of the ungual of pedal digit two: greater than the length of the ungual of pedal digit one (0); between 90 and 100 per cent of the length of the ungual of pedal digit one (1); less than 90 per cent of the length of the ungual of pedal digit one (2). Ordered.

362. Size of the ungual of pedal digit three: greater than 85 per cent of the ungual of pedal digit two in all linear dimensions (0); less than 85 per cent of the ungual of pedal digit two in all linear dimensions (1).

363. Number of phalanges in pedal digit four: four (0); fewer than four (1).

364. Phalanges of pedal digit five: present (0); absent (1).

365. Femoral length: less than 200 mm (0); between 200 and 399 mm (1); between 400 and 599 mm (2); between 600 and 799 mm (3); between 800 and 1000 mm (4); greater than 1000 mm (5). Ordered. **EXCLUDED**

366. **Laminae/ridges extending from the basipterygoid process onto the parasphenoid rostrum: extend parallel untill they fade into the ventral margin of the cultriform process (0); converge anteromedially on the ventral surface of the cultriform process (1). (this study)**

367. **Angle between basipterygoid process and cultriform process of the parabasisphenoid: < 90 degress (0); 90 degress (1); > 90 degrees (2). (This study – modified from Butler *et al.,* 2008)**

368. Length of the basisphenoid (from the basipterygoid process to the basisphenoidal component of the basal tubera) in relation to the length of the basioccipital (from the basioccipital component of the basal tubera to posterior limit of the condyle): longer or equal (0); shorter (1). (this study)

369. Notch in the posterodorsal margin of the lateral portion of the parabasisphenoid: absent (0); present (1). (this study)

370. Number of foramina in the otoccipital between the exoccipital pillar (excluding the foramina for the hypoglossal nerve) posteriorly and fenestra ovalis anteriorly: one (0), two (1). (this study)

371. Unossified gap between the basioccipital and basisphenoidal component of the basal tubera and ventral ramus of the opistothic: absent (0); present (1). (this study)

APPENDIX FOR CHAPTER 6

For the phylogenetic analysis used to establish the phylogenetic position of the Oxford Braincase in the context of Sauropodomorpha evolution we used a expanded version of the dataset of Chapter 5, which in turn corresponds to an updated and revised version of dataset presented in previous works on Sauropodomorpha phylogeny (e.g. Yates, 2007b; Otero & Pol, 2013; Apaldetti *et al.,* 2014, McPhee *et al.,* 2014; 2015). Modifications in relation to the original dataset of Bronzati & Rauhut (Chapter 5) consist in the inclusion of the Oxford Braincase as an Operational Taxonomic Unit and the addition of 4 new characters (372-275) used in previous works focusing on the phylogenetic relationships of sauropods (Wilson, 2005; Carballido *et al.*, 2012).

The following characters were set as additive (also followed by ORDERED in the characters list of Chapter 5): 8, 13, 19, 23, 40, 57, 69, 92, 102, 117, 121, 131, 144, 147, 149, 150, 157, 162, 167, 169, 170, 177, 207, 210, 225, 230, 237, 245, 255, 257, 270, 283, 304, 310, 318, 338, 351, 354, 356, 361, 365. Yet, following Bronzati & Rauhut (Chapter 5), characters 86 and 365 were set as innactive because of problems in character construction. For the principal co-ordinate analyses, as explained in the main document, five taxa were included in the dataset (*Camarasaurus lentus, Dicraeosaurus sattleri, Giraffatitan brancai, Jobaria tiguidensis, Tornieria Africana*) and only those characters related to braincase anatomy were used, namely: 58, 59, 60, 72, 73, 74, 75, 76, 77, 78, 79, 80, 81, 82, 83, 84, 85, 366-375 (see also list of Chapter 5).

Extra characters

372. Otosphenoidal crest: low and not projecting posterolaterally (0); developed as a lamina projecting posterolaterally (1). (new character)
373. Frontal, anteroposterior length: approximately twice (0); or less than minimum transverse breadth (1). (Wilson, 2002: character 20)
374. Parietal, distance separating supratemporal fenestrae: less than (0); or twice the long axis of supratemporal fenestra (1). (Wilsson, 2002: character 24).
375. Supratemporal region, anteroposterior length: temporal bar longer (0); or shorter anteroposteriorly than transversely (1). (Wilson, 2002: character 28).

Reduced strict consensus tree

Figure S6.1: Reduced strict consensus trees obtained in the phylogenetic analyses with letters 'a' and 'b' indicating the alternative positions occupied by the OTUs *Blikanasaurus* and 'Oxford Braincase' (respectively) in the different MPT's.

CURRICULUM VITAE – March 2017

PERSONAL DETAILS

Full name: Mario Bronzati Filho
Date and place of birth: 26/06/1986 Campinas – SP. Brazil
Nationality: Brazilian

EDUCATION

2006 – 2009:   BSc Biological Sciences, Universidade de São Paulo – USP, Faculdade de Filosofia Ciências e Letras de Ribeirão Preto – FFCLRP, Departamento de Biologia, Ribeirão Preto - SP, Brazil. Monograph title: "*Phylogenetic studies of Crocodyliformes with the construction of a supertree using the MRP method*", 83 pp (original title in Portuguese). Supervisor: Max C. Langer (FFCLRP - USP). Funding: FAPESP (Brazilian Agency).

2006-2010   Teaching Degree in Biological Sciences, Universidade de São Paulo – USP, Faculdade de Filosofia Ciências e Letras de Ribeirão Preto – FFCLRP, Departamento de Biologia, Ribeirão Preto - SP, Brazil.

2010-2012:   MSc Comparative Biology, Universidade de São Paulo, USP. Departamento de Biologia, *Campus* de Ribeirão Preto/SP, Brazil. Project title: "*Morphological patterns and shifts of diversification in the evolution of Crocodyliformes*". Supervisor: Max C. Langer. Funding: FAPESP (Brazilian Agency).

Since Oct/2013-: PhD Candidate, Ludwig-Maximilians-University, Faculty of Geosciences, Department of Earth- and Environmental Sciences, Munich, Germany.

Since Oct/2013: Researcher at the Bayerische Staatssammlung für Paläontologie und Geologie, Munich, Germany.

PUBLICATIONS (Articles in periodics)

Cabreira, S.F., Kellner, A.W.A., Dias-da-Silva, S., Silva, L.R., **Bronzati, M.**, Marsola, J.C.A., Müller, R.T., Bittencourt, J.S., Batista, B.J., Raugust, T., Carrilho, R., Brodt, A., Langer, M.C. (2016). A unique Late Triassic dinosauromorph assemblage reveals dinosaur ancestral anatomy and diet. *Current Biology*, 26(22), 3090-3095.

Godoy, P. L.; **Bronzati, M**.; Eltink, E.; Marsola, J. C. DE A.; Cidade, G. M.; Langer, M. C.; Montefeltro, F. C. (2016). Postcranial anatomy of Pissarrachampsa sera (Crocodyliformes, Baurusuchidae) from the Late Cretaceous of Brazil: insights on lifestyle and phylogenetic significance. *PEERJ*, v. 4, p. e2075 (**Joint first authors: Godoy and Bronzati**)

Bronzati, M.; Montefeltro, F. C.; Langer, M. C. (2015). Diversification events and the effects of mass extinctions on Crocodyliformes evolutionary history: *Royal Society Open Science*, v. 2, p. 140385.

Bronzati, M.; Montefeltro, F. C. and Langer, M. C. (2012*)* "A species-level supertree of Crocodyliformes". *Historical Biology,* 24: 598-606.

PUBLICATIONS (Abstracts)

BRONZATI, M.; BENSON, R. B.; RAUHUT, O.W.M. Sauropod braincase anatomy as a product of rapid morphological transformation. In: 14th Annual Meeting of the European Association of Vertebrate Palaeontologists, 2016, Haarlem, The Netherlands. 14th Annual Meeting of the European Association of Vertebrate Palaeontologists Haarlem, The Netherlands, 6-10 July 2016 Abstracts, 2016.

BRONZATI, M.; RAUHUT, O. W. M. . ?Using the brain? for phylogenetic and paleobiological inferences in early dinosaurs and sauropodomorphs. In: 17th Annual Meeting of the Gesellschaft für Biologische Systematik, 2016, Munich, Germany. Abstracts of the 17th Annual Meeting of the Gesellschaft für Biologische Systematik, 2016. v. 88.

BRONZATI, M.; Langer, M. C. ; RAUHUT, O. W. M. . Braincase evolution in early dinosaurs: new evidences from Saturnalia tupiniquim (Late Triassic of Brazil). In: V Congreso Latinoamericano de Paleontologia de Vertebrados, 2015, Colonia, Uruguai. Resumos do V Congresso Latino-americano de Paleontologia de Vertebrados, 2015.

NAIR, J. ; YATES, A. M. ; **BRONZATI, M**. ; WEISBECKER, V. ; SALISBURY, S. W. . A New Braincase of the Near-Sauropod Dinosaur Melanorosaurus (Late Triassic, Southern Africa), and its Systematic and Phylogenetic Implications. In: 15th Conference on Australasian Vertebrate Evolution, Palaeontology, and Systematics, 2015, Alice Springs, Australia. Abstracts of the 15th Conference on Australasian Vertebrate Evolution, Palaeontology, and Systematics, 2015.

STOCKDALE, M. ; BENTON, M. ; **BRONZATI, M.** ; ANDRADE, M. B. ; THOMAS, G. . Temperature-driven evolution and evolutionary stasis among the Crocodylomorpha. In: 63RD Symposium for Vertebrate Palaeontology and Comparative Anatomy, 2015, Southhampton, UK. Abstracts of the 63RD Symposium for Vertebrate Palaeontology and Comparative Anatomy, 2015, Southhampton, 2015.

STOCKDALE, M. ; BENTON, M. ; **BRONZATI, M**. ; ANDRADE, M. B. ; THOMAS, G. . Phylogeny and macroevolution of crocodylomorphs.. In: 59th Annual Meeting of the Palaeontological Association, 2015, Cardiff, UK. Abstracts of the 59th Annual Meeting of the Palaeontological Association, 2015.

Godoy, P. L. ; **BRONZATI, M** . ; LANGER, MAX C. ; Eltink, E. ; Marsola, J. C. ; CIDADE, G. M. ; MONTEFELTRO, FELIPE C. . The postcranial anatomy of Pissarrachampsa sera (Mesoeucrocodylia, Baurusuchidae), from the Late Cretaceous of Brazil. In: 75th Annual Meeting of the Society of Vertebrate Paleontology, 2015, Dallas. Meeting Program & Abstracts of the 75th Annual Meeting of the Society of Vertebrate Paleontology, 2015.

BRONZATI, M.; RAUHUT, O. W. M. . Braincase evolution in Sauropodomorpha based on new evidences from Efraasia minor of the Late Triassic of Germany. In: V Congresso Latino-americano de Paleontologia de Vertebrados, 2015, Colônia, Uruguai. Resumos do V Congresso Latino-americano de Paleontologia de Vertebrados, 2015.

Curriculum Vitae

BRONZATI, M.; HOLWERDA, F. ; RAUHUT, O. W. M. . Redescription of the braincase of Efraasia minor (Dinosauria, Sauropodomorpha) from the Upper Triassic of Germany, with comments on sauropodomorph phylogeny. In: 13th Annual Meeting of the European Association of Vertebrate Palaeontologists, 2015, Opole, Polônia. 13th Annual Meeting of the European Association of Vertebrate Palaeontologists Opole, Poland, 8-12 July 2015 ? Abstracts, 2015.

BRONZATI, M.; Langer, M. C. ; RAUHUT, O. W. M. . The braincase of Saturnalia tupiniquim and the evolution of the braincase in sauropodomorpha. In: 74th Annual Meeting of the Society of Vertebrate Paleontology, 2014, Berlin, Alemanha. Abstracts of papers 74th Annual Meeting of the Society of Vertebrate Paleontology, 2014, 2014. v. 1. p. 98-98.

Bronzati, M.; Montefeltro, F. C. and Langer, M. C. (2012) "*Morphological Patterns in Crocodyliformes*." Reunião Regional da Sociedade Brasileira de Paleontologia – Paleo SP 2012 *Oral presentation

Bronzati, M. ; Montefeltro, F. C. ; Langer, M. C. . Pulsos de diversificação em Crocodyliformes: padrões cladogenéticos utilizando super-árvores. In: VIII Simpósio Brasileiro de Paleontologia de Vertebrados, 2012, Recife-PE. Boletim de Resumos do VIII Simpósio Brasileiro de Paleontologia de Vertebrados, 2012. *Poster Presentation

Bronzati, M.; Montefeltro, F. C. and Langer, M. C. (2011) "What are independent phylogenetic analyses? A discussion based on the construction of the Crocodyliformes supertree" *In* XXX Meeting of the Willi Hennig Society, São José do Rio Preto, Brazil. Hennig XXX Abstracts pp 180-181. *Poster Presentation.

Bronzati, M.; Montefeltro, F. C. and Langer, M. C. (2011) "Using *IterPCR script* on a supertree context: an example using fossil Crocodyliformes. *In* IV Congreso Latinoamericano de Paleontologia de Vertebrados, San Juan, Argentina. *Published online.* – *Oral Presentation.

Langer, M. C. ; Iannuzzi, R. ; Richter, M. ; Laurini, C. R. ; Eltink, E. ; França, M. A. G. ; **Bronzati, M**. . De volta ao Riacho Pedra de Fogo : fósseis permianos da Bacia do Parnaíba no leste do Maranhão. In: XXII Congresso Brasileiro de Paleontologia, 2011, Natal-RN. Atas do XXII Congresso Brasileiro de Paleontologia, 2011. v. 1.

Godoy, P. L. ; Montefeltro, F. C. ; Eltink, E. ; Vila Nova, B. C. A. ; Marsola, J. C. A. ; **Bronzati, M**. ; Venâncio, V. ; Fachini, T. S. ; Langer, M. C. . Novo espécime de Baurusuchidae (Crocodyliformes, Mesoeucrocodylia) de General Salgado-SP (Grupo Bauru, Cretáceo Superior). In: XXII Congresso Brasileiro de Paleontologia, 2011, Natal-RN. Anais do XXII Congresso Brasileiro de Paleontologia, 2011. v. 1. *Poster Presentation

Bronzati, M.; Montefeltro, F. C. and Langer, M. C (2010) "*Phylogenetic studies of Crocodyliformes with the construction of a supertree using the MRP method*" (English title) *In* VII Simpósio Brasileiro de Paleontologia de Vertebrados, 2010, Rio de Janeiro. Boletim de Resumos do VII SBPV. p. 51. *Oral Presentation.

Montefeltro, F. C.; Eltink, E**.**; França, M. A. G.; Marsola, J. C**.; Bronzati, M**.; Godoy, P. L.; Langer, M. C. (2010) "New Crocodyliformes of the Vale do Rio do Peixe Formation (Bauru Group, Late Cretaceous), Campina Verde, MG" (original title in Portuguese). *In*: VII Simpósio Brasileiro de Paleontologia de Vertebrados, 2010, Rio de Janeiro, Brazil. Boletim de Resumos do VII SBPV. p. 51. *Poster Presentation.

CONFERENCES **A**TTENDED (without presentations)

VI Simpósio Brasileiro de Paleontologia de Vertebrados (*VI Brazilian Symposium of Vertebrate Paleontology*), Ribeirão Preto-SP, Brazil; May 28 – 30, 2008.

GRANTS

2006 – 2009: FAPESP

Phylogenetic studies of Crocodyliformes with the construction of a supertree using the MRP method", Supervisor: Max C. Langer

2010 - 2012 - FAPESP

"Morphological patterns and shifts of diversification in the evolution of Crocodyliformes". Supervisor: Max C. Langer

Since 2013 - CNPq/CsF Program (Sciente without borders Programm)

Description of the skull of Saturnalia tupiniquim: implications on the evolution of the braincase and phylogenetic relationships of the Sauropodomorpha.

PUBLIC LECTURES

Supertrees: a necessary not so evil? - University of São Paulo - Postgraduate Course: Molecular Phylogeny of Hexapoda. Organiser: Eduardo Almeida

Workshops Attended

TNT as a cladistic tool (24 hours/100% frequency). USP – FFCLRP , Ribeirão Preto, Brazil, 15-18 August, 2009. Speaker: Peterso Lásaro Lopes. Organizer: Programa de Pós Graduação em Entomologia e Programa de Pós-Graduação em Biologia Comparada – FFCLRP – USP.

III Workshop on Phylogenetic Systematic provided by the Willi Hennig Society (32 hours/100% frequency). UNESP, São José do Rio Preto, Brazil, 25-28 July, 2011. Speakers: John Wenzel, James Carpenter, Eduardo Almeida and Ward Wheeler. Organizer: Fernando B. Noll.

São Paulo School of Advanced Sciences (100 hours/100% frequency). Ilha Bela, Brazil 19-31 August 2012. Organizer: FAPESP; Coordinator: Antonio C. Marques.

Introduction to Virtual Palaeontology and computed tomography (16 hours/100% Frequency). Munich, Germany, 21-23 October, 2014. Speaker: Stephan Lautenschlager.

TEACHING **A**CTIVITIES

Demonstration:
- Practical classes, "Geology", 2007 (FFCLRP - USP, Ribeirão Preto).
- Practical classes, "Paleontology", 2010 (FFCLRP - USP, Ribeirão Preto).
- Teacher assistant (PAE Program) – "Paleontology", 2011 (FFCLRP - USP, Ribeirão Preto).